Coordination Chemistry Reviews, 96 (1989) 89–251
Elsevier Science Publishers B.V., Amsterdam – Printed in The Netherlands

MIXED-VALENCE COMPOUNDS OF THE EARLY TRANSITION METALS

CHARLES G. YOUNG

Department of Chemistry, La Trobe University, Bundoora, Vic., 3083 (Australia)

(Received 17 January 1989)

CONTENTS

ABBREVIATIONS

acac	2,4-pentanedionate
aq	represents water coordination sphere or aqueous solution
arphos	1,2-bis(diphenylarsino)ethane
$bbscH_4$	1,2-bis(salicylideneimino)-1,2-bis(salicylideneiminomethyl)-cyclohexane
bdiol	butane-2,3-diolate
bdta	butanediaminetetraacetate

0010-8545/89/$57.05 © 1989 Elsevier Science Publishers B.V.

biphenH_2	2,2′-biphenol
bispicen	*N*,*N*-bis(2-pyridylmethyl)ethane-1,2-diamine
bpmpH	2,6-bis[bis(2-pyridylmethyl)aminomethyl]-4-methylphenol
bpy	2,2′-bipyridine
^{n}Bu	*n*-butyl
^{t}Bu	*t*-butyl
cyclam	1,4,8,11-tetraazacyclotetradecane
cyclen	1,4,7,10-tetraazacyclododecane
cyst	cysteinate
18-C-6	18-crown-6, 1,4,7,10,13,16-hexaoxocyclooctadecane
3-Clpy	3-chloropyridine
4-CNpy	4-cyanopyridine
Cp	η^5-cyclopentadienyl, $C_5H_5^-$
Cp*	η^5-pentamethylcyclopentadienyl, $C_5Me_5^-$
CT	charge transfer
dhphH_6	1,4-dihydrazineophthalazine
dme	1,2-dimethoxyethane
dmf	dimethylformamide
dmpe	1,2-bis(dimethylphosphino)ethane
dmso	dimethyl sulphoxide
dppe	1,2-bis(diphenylphosphino)ethane
dth	2,5-dithiahexane
dtsbH_4	2,3-dimethyl-1,2,3,4-tetrakis(salicylideneimino)butane
DOTP	1,1-dimethyl-3-oxobutyltriphenylphosphonium
edta	ethylenediaminetetraacetate
ESR	electron spin resonance
Et	ethyl
Etcyst	cysteinate ethyl ester
EXAFS	extended X-ray absorption fine structure
FF	*N*,*N*-bis(5-(*o*-phenyl)-10,15,20-triphenylporphyrin)urea
gly	glycinate, $NH_2CH_2CO_2^-$
hedta	*N*-(hydroxyethyl)ethylenediaminetriacetate
hpH	2-hydroxypyridine
ida	iminodiacetate
ImH	imidazole
K_{comp}	comproportionation constant
L-ImH	2,6-bis[(bis((1-methylimidazol-2-yl)methyl)amino)methyl]-4-methylphenol
mhpH	6-methyl-2-hydroxypyridine
Me	methyl
MeCp	η^5-methylcyclopentadienyl, $C_5H_4Me^-$
4-Mepy	4-methylpyridine

3,5-Me_2py	3,5-dimethylpyridine
Me_3tcn	*N*,*N*′,*N*″-trimethyl-1,4,7-triazacyclononane
MO	molecular orbital
nbd	norbornadiene
nta	nitrilotriacetate
NMR	nuclear magnetic resonance
5-NO_2-saldien	Schiff base of diethylenetriamine and 5-nitrosalicylaldehyde
ox	oxalate
oxine	8-hydroxyquinolate
OAc	acetate, $MeCO_2^-$
OEC	oxygen-evolving complex
OEP	octaethylporphyrin
pdt	propane-1,3-dithiolate
peida	(*S*)-[[1-(2-pyridyl)ethyl]imino]diacetate
Ph	phenyl
phen	1,10-phenanthroline
4-Phpy	4-phenylpyridine
pip	piperidine
pmida	[[(2-pyridyl)methyl]imino]diacetate
py	pyridine
pz	pyrazolyl, $C_3H_3N_2^-$
^{i}Pr	isopropyl
^{i}PrCp	η^5-isopropylcyclopentadienyl, $C_5H_4{}^iPr^-$
^{n}Pr	*n*-propyl
quin	quinoline
R_4bitt^{2+}	3,5-bis(*N*,*N*-dialkyliminio)-1,2,4-trithiolane dication
sal	salicylate
saldien	Schiff base of diethylenetriamine and salicylaldehyde
salhpH_2	2-(salicylideneamino)-1,3-dihydroxy-2-methylpropane
Su	sulphosalicylate anion
tcn	1,4,7-triazacyclononane
thf	tetrahydrofuran
tht	tetrahydrothiophene
tmtaa	benzotetramethyltetraaza[14]annulene
tpa	tris(2-pyridylmethyl)amine
tren	2,2′,2″-triaminotriethylamine
ttha	triethylenetetraminehexaacetate
TCNQ	7,7,8,8-tetracyanoquinonedimethane
TPP	tetraphenylporphyrin
TpTP	tetra-*p*-tolylporphyrin
XPS	X-ray photoelectron spectroscopy

Greek symbols

ϵ extinction coefficient ($M^{-1}\,cm^{-1}$)

A. INTRODUCTION

The study of mixed-valence compounds has a long and intriguing history [1,2]. For more than two centuries after the discovery of the first mixed-valence compound, Prussian blue [3,4], mixed-valence chemistry remained a rather mysterious science. However, in the past 20 years the study of mixed-valence compounds has developed into a field with important ramifications in chemistry, physics, geology and biology [5]. The growth in this area was triggered in 1967 by a number of reviews concerned with the experimental and theoretical aspects of mixed valency [1,6,7]. Since then, progress in mixed-valence chemistry has been dramatic and a wealth of knowledge has been amassed. The most extensive and systematic studies to date have centred on compounds of group 8–11 * transition metals. In particular, compounds of iron [2,8], ruthenium [2,8], platinum [2,9] and copper [10] have been widely studied and reviewed. For these and related elements, the preparative [11,12] and theoretical [2,6,7,13,14] principles of mixed valency are now, to a large extent, well developed. The mixed-valence chemistry of the early transition metals is considerably less developed, yet a remarkable variety of unique and structurally diverse mixed-valence compounds, ranging from solid state reduced halides and oxides to esoteric molecular species, are formed by these elements. Their wide range of oxidation states, coordination numbers and geometries provide enormous potential for the formation of mixed-valence compounds, and many of these may be expected to possess distinctive bonding, chemistry and applications. Moreover, the importance of mixed-valence centres in biological and chemical catalysis provides great stimulus to this area, particularly in titanium, molybdenum, manganese and rhenium chemistry. It is noteworthy that mixed-valence compounds of the early transition metals have not been reviewed. This is a likely consequence of the sheer number and diversity of such compounds and the ineffectiveness of computer-assisted literature searches. It is hoped that this review will stimulate the systematic study of these compounds and facilitate the continued growth of this fascinating area.

* The periodic group notation is in accord with recent actions by IUPAC and ACS nomenclature committees. A and B notation is eliminated because of wide confusion. Groups IA and IIA become groups 1 and 2. The *d*-transition elements comprise groups 3–12, and the *p*-block elements comprise groups 13–18.

(i) Scope and organization

This review surveys mixed-valence compounds of the group 4–7 transition elements. Only compounds containing discrete homometallic molecules or ions having an independent existence in solution or in the solid state are considered. Consequently, many interesting and important compounds which have an extended structure in the solid state do not fall within the scope of this review. Both coordination and organometallic compounds are reviewed herein but binary carbonyl clusters and many of their derivatives have been excluded due to the difficulty of treating their structure and bonding within a mixed-valence context. While it is not feasible to cover solution species formed during routine electrochemical studies, isolated and/or well-characterized species formed by electrochemical methods are treated. In addition, complexes observed during kinetic studies of redox processes are not discussed unless they have been reasonably well characterized. As far as possible the relevant literature has been exhaustively reviewed up to the end of 1987. The literature available up to April 1989 is included as a note added in proof. Apologies go to the authors of any articles which have been overlooked. Wherever possible, inconsistencies and inaccuracies in the existing literature have been noted and corrected data have been included.

The review is organized into four main sections (Sections B–E), each describing a particular group of elements. For each element, a general survey of its mixed-valence chemistry is followed by a detailed discussion of individual compounds and their properties. Compounds are discussed in order of increasing nuclearity, and compounds of a given nuclearity are discussed in order of decreasing average oxidation state. For example, dinuclear molybdenum compounds of average oxidation state 5.5 (formally $Mo^{V}Mo^{VI}$) are discussed first, followed by those of average oxidation state 5.0 (formally $Mo^{IV}Mo^{VI}$) and so on. Compounds of the same average oxidation state are arranged according to the lower formal oxidation state of the metal. Thus for dinuclear tungsten compounds of average oxidation state 3, $W^{II}W^{IV}$ compounds are discussed first followed by those of $W^{0}W^{VI}$. It is hoped that this organization will permit the rapid location of compounds according to their nuclearity, average oxidation state and formal oxidation states. Tables are organized in a similar fashion. However, owing to the limited characterization of some compounds, only data for selected well-characterized compounds are tabulated. Concluding remarks (Section F) complete the review.

TABLE 1

Properties of selected mixed-valence compounds of titanium

Compound	Ti oxidation state		Structure	Ti...Ti distance [a] (Å)	μ_{eff} (BM)	ESR g	IR or near-IR spectrum (cm^{-1}/nm) (ϵ)	Electronic spectrum (nm) (ϵ)	Ref.
	Formal	Average							
$[Ti(OPh)_2Cl(thf)_2]_2H$	III, IV	3.5	**1**	–	0.90/Ti [b]	1.931 [c] 1.945 1.979	$\nu(Ti_2H)$ [d] ν(TiCl)440	–	15
$Cp_4Ti_2(\mu\text{-}NH_2)(\mu\text{-}NH)$	III, IV	3.5	**2**	3.392(4)	0.95/Ti	1.979	1300, 1540 1650, 1860 [g]	495 (3700) [h]	18
$[Ti(OPh)_2]_2(N_2)H$	II, III	2.5	**4**	–	0.76/Ti [b]	1.912 [c] 1.943 1.982	$\nu(N_2)$ [d] ν(TiH) [d]	–	15
$Cp_2Ti\{\mu\text{-}(\eta^1\text{:}\eta^5\text{-}C_5H_4)\}TiCp$	II, III	2.5	–	–	–	–	1120 (144)	486 (260) 640 (183)	21
$Cp_2Ti\{\mu\text{-}(\eta^1\text{:}\eta^5\text{-}C_5H_4)\}TiCp(thf)$	II, III	2.5	Fig. 1	3.336(1)	–	–	1120 (144)	486 (260) 640 (183)	21
$Cp_6Ti_3\{\mu\text{-}OC(NPh)_2\}_2$	III_2, IV	$3\frac{1}{3}$	Fig. 2	Long	1.72	–	–	–	27
$[Ti_3(\mu\text{-}Cl)_6(C_6Me_6)_3]Cl$	II_2, III	$2\frac{1}{3}$	Fig. 13(c)	–	1.84	–	–	–	28

$[Ti(OPh)_2]_3H$	II_2, III	$2\frac{1}{3}$	**7** or **8**	–	0.69/Ti [b]	1.913 [c] 1.941 1.964	–	–	15
$Ti_4(OPr)_{12}O$	III_2, IV_2	3.5	–	–	–	1.96 [e] 3.98, 1.95 [f]	–	–	16
$[\mu_3\text{-}N_2\text{-}(C_{10}H_8)(C_5H_4)Ti_4Cp_5]X$ $X = [Cp_2Ti(C_6H_{14}O_3)]$	II_3, III	2.25	Fig. 3	1–2, 3.334(4) 2–3, 3.949(4) 2–4, 4.881(3) 3–4, 3.101(3)		–	$\nu(N_2)$ 1282	–	23
$Cp_5Ti_5(\mu_3\text{-}S)_6$	III_3, IV_2	5.6	Fig. 4(a)	av. 3.101(3)	1.66	1.993	–	–	33
$Cp_6Ti_6(\mu_3\text{-}O)_8$	III_2, IV_4	$3\frac{2}{3}$	Fig. 4(b)	av. 2.891	Diamagnetic	–	–	–	34

[a] Where more than one distance is quoted, the preceding numbers identify the atoms involved, e.g. when prefixed by 1–2, the distance given is between Ti(1) and Ti(2).

[b] By Evans method in thf–benzene.

[c] In frozen thf solution at 133 K.

[d] Not observed.

[e] In benzene at 295 K, assigned to a dinuclear species.

[f] In frozen benzene solution or solid state.

[g] Solid state reflectance spectrum.

[h] Benzene solution.

B. MIXED-VALENCE COMPOUNDS OF THE GROUP 4 ELEMENTS

(i) Titanium compounds

(a) General survey

The mixed-valence chemistry of titanium is dominated by alkoxy and η^5-cyclopentadienyl complexes, and even in the case of the many organometallic species, is limited to the high valence states (II and higher). This behaviour parallels trends in the chemistry of mononuclear and isovalent titanium compounds. A total of about 17 compounds have been reported but quite a number of these have not been adequately characterized. Dinuclear compounds are restricted to $Ti^{III}Ti^{IV}$ and $Ti^{II}Ti^{III}$ species and of the seven reported, only one has been structurally characterized. This compound, $Cp_2Ti\{\mu\text{-}(\eta^1 : \eta^5\text{-}C_5H_4)\}TiCp(thf)$, its precursor, $Cp_2Ti\{\mu\text{-}(\eta^1 : \eta^5\text{-}C_5H_4)\}TiCp$, and various dinuclear and tetranuclear derivatives also constitute the largest family of related titanium compounds. Oxygen donor ligands are a feature of most known $Ti^{III}Ti^{IV}$ compounds although one cyclopentadienyl complex derived from $Cp_2Ti\{\mu\text{-}(\eta^1 : \eta^5\text{-}C_5H_4)\}TiCp(thf)$ is thought to possess a $Ti^{III}Ti^{IV}$ core. Poorly characterized $[Ti(OPh)_2]_2(N_2)H$, $Cp_2Ti\{\mu\text{-}(\eta^1 : \eta^5\text{-}C_5H_4)\}TiCp$ and $Cp_2Ti\{\mu\text{-}(\eta^1 : \eta^5\text{-}C_5H_4)\}TiCp(thf)$ are the only known $Ti^{II}Ti^{III}$ compounds. A number of very different trinuclear complexes, with formally $Ti_2^{III}Ti^{IV}$ and $Ti_2^{II}Ti^{III}$ metal skeletons and disparate ligand types (chlorides, phenoxides, ureylenes, arenes, cyclopentadienyls and hydrides) are known. As with dinuclear compounds, only one of these, the diphenylureylene complex $Cp_6Ti_3\{\mu\text{-}OC(NPh)_2\}_2$, has been structurally characterized. Tetranuclear, pentanuclear and hexanuclear compounds exist but are quite rare compared with dinuclear and trinuclear compounds. The best characterized tetranuclear compound is another derivative of $Cp_2Ti\{\mu\text{-}(\eta^1 : \eta^5\text{-}C_5H_4)\}TiCp$, formed by its reaction with N_2. A feature of the pentanuclear and hexanuclear compounds which have been structurally characterized, is the coexistence of thio, oxo and cyclopentadienyl ligands in these complexes.

Properties of selected mixed-valence compounds of titanium are summarized in Table 1.

(b) Dinuclear compounds

Very few dinuclear $Ti^{III}Ti^{IV}$ compounds have been reported and none have been unambiguously characterized. For example, the reduction of $[TiCl_2(OPh)_2]_2$ with $NaBH_4$ in thf yields a yellow compound formulated as $[Ti(OPh)_2Cl(thf)_2]_2H$ (**1**) on the basis of chemical, magnetic and IR and ESR studies [15]. Also, ESR studies indicate that purple $Ti_4(O^iPr)_{12}O$ exists as a dinuclear $Ti^{III}Ti^{IV}$ species in solution [16]. In benzene solution a strong

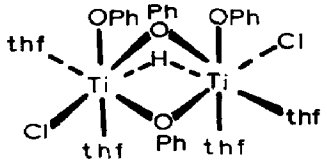

1

signal exhibiting ^{47}Ti ($I = 7/2$, 7.75% abundance) and ^{49}Ti ($I = 7/2$, 5.51% abundance) hyperfine coupling is observed at $g = 1.96$. The signal is assigned to species such as $Ti_2(O^iPr)_7$ and/or $Ti_2(O^iPr)_5O$. A transient $Ti^{III}Ti^{IV}$ complex has also been observed in kinetic studies of the oxidation of Ti(hedta)(H_2O) with [VO(hedta)]$^-$ [17]. The blue complex ($\lambda_{max} \approx 800$ nm, $\epsilon = 47$) is also formed by the autoxidation of Ti(hedta)(H_2O) but its exact nature remains unknown.

Another $Ti^{III}Ti^{IV}$ complex, red $Cp_2Ti_2(\mu\text{-}NH_2)(\mu\text{-}NH)$ (**2**), results from

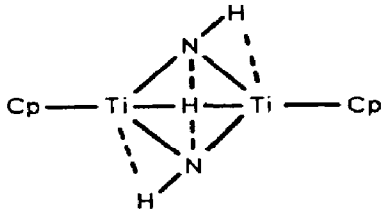

2

the formal oxidation of $Cp_2Ti\{\mu\text{-}(\eta^1 : \eta^5\text{-}C_5H_4)\}TiCp$ (**3**) with NH_3 [18]. Although the planar array of Ti_2N_2 atoms was established by X-ray diffraction the location of the hydrogen atoms is based on indirect arguments. The solid exhibits near-IR bands at 1300, 1540, 1650 and 1860 nm but these bands are absent in solution. Compound **2** reacts with CO and CO_2 to yield isocyanate and carbamate compounds respectively, which have not been fully characterized [19]. Related red products are isolated from the reactions of **3** with primary and secondary amines [18].

The characterization of many $Ti^{II}Ti^{III}$ compounds also leaves much to be desired. Treatment of a thf solution of $[TiCl_2(OPh)_2]_2$ with Na/Hg or potassium under N_2 yields a purple compound formulated as $[Ti(OPh)_2]_2(N_2)H$ (**4**) on the basis of chemical, magnetic, molecular weight and IR

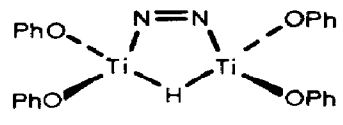

4

spectroscopic properties [15]. Interestingly, the same reaction in toluene

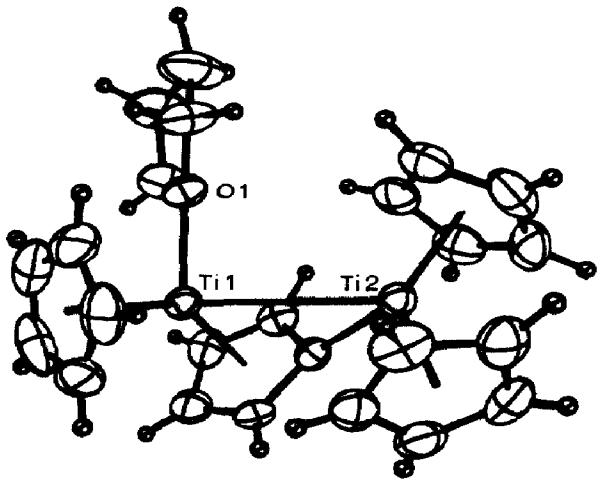

Fig. 1. The molecular structure of **5**. Reproduced with permission from ref. 21.

results in the formation of $[Ti(OPh)_2]_3H$ (vide infra). A brown pyrocatecholate derivative, $[Ti(O_2C_6H_4)]_2(N_2)H$, was also reported and similarly characterized [15]. However, in attempts to produce titanocene and derivatives thereof, Pez, Armor and coworkers have isolated some interesting and well-characterized mixed-valence compounds [18–23]. One of the early achievements of Pez's group was the synthesis of the $Ti^{II}Ti^{III}$ compound **3** and the structural characterization of its thf adduct $Cp_2Ti\{\mu\text{-}(\eta^1:\eta^5\text{-}C_5H_4)\}TiCp(thf)$ (**5**) [20,21]. Grey–black **3** is produced upon reduction of Cp_2TiCl_2 with potassium naphthalene at $-80\,^{\circ}C$, followed by ambient temperature work-up. The X-ray structure of **5**, formed upon the dissolution of **3** in thf, is shown in Fig. 1. The molecule contains three η^5-cyclopentadienyl ligands and one bridging $\eta^1:\eta^5$-cyclopentadienyl ligand arranged around a dinuclear Ti_2 core. The Ti–Ti distance of 3.336(4) Å is consistent with a metal–metal bond between the formally Ti^{II} and Ti^{III} atoms. One thf molecule is bonded to the Ti^{II} atom. Compound **3** exhibits a near-IR absorption at 1120 nm ($\epsilon = 144$) which is not present in related isovalent dimers and is therefore assigned to an intervalence CT transition. Hydride ligands are commonplace in "titanocene" chemistry [20] and the presence of a hydride in **3** or **5** would invalidate the mixed-valence formulations above. Pez et al. [21,22] could find no chemical or crystallographic evidence for the presence of a hydride ligand in these compounds, although they admit that it is difficult to discount its presence completely. Reactions involving **3** have produced both dinuclear $Ti^{III}Ti^{IV}$ (e.g. **2**) and tetranuclear $Ti^{II}_2Ti^{III}_2$ compounds (e.g. **9**, **10** and **11**).

(c) Trinuclear compounds

A number of trinuclear compounds have been reported but few have been

thoroughly characterized. For example, $Cp_3Ti_3(\mu\text{-}O)_4(NO)$ is reportedly formed upon reaction of Cp_2TiR_2 (R = Ph, CH_2Ph) with NO gas [24]. Further, two ill-defined chlorotitanium compounds have been reported by Schram and coworkers [25,26]. One of these, originally formulated as the trinuclear compound $(PPh_3)_3Pt(TiCl_4)_3$, was isolated upon reaction of $Pt(PPh_3)_3$ and $TiCl_4$ [25]. This formally Pt(0) compound was postulated to form via insertion of $TiCl_4$ into the Pt–P bonds of $Pt(PPh_3)_3$. However, on the basis of subsequent ^{31}P NMR, XPS, ESR and magnetic susceptibility studies, the compound was re-formulated as $[PtCl(PPh_3)_3][Ti_3Cl_{11}]$ [26]. The existence of the formally $Ti_2^{III}Ti^{IV}$ anion $[Ti_3Cl_{11}]^-$ has not been confirmed by an X-ray structure. The second chlorotitanium compound reported by Schram and coworkers [25,26] is pentanuclear and is discussed in Section B(i)(e).

Maroon $Cp_6Ti_3\{\mu\text{-}OC(NPh)_2\}_2$ (**6**) is the only structurally characterized trinuclear mixed-valence compound of titanium [27]. Addition of an ether solution of $Cp_2Ti(CO)_2$ to neat PhNCO leads to rapid gas evolution and the precipitation of **6** according to eqn. (1):

$$3Cp_2Ti(CO)_2 + 4PhNCO \rightarrow \mathbf{6} + 8CO \quad (1)$$

Molecules of **6** are composed of two $Cp_2Ti\{OC(NPh)_2\}$ moieties symmetrically linked to a central Cp_2Ti unit through the carbonyl oxygen atoms of the diphenylureylene ligands formed during synthesis (Fig. 2). The complex has a magnetic moment of 1.72 BM per titanium atom at 296 K. To account for the structural and magnetic properties of the compound, Ti(1) is as-

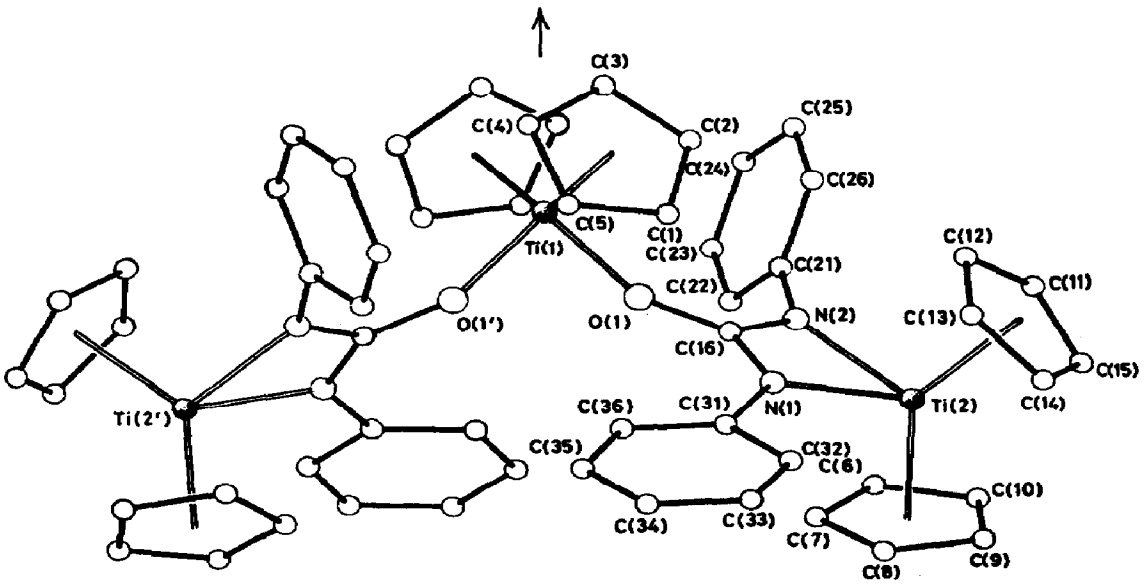

Fig. 2. The molecular structure of **6**. Reproduced with permission from ref. 27.

signed as Ti^{IV} while Ti(2) and Ti(2′) are assigned as Ti^{III}. Thermal rearrangement of **6** in hot toluene leads to the formation of Ti^{IV} and dinuclear Ti^{III} complexes, according to eqn. (2):

$$\mathbf{6} \rightarrow Cp_2Ti\{OC(NPh)_2\} + Cp_4Ti_2\{OC(NPh)_2\} \quad (2)$$

Trinuclear $[Ti_3(\mu\text{-}Cl)_6(C_6Me_6)_3]Cl$ is formed upon careful hydrolysis of the product resulting from the reaction of $TiCl_4$, aluminium and $AlCl_3$ in molten hexamethylbenzene [28]. On the basis of elemental analysis, IR spectroscopy and magnetic measurements the cation was proposed to possess a triangular Ti_3 core, bridged along each edge by two μ-Cl ligands, with η^6-C_6Me_6 ligands bound to each titanium atom. This structure is supported by X-ray structures of related zirconium (Fig. 5), niobium and tantalum complexes. The synthesis of the same compound via hydrolysis of $[TiCl(C_6Me_6)]AlCl_4$ was subsequently reported by Dzierzgowski et al. [29]. They suggested the possible presence of a μ_3-O group in the compound which is unlikely, given the structures of related zirconium, niobium and tantalum compounds.

Treatment of a toluene solution of $[TiCl_2(OPh)_2]_2$ with Na/Hg or potassium leads to the isolation of a very air-sensitive grey compound formulated as $[Ti(OPh)_2]_3H$ and proposed to have one of the structures **7** or **8** [15]. The formally $Ti^{II}_2Ti^{III}$ compound has an effective magnetic moment

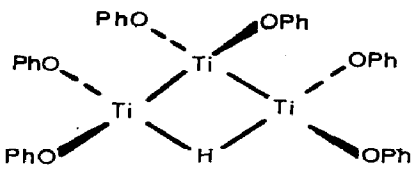

7

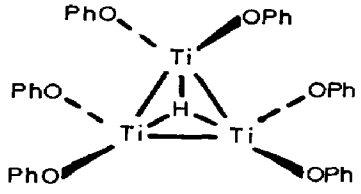

8

of 0.69 BM between −100° and 60°C and exhibits a broad ESR signal. Flamini et al. [15] suggest that previously reported $Ti(OCH_2Ph)_2$ [30] may possess a similar formulation. The same reaction in thf under N_2 results in the formation of **4**.

(d) Tetranuclear compounds

Purple $Ti_4(O^iPr)_{12}O$ is produced by the reaction of $Ti(O^iPr)_4$ and $LiBH_4$ in ether [16]. Variable-temperature ESR experiments suggest the presence of dinuclear $Ti^{III}Ti^{IV}$ species in solution (Section B(i)(b)) and tetranuclear $Ti^{III}_2Ti^{IV}_2$ species in frozen solution or solid states. The ESR spectrum of the tetranuclear species exhibits a sharp singlet at $g = 3.98$, assigned to a $\Delta M_S = 2$ transition due to a singlet–triplet state arising from the magnetic dipole–dipole interaction of two Ti^{III} atoms, along with signals due to

$\Delta M_S = 1$ transitions. The two Ti^{III} atoms are adjacent and probably bridged by μ-O^{i}Pr ligands. A second $Ti_2^{III}Ti_2^{IV}$ compound, the diamagnetic tetranuclear hydride $Ti_4(OEt)_{13}H$, has been reported by Sabo and Gervais [31].

It has been postulated that a third $Ti_2^{III}Ti_2^{IV}$ compound forms upon the reaction of $TiBr_4$ with KBH_4 in liquid ammonia. Green $[NH_4 \cdot NH_3]_2[Ti_4Br_4(NH_2)_{12}]$ was characterized by elemental analysis, redox titrations, chemical properties and XPS [32]. A range of mixed-valence derivatives of this compound has also been reported but the integrity of these materials has not been established nor have any been structurally characterized.

Complex **3** and several other "titanocenes" react with N_2 to give deep blue complexes [20,22,23], some of which are purported to be tetranuclear mixed-valence species. In non-polar solvents, **3** reversibly binds N_2 to form deep blue $[Cp_3Ti_2(C_5H_4)]_2(\mu\text{-}N_2)$ (**9**) [22]. The nitrogen ligand in this complex is proposed to link the formally Ti^{II} atoms of two equivalent molecules of **3**; each nitrogen atom occupies the same coordination site as does the coordinated thf molecule in **5**. Interestingly, **3** does not react with N_2 in thf presumably because a thf molecule blocks the reactive Ti^{II} binding site. Dihydrogen is also reversibly bound by **3** in toluene to form the analogous complex $[Cp_3Ti_2(C_5H_4)]_2H_2$ (**10**) [22]. In polar ether solvents, **3** reacts with N_2 to give a variety of products. When followed by a lengthy work-up, the reaction of **3** and N_2 in dme leads to dark red crystals of $[\mu_3\text{-}N_2\text{-}\{\mu\text{-}(\eta^5\text{:}\eta^5\text{-}C_{10}H_8)\}\{\mu\text{-}(\eta^1\text{:}\eta^5\text{-}C_5H_4)\}Ti_4Cp_5][Cp_2Ti(C_6H_{14}O_3)] \cdot C_6H_{14}O_3$ (**11**, $C_6H_{14}O_3$ = bis(2-methoxyethyl)ether) [23]. An X-ray structure of **11** revealed a tetranuclear cation with the structure shown in Fig. 3. The

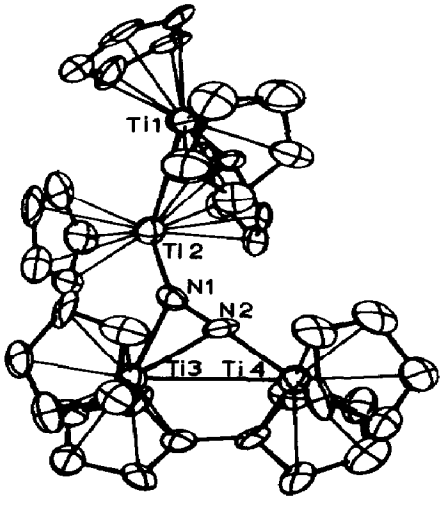

Fig. 3. Structure of the μ_3-N_2-$\{\mu\text{-}(\eta^5\text{:}\eta^5\text{-}C_{10}H_8)\}\{\mu\text{-}(\eta^1\text{:}\eta^5\text{-}C_5H_4)\}Ti_4Cp_5$ unit in **11**. Reproduced with permission from ref. 23.

cation consists of two dinuclear titanium moieties linked by the bridging N_2 molecule. The N_2 molecule is σ-bonded to the formally Ti^{II} (Ti2) atom of a μ-(η^1 : η^5-C_5H_4)Ti_2Cp_3 fragment and σ- and π-bonded to the two Ti^{II} atoms (Ti3 and Ti4) of a μ-(η^5 : η^5-$C_{10}H_8$)Ti_2Cp_2 unit. The dramatically lowered bond order of the N_2 molecule in **9** suggests that mixed-valence species may be important in the titanium-catalysed reduction of N_2 to NH_3. Compound **11** remains the only structurally characterized tetranuclear mixed-valence compound of titanium.

(e) Pentanuclear compounds

Two ill-defined chlorotitanium compounds with mixed-valence formulations have been reported by Schram and coworkers [25,26]. One of these, a trinuclear compound, was discussed in Section B(i)(c). The second, originally formulated as the pentanuclear Pt(0) compound $(PPh_3)_3Pt(TiCl_4)_5$, was isolated upon the reaction of $Pt(PPh_3)_3$ and $TiCl_4$ [25]. On the basis of subsequent ^{31}P NMR, XPS, ESR and magnetic susceptibility studies, the compound was re-formulated as $[PtCl(PPh_3)_3][Ti_5Cl_{19}]$ [26]. The existence of the formally $Ti^{III}_2Ti^{IV}_3$ anion $[Ti_5Cl_{19}]^-$ has not been confirmed by X-ray diffraction studies.

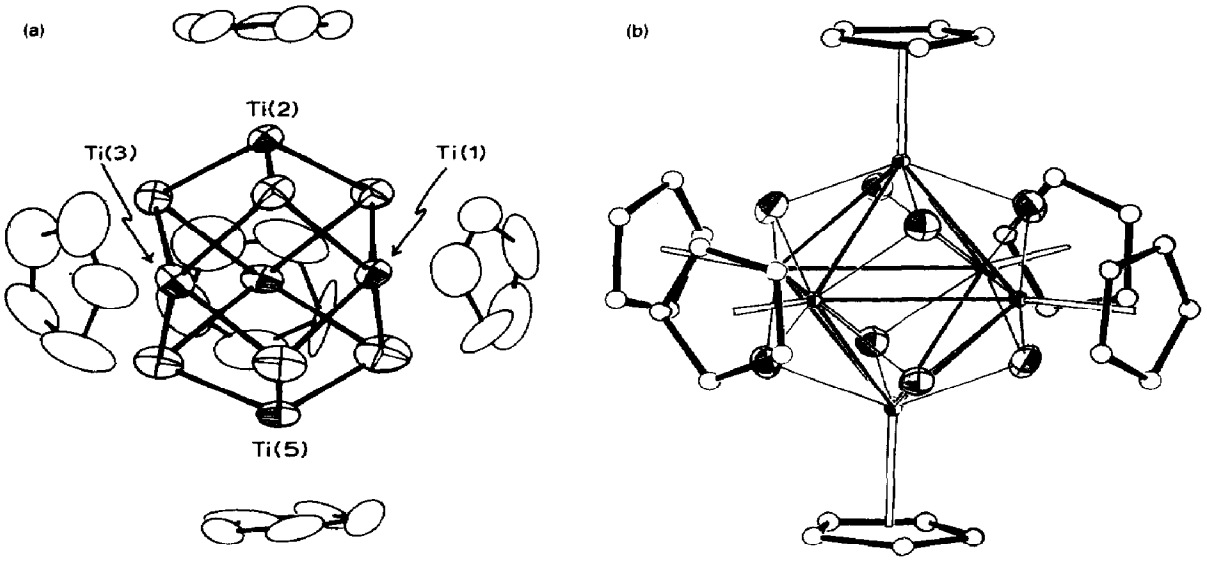

Fig 4. (a) The molecular structure of **12**. Average Ti–S distances are: Ti(1)–S = 2.474 Å, Ti(2)–S = 2.286 Å, Ti(3)–S = 2.463 Å, Ti(4)–S = 2.486, Ti(5)–S = 2.272 Å. Reproduced with permission from ref. 33. (b) The structure of **13** at −160 °C. Titanium and oxygen atoms are shown as small and large sectioned atoms respectively, while carbon atoms are shown as open spheres. Reproduced with permission from ref. 34. The compounds **14** and **15** exhibit similar structures [37].

The reaction of $Cp_2Ti(CO)_2$ with H_2S produces the green–brown thio cluster $Cp_5Ti_5(\mu_3\text{-}S)_6$ (**12**) [33]. The X-ray structure of **12** is shown in Fig. 4(a). The cluster is composed of a Jahn–Teller distorted trigonal bipyramidal Ti_5 core. The faces of the bipyramid are capped with triply bridging thio ligands and each titanium atom is bonded to a Cp ligand. The structure resembles that reported for $Cp_5V_5(\mu_3\text{-}O)_6$ (Section C(i)(e)). The paramagnetism ($\mu_{eff} = 1.66$ BM) and ESR properties ($g = 1.993$) of **12** are consistent with the presence of a single unpaired electron. The assignment of oxidation states III and IV to the equatorial and axial titanium atoms respectively is supported by the observed Ti–S distances.

(f) Hexanuclear compounds

The reaction of Cp_2TiCl_2 with hydrogen and CO leads to the formation of a diamagnetic blue cluster, $Cp_6Ti_6(\mu_3\text{-}O)_8$ (**13**), the structure of which is shown in Fig. 4(b) [34]. Planar Cp rings are located at the apices of a Ti_6 octahedron while each face is capped by a μ_3-O atom. The high symmetry and diamagnetism of the complex precludes a localized $Ti^{IV}_4Ti^{III}_2$ description. The suggestion that **13** is formed upon the reaction of Cp_2TiCl_2 with water [34] was confirmed by later studies by Bottomley et al. [33]. Compound **13** is also reportedly formed when $[Cp_2Ti]_2(CO_3)$ is refluxed for extended periods in toluene [35]. This compound represents the first in a series of compounds, $Cp_mM_mO_n$, where m and n satisfy Euler's theorem; other members include $Cp_5V_5(\mu_3\text{-}O)_6$ (Section C(i)(e)) and $Cp_4Cr_4(\mu_3\text{-}O)_4$ (Section D(i)(e)). The electronic and molecular structures of these clusters have been probed by theoretical studies [36] and the diamagnetism of the $Ti^{III}_2Ti^{IV}_4$ complex is accounted for by placing the two excess electrons into a HOMO of a_{1g} symmetry.

A number of related oxochloro–Ti complexes, $L_6Ti_6(\mu_3\text{-}O)_4(\mu_3\text{-}Cl)_4$ (**14**) and $L_6Ti_6(\mu_3\text{-}O)_6(\mu_3\text{-}Cl)_2$ (**15**, L = Cp, MeCp) are produced upon reduction of $L_4Ti_4Cl_4(\mu\text{-}O)_4$ or $[CpTiCl_2]_2\text{-}\mu\text{-}O$ with aluminium, zinc or $HSnBu^n_3$ [37]. Complexes **14** and **15** are hydrolysed to the mixed-valence species $L_6Ti_6(\mu_3\text{-}O)_8$. X-ray diffraction studies reveal that $(MeCp)_6Ti_6(\mu_3\text{-}O)_4(\mu_3\text{-}Cl)_4$ and $Cp_6Ti_6(\mu_3\text{-}O)_6(\mu_3\text{-}Cl)_2$ possess structures analogous to that of **13** (Fig. 4(b)). The isovalent Ti^{III} complexes **14** contain two unpaired electrons while the $Ti^{III}_4Ti^{IV}_2$ complexes **15** are diamagnetic. The magnetic properties of these complexes may be explained by a symmetry modification of the MO scheme developed by Bottomley and Grein [36].

Depending on the stoichiometry employed, a number of products may be obtained from the reaction of Cp_2TiCl_2 and Li_3N in thf. Mass spectra indicate the formation of $Cp_6Ti_6(C_5H_4)_2N$ and $Cp_6Ti_6(C_5H_4)_2N_3$ when $Cp_2TiCl_2 : Li_3N$ mole ratios of 4 : 2.8 and 1 : 1 respectively are employed in the reaction [38].

(ii) Zirconium compounds

(a) General survey

Discrete mixed-valence compounds of zirconium are limited to salts of $[Zr_3(\mu\text{-}Cl)_6(C_6Me_6)_3]^{n+}$ ($n = 1, 2$) and like most mixed-valence compounds of titanium, these formally $Zr^{II}Zr_2^{III}$ and $Zr_2^{II}Zr^{III}$ complexes are organometallic species. The dominance of the IV oxidation state in zirconium chemistry is likely to be a prime factor limiting the mixed-valence chemistry of this element. The poorly developed coordination chemistry of Zr^{III}, Zr^{II}, Zr^{I} and Zr^{0} provides little scope for the formation of mixed-valence combinations. Disproportionation of Zr^{III} into Zr^{IV} and Zr^{II} accounts for the absence of $Zr_x^{III}Zr_y^{IV}$ and $Zr_x^{II}Zr_y^{III}$ species although recently prepared dinuclear Zr^{III} compounds may, through suitable redox reactions, provide the opportunity to produce discrete dinuclear mixed-valence species of this type. Nevertheless, zirconium does possess a rich mixed-valence chemistry based on solid state reduced halides and chalcogenides. However, compounds of this type are outside the scope of this review. Corbett's group at Iowa State University has been prolific in this area and the reader is encouraged to consult refs. 39–42 and references cited therein. In the reduced halides and their derivatives, zirconium clusters of varying nuclearity are condensed into infinite chain and sheet structures of considerable intricacy; the degree of cluster condensation is dictated by the oxidation state of the metal [39–43]. Corbett's [40] elegant studies of the group 3 halides have revealed related behaviour in these materials. Structures composed of hexanuclear Zr_6 clusters which encapsulate boron, carbon, aluminium and silicon atoms are among the most recent achievements in this area [42]. All these compounds exhibit strong metal–metal bonding and highly delocalized band structures.

(b) Trinuclear compounds

Discrete mixed-valence compounds of zirconium are limited to trinuclear clusters of the type $[Zr_3(\mu\text{-}Cl)_6(C_6Me_6)_3]^{n+}$ ($n = 1, 2$). The first compound of this type was reported by Fischer and Röhrscheid in 1966 [28]. The reduction of $ZrCl_4$ in a molten mixture of hexamethylbenzene, aluminium and $AlCl_3$ produced $[Zr_3(\mu\text{-}Cl)_6(C_6Me_6)_3]Cl$, characterized by elemental analysis, IR spectroscopy and magnetic susceptibility data. In 1981, Stollmaier and Thewalt [44] reported the synthesis and X-ray structural characterization of $[Zr_3(\mu\text{-}Cl)_6(C_6Me_6)_3][Al_2Cl_7]_2$ (**16**). This compound is produced when $ZrCl_4$, C_6Me_6, aluminium and $AlCl_3$ are reacted together in refluxing benzene (the $Al : AlCl_3$ ratio used was much larger than that employed by Fischer and Röhrscheid [28]). The isolation of different products from the above reactions may be simply due to the different reaction conditions employed or to the preferential crystallization of one of the

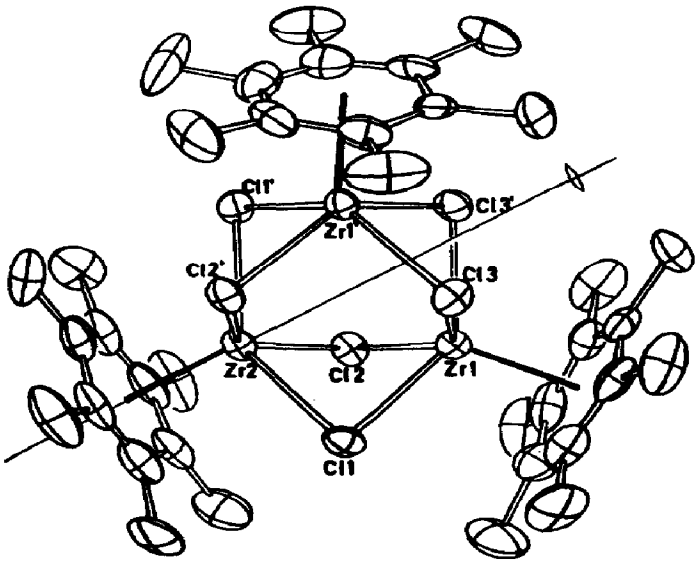

Fig. 5. Structure of the cation in **16**. Analogous structures are possessed by titanium, niobium and tantalum compounds. Reproduced with permission from ref. 44.

simultaneously formed $[Zr_3(\mu\text{-}Cl)_6(C_6Me_6)_3]^{n+}$ cations. The structure of the $[Zr_3(\mu\text{-}Cl)_6(C_6Me_6)_3]^{2+}$ cation in **16** is shown in Fig. 5. It consists of a triangular Zr_3 core ($Zr \cdots Zr = 3.35$ Å) bridged along each edge by two μ-Cl ligands ($Zr\text{–}Cl = 2.56$ Å), with a η^6-C_6Me_6 ligand coordinated to each zirconium atom. The small Zr–Cl–Zr angle of 80° suggests a degree of Zr–Zr bonding. The structure is identical to that proposed for $[M_3(\mu\text{-}Cl)_6(C_6Me_6)_3]^+$ (M = Ti, Zr) by Fischer and Röhrscheid [28] and is also exhibited by related niobium and tantalum complexes (Sections C(ii)(c) and C(iii)(c)). The trinuclear $[Zr_3(\mu\text{-}Cl)_6]^{n+}$ core is also observed in reduced mixed-valence zirconium chlorides [45].

(c) Hexanuclear compounds

Recently, Cotton et al. [46] reported the synthesis of a hexanuclear cluster formulated as $Zr_6(\mu\text{-}Cl)_{12}(PMe_2Ph)_6$ on the basis of an X-ray diffraction study. The complex possesses an octahedral cluster structure typical of $[M_6(\mu\text{-}X)_{12}L_6]^{n+}$ complexes. However, the recently recognized presence of carbon, nitrogen or beryllium atoms within the Zr_6 clusters in the compounds characterized by Corbett et al. raises the question of whether an atom resides at the centre of the Zr_6 cluster of $Zr_6Cl_{12}(PMe_2Ph)_6$. The authors believe this is not the case, although the presence of a hydride ligand, which would make the complex a formally mixed-valence complex, cannot yet be discounted.

(iii) Hafnium compounds

(a) General survey

The chemistry of hafnium is the least developed chemistry of the elements treated in this review. Given the relative scarcity of mixed-valence complexes of its congeners, titanium and more especially zirconium, it is not surprising that, within the scope of this review at least, there appears to be no known mixed-valence complexes of this element.

C. MIXED-VALENCE COMPOUNDS OF THE GROUP 5 ELEMENTS

(i) Vanadium compounds

(a) General survey

In a recent review, Boas and Pessoa [47] included mixed-valence chemistry among the recent developments in vanadium chemistry and predicted that the area would be one of rapid growth. However, to date, the mixed-valence chemistry of vanadium has developed slowly in comparison with that of other early transition metals, notably molybdenum, manganese and rhenium. Nevertheless, there are great opportunities for the realization of interesting chemistry. The majority of mixed-valence vanadium compounds contain the metal in oxidation states of II through V. In keeping with the oxidative and hydrolytic stabilities of mononuclear complexes, oxo–$V^{IV}V^{V}$ complexes are most stable while those containing V^{II} and V^{III} have only transient existence. Organometallic complexes containing V^{-1} have been reported but compounds containing V^{I} and V^{0} remain unknown. Com-

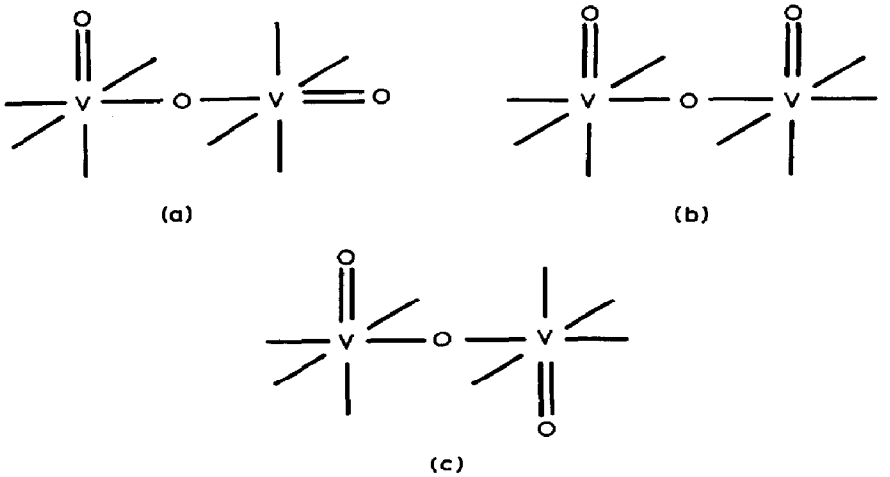

Fig. 6. Proposed and established core structures of $[V_2O_3]^{n+}$ complexes.

pounds containing the $[V_2O_3]^{3+}$ core constitute the largest class of mixed-valence compounds known for vanadium. These binuclear complexes may be classified into two groups. In the first group, the complexes possess localized V^{IV} and V^{V} centres apparently due to zero overlap of d_{xy} orbitals across the oxo bridge. Members of this group exhibit eight-line ESR spectra (^{51}V, 99.9%, $I = 7/2$) and, although no crystal structures are yet available it has been proposed that they possess the structure shown in Fig. 6(a). Related isovalent V^{V} complexes are, however, known to possess the *syn*-dioxo-μ-oxo core structure shown in Fig. 6(b). Moreover, one valence-trapped compound, $Na[V_2O_3(peida)_2] \cdot NaClO_4 \cdot H_2O$, contains a distorted *anti*-dioxo-μ-oxo core related to the structure shown in Fig. 6(c). It would therefore seem that all three structures represent viable core units for the first group of $[V_2O_3]^{3+}$ compounds. Members of the second, larger, group possess delocalized structures and exhibit 15-line ESR spectra as a result of hyperfine coupling to two ^{51}V nuclei. Numerous polyamine polycarboxylic acid complexes of this type have been reported and structurally characterized; all possess an *anti*-$[V_2O_3]^{3+}$ core (Fig. 6(c)) which permits orbital overlap across the oxo bridge. Even the aquated $[V_2O_3]^{3+}$ ion has been characterized. Dinuclear $V^{III}V^{IV}$ and $V^{II}V^{IV}$ compounds are extremely unstable, the latter being long-lived intermediates in inner-sphere electron transfer processes. Two organometallic bis(fulvalene)-$V^{II}V^{III}$ complexes $[V_2(\eta^5 : \eta^5\text{-}C_{10}H_8)_2]^+$ and $[V_2(\eta^5 : \eta^5\text{-}C_{10}H_8)_2(CO)_2]^+$ are known to exist. The most reduced dinuclear compound is the organometallic $V^{-I}V^{III}$ compound $Cp_2V(\mu\text{-}CO)V(CO)_5$. Only a handful of high nuclearity compounds are known. Trinuclear complexes possessing linear and triangular structures exemplified by $V_2^{-I}V^{II}$ μ_2-η^2-carbonyl complexes and $V_3(\mu_3\text{-}O)(O_2CCF_3)_6(thf)_3$ respectively have been reported. Known pentanuclear compounds, members of the series obeying Euler's theorem, possess the formulae $L_5V_5E_6$ (E = O, L = Cp; E = S, L = MeCp). Interestingly, from an electronic point of view, the corresponding dications and various derivatives have also been isolated. The presence of high valent oxo–$V^{II,IV,V}$ cores is an unusual feature of these organometallic species. In the very high nuclearity league, nonanuclear, decanuclear and pentadecanuclear $V_x^{IV}V_y^{V}$ compounds are known. One of these compounds, $K_7[V_9O_{16}(bdta)_4]$, is clearly related to the dinuclear $[V_2O_3]^{3+}$ compounds, the anion being an aggregation of four $[V_2O_3]^{3+}$ units around a central V^{V} atom. The most interesting high nuclearity complexes are undoubtedly the *closo* oxovanadates, which may be expected to possess a rich but still undiscovered chemistry owing to the ability of vanadium to exhibit highly variable geometries and its reluctance to form a restricted number of metal–metal-bonded clusters (cf. niobium and tantalum).

Properties of selected mixed-valence compounds of vanadium are summarized in Table 2.

TABLE 2

Properties of selected mixed-valence compounds of vanadium

Compound	V oxidation state		Structure	ESR spectrum	μ_{eff} (BM)	Electronic spectrum (nm) (ϵ)	Ref.
	Formal	Average					
$(N^nBu_4)[V_2O_3(oxine)_4]$	IV, V	4.5	Fig. 6(a)–6(c)?	8-line, $g = 1.98$	–	725 (86)	48, 51–52
$V_2O_3(acac)_3(bpy)$	IV, V	4.5	Fig. 6(a)?	–	1.70	790 (45), 440 (1670)	54
$Na[V_2O_3(peida)_2]\cdot NaClO_4\cdot H_2O$	IV, V	4.5	Fig. 7	–	–	980 (1200), 735 (940), 565 (470)	55
$(NH_4)_3[V_2O_3(nta)_2]\cdot 3H_2O$	IV, V	4.5	Fig. 6(c) V–O = 1.607 Å	15-line, $g = 1.981$ $A = 52\times10^{-4}$ cm^{-1}	–	1000 (350), 750 (380), 583 (240)	56
$[V_2O_3(pmida)_2]^-$ $K(18\text{-C-}6)^+$, H^+ salts	IV, V	4.5	Fig. 8	15-line, $g = 1.969$ $A = 54$ G	1.79	1000 (1070), 715 (915), 565 (515)	58, 59
$[V_2O_3(aq)]^{3+}$ (in situ)	IV, V	4.5	–	–	–	990 (sh), 825 (112), 662 (118), 570 (130)	60
$[V_2(\eta^5{:}\eta^5\text{-}C_{10}H_8)_2]PF_6$	II, III	2.5	–	8-line, $g = 1.978$ $A = 50$ G	0–1.2	900 (412), 690 (706), 388 (3470)	64
$[V_2(\eta^5{:}\eta^5\text{-}C_{10}H_8)_2(CO)_2]PF_6$	II, III	2.5	–	$g = 2.007$	1.7	Insoluble	64
$Cp_2V(\mu\text{-CO})V(CO)_5$	−I, III	1.0	Fig. 9(a)	$g = 1.99$, ascribed to V^{IV} impurity	2.77	–	68
$V_3(\mu_3\text{-O})(O_2CCF_3)_6(thf)_3$	II, III_2	$2\frac{2}{3}$	Fig. 10 V…V = 3.357(11) Å	–	–	–	72
$[V(thf)_4][V(CO)_6]_2$	$-I_2$, II	0	Fig. 9(b)	–	–	–	76
$Cp_5V_5(\mu_3\text{-O})_6$	III_3, IV_2	3.4	–	$g = 1.972$ Broad, glass only	0.93 (293 K)	–	78, 79
$K_7[V_9O_{16}(bdta)_4]\cdot 27H_2O$	IV_4, V_5	$4\frac{5}{9}$	Fig. 11	Unresolved	1.76 per V^{IV} V^V pair	1020 (800), 900 (900) 720 (950), 585 (850) (ϵ, per V^{IV} V^V pair)	59
$(NEt_4)_4[V_{10}O_{26}]\cdot H_2O$	IV_2, V_8	4.8	Fig. 12(a)	15-line, $g = 1.96$ $A = 51$ G	ca. 1.9	825, 505	85, 86
$(NMe_4)_6[V_{15}O_{36}]Cl\cdot 4H_2O$	IV_8, V_7	$4\frac{7}{15}$	Fig. 12(b)	–	3.9	–	88
$K_8[V_{19}O_{40}H]\cdot 11H_2O$	IV_6, V_{13}	$4\frac{13}{19}$	See ref. 90	–	–	–	90

(b) Dinuclear compounds

The first $[V_2O_3]^{3+}$ complex was reported in 1975 by Reichel and Sawyer [48]. Their electrochemical studies of V^{III}, V^{IV} and V^{V} complexes of oxine revealed the formation of a mixed-valence complex upon the reduction of $VO(OMe)(oxine)_2$ in the presence of water or direct reduction of $VO(OH)(oxine)_2$. The electrochemical species was identical with yellow $(N^nBu_4)[V_2O_3(oxine)_4]$ (**17**) prepared by simply mixing equimolar amounts of $VO(OH)(oxine)_2$, $VO(oxine)_2$ and N^nBu_4OH in methanol. The mixed-valence anion and its mononuclear V^{IV} precursor, $VO(oxine)_2$, exhibit eight-line ESR spectra characteristic of localized V^{IV} centres. Splittings on the high field end of the spectrum of **17** were interpreted in terms of a V^{IV} coordination sphere different from that of $VO(oxine)_2$ or possibly some exchange of the IV and V oxidation states. Similar features in the ESR spectrum of $[VO(ttha)]^{4-}$ have been ascribed to the presence of the dinuclear V^{IV} ion, casting doubt on the integrity of the ESR-active species in the oxine system [49]. A weak band at 725 nm has been assigned to an intervalence CT transition and the complex was shown to be reversibly oxidized to the corresponding binuclear V^{V} complex [50]. This system has been reinvestigated by Jeannin and coworkers [51,52] who confirmed Reichel and Sawyer's observations and reported that **17** could be formed from *cis*-$[VO_2(oxine)_2]^-$ and $VO(oxine)_2$ in MeCN. It was proposed that the complex forms via a simple addition reaction in which one of the oxo groups of $[VO_2(oxine)_2]^-$ coordinates to the sixth position of the $VO(oxine)_2$ molecule. The structure proposed by Jeannin and coworkers (Fig. 6(a)) has not been confirmed by crystallographic studies. However, the structure does account for the absence of electron delocalization by requiring the interaction between the two d_{xy} orbitals to be zero. A bent V–O–V bridge has also been proposed to account for the weak electronic interaction [50]. Interestingly, the structure of the isovalent V^{V} complex, $V_2O_3(oxine)_4$ (**18**), does not possess the structure shown in Fig. 6(a) but instead exhibits a *syn*-$[V_2O_3]^{4+}$ core (Fig. 6(b), V–O–V = 173.4(4)°) [53]. This result and the reversible oxidation of **17** to **18** [50] suggest a related structure for **17**. It would be of great interest to crystallize and structurally characterize **17** in order to resolve the origin of the observed valence localization. The structure shown in Fig. 6(a) has also been proposed for green $V_2O_3(acac)_3(bpy)$, formed by the reaction of $VO(acac)_2$ and bpy in methanol [54]. A magnetic moment of 1.70 BM was reported for the complex but unfortunately the ESR spectrum of the complex was not reported.

The crystal structure of one valence-trapped $[V_2O_3]^{3+}$ complex has been reported. The structure of the anion in $Na[V_2O_3(peida)_2] \cdot NaClO_4 \cdot H_2O$ (Fig. 7) is composed of inequivalent vanadium centres indicative of localized valencies [55]. The inequivalence is manifest in differing V–O bond lengths,

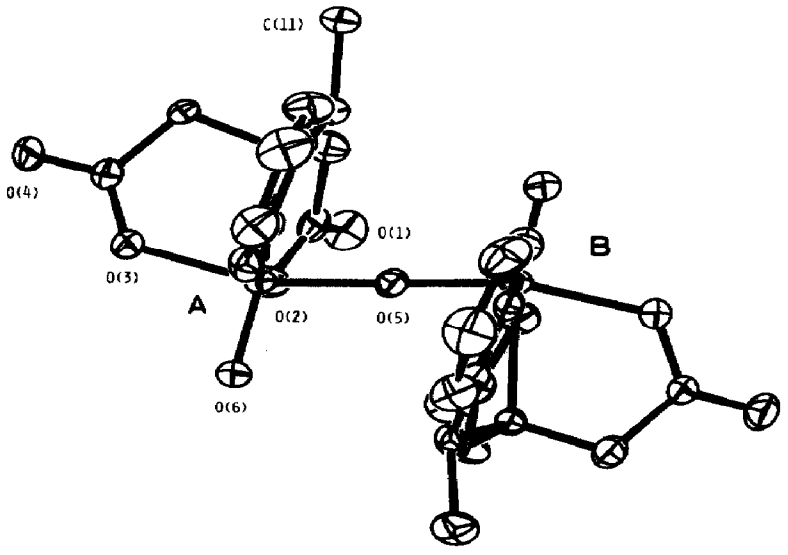

Fig. 7. Structure of the $[V_2O_3(peida)_2]^-$ anion. Bond distances and angles include V_A–O(5) = 1.875(4) Å, V_B–O(5) = 1.763(4) Å, V_A–O(6) = 1.622(4) Å, V_B–O(6) = 1.613(4) Å, V_A–O(5)–V_B = 179.5(3)°. Reproduced with permission from ref. 55.

the deviation of the $[V_2O_3]^{3+}$ core from the true *anti*-planar structure (the torsion angle between the V=O bonds being 164.3(2)°), and an unsymmetrical ion distribution around the complex in the solid state. A comparison with the structures of the corresponding V^{IV} and V^{V} monomers and the ion distribution around the complex strongly suggest that V_A and V_B possess oxidation states of IV and V respectively, making it a Class II ion in the Robin and Day classification [1]. An absorption at about 1000 nm has been assigned to the intervalence CT transition.

The very weak electronic interaction of vanadium ions in the above complexes contrasts with the strong interaction exhibited by *anti*-$[V_2O_3]^{3+}$ complexes possessing the core geometry shown in Fig. 6(c). Nishizawa et al. [56] produced the first compound of this type when deep blue crystals of $(NH_4)_3[V_2O_3(nta)_2] \cdot 3H_2O$ (**19**) were precipitated from an aqueous solution containing $K[VO(nta)(H_2O)]$, $K[VO_2(nta)]$ and NH_4ClO_4. A 15-line ESR spectrum indicative of electron delocalization over two equivalent ^{51}V centres is characteristic of **19**. The spectrum is complicated by the signal of $[VO_2(nta)]^{2-}$, this complex being produced in the equilibrium shown in eqn. (3) ($K = 20$ dm^3 mol^{-1} at 25 °C):

$$[VO(nta)(H_2O)]^- + [VO_2(nta)]^{2-} = [V_2O_3(nta)_2]^{3-} + H_2O \qquad (3)$$

The equilibrium also accounts for the observation of the dinuclear species upon oxidation of $[VO(nta)(H_2O)]^-$ with nitrite [57]. The X-ray structure of the compound has been determined [56]. In the solid state, molecular C_i

symmetry dictates a linear V–O–V unit and *anti*-disposed V=O groups (V–O = 1.607 Å). The structure permits non-zero overlap of the d_{xy} orbitals of vanadium, and experimental data clearly indicate that both vanadium centres are equivalent in solution and the solid state. A derivative of **19**, $Na_3(18\text{-C-}6)_3[V_2O_3(nta)_2] \cdot 9H_2O$, and various salts of $[V_2O_3(pmida)_2]^-$ were reported soon after [58]. For the latter complexes, dissolution in poorly coordinating solvents allowed spectra to be recorded without dissociation into monomers. A 15-line room-temperature ESR spectrum is exhibited by $[V_2O_3(pmida)_2]^-$, and the crystal structure of $H[V_2O_3(pmida)_2] \cdot 4H_2O$ revealed the structure shown in Fig. 8 [58,59]. Small deviations from centrosymmetry are assigned to an asymmetric localization of the H^+ ions rather than to valence trapping [59]. The profile of the intervalence CT band at 1000 nm ($\epsilon = 1070$) was simulated using the vibronic coupling model of Wong and Schatz [13] yielding parameters consistent with strongly delocalized systems, very near to Robin and Day's [1] Class III systems. Single-crystal spectra and magnetic and electrochemical studies have also been reported [59] and a comproportionation constant of 10^{24} has been estimated. The observation of the mixed-valence $[V_2O_3(aq)]^{3+}$ complex, the "naked" core for the species discussed above, has also been reported [60] but has not been characterized by ESR spectroscopy. This complex exists in equilibrium with the aquadioxo–V^V and aquaoxo–V^{IV} ions in perchloric, sulphuric or hydrochloric acid media. In 8.7 M $HClO_4$ the formation

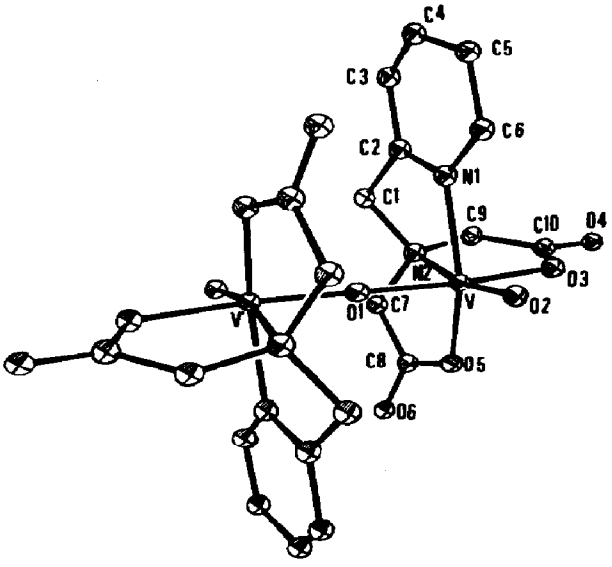

Fig. 8. Structure of the $[V_2O_3(pmida)_2]^-$ anion. Bond distances and angles include V–O(1) = 1.79(2) Å, V–O(2) = 1.592(4) Å, V–O(1)–V = 175.3(7)°. Reproduced with permission from ref. 59.

constant is only 8.1 M^{-1} and the value is even lower (0.8 M^{-1}) in 5 M $HClO_4$. It is proposed that the complex forms by the substitution of a coordinated water molecule of $[VO(aq)]^{2+}$ by an oxo group of $[VO_2(aq)]^+$. An absorption at 990 nm has been assigned to the intervalence CT transition but the low intensity was taken as evidence for a bent or otherwise distorted $[V_2O_3]^{3+}$ unit. Attempts to prepare related bdta complexes yielded a novel nonanuclear complex which is discussed in Section C(i)(f).

Lower oxidation state mixed-valence complexes of polyamine polycarboxylic acid ligands are unstable and have not been isolated and structurally characterized. A superoxo intermediate, which spontaneously converts to a mixed-valence $V^{III}V^{IV}$ complex, may be intercepted during the oxidation of $[V_2O(ttha)]^{2-}$ with O_2 [49]. The same complex may be generated by mixing equimolar amounts of VCl_3, $VOSO_4$ and ttha at pH 7. Pairs of $V^{III}V^{IV}$ complexes undergo electron-cross transfer to form isovalent species; the comproportionation constant of the $V^{III}V^{IV}$ complex, in contrast with that of $[V_2O_3(pmida)_2]^-$ (10^{24}), is only 0.15 ± 0.04. Kinetic studies of the reaction of aqueous V^{II} and V^{IV} ions provide evidence for the formation of a brown intermediate prior to electron transfer and concomitant formation of V^{III} [61]. Originally described as the hydrolytic dimer of V^{III}, $[V_2O(aq)]^{4+}$, this complex is thought to be a valence-trapped $V^{II}V^{IV}$ species. Similar intermediates have been observed in related studies. Thus the cross-reaction of $[V(hedta)]^-$ and $[VO(hedta)]^-$ forms a detectable red $V^{II}V^{IV}$ species which undergoes a ligand rearrangement controlled intramolecular electron transfer process to form $[V_2^{III}O(hedta)_2]^{2-}$ [62,63]. A corresponding intermediate is also formed in the edta system [62]. These intermediates are unusually long lived in comparison with other inner-sphere electron transfer intermediates.

Ferricenium oxidation of $V_2(\eta^5 : \eta^5\text{-}C_{10}H_8)_2$ ($C_{10}H_8$ = fulvalene) results in the formation of the deep purple $V^{II}V^{III}$ complex $[V_2(\eta^5 : \eta^5\text{-}C_{10}H_8)_2]^+$ which has been isolated as the PF_6^- salt (**20**) [64]. In an analogous manner, brown $[V_2(\eta^5 : \eta^5\text{-}C_{10}H_8)_2(CO)_2]PF_6$ (**21**) may be prepared from $V_2(\eta^5 : \eta^5\text{-}C_{10}H_8)_2(CO)_2$. Magnetic susceptibility studies indicate that both compounds possess one unpaired electron, but whereas **21** exhibits spin-only behaviour, **20** exhibits behaviour consistent with intermolecular antiferromagnetic coupling in the solid state. In solution, **20** exhibits an eight-line ESR spectrum ($g = 1.978$, $A = 50$ G) indicative of a trapped-valence species while the solid state ESR spectrum of **21** ($g = 2.007$) exhibits no informative hyperfine structure. Other dinuclear $V^{II}V^{III}$ complexes have been reported but remain poorly characterized [65,66].

Extending earlier work by Calderazzo and Bacciarelli [67], Osborne et al. [68] prepared the $V^{-I}V^{III}$ μ_2-η^2-carbonyl complex, $Cp_2^*V(\mu\text{-}CO)V(CO)_5$, via the reaction of Cp_2^*V and $V(CO)_6$ in pentane. The structure of the complex

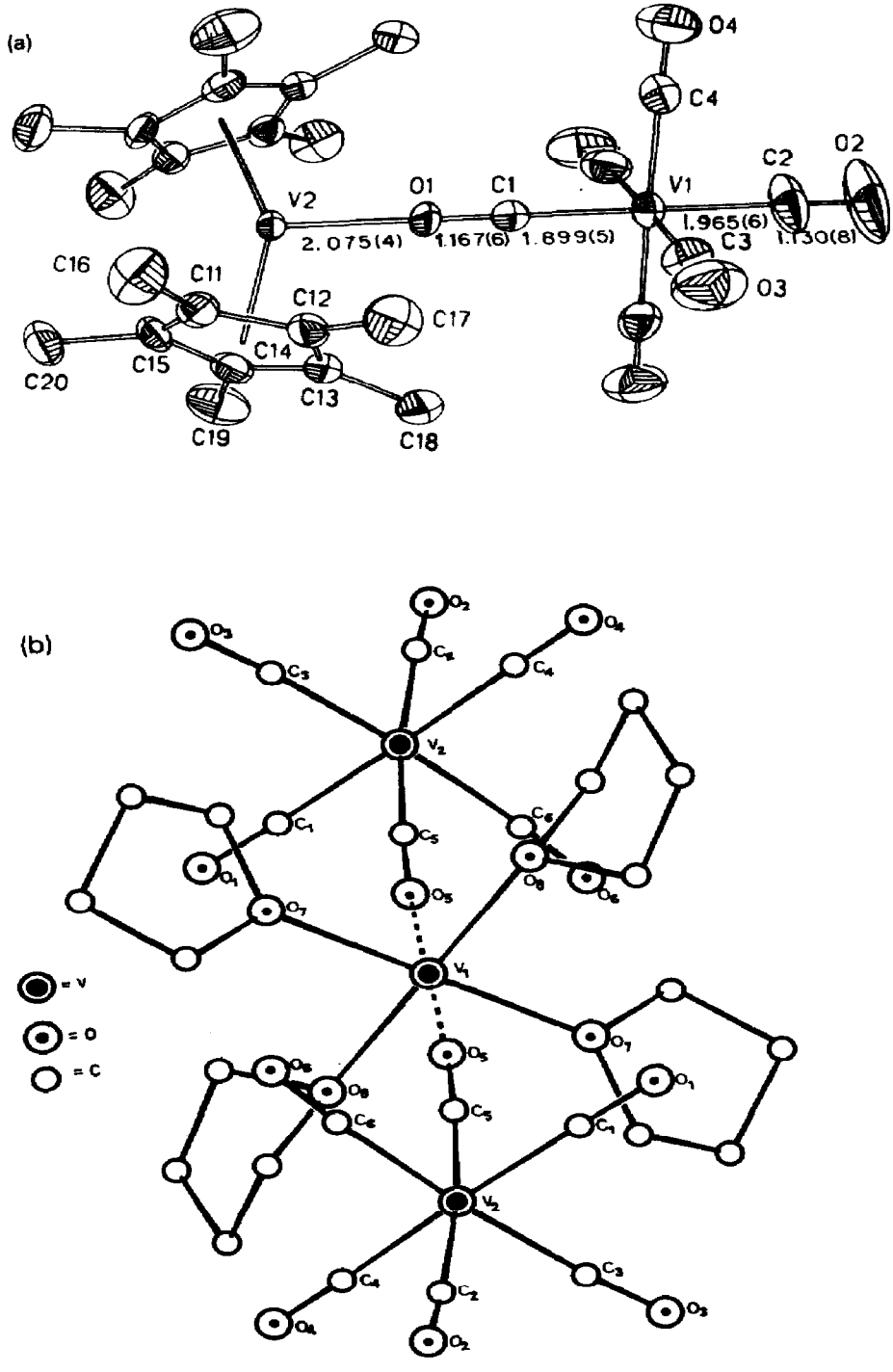

Fig. 9. Structures of μ_2-η^2-carbonyl complexes of vanadium. (a) $Cp^*_2V(\mu\text{-}CO)V(CO)_5$. Reproduced with permission from ref. 68. (b) $[V(thf)_4][V(CO)_6]_2$. Reproduced with permission from ref. 76.

is shown in Fig. 9(a). The molecule possesses a linear V–C–O–V bond with V–O = 2.075(4) Å, C–O = 1.167(6) Å and V–C = 1.899(5) Å. The other structural parameters are consistent with a predominantly ionic interaction of $[Cp_2^*V]^+$ and $[V(CO)_6]^-$ moieties. However, molecular orbital calculations suggest a small covalent π back-donation from a t_{2g} orbital on $[V(CO)_6]^-$ into a partially occupied π orbital on the $[Cp_2^*V]^+$ fragment. Support for the presence of a V^{III} (d^2) centre and a diamagnetic V^{-I} (d^6) centre is provided by magnetic susceptibility data which reveal the presence of two unpaired electrons. Related $V_2^{-I}V^{II}$ complexes are discussed in Section C(i)(c).

(c) Trinuclear compounds

A number of transition metals from trinuclear oxo-centred basic carboxylate complexes with the general structure shown in Fig. 10. Both isovalent M^{III} and mixed-valence $M^{II}M_2^{III}$ complexes are known for vanadium, chromium, tungsten and manganese. Following earlier reports of compounds variously formulated as $V_3(OH)(OAc)_8$, $H[V_3O(OAc)_8]$ and $[V_3O(OAc)_7(HOAc)]_n$ [69–71], the complexes $[V_3(\mu_3\text{-}O)(OAc)_6(HOAc)_2(thf)]^+$ and $V_3(\mu_3\text{-}O)(O_2CCF_3)_6(thf)_3$ (**22**) were reported by Cotton et al. [72]. Dark green **22** was isolated upon work-up of the reaction of $VCl_2 \cdot 2thf$

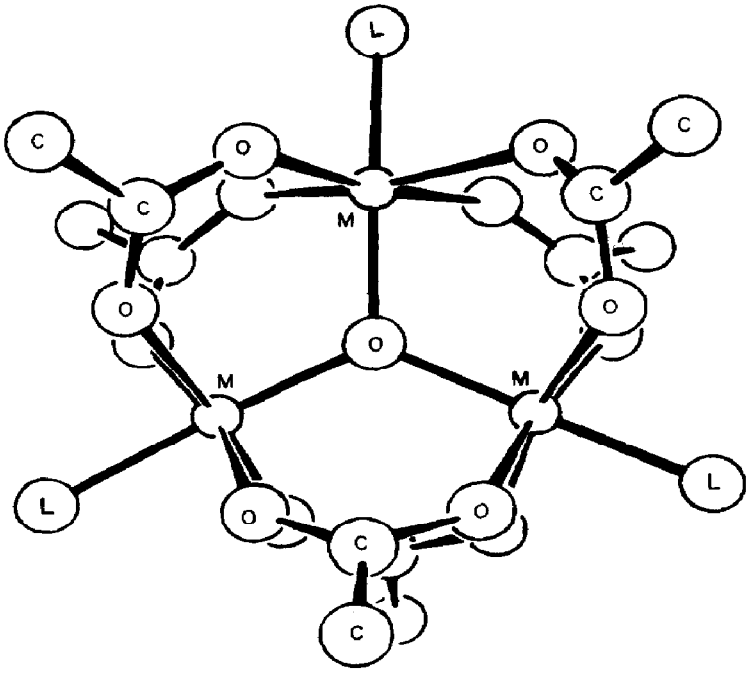

Fig. 10. General structure of oxo-centred basic metal carboxylates of formula $[M_3(\mu\text{-}O)(O_2CR)_6L_3]^{n+}$. Reproduced with permission from ref. 72.

and CF_3CO_2Na in CH_2Cl_2–thf (3 : 1 v/v). There is no structural evidence for valence localization in this $V^{II}V_2^{III}$ complex. Indeed, the question of what factors are important in determining the character (localized or delocalized) of such mixed-valence species remains unresolved. For the related cationic complex, structural evidence suggests that the three non-bridging ligands are neutral and a V_3^{III} formulation is assigned accordingly. Related mixed-valence complexes of chromium, tungsten and manganese are discussed in Section D(i)(c), Section D(iii)(c) and Section E(i)(c) respectively.

Several carbonyl–V complexes form as a result of the disproportionation of $V(CO)_6$ in the presence of hard Lewis bases (eqn. (4), B = base) [73]:

$$3V(CO)_6 + 6B \rightarrow [VB_6]^{2+} + 2[V(CO)_6]^- + 6CO \quad (4)$$

Salts of the type $[VB_6][V(CO)_6]_2$ are commonly formed by this reaction but isocarbonyl-bridged compounds have also been isolated and characterized. For example, the reaction of $V(CO)_6$ and base in benzene results in the formation of $[VB_4][V(CO)_6]_2$ (B = thf, acetone, picoline, MeCN) [74,75]. The presence of linear μ_2-η^2-carbonyl ligands in the thf derivative has been recently demonstrated by X-ray crystallography [76]. The structure of $[V(thf)_4][V(CO)_6]_2$ (Fig. 9(b)) reveals that the V^{II} atoms of the $V(thf)_4$ moiety are coordinated by the oxygen atoms of carbonyl ligands on adjacent V^{-I} atoms as well as by those of the four thf ligands [76]. A near-linear V–C–O–V group is formed wherein the V–O(CO) distances (2.079 Å) are shorter than the V–O(thf) distances (2.170 Å).

(d) Tetranuclear compounds

Green $Cp_2VI(NO)$ is slowly converted to golden–brown $Cp_4V_4I_2(NO)_2(\mu\text{-}O)_4$ in thf solution [77]. The eight-membered V_4O_4 ring in this compound is non-planar and each vanadium atom is coordinated to a cyclopentadienyl ligand. Two pairs of different vanadium centres are distinguished by coordination to either a nitrosyl or iodo ligand. The mechanism of formation of the complex and the actual oxidation states of the various metal atoms remain obscure.

(e) Pentanuclear compounds

A variety of cyclopentadienyloxovanadium complexes have been prepared by Bottomley and coworkers [78–81]. Black $Cp_5V_5(\mu_3\text{-}O)_6$ (**23**), formed in the reaction of VCp_2 and N_2O at −78 °C, possesses a structure similar to that of $Cp_5Ti_5(\mu_3\text{-}S)_6$ (Fig. 4(a)) [78,79]. A trigonal bipyramidal arrangement of vanadium atoms is observed; each vanadium atom is capped by a Cp ring and each face of the polyhedron is capped by an oxygen atom. The oxygen atoms lie 1.128 Å above the triangular faces and are displaced 0.29 Å from the centre of the face towards the axial vanadium atoms (V_{ax}–O =

1.861(5) Å, V_{eq}–O = 1.992(6) Å) and the V_{ax}–Cp bonds are significantly longer than the V_{eq}–Cp bonds. These differences are interpreted in terms of localized V^{IV} and V^{III} centres at axial and equatorial positions respectively. A weak interaction of the V^{IV} centres is the possible cause of the low magnetic moment of the complex (0.93 BM). Recently, the sulphur analogue, $(MeCp)_5V_5S_6$, and the X-ray structure of a derivative, $[(MeCp)_5V_5S_6]$-$(TCNQ)_2$, were reported [82]; a trigonal bipyramidal structure, related to that of **23**, was observed. These complexes are the second members of the series $Cp_mM_mO_n$, where m and n satisfy Euler's theorem. Related compounds, derived from $Cp_6V_6(\mu_3\text{-}O)_8$ display a remarkable structural diversity [79–81]. The electronic structures of the $Cp_5V_5O_6$ and $Cp_6V_6O_8$ complexes and their derivatives have been explored using theoretical calculations [36].

(f) High nuclearity compounds

Attempts to prepare $[V_2O_3]^{3+}$ complexes of bdta yielded the novel nonanuclear compound, $K_7[V_9O_{16}(bdta)_4] \cdot 27H_2O$ [59]. The $[V_9O_{16}(bdta)_4]^{7-}$ anion, shown in Fig. 11, is composed of four dinuclear $V^{IV}V^{V}$ units linked via oxygen bridges to a central $[VO_4]^{3-}$ tetrahedron. While maintaining the common *anti*-planar $[V_2O_3]^{3+}$ core structure (see Fig. 6(c)) the mixed-valence arms possess inequivalent vanadium centres. Structural parameters (e.g. V(1)–O(7) and V(3)–O(8) ca. 1.70 Å vs. V(2)–O(7) and V(4)–O(8) ca. 1.91 Å) suggest that the proximal and distal (to V(5)) vanadium atoms

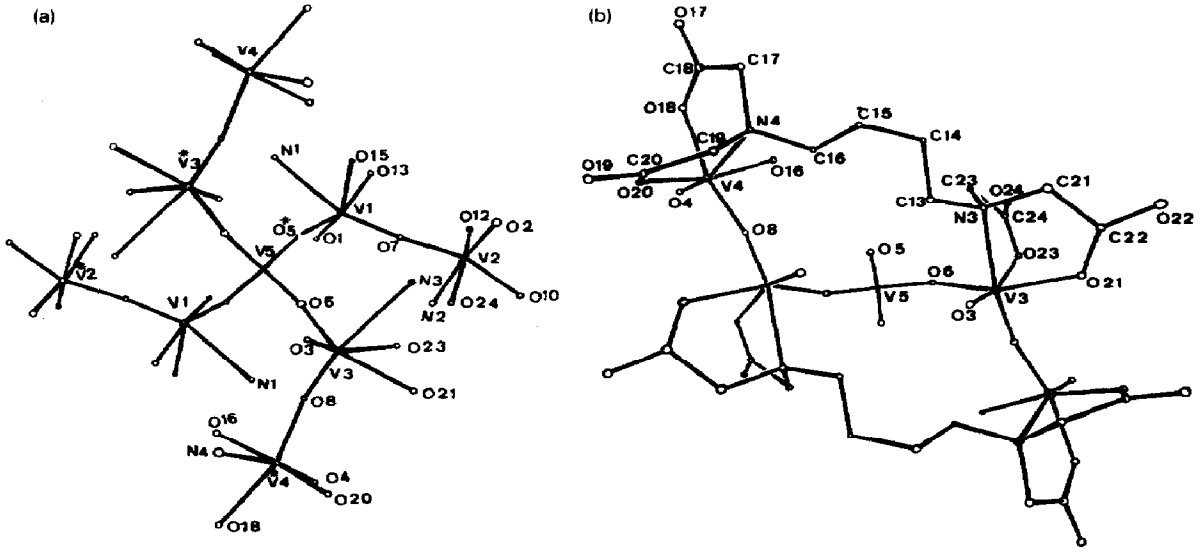

Fig. 11. Structure of the $[V_9O_{16}(bdta)_4]^{7-}$ anion: (a) the arrangement of the V^{IV} V^{V} pairs about the central tetrahedral V^{V} atom; (b) the coordination mode of two of the $bdta^{4-}$ ligands. Reproduced with permission from ref. 59.

possess more V^{V} and V^{IV} character respectively. The intervalence CT band is split into two components (900 nm, 1020 nm, shoulder).

High valent vanadium chemistry is dominated by the formation of oxo complexes, particularly isopolyvanadates and heteropolyvanadates. Many mixed-valence compounds of vanadium, some derived from the direct reduction of vanadates, possess infinite solid state structures which have no independent existence in solution. A number of interesting mixed-valence polyvanadic acid gels are also formed by the polymerization of decavanadic acid [83]. However, several discrete mixed-valence isopolyvanadate ions have been described. In 1964, Ostrowetsky reported that a number of species formed in solutions containing V^{IV} and V^{V} [84]. At $8 \leqslant pH \leqslant 10$ ill-defined $(V_2^{IV}V^{V})_n$ species were postulated to form and a solid formulated as $Na_3[V_6O_{15}H]$ was isolated. At lower pH a variety of decanuclear $V_3^{IV}V_7^{V}$ and $V_7^{IV}V_3^{V}$ complexes, postulated to form via a $V_2^{IV}V_8^{V}$ complex, were observed. A $V_2^{IV}V_8^{V}$ complex has subsequently been characterized. Deep violet $(NEt_4)_4[V_{10}O_{26}] \cdot H_2O$ (**24**), formed by the hydrolytic dissociation of $VO(acac)_2$ in the presence of NEt_4Cl, was first reported in 1968 [85]. At that time the compound was incorrectly formulated as $(NEt_4)[V_{10}O_{28}H_4]$ on the basis of redox titrations, electronic, IR and ESR spectroscopic and magnetic studies. The electronic spectrum of the compound exhibits a very broad and intense band at ca. 500 nm, assigned to an intervalence CT and a 15-line ESR spectrum consistent with the interaction of the unpaired electrons with two equivalent ^{51}V nuclei. The true stoichiometry of the compound and its novel structure was revealed by a recent crystallographic study [86]. As shown in Fig. 12(a), the anion in **24** is composed of a crown of eight vertex-shared tetrahedral VO_4 units capped above and below by two vanadium atoms with tetragonal pyramidal geometries [V(1) and V(6)]. The tetrahedral and pyramidal units have V–O distances typical of V^{V} and V^{IV} centres respectively. The average V–V distances are as follows: V^{V}–V^{V}, 3.25 Å; V^{V}–V^{IV}, 3.59 Å; V^{IV}–V^{IV}, 4.44 Å. The distance between the V^{IV} atoms is similar to that found in other binuclear V^{IV} complexes which exhibit electron coupling. A related compound, formulated as $(NEt_4)_4[V_{10}O_{26}F_2H_2]$ and having spectroscopic properties similar to those of **24**, was reported in 1969 [87] but the true stoichiometry and structure of this compound remains unknown.

The reduction of V^{V} with S^{2-} and rapid exchange of oxygen for sulphur takes place in hot aqueous solutions of $[VS_4]^{3-}$. In the presence of added NMe_4Cl, these reactions lead to the precipitation of the brown pentadecanuclear $V_8^{IV}V_7^{V}$ compound $(NMe_4)_6[V_{15}O_{36}]Cl \cdot 4H_2O$ (**25**) [88]. The structure of the anion in **25** is shown in Fig. 12(b). The complex is composed of 15 tetragonal VO_5 pyramids linked to form a spheroidal D_{3h} molecule. The vanadium atoms reside on the surface of a sphere of radius 3.45 ± 0.1 Å

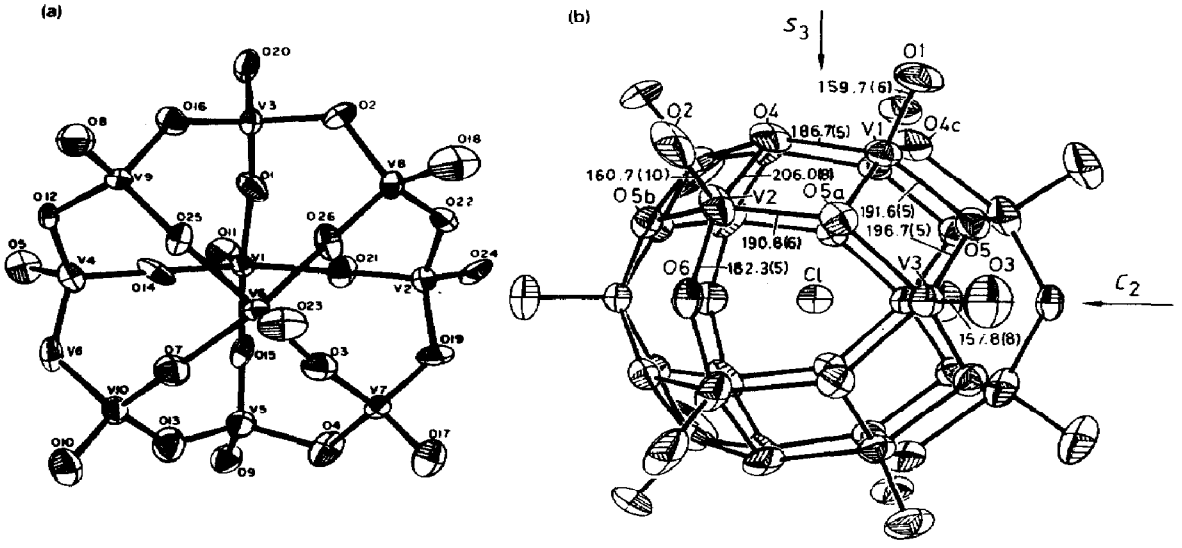

Fig. 12. (a) Structure of the $[V_{10}O_{26}]^{4-}$ anion in **24**. Reproduced with permission from ref. 86. (b) Structure of the $[V_{15}O_{36}]^{5-}$ anion with entrapped Cl^- ion in **25**. Other distances include $V_1-V_2 = 2.933(2)$ Å, $V_1-V_3 = 3.000(2)$ Å. Reproduced with permission from ref. 88.

centred around the encapsulated chloride ion. The compound was further characterized by elemental and thermal analysis, IR spectroscopy and magnetic measurements ($\mu_{eff} = 3.9$ BM). According to an earlier report [89], homogeneous acidification of $[VS_4]^{3-}$ solutions results in the formation of $Na_6V_8^{IV}V_2^{V}O_{24} \cdot 8H_2O$, $K_6V_8^{IV}V_2^{V}O_{24} \cdot 5H_2O$ and $(NH_4)_4V_3O_8 \cdot 0.5H_2O$.

Even larger polyanions may be precipitated from the intensely coloured solutions obtained by mixing V^{IV} and V^{V} in acidic solution [90]. Blue–violet anions with variable composition ($V^{IV}:V^{V} = 5:14$–$7:12$) possess nuclearities of 19! This is consistent with the X-ray structure of $K_8[V_{19}O_{40}H] \cdot 11H_2O$, which revealed the existence of discrete $[V_{19}O_{40}H]^{8-}$ ions composed of 18 VO_n polyhedra surrounding a central VO_4 tetrahedron. Analysis of the V–O distances aided the location of the six valence-trapped V^{IV} atoms and the hydrogen atom. The positions of the V^{IV} atoms and the paramagnetism of the compound indicate pairing of four spins in two proximate $V^{IV}-V^{IV}$ pairs while the other two V^{IV} centres are isolated and paramagnetic. The structure of $[V_{19}O_{40}H]^{8-}$ resembles that published [91] for the anion in $K_{12}[V_{18}O_{42}] \cdot 15$–$16H_2O$, except that the cavity within the vanadium skeleton is occupied by the VO_4 unit rather than H_2O or K^+. Some of the species reported by Ostrowetsky [84] may have related compositions and structures.

It is interesting to note that mixed-valence and magnetically coupled vanadate domains have been observed in heteropolytungstate anions which have Keggin [92] and Dawson [93] structures. In the Dawson-type anion

$[P_2W_{15}V^{IV}V_2^{V}O_{62}]^{10-}$ the degree of electron delocalization is temperature dependent; ESR spectra at 350 K are consistent with rapid (greater than 10^8) intramolecular electron hopping among three equivalent ^{51}V nuclei, while spectra at 5 K indicate electron trapping on a single vanadium centre. Further discussion of isopolyanions and heteropolyanions may be found in recent reviews by Pope [94,95].

(ii) Niobium compounds

(a) General survey

Niobium as well as tantalum exhibit a strong tendency to form metal–metal bonds in compounds of low oxidation state, and both elements display a rich cluster chemistry as a result of this behaviour. As a consequence the mixed-valence chemistry of these elements differs markedly from that of their first row congener. With few exceptions, mixed-valence compounds of niobium are either trinuclear or hexanuclear and possess strong metal–metal bonds. To date, known dinuclear compounds are restricted to the $Nb^{III}Nb^{IV}$ complexes $Cp_4Nb_2Cl_3$ and $[Cp_4Nb_2Cl_2]^+$. Triangular clusters of the type shown in Fig. 13 are a feature of all but one of the known trinuclear niobium complexes. The mixed-valence binary halides of niobium are composed of triangles of niobium atoms linked by intercluster halides and their extended solid state structure precludes them from discussion. A number of trinuclear bi-oxocapped trinuclear clusters of the type $[Nb_3(\mu_3\text{-}O)_2(O_2Y)_6L_3]^{n\pm}$ (Fig. 13(a)), formally $Nb^{III}Nb_2^{IV}$ complexes with an average oxidation state of $3\frac{2}{3}$, have been reported. The first of these, $[Nb_3(\mu_3\text{-}O)_2(SO_4)_6(H_2O)_3]^{5-}$, was reported as early as 1912 but was only recently structurally characterized. This spurred further work which resulted in the characterization of related $[Nb_3(\mu_3\text{-}O)_2(O_2CR)_6L_3]^+$ complexes. Recently, the characterization of $[Nb_3(\mu_3\text{-}S)(\mu\text{-}O)_3(NCS)_9]^{6-}$ and $Nb_3(\mu_3\text{-}CNBu^t)(\mu\text{-}Cl)_3Cl_5(CN^tBu)_4$ has provided evidence for the formation of complexes containing the $[Nb_3(\mu_3\text{-}X)(\mu\text{-}Y)_3]^{n\pm}$ core (Fig. 13(b)). The latter complex possesses an average oxidation state of $2\frac{2}{3}$. In still lower oxidation states a remarkable series of $[Nb_3(\mu\text{-}Cl)_6(C_6Me_6)_3]^{n+}$ ($n = 1$–4) complexes (Fig. 13(c)) are known to exist. Only one tetranuclear compound, the $Nb_2^{III}Nb_2^{IV}$ complex $Nb_4Br_{10}(Se)(Se_2)(MeCN)_4$, has been reported. The hexanuclear cluster halides form the largest class of mixed-valence niobium compounds. These compounds are based on the cluster cores shown in Fig. 14. Complexes of the type $[Nb_6(\mu\text{-}X)_{12}]^{n+}$ (X = Cl, Br; $n = 2$, 3, 4) are composed of an octahedron of niobium atoms, the edges of which are bridged by μ-X ligands while other ligands coordinate each metal atom (Fig. 14(a)). Complexes of the type $[Nb_6(\mu_3\text{-}X)_8]^{n+}$ (X = I; $n = 0$, 2, 3) are composed of an octahedron of niobium atoms, the faces of which are capped by μ_3-X ligands

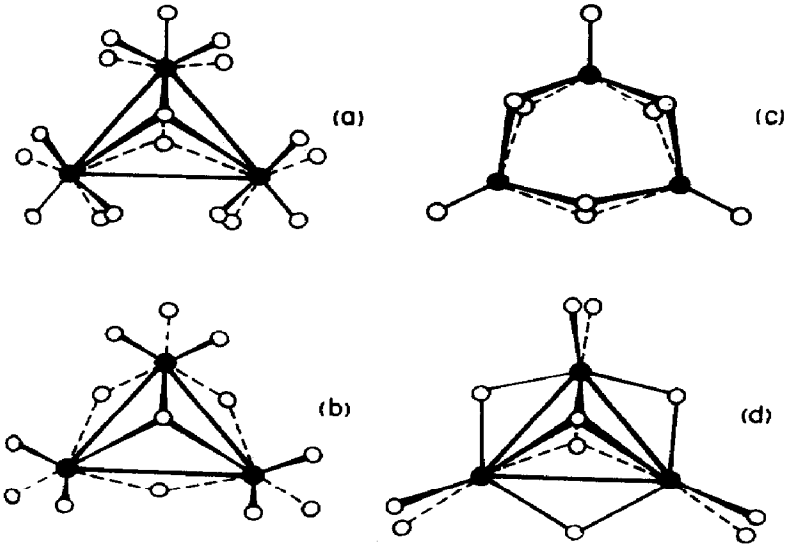

Fig. 13. General structures of triangular trinuclear metal complexes. For many complexes empty circles represent the donor atoms of edge-bridging bidentate ligands.

arranged in a cubic array (Fig. 14(b)). Other ligands are coordinated to each metal atom. These compounds contain tightly bound clusters, with Nb–Nb distances close to those in the metal itself. While many of the binary halides exhibit extended solid state structures, a large number of discrete hexanuclear derivatives have been prepared and characterized. The chemistry of the hexanuclear cluster compounds of niobium and tantalum has been extensively reviewed [43,96–101]. Structural studies were recently reviewed by Holloway and Melnik [102].

Properties of selected mixed-valence compounds of niobium are summarized in Table 3.

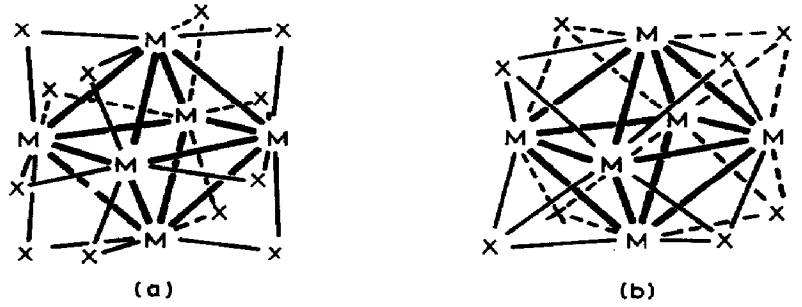

Fig. 14. The two octahedral cluster cores observed in hexanuclear complexes: (a) the $[M_6(\mu\text{-}X)_{12}]^{n+}$ core and (b) the $[M_6(\mu_3\text{-}X)_8]^{n+}$ core. In discrete complexes, the metal atoms are further coordinated by a terminal ligand.

TABLE 3

Properties of selected mixed-valence compounds of niobium

Compound	Nb oxidation state		Structure	Nb...Nb distance [a] (Å)	Magnetic properties	Ref.
	Formal	Average				
$Cp_4Nb_2Cl_3$	III, IV	3.5	–	–	$\mu = 1.81$ BM (293 K)	103
$K_4(H_5O_2)[Nb_3(\mu_3\text{-}O)_2(SO_4)_6(H_2O)_3]$	III, IV_2	$3\frac{2}{3}$	Fig. 13(a)	1–2, 2.875(1) 1–3, 2.889(1) 2–3, 2.892(1)	–	108–117
$[Nb_3(\mu_3\text{-}O)_2(O_2C^tBu)_6(thf)_3]BPh_4$	III, IV_2	$3\frac{2}{3}$	Fig. 13(a)	1–2, 2.834(1) 1–3, 2.855(1) 2–3, 2.838(1)	$\mu = 1.3$ BM (293 K) No ESR signal at 77 K	117, 119
$[Nb_3(\mu_3\text{-}O)_2(OAc)_6(thf)_3][NbOCl_4(thf)]$	III, IV_2	$3\frac{2}{3}$	Fig. 13(a)	av. 2.843(3)	–	117
$(NH_4)_3(NMe_4)_3[Nb_3(\mu_3\text{-}S)(\mu\text{-}O)_3(NCS)_9]$	III, IV_2	$3\frac{2}{3}$	Fig. 13(b)	av. 2.763(3)	–	117
$Sm[Nb_3Cl_{14}]$	III, IV_2	$3\frac{2}{3}$	**26** or **27**	3.042(9)	$\mu = 1.60$ BM (281.9 K)	120
$Nb_3Cl_8(^tBuNC)_5$	II, III_2	$2\frac{2}{3}$	Fig. 15	1–2, 2.875(1) 1–3, 3.220(1) 2–3, 3.207(1)	ESR, decet $g = 1.95$, $A(^{93}Nb) = 130$ G	123, 125
$[Nb_3(\mu\text{-}Cl)_6(C_6Me_6)_3](TCNQ)_2$	II, III_2	$2\frac{2}{3}$	Fig. 13(c)	1–2, 3.327(2) 2–3, 3.344(3)	ESR (solid) broad, isotropic, $g = 1.996$	130
$[Nb_3(\mu\text{-}Cl)_6(C_6Me_6)_3]Cl$	II_2, III	$2\frac{1}{3}$	Fig. 13(c)	–	–	129
$Nb_3(\mu_3\text{-}Cl)(\mu\text{-}Cl)_3Cl_3(PMe_2Ph)_6$	II_2, III	$2\frac{1}{3}$	Fig. 13(b)	2.831(3)	Diamagnetic	133
$Nb_4Br_{10}(Se)(Se_2)(MeCN)_4$	III_2, IV_2	3.5	Fig. 16	1–1′, 2.886(1)	Diamagnetic	134
$K_4[Nb_6Br_{18}]$	–	$2\frac{2}{3}$	Fig. 14(a)	2.968(3) –2.975(1)	–	138
$Nb_6I_8(NH_2Me)_6$	–	$1\frac{1}{3}$	Fig. 14(b)	2.695(5) –2.870(4)	Diamagnetic	143

[a] Where more than one distance is quoted the preceeding numbers identify the atoms involved, e.g. when prefixed by 1–2, the distance given is between Nb(1) and Nb(2).

(b) Dinuclear compounds

Only two dinuclear mixed-valence compounds of niobium are known to exist. Reduction of Cp_2NbCl_2 to Cp_2NbCl proceeds via the purple $Nb^{III}Nb^{IV}$ compound $Cp_4Nb_2Cl_3$, which may be independently prepared by mixing solutions of the first two mentioned compounds [103]. It is proposed that the compound possesses a single μ-Cl ligand which links Cp_2NbCl units. The cation $[Cp_4Nb_2Cl_2]^+$, prepared by chloride abstraction from $Cp_4Nb_2Cl_3$, is proposed to possess a di-μ-Cl bridge. Detailed electrochemical studies of the reduction of Cp_2NbCl_2 also reveal the formation of $Cp_4Nb_2Cl_3$ and other mixed-valence species such as $[Cp_4Nb_2Cl_2]^-$ [104].

Other postulated dinuclear complexes have been disproved or remain to be thoroughly characterized. Matsuda et al. [105] postulated the formation of an $Nb^{IV}Nb^{V}$ complex upon photochemical reduction of $[(TpTP)Nb]_2(\mu\text{-}O)_3$ but this claim was subsequently disproved by Anderson et al. [106]. Spectrophotochemical studies revealed that the reduced and oxidized forms of $[(TpTP)Nb]_2O_3$ and $[(OEP)Nb]_2O_3$ do exhibit ESR signals typical of Nb^{IV} but these signals were due to monomeric species produced by chemical reactions accompanying photochemical reduction. Reaction of $KNb(SO_4)_2 \cdot 4H_2O$ with phosphoric acid in aqueous H_2SO_4 solution results in the formation of a red–brown solid after neutralization with Na_2CO_3. Analysis and redox titrations indicate the formulation of $Nb^{V}O[Nb^{III}(PO_4)_2] \cdot 6H_2O$ but the structure and nuclearity of the compound remain unknown [107].

(c) Trinuclear compounds

The $[Nb_3(\mu_3\text{-}O)_2(\mu\text{-}SO_4)_6(H_2O)_3]^{5-}$ complex has a long history which reaches back to early attempts to separate and characterize niobium (then columbium) and tantalum. The red–brown anion was first prepared by Ott [108] by the electrochemical reduction of $NbCl_5$ in concentrated sulphuric acid. Ott, who believed the complex to contain Nb^{III}, formulated the ammonium salt as $(NH_4)_2SO_4 \cdot Nb_2(SO_4)_3 \cdot H_2SO_4 \cdot 6H_2O$. Formulations such as $4K_2O \cdot Nb_2O_5 \cdot 2Nb_2O_3 \cdot 12H_2SO_4 \cdot 12H_2O$ and $4K_2O \cdot Nb_2O_5 \cdot 2Nb_2O_3 \cdot 13H_2SO_4 \cdot 16H_2O$ were later assigned to the potassium salt [109–111]. Subsequent investigations of this system were carried out by Golibersuch and Young [112] and Russian workers [113,114]. Golibersuch and Young [112] established that upon completion of the electrolytic reduction the niobium had attained an oxidation state of 3.7 and they isolated alkali metal salts containing niobium in the same oxidation state (3.68 ± 0.02). Further, their analytical and conductimetric data indicated formulations such as $K_4Nb_3(OH)_3(SO_4)_6 \cdot 9H_2O$ or $K_8Nb_6O_3(SO_4)_{12} \cdot 21H_2O$. The Russian workers [113,114] proposed a hexanuclear structure, formulating the ammonium salt as $(NH_4)_8[Nb_6O_3(SO_4)_{12}] \cdot xH_2O$. In 1980, Bino [115,116] reported the X-ray structure of the potassium salt and established the

correct formula as trinuclear $K_4(H_5O_2)[Nb_3(\mu_3\text{-}O)_2(\mu\text{-}SO_4)_6(H_2O)_3] \cdot 5H_2O$. Later, Cotton and coworkers [117,118] reported the isolation and X-ray structure of $(NH_4)_3(H_3O)_2[Nb_3(\mu_3\text{-}O)_2(SO_4)_6(H_2O)_3] \cdot 3H_2O$, formed by the reaction of $Nb_2Cl_6(thf)_3$ with 40–70% H_2SO_4 in thf followed by precipitation with $(NH_4)_2SO_4$. The anion exhibits the typical $[M_3(\mu_3\text{-}X)_2(O_2Y)_6L_3]^{n\pm}$ structure depicted in Fig. 13(a). The $[Nb_3(\mu_3\text{-}O)_2(\mu\text{-}SO_4)_6(H_2O)_3]^{5-}$ molecule has virtual D_{3h} symmetry and a trigonal bipyramidal $[Nb_3O_2]^{17+}$ core with oxygen atoms above and below a triangle of niobium atoms. Two sulphate ligands bridge each edge of the triangle and three water molecules complete the niobium coordination spheres. The average Nb–Nb and Nb–μ_3-O bond distances are 2.886(1) Å and 2.052(9) Å respectively. The charge on the cluster indicates an average oxidation state of $3\frac{2}{3}$ in agreement with the results of the redox titrations performed by Golibersuch and Young [112]. The complex possesses four core valence electrons, giving rise to an Nb–Nb bond order of 2/3, which is consistent with the Nb–Nb distance reported above. An intermediate green complex observed in the syntheses [112,118] has been tentatively assigned as $[Nb_3(\mu_3\text{-}O)_2(\mu\text{-}SO_4)_6(H_2O)_3]^{6-}$ [118]. Mixed-valence molybdenum and tungsten complexes of this general type are also known (Sections D(ii)(c) and D(iii)(c)).

Cotton et al. [117,119] have reported further examples of $[Nb_3(\mu_3\text{-}O)_2(O_2Y)_6L_3]^{n\pm}$ complexes. The reaction of $Nb_2Cl_6(SMe_2)_3$ with sodium carboxylates in benzene–thf results in the formation of red complexes $[Nb_3(\mu_3\text{-}O)_2(O_2CR)_6(H_2O)_3]^+$ (R = Ph, 'Bu) [119]. The first cation was isolated as the $[NbOCl_4(thf)]^-$ salt and remains incompletely characterized. The second cation has been fully characterized as the BPh_4^- salt. The structure of the $[Nb_3(\mu_3\text{-}O)_2(O_2C'Bu)_6(thf)_3]^+$ cation is shown in Fig. 13(a); it consists of a trigonal bipyramidal $[Nb_3O_2]^{7+}$ core with oxygen atoms 1.204(1) Å above and below a triangle of niobium atoms. Two $'BuCO_2^-$ ligands bridge each edge of the triangle and three thf molecules complete the niobium coordination spheres. An analogous cation structure was reported for $[Nb_3(\mu_3\text{-}O)_2(OAc)_6(thf)_3][NbOCl_4(thf)]$ prepared by the reaction of $Nb_2Cl_6(tht)_3$ and acetic acid–acetic anhydride (1 : 1 v/v). The mean Nb–Nb distance in this case was 2.843(3) Å [117].

Evidence for the formation of $[Nb_3(\mu_3\text{-}X)(\mu\text{-}Y)_3L_9]^{n\pm}$ compounds has also been provided by Cotton's group [117]. Chromatographic work-up of the reaction of $Nb_2Cl_6(tht)_3$ and aqueous HCl afforded a green cation proposed to be $[Nb_3O_4(H_2O)_9]^{n+}$ or an oxo–Nb^{III} complex. Reaction of the green complex with NH_4NCS and NMe_4Br in methanol yielded black crystals of $(NH_4)_3(NMe_4)_3[Nb_3(\mu_3\text{-}S)(\mu\text{-}O)_3(NCS)_9] \cdot MeOH$, which were characterized by X-ray crystallography. The anion exhibits the structure shown in Fig. 13(b).

The air- and water-sensitive $Nb^{III}Nb_2^{IV}$ compound, $Sm[Nb_3Cl_{14}]$, is formed when a toluene solution of $NbCl_5$ is reacted with a slurry of samarium metal in methylcyclohexane [120]. The temperature-dependent magnetism of the compound is due entirely to Sm^{3+} and thus the $[Nb_3Cl_{14}]^{3-}$ anion contains no unpaired electrons. The structure of the compound has been probed using EXAFS spectroscopy, which gives Nb–Cl(terminal), Nb–Cl(bridge) and Nb–Nb distances of 2.324(8) Å, 2.552(25) Å and 3.042(9) Å respectively. The EXAFS data are consistent with both structures **26** and **27**, which correspond to the formulations $Sm[Nb_3Cl_{14}]$ and $Sm[Nb_3Cl_{12}]Cl_2$ respectively. A triangular $[Nb_3Cl_{12}]^-$ cluster was discounted on account of the very

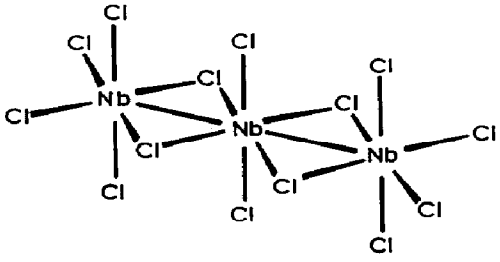

26

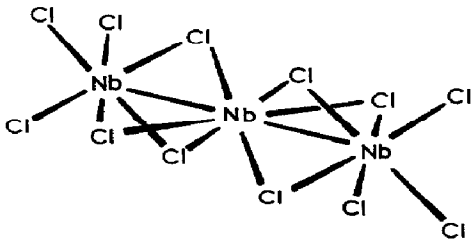

27

short Nb–Nb distance. The central d^2 Nb^{III} atom is proposed to form $\sigma^2\pi^2$ metal–metal bonds with the terminal d^1 Nb^{IV} atoms, accounting for the diamagnetism of the anion. The linear structures contrast with the triangular Nb_3-core structures observed for all other trinuclear niobium compounds. It is also possible that this compound exhibits an extended structure in the solid state. Blue $Nb_3Cl_8(SMe_2)_2(OEt_2)$ is reported to form from the reduction of $NbCl_5$ using magnesium metal in the presence of SMe_2. The compound is insoluble or decomposes upon dissolution and remains to be adequately characterized [121].

The reaction of $CpNb(CO)_3(PPh_3)$ with anhydrous HCOOH in boiling xylene produces the black trinuclear compound $[CpNb(O_2CH)]_3(\mu_3\text{-}O)(\mu\text{-}O)(\mu\text{-}OH)_2$ [122]. The compound has been characterized by elemental analysis, IR spectroscopy, magnetic susceptibility studies and X-ray crystallography. The compound is formulated as an Nb^{IV} compound, primarily on the basis of its magnetic properties, but mixed-valence formulations cannot be discounted on the basis of analytical and crystallographic data.

A number of products are formed in the reaction of $Nb_2Cl_6(SMe_2)_3$ and ^{t}BuNC [123–125]; these include $Nb_3Cl_8(^t\text{BuNC})_5$ (**28**) and $Nb_2Cl_6(^t\text{BuNC})_6$ (**29**), the former being an $Nb^{II}Nb_2^{III}$ complex. The X-ray structure of the red–brown **28** is shown in Fig. 15 [123,125]. The niobium atoms in **28** define an isosceles triangle with a bridging chlorine atom below each edge and a

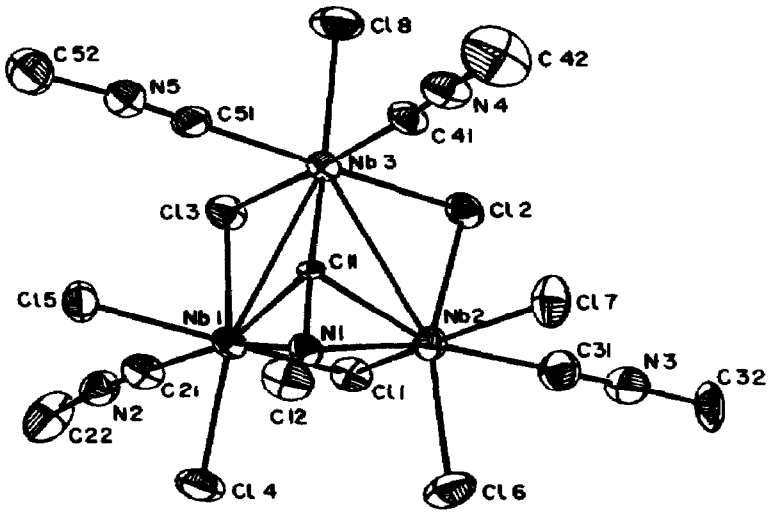

Fig. 15. The molecular structure of **28** drawn for clarity without the methyl groups of the 'BuNC ligands. Reproduced with permission from ref. 125.

multiply bridging isocyanide ligand above the Nb_3 triangle. The Nb(1)–Nb(2) distance (2.875(1) Å), which is indicative of a two-electron bond, is considerably shorter than the other two Nb–Nb distances (average, 3.213 Å). In solution, **28** exhibits a well-resolved ESR spectrum, a symmetrical decet (^{93}Nb, $I = 9/2$, $g = 1.95$, $A = 130$ G), indicative of a doublet ground state. While an unambiguous assignment of the oxidation states has not been possible, it is likely that the unpaired electron is localized on Nb(3), making it Nb^{II}, while the other niobium atoms are in oxidation state III. The Nb^{III} centres participate in a $\sigma^2\pi^2$ metal–metal bond.

Niobium forms a series of trinuclear $[Nb_3(\mu\text{-}Cl)_6(C_6Me_6)_3]^{n+}$ ($n = 1$–4) complexes. Green $[Nb_3Cl_6(C_6Me_6)_3]Cl$, first reported by Fischer and Röhrscheid [28], will be discussed before the oxidized forms. The compound was prepared by the reaction of $NbCl_5$ with C_6Me_6 in the presence of aluminium and $AlCl_3$. The analogous bromo complex was subsequently reported by King and coworkers [126,127] but is less stable towards hydrolysis than is the chloro compound. The trinuclear structure of $[Nb_3(\mu\text{-}Cl)_6(C_6Me_6)_3]^+$ was demonstrated by X-ray crystallography. The first determination, reported by Churchill and Chang [128], was of low precision ($R = 0.12$) owing to small crystal size and disorder. The trinuclear C_{3h} structure with Nb–Nb distances of 3.334(6) Å was consistent with an Nb–Nb bond order of 1/3. In keeping with an earlier postulate by King and coworkers [126,127] (vide infra), Churchill and Chang postulated that oxidation to the dication was accompanied by dimerization. Later, a high precision structure determination of $[Nb_3(\mu\text{-}Cl)_6(C_6Me_6)_3]Cl \cdot 3CHCl_3$ was re-

ported by Stollmaier and Thewalt [129]. The cation possesses a highly symmetrical D_{3h} structure (Fig. 13(c), where the terminal ligands are C_6Me_6) similar to that of the zirconium analogue (Fig. 5), with Nb–Nb and Nb–Cl distances of 3.347(4) Å and 2.504(2) Å respectively. The hexamethylbenzene rings are not planar. The $[Nb_3(\mu\text{-}Cl)_6(C_6Me_6)_3]^+$ complex is readily oxidized to analogous dications, trications and tetracations. The dication is formed upon oxidation with reagents such as Ce^{IV}, *N*-bromosuccinimide, iodine and oxygen [126,127]. Oxidation using $(NH_4)_2[Ce(NO_3)_6]$ results in the formation of water-soluble $[Nb_3(\mu\text{-}Cl)_6(C_6Me_6)_3][Ce(NO_3)_6]$ which may be converted to the insoluble BF_4^-, SCN^- and BPh_4^- salts. Analogous bromo complexes have been reported but are less stable. King and coworkers [126,127] reported that the complexes were diamagnetic and postulated that the oxidation of $[Nb_3(\mu\text{-}Cl)_6(C_6Me_6)_3]^+$ was accompanied by dimerization, leading to the hexanuclear cluster $[Nb_6Cl_{12}(C_6Me_6)_6]^{4+}$. The electrochemical reversibility observed for this oxidation was explained in terms of the slow rate of dimerization relative to the voltammetric time scale. The hexanuclear structure has been disproved by the X-ray structure of purple $[Nb_3(\mu\text{-}Cl)_6(C_6Me_6)_3](TCNQ)_2$ (**29**) which is formed when $[Nb_3(\mu\text{-}Cl)_6(C_6Me_6)_3]PF_6$, LiTCNQ and TCNQ are reacted together in hot MeCN [130]. Compound **29** is composed of an unusual zigzag array of trinuclear $[Nb_3(\mu\text{-}Cl)_6(C_6Me_6)_3]^{2+}$ cations and TCNQ anion dimers; the structure of the dication is the same as that observed for the monocation and its zirconium analogue (see Figs. 5 and 13(c)). The mean Nb–Nb distance is 3.335(9) Å and the hexamethylbenzene rings are bent. The compound is paramagnetic, and polycrystalline samples exhibit a broad nearly isotropic ESR signal at $g = 1.996$. The trinuclearity of the dication has been placed on firm ground by the recent studies of Boyd et al. [131]. Cyclic and square wave voltammetry and controlled potential electrolysis of $[Nb_3(\mu\text{-}Cl)_6(C_6Me_6)_3]^+$ at inert solid electrodes revealed three quasi-reversible oxidations in the range 0.223–1.16 V (vs. Ag/AgCl). Analogous complexes in four stable oxidation states may be generated, but while $[Nb_3(\mu\text{-}Cl)_6(C_6Me_6)_3]^{2+}$ may be isolated and characterized, the fragile 3 + and 4 + ions have not been isolated in substance. In contrast with the reported diamagnetism of the dication, Boyd et al. report effective solution and solid state magnetic moments consistent with one unpaired electron in this complex. Further, the electrochemically oxidized complexes are stable for many hours. The analogous tantalum system has been investigated [127].

The structures of the lower halides of niobium, Nb_3X_8 (X = Cl, Br, I), consist of infinite arrays of $Nb_3(\mu_3\text{-}X)(\mu\text{-}X)_3X_9$ units linked together by a sharing of the terminal halide ligands [132]. Cotton et al. [133] have reported the synthesis and X-ray structure of a discrete trinuclear complex $Nb_3(\mu_3\text{-}Cl)(\mu\text{-}Cl)_3Cl_3(PMe_2Ph)_6$ (Fig. 13(b)), which is formed upon reduction of

$[NbCl_2(thf)]_2(\mu\text{-}Cl)_2(\mu\text{-tht})$ with Na/Hg in the presence of PMe_2Ph. The complex has virtual C_3 symmetry and is composed of a trinuclear $Nb_3(\mu_3\text{-}Cl)(\mu\text{-}Cl)_3$ core surrounded by terminal chloro and PMe_2Ph ligands. The compound is diamagnetic, consistent with a singlet ground state for this eight-electron species.

(d) Tetranuclear compounds

The reaction of $NbBr_4(MeCN)_2$ and Sb_2Se_3 in acetonitrile results in the formation of $Nb_4Br_{10}(Se)(Se_2)(MeCN)_4$ according to eqn. (5) [134]:

$$4NbBr_4(MeCN)_2 + Sb_2Se_3 \xrightarrow[50\,^\circ C,\ 7\ days]{MeCN} Nb_4Br_{10}(Se)(Se_2)(MeCN)_4 + 2SbBr_3 \quad (5)$$

The compound is composed of the discrete tetranuclear C_s molecules shown in Fig. 16. A central $(MeCN)_2Br_2Nb(\mu\text{-}Se_2)(\mu\text{-}Se)NbBr_2(MeCN)_2$ fragment is linked by μ-Br and μ-Se ligands to two $NbBr_3$ units. The Se(3) atom is bound to all four niobium atoms in the complex. The Nb(1)–Nb(1′) distance of 2.886(1) Å is indicative of an Nb–Nb single bond between these atoms, which are assigned an oxidation state of IV. The other niobium atoms, Nb(2) and Nb(3), are assigned an oxidation state of III. The diamagnetism of the compound is consistent with localized low spin Nb^{III} and metal–metal-bonded Nb^{IV} atoms. This compound possesses an interesting structural similarity to the infinite chain compound $Nb_3Se_5Cl_7$ [135].

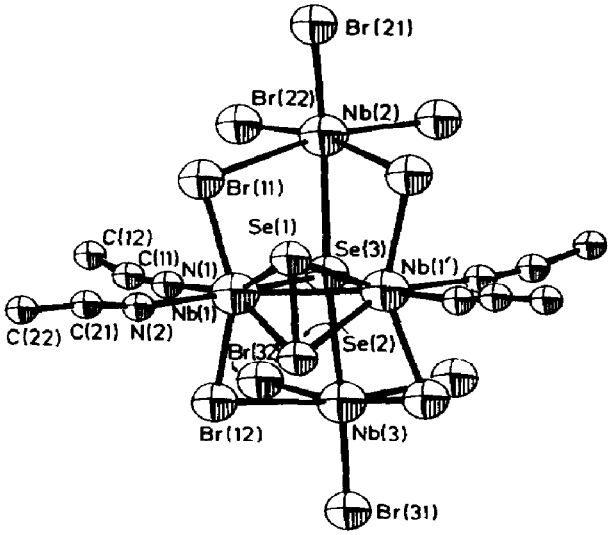

Fig. 16. Structure of $Nb_4Br_{10}(Se)(Se_2)(MeCN)_4$. Reproduced with permission from ref. 134.

(e) Hexanuclear and octanuclear compounds

As previously indicated, the chemistry of the mixed-valence hexanuclear cluster compounds of niobium has been extensively reviewed [43,96–102]. The reader is referred to these articles for an overview of this area. The most recent and significant work is briefly described below. The bridging halide ligands within the $[Nb_6X_{12}]^{n+}$ cores are relatively inert to substitution, but the higher lability of the "centrifugal" ligands allows the production of mixed halides, hydrates and oxygen donor ligand derivatives of the form $[(Nb_6X_{12})X'_qL_{6-q}]^{(n-q)\pm}$ (X = Cl, Br; Y = F, Cl, Br, I, OH; L = neutral donor). In 1981 the first non-oxygen donor ligand derivatives were reported by Klendworth and Walton [136]. Green complexes, $Nb_6Cl_{14}(PR_3)_4$ (R_3 = $^nPr_3$, Et_3, Et_2Ph), were prepared by the reaction of phosphine with $Nb_3Cl_{14} \cdot 8H_2O$, ligand displacement of dmso from $Nb_6Cl_{14}(dmso)_4$ or phosphine-induced reduction of $Nb_6Cl_{15} \cdot 7H_2O$ [136]. Electrochemical studies of the phosphine complexes reveal the presence of three reversible couples, two one-electron oxidations and a single reduction. Chemical oxidation of $Nb_6Cl_{14}(P^nPr_3)_4$ with $NOPF_6$ results in the formation of yellow $[Nb_6Cl_{14}(P^nPr_3)_4]PF_6$. This compound exhibits a 49-line ESR spectrum in CH_2Cl_2 at room temperature ($g = 1.948$, $A = 20.6$ G), indicating coupling of the electron with six equivalent niobium nuclei (55 lines predicted). The ESR spectrum is virtually identical with that of $[Nb_6Cl_{18}]^{3-}$ [137]. The X-ray structure of $K_4[Nb_6Br_{18}]$ has been reported [138]. The compound is isostructural with $K_4[Nb_6Cl_{18}]$ [139] and possesses discrete $[Nb_6Br_{18}]^{4-}$ clusters of the type shown in Fig. 14(a).

Compounds based on the $[Nb_6X_8]^{n+}$ core unit are currently limited to the subiodides and until recently only solid state materials had been characterized. Thus three-dimensional networks of $[Nb_6I_8]^{n+}$ ($n = 3, 2$) clusters linked via iodo bridges are found in Nb_3I_{11} [140,141] and $CsNb_6I_{11}$ [142] respectively. A recent development in this area is the characterization of the intracluster hydride compounds Nb_6HI_{11} and $CsNb_6HI_{11}$ [141,142]. Another significant development is the synthesis of a discrete complex possessing the $[Nb_6I_8]^0$ core. The reaction of Nb_6I_{11} with a solution of NH_2Me in ethanol results in the formation of dark brown $Nb_6I_8(NH_2Me)_6$ (**30**) [143]. Molecules of **30** are composed of an octahedral Nb_6I_8 core with six methylamine ligands bound at its corners. Unlike Nb_6I_{11} and related compounds, the clusters in **30** are not linked together to form an extended lattice. This compound also exhibits the lowest oxidation state yet observed in a niobium cluster compound. The bonding in the $[Nb_6X_8]^{n+}$ clusters has received theoretical treatment [144].

In the late sixties, Bradley et al. [145] reported the X-ray structures of several hydrolysed metal alkoxides and the X-ray structure of $Nb_8O_{10}(OEt)_{20}$. The molecule is composed of eight slightly distorted NbO_6

octahedra. Two sets of three edge-shared octahedra are linked by two bridging octahedra through corner sharing.

(iii) Tantalum compounds

(a) General survey

The mixed-valence chemistry of tantalum strongly resembles that of niobium, especially with respect to the formation of hexanuclear cluster compounds. However, there are notably fewer trinuclear and tetranuclear mixed-valence complexes known for tantalum. Only two dinuclear complexes, $Cp_4Ta_2Cl_3$ and $[Cp_4Ta_2Cl_2]^+$, are known at present. Trinuclear compounds are restricted to salts of the $[Ta_3(\mu\text{-}Cl)_6(C_6Me_6)_3]^{n+}$ ($n = 1, 2$) cations, which are formally $Ta_2^{II}Ta^{III}$ and $Ta^{II}Ta_2^{III}$ complexes respectively. Mixed-valence compounds containing mono- and bi-capped triangular Ta_3 cores are not yet known, although the recent synthesis of the complexes $[M_3(\mu_3\text{-}Cl)(\mu\text{-}Cl)_3Cl_6(PEt_3)_3]^-$ (M = Nb, Ta) [46] suggests that trinuclear μ_3-O complexes of tantalum will eventually be described. Tetranuclear mixed-valence compounds remain unknown. The hexanuclear cluster halides form by far the largest class of mixed-valence tantalum compounds. These compounds contain the $[Ta_6(\mu\text{-}X)_{12}]^{n+}$ cluster core shown in Fig. 14(a). In discrete molecular species the tantalum atoms are further coordinated by six terminal ligands while in reduced halides these centrifugal ligands serve as intercluster bridging ligands. The chemistry and structure of the hexanuclear clusters of tantalum have been extensively reviewed [43,96–101]. Structural studies have been recently reviewed by Holloway and Melnik [146].

(b) Dinuclear compounds

A dinuclear mixed-valence compound of tantalum was first reported in 1977 [147]. Purple $Cp_4Ta_2Cl_3$ was characterized by elemental analysis, X-ray fluorescence, IR and mass spectral and magnetic susceptibility studies. The synthesis of the compound from $TaCl_5$ and NaCp required the addition of reducing $LiPPh_2$ which was converted to P_2Ph_4. The complex was subsequently prepared by Na/Hg reduction of Cp_2TaCl_2 [148]. The $[Cp_4Ta_2Cl_3]^+$ cation has also been reported [148]. Analogous niobium complexes were discussed in Section C(ii)(b).

(c) Trinuclear compounds

The brown trinuclear complex $[Ta_3(\mu\text{-}Cl)_6(C_6Me_6)_3]Cl$, first reported by Fischer and Röhrscheid [28], has been subject to studies paralleling those previously described for the niobium analogue (Section C(ii)(c)). The complex is prepared by the reaction of $TaCl_5$ and C_6Me_6 in the presence of aluminium and $AlCl_3$ [28]. The $[Ta_3(\mu\text{-}Cl)_6(C_6Me_6)_3]^+$ complex is oxidized

to the dication using methanolic $(NH_4)_2[Ce(NO_3)_6]$ or *N*-bromosuccinimide; the dication has been isolated as the PF_6^- and NCS^- salts [126,127]. The bromo complex $[Ta_3(\mu\text{-}Br)_6(C_6Me_6)_3]^+$ is prepared in an analogous fashion and undergoes a similar oxidation reaction. On the basis of an incorrectly determined diamagnetism, King et al. [126,127] postulated the dimerization of the dications (M = Nb, Ta) to form the hexanuclear complexes $[M_6(\mu\text{-}Cl)_{12}(C_6Me_6)_6]^{4+}$. This proposition has not been supported by subsequent crystallographic [130] and electrochemical studies [131] on the niobium system (see Section C(ii)(c)). It is likely that both tantalum complexes possess structures similar to those established for $[Nb_3(\mu\text{-}Cl)_6(C_6Me_6)_3]^+$ [129] and $[M_3(\mu\text{-}Cl)_6(C_6Me_6)_3]^{2+}$ (M = Zr (Fig. 5) [44], Nb [130]).

(d) Hexanuclear compounds

Evidence for the formation of $[Ta_6(\mu\text{-}X)_{12}]^{n+}$ (X = Cl, Br; $n = 2, 3, 4$) clusters was accumulated in the late sixties and examples of each type were structurally characterized. Only recent and significant results are presented below as this area has been adequately reviewed [43,96–101,146]. The first P-donor ligand derivatives of $[Ta_6Cl_{12}]^{n+}$ ($n = 2, 3, 4$) were reported in 1981 by Klendworth and Walton [136]. The compound $Ta_6Cl_{14}(P^nPr_3)_4$ was prepared by the direct reaction of $Ta_6Cl_{14} \cdot 6H_2O$ with P^nPr_3 in ethanol. Oxidation with suitable amounts of $NOPF_6$ lead to the salts $[Ta_6Cl_{14}(P^nPr_3)_4](PF_6)_x$ ($x = 1, 2$). Two electrochemical oxidations were also observed, but in contrast with analogous niobium chemistry, reduction of $Ta_6Cl_{14}(P^nPr_3)_4$ was not observed. The tantalum complexes were characterized by electronic, ESR and photoelectron spectroscopy. Recently, it was discovered that the reaction of air-oxidized solutions of $[Ta_6Cl_{12}]^{4+}$ with concentrated HCl or HBr resulted in spontaneous reduction to $[Ta_6Cl_{12}]^{3+}$, together with oxidation of some cluster units to Ta_2O_5 [149]. The structure of $NMe_4[Ta_6Cl_{12}(H_2O)_6]Br_4$ was determined. It consists of discrete $[Ta_6Cl_{12}(H_2O)_6]^{3+}$ ions with the structure shown in Fig. 14(a), linked via hydrogen bonding to the bromide counter-ions. The distance of 2.9059(2) Å between tantalum atoms is the shortest found in hexanuclear tantalum compounds. The compound is isostructural with $H_2[Ta_6Cl_{12}] \cdot 6H_2O$ which contains the $[Ta_6Cl_{12}]^{2+}$ cation [150]. Irradiation of $[Ta_6Br_{12}]^{2+}$ in deoxygenated HCl solution led to photo-oxidation of the cluster and the formation of hydrogen according to eqn. (6), possibly via the intermediate formation of $[Ta_6Br_{12}]^{2+*}$ [151]:

$$[Ta_6Br_{12}]^{2+} + H^+ \rightarrow [Ta_6Br_{12}]^{3+} + \tfrac{1}{2}H_2 \qquad (6)$$

An esoteric application of the $[Ta_6(\mu\text{-}Cl)_{12}]^{n+}$ complexes is their intercalation and subsequent oxidation to metal oxide aggregates in pillared clays

such as montmorillonite [152]. The electronic structure of hexanuclear tantalum complexes has recently been subject to theoretical treatment [144].

D. MIXED-VALENCE COMPOUNDS OF THE GROUP 6 ELEMENTS

(i) Chromium compounds

(a) General survey

In contrast with the extensive mixed-valence chemistry of its second and third row congeners, chromium forms only a limited number of mixed-valence compounds. Although chromium shares the wide range of oxidation states characteristic of the other group 6 elements, the unique redox and kinetic properties of chromium conspire to "limit" its coordination chemistry [153]. The most stable and important oxidation state is Cr^{III} while Cr^{IV}, Cr^{V} and Cr^{VI} are relatively unimportant due to their powerful oxidizing ability. Disproportionation into Cr^{III} and Cr^{VI} complexes is also a feature of Cr^{IV} chemistry and Cr^{II} compounds are very labile. The low valence chemistry of chromium is dominated by organometallic species, notably carbonyl and arene complexes and their derivatives. The limited mixed-valence chemistry of chromium is a consequence of the general behaviour pattern described above. Dinuclear complexes are restricted to incompletely characterized carbonyl–$Cr^{0}Cr^{I}$ complexes, $Cr_2(CO)_{10}(\mu\text{-Y})$ (Y = I, NCS, CN), and a series of arene–$Cr^{0}Cr^{I}$ complexes, **31**$^{+}$–**38**$^{+}$, derived from dinuclear Cr^{0} or Cr^{II} precursors. Dinuclear combinations of higher oxidation state centres are apparently unstable and have not yet been reported. Most notable in this regard, and again in contrast with molybdenum and tungsten chemistry, is the absence of $Cr^{II}Cr^{III}$ complexes derived from the ubiquitous $[Cr^{4}Cr]^{4+}$ core [154]. The majority of other mixed-valence chromium compounds contain Cr^{III} in combination with Cr^{II}, Cr^{IV} and possibly Cr^{VI}. A number of trinuclear $Cr_2^{III}Cr^{IV}$ and $Cr^{II}Cr_2^{III}$ compounds are known and all but one of these possess a triangular array of chromium atoms. The basic carboxylates $Cr_3O(O_2CCF_2H)_6L_3$ (L = py, 4-CNpy) exhibit structures analogous to those of related vanadium, tungsten and manganese complexes and appear to be valence delocalized. A unique structure involving bridging thio ligands has been established in the case of $Cr_3(\mu_3\text{-S})_2(\mu\text{-S})_3(dmpe)_3$, the most oxidized of the unambiguously characterized complexes. Novel $Cp_2Cr_3(\mu\text{-}O_2CCF_3)_6$, a linear $Cr^{II}Cr_2^{III}$ complex with localized valencies, has also been characterized. There are no known tetranuclear mixed-valence compounds of chromium. Two trinuclear $Cr^{II}Cr_2^{III}$ units share the corner Cr^{II} atom in $[Cp_2Cr_2(\mu_3\text{-S})_2(\mu\text{-S}^{t}Bu)]_2Cr$, an example of a pentanuclear compound. Other higher nuclearity complexes remain to be adequately characterized.

TABLE 4

Properties of selected mixed-valence compounds of chromium

Compound	Cr oxidation state		Structure	Cr ··· Cr distance [a] (Å)	ESR spectrum [b]		Ref.
	Formal	Average			g	A (G)	
$Cr_2(\mu\text{-}I)(CO)_{10}$	0, I	0.5	–	–	–	–	155–157
31$^+$	0, I	0.5	–	–	Fluid, 1.9868	$A(22\ ^1H) = 1.75$	160
					Frozen, $g_{\parallel} = 2.003$,	$A_{\parallel}(^1H) = 3.2$,	
						$A_{\perp}(^1H) = 3.7$	
					$g_{\perp} = 1.9792$	$A_{\perp}(^{53}Cr) = 26$	
32$^+$	0, I	0.5	–	–	Fluid, 1.9856	Unresolved	160
					Frozen, $g_{\parallel} = 2.0025$	$A_{\parallel}(^1H) = 3.2$,	
						$A_{\perp}(^1H) = 3.7$	
					$g_{\perp} = 1.9792$	$A_{\perp}(^{53}Cr) = 26$	
34$^+$	0, I	0.5	–	–	Frozen, $g_1 = 2.098$	$A_1(1\ ^{31}P) = 27.9$	161
					$g_2 = 2.033$	$A_2(1\ ^{31}P) = 31.6$	
					$g_3 = 1.991$	$A_3(1\ ^{31}P) = 30.4$	
35$^+$	0, I	0.5	Fig. 17	4.374(2)	Fluid, 2.017	$A(2\ ^{31}P) = 12.8$ [c]	161

36^+	0, I	0.5	–	–	Fluid, 2.022 Frozen, $g_1 = 2.059$ $g_2 = 2.008$ $g_3 = 1.997$	$A(2\,^{31}P) = 14.9$ $A(2\,^{31}P) = 14.7$ $A(2\,^{31}P) = 14.0$ $A(2\,^{31}P) = 14.8$	161
37^+	0, I	0.5	–	–	Fluid, 2.019	$A(2\,^{75}As) = 13.7$ [c]	161
$Cr_3(\mu_3\text{-}S)_2(\mu\text{-}S)_3(dmpe)_3$	III_2, IV	$3\frac{1}{3}$	Fig. 13(d)	1–2, 2.647(7) 1–3, 2.552(6) 2–3, 2.565(8)	Diamagnetic		162
$Cr_3(\mu_3\text{-}O)(O_2CCF_2H)_6(py)_3$	II, III_2	$2\frac{2}{3}$	Fig. 10	3.356(2)	–	–	163
$Cr_3(\mu_3\text{-}O)(O_2CCF_2H)_6(CN\text{-}py)_3$	II, III_2	$2\frac{2}{3}$	Fig. 10	3.336(1)	–	–	163
$Cp_2Cr_3(\mu\text{-}O_2CCF_3)_6$	II, III_2	$2\frac{2}{3}$	Fig. 18	1–2, 3.717(1)	–	–	164
$[Cp_2Cr_2(\mu\text{-}S)_2(\mu\text{-}S^tBu)]_2Cr$	II, III_4	2.8	Fig. 19	1–2, 2.933(2) 1–3, 2.889(2) 2–3, 2.665(2)	–	–	168

[a] Where more than one distance is quoted the preceding numbers identify the atoms involved, e.g. when prefixed by 1–2, the distance given is between Cr(1) and Cr(2).

[b] Spectra in CH_2Cl_2 (fluid) or CH_2Cl_2–$C_2H_4Cl_2$ (frozen). The number and type of coupled nuclei (where reported) are quoted along with the A values.

[c] Spectra unresolved for frozen media.

Properties of selected mixed-valence compounds of chromium are summarized in Table 4.

(b) Dinuclear compounds

The simplest mixed-valence chromium compound yet reported is $Cr_2(\mu\text{-}I)(CO)_{10}$. This deep-red, paramagnetic Cr^0Cr^I complex was isolated as an intermediate during the iodine oxidation of either $Na_2[Cr_2(CO)_{10}]$ or $Na[Cr(CO)_5I]$ [155,156]. The complex, which is only stable below $-25°C$, has been characterized by analysis and IR and magnetochemical data. IR data support a structure consisting of octahedral chromium centres linked by a linear iodo bridge [156,157]. However, the compound has not been structurally characterized. The structurally characterized isovalent compound $(Ph_3PNPPh_3)[Cr_2(\mu\text{-}I)(CO)_{10}]$ exhibits a Cr–I–Cr angle of 117.9(1)° [158]. The mixed-valence core is not maintained upon reaction with N- or P-donor ligands; substituted mononuclear carbonyl–Cr(0) and carbonyl–Cr(I) complexes are formed instead [159]. Related $Cr_2(\mu\text{-}Y)(CO)_{10}$ (Y = SCN, CN) complexes have been reported and investigated by IR spectroscopy [157].

A variety of Cr^0Cr^I complexes have been derived from (η^6-arene)dichromium(0) complexes. The first complexes of this type, the monocations **31**$^+$–**32**$^+$, were reported by Elschenbroich and Heck [160]. The mixed-valence monocations were obtained by the electrochemical reduction of the

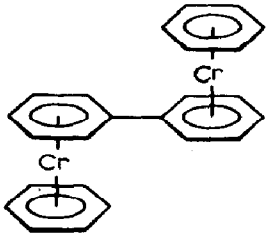

31

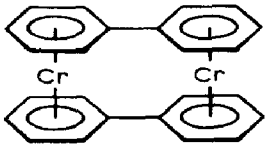

32

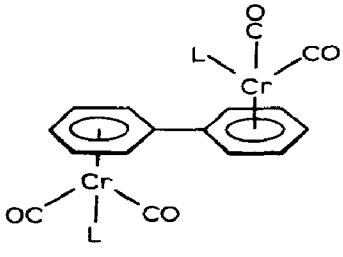

33, L = CO

34, L = PPh_3

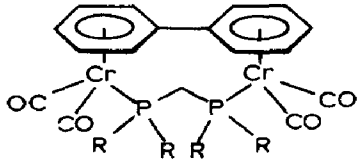

35, R = Ph

36, R = Me

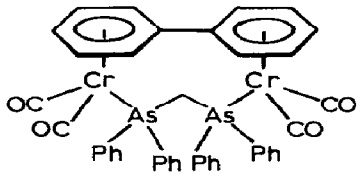

37

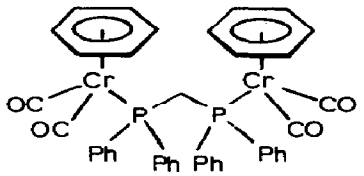

38

dications 31^{2+}–32^{2+}, produced by the air oxidation of (η^6-arene)dichromium(0) complexes **31**–**32**. Solution ESR spectra of 31^+ reveal hyperfine features due to coupling of the electron to 22 ^{1}H nuclei ($A = 1.75$ G), indicating that the unpaired electron is delocalized over both bis(arene)chromium moieties. In contrast, glassy media ESR spectra of both 31^+ and 32^+ are indicative of the interaction of the unpaired electron with protons of only one such moiety. It has been suggested that the spin localization observed in the glassy state may result from ion-pair formation. Related phosphine- and arsine-bridged Cr^0Cr^1 complexes have been recently prepared [161]. The monocations 33^+–38^+, derived from **33**–**38**, have been characterized by IR and ESR spectroscopy and, in the case of 35^+, by X-ray crystallography. They may be prepared by either bulk electrolysis or ferricenium oxidation of the Cr(0) precursors. The glass medium ESR signal of maroon 34^+ at 273 K was interpreted in terms of a rhombic g tensor with a resolved doublet, arising from coupling to a single ^{31}P nucleus ($I = \frac{1}{2}$, $A = 30.0$ G), along each of the three principal directions. The ESR data suggest that the unpaired electron spin density is essentially localized on one side of the 34^+ molecule. A valence-localized structure in solution is also

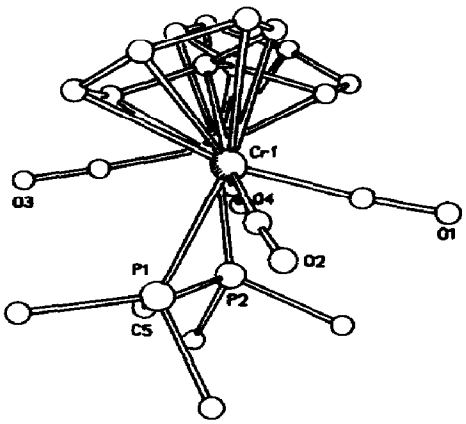

35

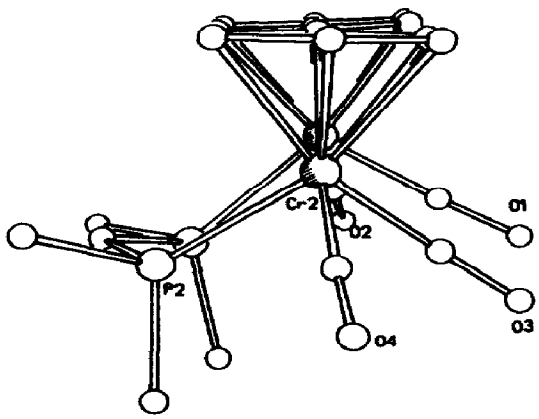

35^+

Fig. 17. Structures of **35** and 35^+ viewed along the Cr · · · Cr vector, highlighting the biphenyl torsion angle. Reproduced with permission from ref. 161.

consistent with IR studies. In their solution ESR spectra, the green phosphine complexes 35^+ and 36^+ display triplets due to coupling with two equivalent ^{31}P nuclei, while the arsine complex 37^+ displays a seven-line ESR spectrum due to coupling with two equivalent ^{75}As nuclei ($I = 3/2$). ESR spectra support a delocalized structure in frozen glass media. The compounds **35** and [**35**]PF_6 have also been structurally characterized and views of **35** and 35^+ are shown in Fig. 17. Although the $Cr(CO)_2P$ units of both complexes are constrained to be on the same side of the biphenyl ligand, the complexes exhibit quite different biphenyl ligand torsion angles. A biphenyl ligand torsion angle of 50.8(3)° is observed in **35** while a nearly planar biphenyl ligand, characterized by a torsion angle of 3.7(4)°, is observed for 35^+. Complexes **35** and 35^+ feature Cr · · · Cr distances of 4.828(1) Å and 4.374(2) Å respectively. There is no crystallographic evidence for the presence of a valence-trapped structure for 35^+. Complex 38^+ is formulated as a localized mixed-valence cation. Complex **33** may be electrochemically oxidized to the corresponding monocation at 260 K. The cation persists for short periods only and spectroscopic characterization has been prevented by decomposition. For complexes 31^+–38^+, the degree of twist of the biphenyl linkage appears to be an important factor in determining the magnitude of the electronic interaction between the metal atoms. Effective uncoupling of the π systems of the arene rings may result in localized valences in complexes with non-planar biphenyl ligands. Thus a twisting of the biphenyl ligand in the singly bridged complexes 31^+, 34^+ and 38^+ may account for the observed valence-trapping in these complexes. Likewise, the near-planar biphenyl ligand geometry of complexes 32^+ and 35^+–37^+ may enhance their valence delocalization.

(c) Trinuclear compounds

An unusual $Cr_2^{III}Cr^{IV}$ complex was recently reported by Arif et al. [162]. Deep purple $Cr_3(\mu_3\text{-}S)_2(\mu\text{-}S)_3(dmpe)_3$ (**39**) is formed by the addition of dmpe to the black suspension formed from $CrCl_3$ and NaSH in methanol at −78 °C. The complex is composed of a triangular Cr_3 unit which is capped on both faces by a μ_3-S atom. The edges of the triangle are bridged by μ-S atoms and each chromium atom bears a bidentate dmpe ligand (Fig. 13(d)). Molecular orbital calculations on the model compound $Cr_3S_5(PH_3)_6$ at D_{3h} symmetry suggest that a second-order Jahn–Teller distortion is responsible for the distortion of **39** from D_{3h} symmetry.

Trinuclear $Cr^{II}Cr_2^{III}$ complexes possessing the oxo-centred basic carboxylate structure, shown in Fig. 10, have been reported by Cotton and Wang [163]. The blue or green complexes $Cr_3(\mu_3\text{-}O)(O_2CCF_2H)_6L_3$ (L = py, 4-CNpy) were slowly precipitated from various solvent systems containing $Cr_2(O_2CCF_2H)_4$ and L. In both complexes, the $CF_2HCO_2^-$ ligands act in a

bridging capacity while the aromatic amine ligands occupy non-bridging equatorial positions (L in Fig. 10). The two structures are very similar and both molecules approximate closely to D_{3h} symmetry. Valence delocalization is consistent with the structural equivalence of the chromium centres in these complexes. While related $M^{II}M_2^{III}$ (M = V, W, Mn) complexes also exhibit valence delocalization, one magnanese complex, $Mn_3O(OAc)_6(3\text{-Clpy})_3$, is known to possess trapped valences.

Cotton and Rice [164] have also reported the synthesis and characterization of a $Cr^{II}Cr_2^{III}$ complex possessing a linear rather than a triangular structure. In an effort to prepare $Cr_2(O_2CCF_3)_4$, these workers investigated the reaction of Cp_2Cr and CF_3CO_2H and found that slow diffusion of toluene solutions of these reactants resulted in the formation of large purple crystals of $Cp_2Cr_3(\mu\text{-}O_2CCF_3)_6$. The compound is postulated to form as a result of combined redox and ligand substitution reactions effected by the strong organic acid. The structure of this compound is shown in Fig. 18. The central Cr^{II} atom possesses a tetragonally distorted octahedral coordination sphere composed of four short (2.01 Å) and two long (2.58 Å) Cr–O bonds. The Cr^{II} atom, which resides at an inversion centre, is linked to two terminal $CpCr^{III}$ units via six $\mu\text{-}CF_3CO_2^-$ ligands. The monodentate $CF_3CO_2^-$ ligands are deprotonated and the $CpCr^{III}O_3$ coordination spheres are very similar to those of other $[CpCrX_3]^-$ complexes. The Cr · · · Cr distances are 3.717(1) Å. No other data were reported.

A simple trinuclear $Cr_2^{-I}Cr^0$ compound, green $Na_2[Cr_3(CO)_{14}]$, is formed upon the reaction of $Cr(CO)_6$ and $NaBH_4$ in refluxing thf [165]. The NMe_4^+ salt has also been reported but the complexes remain poorly characterized.

(d) Tetranuclear compounds

Although tetranuclear mixed-valence chromium complexes are unknown,

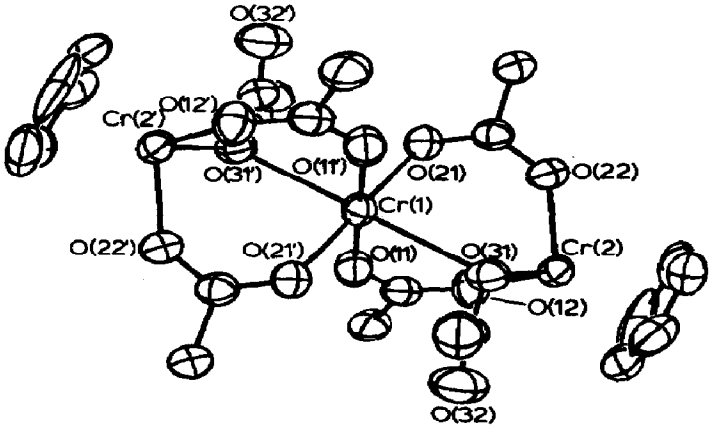

Fig. 18. Structure of $Cp_2Cr_3(\mu\text{-}O_2CCF_3)_6$. Reproduced with permission from ref. 164.

it is interesting to note the synthesis and characterization of deep blue $Cp_4Cr_4O_4$ [166] which is the third member of the $Cp_mM_mO_n$ series where m and n satisfy Euler's theorem. The related complexes $(MeCp)_4Cr_4O_4$ and $(MeCp)_4Cr_4S_4$ have also been reported [167]. Two mixed-valence members of the series, $Cp_6Ti_6O_8$ and $Cp_5V_5O_6$, have been discussed in Section B(i)(f) and Section C(i)(e) respectively.

(e) Pentanuclear compounds

One pentanuclear $Cr^{II}Cr_4^{III}$ complex has been reported; irradiation of a mixture of $Cp_2Cr_2(\mu\text{-S})(\mu\text{-S}^t\text{Bu})_2$ and $(C_6H_6)Cr(CO)_3$ leads to the formation of the black complex $[Cp_2Cr_2(\mu_3\text{-S})_2(\mu\text{-S}^t\text{Bu})]_2Cr$ [168]. The structure of the complex (Fig. 19) reveals a metal spirane unit with two perpendicular Cr_3 triangles linked via the shared Cr(1) atom. Each triangle of chromium atoms is capped by two μ_3-S atoms. The bond lengths between the terminal Cr(2)–Cr(3) and Cr(2′)–Cr(3′) atoms (2.665(1) Å) are virtually identical to the Cr–Cr bond length of $Cp_2Cr_2(\mu\text{-S})(\mu\text{-S}^t\text{Bu})_2$ (2.689 Å), indicating the preservation of the Cr=Cr double bond despite the bonding to Cr(1). The unique Cr(1) atom is assigned an oxidation state of II while the four remaining chromium atoms are assigned an oxidation state of III.

(f) High nuclearity compounds

The addition of H_2O_2 to an acidic solution of a chromate salt results in the formation of an unstable blue complex which can be extracted into diethyl ether [169]. The composition of this complex has not been unambigu-

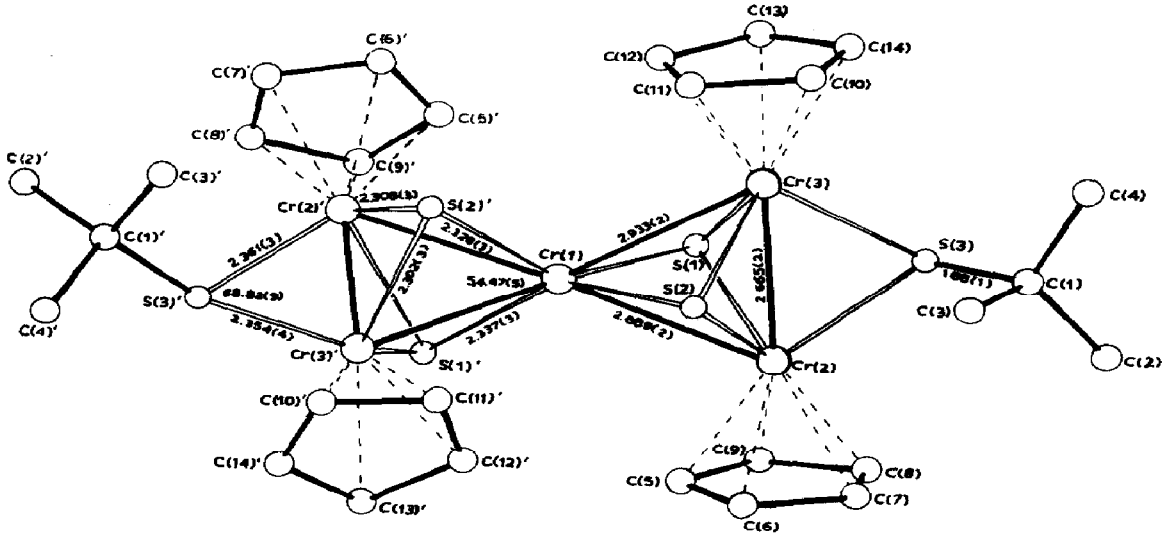

Fig. 19. Structure of $[Cp_2Cr_2(\mu_3\text{-S})_2(\mu\text{-S}^t\text{Bu})]_2Cr$. Reproduced with permission from ref. 168.

ously established but formulations such as $Cr_2^{III}(Cr_2^{VI}O_{10})_3$ have been proposed [170]. When the reaction is performed in the presence of sulphosalicylic acid a compound with the formulation $(Cr^{III}Su)_3[Cr^{III}(Cr_2^{VI}O_{10})_3]$ is reported to form [171,172]. The difficult chemistry of this system remains to be resolved satisfactorily.

(ii) Molybdenum compounds

(a) General survey

In terms of mixed-valence chemistry, molybdenum is the element par excellence. The popularity of molybdenum chemistry, chiefly a result of its importance in biological and chemical catalysis, combined with the element's ability to form stable complexes with a wide variety of oxidation states ($-$II to VI), coordination numbers and geometries accounts for its well-developed mixed-valence chemistry. Indeed, a remarkable variform and structural diversity are manifest by the mixed-valence compounds of molybdenum. Compounds exhibiting all formal oxidation states with the exception of $-$II and $-$I are known to exist. A wide variety of nuclearities, dinuclear through decanuclear and beyond, characterize these materials. Molybdenum forms about 30 distinct dinuclear mixed-valence compounds, and examples with integral and half-integral oxidation states of 5.5 through 0.5, with the exception of 4.0 and 1.0, have been reported. High valence $Mo^{V}Mo^{VI}$ complexes such as $[Mo_2O_4(\mu\text{-}O)(Me_3tcn)_2]^+$ are rare and none have been isolated and structurally characterized. In contrast, a variety of well-characterized $Mo^{IV}Mo^{VI}$ compounds are known, the majority of which are derived from reactions involving $[MoS_4]^{2-}$; the $[MoS_4]^{2-}$ fragment comprises a portion of the molecular structure in such compounds. Isolable compounds in which molybdenum has an average oxidation state of 4.5 are of two types. The first type, the majority, are dithiocarbamate complexes of oxo–$Mo^{IV}Mo^{V}$. The most studied of these, $[Mo_2(\mu\text{-}O)(S_2CNR_2)_6]^+$, have been characterized by spectroscopic and crystallographic studies. Although structurally characterized in a mixed crystal, synthetic limitations have prevented a deeper understanding of the interesting $[Mo_2O_2(\mu\text{-}O)(S_2CNEt_2)_4]^-$ complex. Recently reported $[Mo_2O_2(S_2CNR_2)_4]^+$ complexes remain to be thoroughly characterized. The second, minor type, are $Mo^{III}Mo^{VI}$ complexes, again derived from and containing $[MoS_4]^{2-}$; an example is $[S_2Mo(\mu\text{-}S)_2MoBr_3(SMe_2)]^{2-}$. Electrochemical and kinetic evidence for the formation of $Mo^{IV}Mo^{V}$ complexes has also been collected, but associated chemical transformations may ultimately result in products of higher nuclearity. A number of $Mo^{III}Mo^{IV}$ complexes of the type $[Cp_2Mo_2(\mu\text{-}SR)_{4-x}(\mu\text{-}SR')_x]^{n+}$ (R = missing, alkyl) are known and a series has been extensively characterized by spectroscopic and crystallographic

studies. A mixed crystal containing $[Mo_2(\mu\text{-}SO_2)(\mu\text{-}S_2)(CN)_8]^{3-}$ has been crystallographically characterized. In contrast with the formation of W_2^{5+} complexes by oxidation of $W_2(O_2CR)_4$ with I_2, the reaction of $Mo_2(OAc)_4$ with this reagent yields the $Mo^{III}Mo^{IV}$ complex $[Mo_2(\mu\text{-}O)(\mu\text{-}I)(\mu\text{-}OAc)I_2(thf)_4]^+$. Molybdenum also forms $[Mo_2Cl_9]^{2-}$, the tungsten analogue of which has been structurally characterized. The Mo^0Mo^{VI} complex $[(CO)_4Mo(\mu\text{-}S)_2MoS_2]^{2-}$ possesses metal centres which differ in formal oxidation state by six units, a feature shared with a trinuclear relative $[(CO)_4Mo(\mu\text{-}S)_2Mo(\mu\text{-}S)_2Mo(CO)_4]^{2-}$ and $W_2(O^iPr)_6(CO)_4$. Strong metal–metal bonds are a feature of $Mo^{II}Mo^{III}$ compounds such as $K_3[Mo_2(SO_4)_4]$ and $[Mo_2(tmtaa)_2]BF_4$, which are formed by oxidation of the isovalent Mo^{II} analogues. The $[Mo_2X_8]^{3-}$ (X = Cl, Br) complexes, originally thought to be produced by oxidation of $Mo_2(OAc)_4$ with HX, are in fact the isovalent hydrido complexes $[Mo_2HX_8]^{3-}$. Oxidation or reduction of other Mo^{II} complexes generally results in relatively unstable species. An unusual phosphine-stabilized Mo^0 centre is observed in the Mo^0Mo^{IV} compound $Mo_2(O^iPr)_4(dmpe)_2$ while an average oxidation state of 0.5 characterizes the organometallic complex $(\eta^7\text{-}C_7H_7)MoX_3Mo(\eta^7\text{-}C_7H_7)$ and related species.

Molybdenum also forms many compounds of higher nuclearity. As is the case with chromium and tungsten, molybdenum forms trinuclear compounds with both linear and triangular structures. Most linear compounds contain bidentate $[MoS_4]^{2-}$ ligands bound to central $[Mo^{IV}E]^{2+}$ (E = O, S) or $[Mo^{II}(NNMe_2)_2]^{2+}$ fragments. In one case, $[(CO)_4Mo(\mu\text{-}S)_2Mo(\mu\text{-}S)_2Mo(CO)_4]^{2-}$, the $[MoS_4]^{2-}$ fragment serves to bridge two $Mo(CO)_4$ units. The remaining trinuclear complexes possess triangular structures; examples of $Mo^{IV}Mo_2^V$, $Mo_2^{IV}Mo^V$, $Mo_2^{III}Mo^{IV}$ and $Mo^{II}Mo_2^{III}$ complexes include $[Mo_3(\mu_3\text{-}CMe)_2(OAc)_6(H_2O)_3]^{2+}$, $[Mo_3(\mu_3\text{-}CMe)_2(OAc)_6(H_2O)_3]^+$, $[Mo_3(\mu_3\text{-}O)(\mu\text{-}Cl)_3(OAc)_3(H_2O)_3]^{2+}$ and $Mo_3HI_7(thf)_3$ respectively. Some very unusual tetranuclear compounds have been reported. Although a number of $Mo_2^VMo_2^{VI}$ complexes are claimed to exist, scrutiny of X-ray crystallographic data reveals a structural anomaly consistent with their formulation as isovalent Mo^V compounds. High valent $Mo_2^{IV}Mo_2^{VI}$ complexes such as $[Mo_4O_{11}(dhphH_2)]^{2-}$ and $[(MeCp)_2Mo_2O_4]_2$ have been structurally characterized and possess unique structures. However, many tetranuclear compounds possess cuboidal structures. These include $Mo_4(\mu_3\text{-}S)_4(\mu\text{-}S_2CNEt_2)_2(S_2CNEt_2)_4$ and derivatives of the aqua ions $[Mo_4S_4(aq)]^{n+}$ ($n = 5, 6$). Oxo, selenido and tellurido analogues of the latter complexes have been recently reported and are presumed to possess similar cuboidal structures. Unique structures characterize $Mo_4O_2(\mu_4\text{-}CO_3)(CO)_2(\mu\text{-}O)_2(\mu\text{-}OH)_4(PMe_3)_6$ and $[Mo_4O_8(OMe)_2(NNPh)_4]^{2-}$, which are examples of $Mo_2^{II}Mo_2^V$ and $Mo_2^0Mo_2^{VI}$ complexes respectively. An interesting case of

isomerism is observed for $[Mo_4Cl_{12}]^{3-}$. This anion adopts both rhombohedral and butterfly cluster core geometries derived from the removal of *trans*-MoCl or *cis*-MoCl units respectively from $[Mo_6Cl_{14}]^{2-}$. Related tetranuclear iodo and pentanuclear complexes are known. Hexanuclear complexes include $Mo_6O_{10}(O^iPr)_{12}$, which possesses an extended serpentine structure, but there are relatively few (cf. niobium and tantalum) octahedral clusters such as $Mo_6(\mu_3\text{-}S)_8(PEt_3)_6$ and derivatives of $[Mo_6X_{14}]^{2-}$. Heptanuclear and decanuclear complexes have been crystallographically characterized. The so-called isopoly and heteropoly blues constitute a large and intriguing class of molybdenum mixed-valence compounds. However, since these compounds have been the subject of recent reviews [94,95,173,174] they will not be discussed herein.

Properties of selected mixed-valence compounds of molybdenum are summarized in Tables 5 and 6.

(b) Dinuclear compounds

Properties of selected dinuclear mixed-valence compounds of molybdenum are summarized in Table 5.

The first strong evidence for the existence of an Mo^VMo^{VI} complex was obtained by Wieghardt and coworkers [175,176]. Reduction of the dinuclear Mo^{VI} complex $[Mo_2O_4(\mu\text{-}O)(Me_3tcn)_2]^{2+}$ with $NaBH_4$ or NH_2NH_2 results in the formation of blue paramagnetic $[Mo_2O_4(\mu\text{-}O)(Me_3tcn)_2]^+$ (**40**). The electronic spectrum of **40** exhibits intervalence CT bands at 753 nm ($\epsilon = 2.6 \times 10^3$) and 909 nm ($\epsilon = 2.7 \times 10^3$). The very stable complex ($K_{comp} = 6 \times 10^{18}$) exhibits an ESR spectrum consistent with electron delocalization over two equivalent molybdenum nuclei ($^{95,97}Mo$, $I = 5/2$, 25% abundance) [176]. The complex, which may also be generated by electrochemical reduction of $[Mo_2O_4(\mu\text{-}O)(Me_3tcn)_2]^{2+}$ in aprotic media [175] or alkaline aqueous solutions [176], is likely to possess a structure similar to that of $[Mo_2O_4(\mu\text{-}O)(Me_3tcn)_2]^{2+}$ [175]. A second green Mo^VMo^{VI} complex is reported to result from the proton-assisted oxidation of orange $Mo^V_2O_2(\mu\text{-}O)_2(gly)_2(H_2O)_2$ [177]. When the oxidation is monitored spectrophotometrically, a new band at 850 nm ($\epsilon = 241$), assigned to an intervalence CT transition, appears. The mixed-valence complex is formulated as an oxo-bridged dinuclear complex containing oxo–Mo^V and dioxo–Mo^{VI} centres, viz. $(gly)(H_2O)MoO(OH)(\mu\text{-}O)MoO_2(gly)(H_2O)$, but it remains to be isolated and unambiguously characterized. Kinetic studies of the oxidation of $[Mo_2O_4(edta)]^{2-}$ [178] and $[Mo_2O_4(aq)]^{2+}$ [179] reveal that these reactions are likely to proceed via Mo^VMo^{VI} intermediates which retain the two bridging oxo ligands.

The oxometallates and thiometallates (M = Mo, W) not only act as precursors to mixed-valence compounds but also frequently appear as

TABLE 5

Properties of selected dinuclear mixed-valence compounds of molybdenum

Compound	Mo oxidation state		Structure	Mo···Mo distance (Å)	μ_{eff} (BM)	ESR spectrum	Electronic spectrum (nm) (ϵ)	Electron configuration	Ref.
	Formal	Average							
$[Mo_2O_4(\mu\text{-}O)(Me_3tcn)_2]^{+}$ [a]	V, VI	5.5	-	-	1.7 [c]	$g = 1.958$	909 (2700) 753 (2600)	-	175, 176
$Mo_2O_4(gly)_2(H_2O)_2(OH)$ [a]	V, VI	5.5	-	-	0.6 [c]	-	850 (241)	-	177
$(MeCp)_2Mo(\mu\text{-}S)_2MoS_2$	IV, VI	5.0	Fig. 20(a)	2.970(1)	Diamagnetic	-	-	-	180–182
$(PPh_4)_2[(S_4)MoS_2MoS_2]$	IV, VI	5.0	Fig. 21(a)	2.859(1)	Diamagnetic	-	422 (6980) 298 (23800)	-	184
$[Mo_2(\mu\text{-}O)(S_2CNEt_2)_6]BF_4$	IV, V	4.5	Fig. 22	ca. 3.70	2.17	-	1310 (1080), 890 (220) 677, 497, 440, 410	-	186, 187
$[Mo_2O_2(S_2CNMe_2)_4]PF_6$	IV, V	4.5	44	-	-	$g = 1.98$, $A = 37$ G	-	-	190
$[Cp_2Mo_2(SC_3H_6S)_2]BF_4$	III, IV	3.5	Fig. 23	2.599(1)	1.68	-	1040 (72), 618 (690) 480 (300), 408 (500)		205, 208
$(MeCp)_2Mo_2S(SMe)(S_2CH_2)$	III, IV	3.5	-	-	-	$g = 1.993$, $A = 14$ G	1360 (975) 523 (1400), 422 (1000)		206, 208
$[Cp_2Mo_2(\mu\text{-}SMe)_4]PF_6$	III, IV	3.5	-	2.617(4)	1.69	$g = 2.009$	-	$\sigma^2\pi^2\delta^*$	210
$[Mo_2(\mu\text{-}SO_2)(\mu\text{-}S_2)(CN)_8]^{5-}$ [b]	III, IV	3.5	Fig. 24	2.790(1)	-	$g = 2.012$ $A = 19.2$ G	980, 340, 305	$\sigma^2\pi^2\delta^*$	211
$[Mo_2OI(OAc)I_2(thf)_4]$- $[MoOI_4(thf)]$	III, IV	3.5	-	2.527(2)	3.14	-	-	$\sigma^2\pi^2\delta$ (or δ^*)	212
$(N^nBu_4)_2[Mo_2Cl_9]$	III, IV	3.5	-	-	2.06	-	975 (163) 781 (171) 654 (265)	-	213, 214
$(NEt_4)_2[(CO)_4MoS_2MoS_2]$	0, VI	3.0	-	-	Diamagnetic	-	467–450, 613–555 [e]	-	217
$K_3[Mo_2(SO_4)_4]\cdot 3.5H_2O$	II, III	2.5	Fig. 25	2.164(2)	1.65	$g_{\parallel} = 1.891$, $A_{\parallel} = 45.2$ [d] $g_{\perp} = 1.909$, $A_{\perp} = 22.9$ [d]	573 (17.5) 412 (16.9)	$\sigma^2\pi^4\delta$	219, 220
$[Mo_2(tmtaa)_2]PF_6$	II, III	2.5	-	2.221	-	$g = 1.959$, $A = 32.2$ [d]	-	$\sigma^2\pi^4\delta$	230
$(N^nBu_4)[Mo_2Br_6]$	II, III	2.5	-	-	1.50	$g = 1.98$	-	$\sigma^2\pi^4\pi^*$	231
$Mo_2(O^iPr)_4(dmpe)_2$	0, IV	2.0	Fig. 26	2.236(1)	Diamagnetic	-	-	$\sigma^2\pi^4$	244
$Mo_2(\mu\text{-}OMe)_3(C_7H_7)_2(CO)_2$	0, I	0.5	Fig. 27	-	1.74	$g = 1.9537$ $A_{Mo} = 46.4$ G $A_H = 5.2$ G	-	-	247

[a] Formed and characterized in solution.

[b] In a mixed crystal of $K_{4+x}[Mo_2(SO_2)(S_2)(CN)_8]_x[Mo_2(SO_2)(S_2)(CN)_8]_{1-x}\cdot 4H_2O$ ($x = 0.3$).

[c] By Evans method.

[d] A values $\times 10^4$ cm^{-1}.

[e] Solvent dependent.

TABLE 6

Properties of selected high nuclearity mixed-valence compounds of molybdenum

Compound	Mo oxidation state		Structure	Mo · · · Mo distance [a] (Å)	μ_{eff} (BM)	Ref.
	Formal	Average				
$(NEt_4)_2[S_2Mo(\mu\text{-}S)_2MoS(\mu\text{-}S)_2MoS_2]$	IV, VI_2	$5\frac{1}{3}$	Fig. 21(b)	2.982(1), 2.924(1)	Diamagnetic	248
$(PPh_4)_2[Mo_3S_8(NNMe_2)_2]$	II, VI_2	$4\frac{1}{3}$	–	–	Diamagnetic	255
$[Mo_3(\mu_3\text{-}CMe)_2(OAc)_6(H_2O)_3]SbF_6$	III, IV_2	$3\frac{2}{3}$	Fig. 13(a)	2.8155(8)	Paramagnetic	256, 257
$Mo_3HI_7(thf)_3$	II, III_2	$2\frac{2}{3}$	Fig. 28	2.487(4)	–	273
$[Mo_3(\mu_3\text{-}O)(\mu\text{-}Cl)_3(OAc)_3(H_2O)_3](ClO_4)Cl$	II, III_2	$2\frac{2}{3}$	Fig. 13(b)	2.550(2)	–	268
$(NHEt_3)_2[Mo_4O_{11}(dhphH_2)]$	IV_2, VI_2	5.0	Fig. 32	1–2, 3.47	Diamagnetic	278
$[(MeCp)_2Mo_2O_4]_2$	IV_2,VI_2	5.0	Fig. 20(b)	1–2, 3.353(2); 2–2′, 3.354(3)	Diamagnetic	180–182
$Mo_4(\mu_3\text{-}N)_2(O^iPr)_{12}$	III_2, VI_2	4.5	Fig. 33	1–1′, 2.552(1); 1–2, 2.918(1)	–	279
$Mo_4(\mu_3\text{-}S)_4(S_2CNEt_2)_6$	III_2, IV_2	3.5	**59**	2.858(5)–2.870(7)	Diamagnetic	280
$K_4[Mo_4O_4(OH)_2(edta)_2]\cdot 12H_2O$	III_2, IV_2	3.5	Fig. 34(a)	1–2, 2.412(1)	Diamagnetic	202, 283
$(NH_4)_6[Mo_4S_4(NCS)_{12}]\cdot 10H_2O$	III_2, IV_2	3.5	–	2.791(1)–2.869(1)	Diamagnetic	284
$Mo_4O_6(\mu_4\text{-}CO_3)(CO)_2(OH)_4(PMe_3)_6$	II_2, V_2	3.5	Fig. 35	2–2′, 2.5522(9)	Diamagnetic	291
$Cs_3[Mo_4S_4(edta)_2]_2\cdot 26H_2O$	III_3, IV	3.25	Fig. 34(b)	1–2, 2.775(2); 1–3, 2.794(2) 1–4, 2.880(2); 2–3, 2.845(2) 2–4, 2.755(2); 3–4, 2.796(2)	2.0	285
$(NHEt_3)_2[Mo_4O_8(OMe)_2(NNPh)_4]$	O_2, VI_2	3.0	Fig. 36	1–3, 3.465	Diamagnetic	292
$(AsPh_4)_2(NEt_4)[Mo_4Cl_{12}]$	II_3, III	2.25	Fig. 29(e)	2.358(2)–2.653(2)	1.72 [b]	293
$(NEt_4)_3[Mo_4Cl_{12}]$	II_3, III	2.25	Fig. 29(d)	2.501(1)–3.392(1)	1.63	293
$(N^nBu_4)_2[Mo_4I_{11}]$	II_3, III	2.25	Fig. 29(c)	1–2, 3.035(5); 3–4, 2.669(5) rest av. 2.542(5)	1.87	294
$(N^nBu_4)_2[Mo_5Cl_{13}]$	II_4, III	2.2	Fig. 29(b)	2.602(3), 2.563(3)	Paramagnetic	295
$Mo_6O_{10}(O^iPr)_{12}$	V_4, VI_2	$5\frac{1}{3}$	Fig. 37	1–2, 2.585(1), 1–1′, 3.353(1) 2–3, 3.285(1)	Diamagnetic	296
$Mo_6(\mu_3\text{-}S)_8(PEt_3)_6$	II_2, IV_4	$2\frac{2}{3}$	Fig. 14(b)	2.664(1)–2.662(1)	Diamagnetic	298
$(N^nBu_4)_4[Mo_{10}O_{28}(SCH_2CH_2O)(MeOH)_2]$	V_4, VI_6	5.6	fig. 38	1–2, 2.681(1); 2–3, 3.110(1) 3–4, 2.640(1)	Diamagnetic	302

[a] Where more than one distance is quoted the preceding numbers identify the molybdenum atoms involved, e.g. when prefixed by 1–2, the distance given is that between Mo(1) and Mo(2).

[b] For structurally analogous $(NPr_4)_3[Mo_4Cl_{12}]$.

recognizable fragments in the structure of such species. As the first of many examples, a variety of $Mo^{IV}Mo^{VI}$ complexes are produced when $(RCp)_2MoCl_2$ (R = H, Me, ^nBu) complexes react with alkali metal or ammonium tetraoxomolybdates and tetrathiomolybdates [180]. While tetranuclear complexes result from reactions involving $[MoO_4]^{2-}$ (Section D(ii)(d)), reactions involving $[MoS_4]^{2-}$ produce orange–red dinuclear complexes. These are exemplified by $(MeCp)_2Mo(\mu\text{-}S)_2MoS_2$, the structure of which is shown in Fig. 20(a) [181,182]. The molybdenum atoms in the tetrahedral MoS_4 and $(RCp)_2Mo$ fragments retain their original oxidation states of VI and IV respectively in these Class I compounds. The $(MeCp)_2Mo(\mu\text{-}O)(\mu\text{-}S)MoO_2$ complex has also been reported [180] and analogous tungsten complexes are discussed in Section D(iii)(b).

Complex equilibria prevail in solutions of $[MS_4]^{2-}$ (M = Mo, W) and sulphur or S_x^{2-} and isovalent and mixed-valence compounds may be isolated from such mixtures [183,184]. Reduction of $(PPh_4)_2[(S_4)MoS(\mu\text{-}S)_2MoS(S_2)]$ with $NaBH_4$ in dmf results in the formation of brown–red $(PPh_4)_2[(S_4)MoS(\mu\text{-}S)_2MoS_2]$, a mixed-valence $Mo^{IV}Mo^{VI}$ complex in which an S_4^{2-} ligand and an $[Mo^{VI}S_4]^{2-}$ ligand are bonded to a thio–Mo^{IV} centre (Fig. 21(a)). The related $Mo^{IV}Mo^{VI}$ complex $[(S_2)MoS(\mu\text{-}S)_2MoS_2]^{2-}$, isolated in a mixed crystal containing PPh_4^+ and $[S_2Mo(\mu\text{-}S)_2MoS_2]^{2-}$, possesses a similar structure except that an S_2^{2-} ligand replaces the S_4^{2-} ligand. Only crystallographic data have been reported in both cases.

Pink–red compounds of general formula $Mo_2O(S_2CNR_2)_2(YC_6H_4CXN_2)_2$ (X = O, Y = H; X = S, Y = H, Cl, OMe) are produced upon reaction of $MoO_2(S_2CNR_2)_2$ and the hydrazines $YC_6H_4CXNHNH_2$ in refluxing

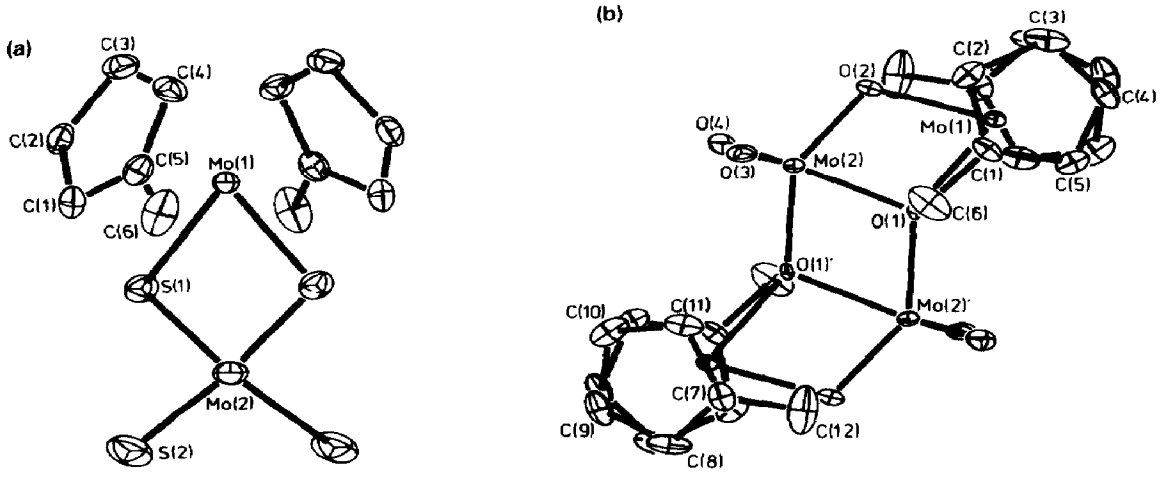

Fig. 20. Structures of (a) $(MeCp)_2Mo(\mu\text{-}S)_2MoS_2$ and (b) $[(MeCp)_2Mo_2O_4]_2$. The analogous tungsten complexes possess similar structures. Reproduced with permission from ref. 182.

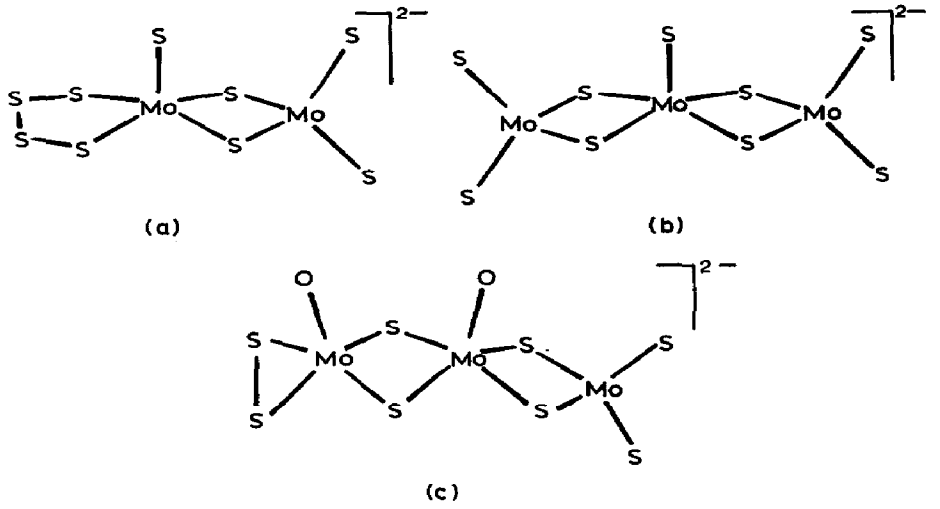

Fig. 21. Some mixed-valence complexes derived from $[MoS_4]^{2-}$: (a) $[(S_4)MoS(\mu\text{-}S)_2MoS_2]^{2-}$, (b) $[S_2Mo(\mu\text{-}S)_2MoS(\mu\text{-}S)_2MoS_2]^{2-}$ and (c) $[(S_2)MoO(\mu\text{-}S)_2MoO(\mu\text{-}S)_2MoS_2]^{2-}$.

methanol (PPh_3 is also a reactant when X = O) [185]. The X-ray structures of $Mo_2O(S_2CNEt_2)_2(C_6H_5CON_2)_2 \cdot CH_2Cl_2$ and $Mo_2O(S_2CNEt_2)_2(ClC_6H_4CSN_2)_2 \cdot CHCl_3$ have been determined, and although it is difficult to assign molybdenum oxidation states in delocalized complexes such as these, both Mo_2^V and $Mo^{IV}Mo^{VI}$ formulations are conceivable. In the mixed-valence formulation the molybdenum atoms bonded to the terminal oxo ligand would be in the higher oxidation state. Aspects of the structures and an electrochemical study of the complexes provide some support for the mixed-valence formulation. The complexes may be electrochemically reduced to mixed-valence anions, $[Mo_2O(S_2CNR_2)_2(YC_6H_4CXN_2)_2]^-$, which exhibit rhombic ESR spectra in frozen solution.

The reactions of $[MoO(S_2CNR_2)_3]X$ (R = Me, Et; X = BF_4^-, PF_6^-, ClO_4^-) and PPh_3 in methanol result in the formation of green–black dichroic crystals of $[Mo_2O(S_2CNR_2)_6]X$, which have been characterized by a variety of physical and spectroscopic techniques and in the case of $[Mo_2O(S_2CNEt_2)_6]BF_4$ (**41**) by X-ray diffraction [186,187]. The cation in **41** comprises two seven-coordinate pentagonal bipyramidal $MoO(S_2CNEt_2)_3$ units linked by a near-linear (175.7°) μ-oxo ligand (Fig. 22). A conspicuous near-IR band at 1310 nm ($\epsilon \approx 1100$) has been assigned to an intervalence CT, owing to its absence in the electrochemically produced Mo^{IV} analogue. The properties of the near-IR band deviate considerably from those predicted by Hush [7] for Class II systems; the bandwidth of the absorption is much narrower than predicted and the energy of the band is solvent independent. The near-IR spectra and the crystallographic equivalence of the molybdenum

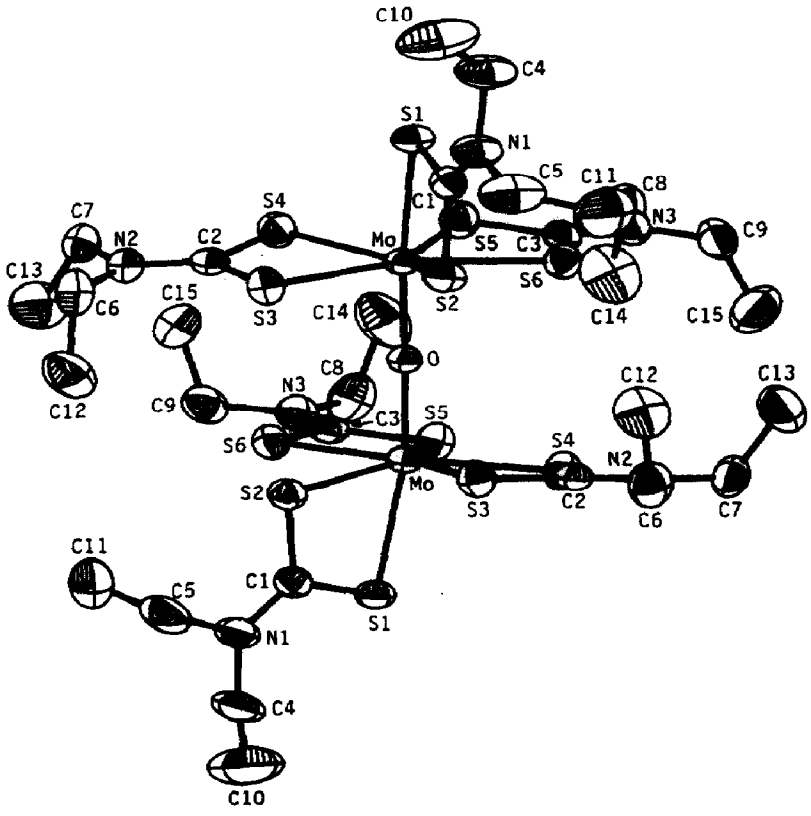

Fig. 22. Structure of the cation in **41**. Reproduced with permission from ref. 187.

atoms support a Class IIIA formulation for these complexes. These compounds are the only synthetically accessible and unambiguously characterized $Mo^{IV}Mo^{V}$ complexes known.

Attempts to prepare $MoO(S_2CNEt_2)_3$ by reacting $MoOCl_3$ and NaS_2CNEt_2 in CH_2Cl_2 resulted in the crystallization of $(H_5O_2)[Mo_2O_3(S_2CNEt_2)_4]_3$ (**42**), which has been characterized by X-ray diffraction and single-crystal ESR studies [188]. Crystals of **42** are proposed to contain co-crystallized $H_5O_2^+$, $[Mo_2O_3(S_2CNEt_2)_4]^-$ (**43**) and $Mo_2O_3(S_2CNEt_2)_4$

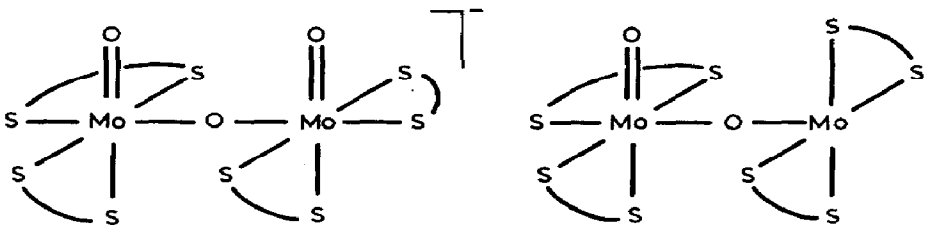

43 44

molecules in a ratio of 1 : 1 : 2. Although the structure and spectroscopic properties of the mixed-valence $Mo^{IV}Mo^{V}$ anion are of particular interest, crystallographic disorder and limitations to the interpretation of the ESR data provide a less than clear picture of the $[Mo_2O_3(S_2CNEt_2)_4]^-$ anion. The unit cell of **42** contains 12 dinuclear complexes, four with C_i symmetry and eight with approximate C_2 symmetry. Half of the C_2-type complexes are proposed to be anionic owing to their proximity to what appear to be $H_5O_2^+$ ions. The ESR spectra of a single crystal of **42** exhibit two distinct signals, attributable to an electron associated with a molybdenum atom. While the ESR spectra were assigned to an unpaired electron in an $[Mo_2O_3(S_2CNEt_2)_4]^-$ anion, the location of the anion in the crystal lattice could not be established. It was concluded that the mixed-valence anion is randomly distributed over all the C_2-type sites and that the unpaired electron is localized on only one molybdenum atom of the anion. This implies that the anion is a Class II mixed-valence species. Unfortunately, attempts to reproduce the synthesis of **42** have failed [189].

A third $Mo^{IV}Mo^{V}$ dithiocarbamate complex has recently been reported [190]. Electrochemical (eqn. (7)) or chemical ($NOPF_6$) oxidation of $MoO(S_2)(S_2CNR_2)_2$ (R = Me, Et)

$$3MoO(S_2)(S_2CNR_2)_2 \rightarrow [Mo_2O_2(S_2CNR_2)_4]^+ + 6S + \text{'MoO'} + R_4bitt^{2+} + 3e^- \quad (7)$$

results in the formation of yellow–orange $[Mo_2O(\mu\text{-}O)(S_2CNR_2)_4]^+$ (**44**) which have been isolated as PF_6^- salts and characterized by elemental analysis, conductivity studies and IR and ESR spectroscopy. ESR spectra are typical of a localized Mo^V centre ($g = 1.98$, $A = 37$ G). Dimerization of **44** is postulated to occur at higher concentrations on the basis of conductivity studies and the appearance of a second ESR signal at $g = 1.97$. The dinuclear cation is proposed to contain a *cis*-$Mo^VO(\mu\text{-}O)(S_2CNR_2)_2$ centre linked via the μ-O ligand to an $Mo^{IV}(S_2CNR_2)_2$ fragment, producing octahedral and square-pyramidal geometries at the Mo^V and Mo^{IV} atoms respectively.

Evidence for $Mo^{IV}Mo^{V}$ complexes has also been obtained from the electrochemical and kinetic studies described briefly below. These species are quite unstable and their ultimate fate depends on the time scale of the experiment. The Mo^V complex $Mo_2O_3(oxine)_4$ is reduced in two reversible one-electron steps to produce $Mo^{IV}Mo^{V}$ and Mo_2^{IV} species [191]. The mixed-valence complex exhibits a long-lived ESR signal and is decomposed by a first-order reaction with $k = 7.2 \times 10^{-2}$ s^{-1}. de Hayes et al. [192] report that the electrochemical reduction of $Mo_2O_2(\mu\text{-}S)_2(S_2CNR_2)_2$ in dmf results in the formation of a mixed-valence tetramer, $[Mo_4O_4(\mu_3\text{-}S)_4(S_2CNR_2)_4]^-$,

which may itself be reduced to the corresponding dianion. Adequate characterization data were provided for neither complex but a rationalization for the formation of a tetramer was subsequently proposed [193]. The studies of de Hayes et al. were extended by Schultz and coworkers [194,195] who reported substantially different electrochemical behaviour in the case of $Mo_2O_2(\mu\text{-}S)_2(S_2CNR_2)_2$. The electrochemistry observed for complexes of general formula $Mo_2E_2(\mu\text{-}E)_2L_2$ ($E = O$ or S, $L = S_2CNEt_2^-$, $S_2P^iPr_2^-$, $S_2C_2(CN)_2^{2-}$ [194], edta, cyst, Etcyst [195]) indicate that the ease of production and chemical stability of the one- and two-electron reduced products increase with increasing sulphur substitution, i.e. $[Mo_2O_4]^{n+} < [Mo_2O_3S]^{n+} < [Mo_2O_2S_2]^{n+}$. However, in no case were these products stable for an extended period of time. Interestingly, Kathirgamanathan et al. [196] report that electrolysis of solutions containing pairs of $[Mo_2O_{4-x}(\mu\text{-}S)_x(cyst)_2]^{2-}$ ($x = 1, 2$) complexes leads to the formation of Mo_3^{IV} and mixed-valence tetranuclear complexes (Section D(ii)(d)). The reversible one-electron reduction of related $[Mo_2S_4]^{2+}$ complexes corroborates the increased stability of the reduced species when the complex possesses a sulphur-rich coordination sphere [197]. The aquated electron, produced in pulse radiolytic experiments, reduces the Mo^V complexes $[Mo_2O_4(edta)]^{2-}$, $[Mo_2O_2(\mu\text{-}S)_2(edta)]^{2-}$, $[Mo_2O_4(ox)_2(H_2O)_2]^{2-}$ and $[Mo_2O_4(cyst)_2]^{2-}$ to the corresponding $Mo^{IV}Mo^V$ trianions [198]. The transient mixed-valence species are rapidly re-oxidized with oxygen with rate constants of 10^8 M^{-1} s^{-1} but in the absence of oxygen decompose in 5–10 s to form unidentified products. In contrast with results drawn from the above electrochemical studies, the presence of sulphur in the coordination sphere does not appear to enhance the stability of the $Mo^{IV}Mo^V$ species. Reduction of triply bridged species such as $[Mo_2O_2(SePh)_6(OMe)]^-$ also produces $Mo^{IV}Mo^V$ species but these are only stable at low temperatures [199]. Chemical reductions often contrast with those produced electrochemically, and it has been stated [200] that $[Mo_2O_4(edta)]^{2-}$ produces $[Mo_2O_2(OH)_2(edta)]^{4-}$ and an $[Mo^{III}Mo^{IV}]_2$ complex when reduced with Zn/Hg. Indeed, the putative $[Mo^{III}Mo^{IV}]_2$ tetramer may be isolated upon oxidation of $[Mo_2(OH)_2(OAc)(edta)]^-$ (Section D(ii)(d)) [201,202]. It is clear from this brief account that many mysteries related to chemical and electrochemical redox reactions of dinuclear Mo^V complexes remain to be solved.

The reactions of $(PPh_4)_2[MoS_4]$ with $MoBr_4$ (with SMe_2 as solvent) and $MoBr_2(NO)_2$ (with MeCN as solvent) produce the μ-thio compounds $(PPh_4)_2[S_2Mo(\mu\text{-}S)_2MoBr_3(SMe_2)]$ and $PPh_4[S_2Mo(\mu\text{-}S)_2MoBr_2(NO)_2]$ respectively [203]. These $Mo^{III}Mo^{VI}$ complexes have been characterized by elemental analysis and IR spectroscopy. Ill-defined species of purported formulation $Mo_2Cl_6(SR)_3$ are formed upon the reaction of $MoCl_5$ and Me_3SiSR in CS_2 [204].

Rakowski DuBois and coworkers have elegantly exploited the redox-active nature of μ-thiocyclopentadienyl–Mo complexes in order to modify the reactivity of the μ-thio ligands. In the course of these studies they have reported several mixed-valence species. The first was prepared and structurally characterized in 1979 [205]. Isovalent $Cp_2Mo_2(SC_nH_{2n}S)_2$ ($n = 2, 3$) complexes undergo two chemical or electrochemical oxidations, the first of which produces green $[Cp_2Mo_2(SC_nH_{2n}S)_2]^+$ which were isolated as BF_4^- salts. The compounds exhibit magnetic moments (1.68 BM) indicative of the presence of one unpaired electron. The structure of the cation in $[Cp_2Mo_2(SC_3H_6S)_2]BF_4$ is shown in Fig. 23. The planes of the propanedithiolate ligands bisect the Mo–Mo bond and the two equivalent halves of the molecule are related by an inversion centre. The Mo–Mo distance of 2.599(1) Å is indicative of a single bond. Subsequently, the $Mo^{III}Mo^{IV}$ complex $(MeCp)_2Mo_2(\mu\text{-}S)(\mu\text{-}SMe)(\mu\text{-}S_2CH_2)$ was prepared by electrochemical and chemical reduction of $[(MeCp)_2Mo_2(\mu\text{-}S)(\mu\text{-}SMe)(\mu\text{-}S_2CH_2)]^+$ [206]. The complex is blue in the solid state but dissolves to produce an intense pink solution exhibiting a near-IR band at 1360 nm ($\epsilon = 975$) and an ESR spectrum with $g = 1.993$ and $A(^{95}Mo) = 14$ G. The complex is methylated with MeI forming another mixed-valence complex, $[(MeCp)_2Mo_2(\mu\text{-}SMe)_2(\mu\text{-}S_2CH_2)]^+$ [206], and undergoes a photochemical reaction to produce the mixed-valence tetramer $[(MeCp)_2Mo_2(\mu\text{-}S)(\mu\text{-}SMe)(\mu\text{-}S_2CH_2)]_2$ [206,207]. These initial studies have been extended and a thorough investigation of the mixed-valence nature of $[Cp_2Mo_2(S)_x(SR)_{4-x}]^n$ ($n = +1, 0, -1$) complexes has been reported [208]. On the basis of cyclic voltammetric and X-ray diffraction studies the complexes are postulated to possess structures

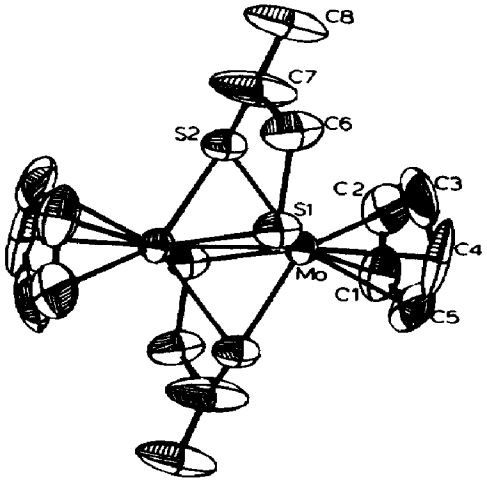

Fig. 23. Structure of the $[Cp_2Mo_2(SC_3H_6S)_2]^+$ cation. Reproduced with permission from ref. 205.

identical with their well-characterized Mo_2^{IV} or Mo_2^{III} precursors. The mixed-valence complexes exhibit near-IR absorptions, the energies and intensities of which are markedly sensitive to ligand type, while the peak widths at half-height are considerably narrower than those predicted for Class II complexes [7]. The spectra are also solvent independent. Measured comproportionation constants for these complexes range from 10^{11} to 10^{15}. Their ESR spectra exhibit features arising from coupling of the unpaired electron to two equivalent molybdenum nuclei, and the low coupling constants ($A = 14$–18 G) are consistent with some ligand contribution to the electron density. An intriguing result is the detection of a tight ion pair of Na^+ and $[(MeCp)_2Mo_2(\mu\text{-}S)_2(S_2CH_2)]^-$ in thf solution. The presence of the ion pair was revealed by hyperfine coupling to molybdenum and the associated sodium counter-ion with spin 3/2 ($A_{Na} = 15$ G). This result is indirect evidence for the presence of spin density on the thio ligands, which is consistent with a contribution of the sulphur *p*-orbitals to the HOMO. The reactivity of the mixed-valence species has also been investigated [206,207]. In a recent report, the redox properties of $[Cp_2Mo_2(\mu\text{-}S_2CH_2)(\mu\text{-}S)(\mu\text{-}SC(H)C(H)Ph)]Br$ were reported [209]. The compound undergoes reversible electrochemical reduction or chemical reduction to form a mixed-valence complex, the ESR spectrum of which indicates electron delocalization over both molybdenum atoms. The mixed-valence complex rapidly disproportionates to analogous Mo^{III} and Mo^{IV} derivatives. A tetranuclear complex is also proposed to result from reactions involving the mixed-valence species. Neutral $Cp_2Mo_2(\mu\text{-}SMe)_4$ is readily oxidized to $[Cp_2Mo_2(\mu\text{-}SMe)_4]^+$ with $AgPF_6$ in ethanol [210]. The isovalent precursor and $[Cp_2Mo_2(\mu\text{-}SMe)_4]PF_6$ exhibit structures composed of two CpMo units linked by four symmetri-

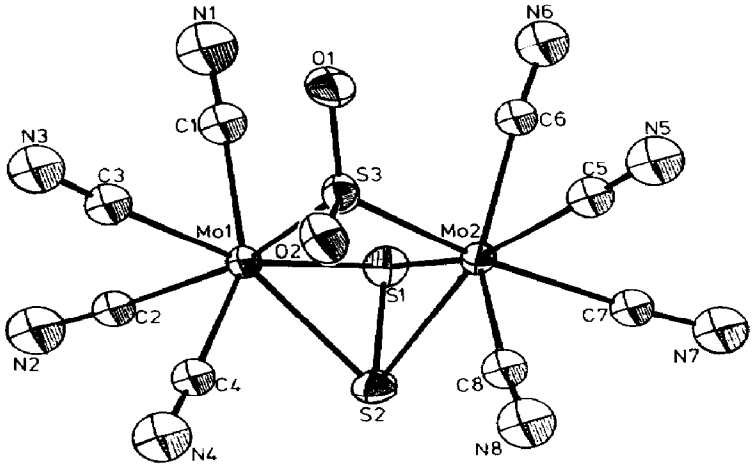

Fig. 24. Structure of the mixed-valence anion in **45**. Reproduced with permission from ref. 211.

cally positioned μ-SMe ligands. The Mo–Mo bond of the monocation is slightly longer (2.617(4) Å) than the Mo–Mo bond in the neutral complex (2.603(2) Å).

Oxygenation of an aqueous solution of $K_6[Mo_2(\mu\text{-}S)_2(CN)_8]$ results in the formation of violet crystals with the composition $K_{4+x}[Mo^{III}Mo^{IV}(\mu\text{-}SO_2)(\mu\text{-}S_2)(CN)_8]_x[Mo_2^{IV}(\mu\text{-}SO_2)(\mu\text{-}S_2)(CN)_8]_{1-x} \cdot 4H_2O$ ($x = 0.3$) (**45**) [211]. The two co-crystallized anions are formed by sequential oxidation of the starting material and both possess the structure shown in Fig. 24 but with apparently different Mo–Mo bond distances. The ESR spectrum of **45** in water is consistent with the interaction of an unpaired electron with two equivalent molybdenum atoms ($g = 2.012$, $A = 19.2$ G). MO calculations show that these species are best described as complexes of SO_2^{2-} and S_2^{2-}, with a metal–metal double bond in the case of the Mo_2^{IV} complex and a reduced bond order in the case of the $Mo^{III}Mo^{IV}$ complex.

An unusual metal–metal-bonded Mo_2^{7+} complex has been reported by Cotton and Poli [212]. The reaction of $Mo_2(OAc)_4$, Me_3SiI and I_2 in thf results in the precipitation of a grey solid formulated as $[Mo_2(\mu\text{-}O)(\mu\text{-}I)(\mu\text{-}OAc)I_2(thf)_4][MoOI_4(thf)]$ on the basis of an X-ray diffraction study. The cation possesses a distorted edge-sharing bi-octahedral structure with a short Mo–Mo separation of 2.527(2) Å. The μ-O and μ-I ligands define the shared edge while the μ-OAc group serves to link axial sites on the two octahedra. Terminal iodide ligands are coordinated *trans* to the acetate donor atoms and the remainder of the coordination spheres are occupied by thf ligands. The cation may possess either a $\sigma^2\pi^2\delta$ or a $\sigma^2\pi^2\delta^*$ electron configuration. While ESR studies were not reported the effective magnetic moment of 3.14 BM at room temperature is consistent with the presence of a single unpaired electron in both the cation and the Mo^V anion. Contrasting with the above result, the oxidation of $W_2(O_2CR)_4$ complexes with Br_2 or I_2 results in the formation of W_2^{5+} complexes (Section D(iii)(b)).

Green crystals of $(N^nBu_4)_2[Mo_2Cl_9]$ (**46**) result from the reaction of $[Mo(CO)_4Cl_3]^-$ and $MoCl_5$ in the presence of N^nBu_4Cl (eqn. (8)) [213,214]:

$$MoCl_5 + N^nBu_4[Mo(CO)_4Cl_3] + N^nBu_4Cl \rightarrow (N^nBu_4)_2[Mo_2Cl_9] + 4CO \quad (8)$$

The anion of **46** is likely to exhibit a confacial bi-octahedral structure similar to those established for $[Mo_2Cl_9]^{3-}$ and $[W_2Cl_9]^{n-}$ ($n = 2, 3$) [215,216]. Variable-temperature magnetic susceptibility measurements are consistent with an appreciable population of $S = 1/2$ and $S = 3/2$ ground and excited states respectively at temperatures greater than 95 K.

The $[MoS_4]^{2-}$ anion acts as a bidentate ligand to carbonyl–Mo^0 fragments to produce Class I compounds with disparate oxidation states. The dinuclear and trinuclear compounds $(NEt_4)_2[(CO)_4Mo(\mu\text{-}S)_2MoS_2]$ and

$(NEt_4)_2[(CO)_4Mo(\mu\text{-}S)_2Mo(\mu\text{-}S)_2Mo(CO)_4]$ are prepared by the reaction of $(NEt_4)_2[MoS_4]$ and $Mo(CO)_4(nbd)$ [217]. The formulation of the complexes as Mo^0Mo^{VI} and $Mo_2^0Mo^{VI}$ species respectively is supported by electrochemical studies but no X-ray diffraction studies have been reported. The six-unit difference in the oxidation states of the metals is exceptional and is matched only by the W^0W^{VI} compound $W_2(O^iPr)_6(CO)_4$ reported by Cotton and Schwotzer [218] (Section D(iii)(b)).

Lavender needles of the Mo_2^{5+} compound $K_3[Mo_2(SO_4)_4] \cdot 3.5H_2O$ (**47**) are formed by slowly mixing solutions of $K_4[Mo_2(SO_4)_4]$ and K_2SO_4 in dilute H_2SO_4 [219,220]. Interestingly, the trianion can also be formed by irradiation of $[Mo_2(SO_4)_4]^{4-}$ in 5 M H_2SO_4, a reaction in which protons act as electron acceptors to yield H_2 [221]. In the anion of **47** (Fig. 25) four bidentate sulphate ions, related by a fourfold axis, bridge the strongly metal–metal-bonded molybdenum atoms. Consistent with a $\sigma^2\pi^4\delta$ electronic configuration, a lengthening of the Mo–Mo bond in $[Mo_2(SO_4)_4]^{3-}$ (2.164(2) Å) relative to that in $[Mo_2(SO_4)_4]^{4-}$ (2.11(1) Å for the $\sigma^2\pi^4\delta^2$ bond) is observed. The structures of the related compounds $K_4[Mo_2(SO_4)_4]\text{-}X \cdot 4H_2O$ (X = Cl [222], Br [223]) have also been reported; they possess the same basic structure as **47** except that $Mo \cdots X$ interactions take the place of $Mo \cdots OH_2$ interactions. Compound **47** is paramagnetic, its behaviour following the Curie law over the temperature range 60–300 K ($\mu_{eff} = 1.65$ BM), and it exhibits an ESR spectrum interpreted in terms of axial symmetry ($g_\parallel = 1.891$, $g_\perp = 1.909$; $|A_\parallel| = 45.2 \times 10^{-4}$ cm^{-1} and $|A_\perp| = 22.9 \times 10^{-4}$ cm^{-1}) and electron delocalization over equivalent molybdenum atoms [220]. A detailed analysis of the vibrational spectrum of **47** has been presented, and strong bands at 373 and 386 cm^{-1} were assigned to ν(Mo–Mo) for non-equivalent ions in the unit cell [224]. Pernick and Ardon

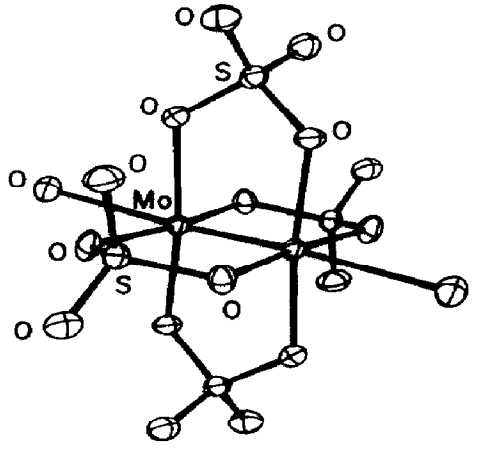

Fig. 25. Structure of the anion in **47**. Reproduced with permission from ref. 220.

[225] subsequently reported that blue $[Mo_2(SO_4)_4]^{3-}$ is stable in 2 N H_2SO_4 but disproportionates in other acids, the latter reaction being reversed by the addition of K_2SO_4. These authors also reported an improved preparation for **47** [225]. The products of the disproportionation reaction were later identified as complexes possessing the $[Mo_2]^{4+}$ and $[Mo_2]^{6+}$ cores [226]. The electrochemical oxidation of $Mo_2(O_2C^iPr)_4$ yields $[Mo_2(O_2C^iPr)_4]^+$; ESR properties indicate delocalization of the unpaired electron over two equivalent molybdenum nuclei [227]. The iodide salts of $[Mo_2(O_2CR)_4]^+$ (R = Et, CMe_3, Ph) are produced by iodine oxidation of $Mo_2(O_2CR)_4$. The compounds are paramagnetic ($\mu_{eff} = 1.66$ BM), possess an Mo–Mo bond order of 3.5 and a $\sigma^2\pi^4\delta$ ground state [228]. Similar electrochemical oxidation of $[Mo_2Cl_8]^{4-}$ produced a short-lived species, presumably $[Mo_2Cl_8]^{3-}$, which could not be observed by ESR spectroscopy. The formation of $[Mo_2(O_2CCF_3)_4]^-$ in pulse radiolysis experiments has also been reported [229].

The redox properties of $Mo_2(tmtaa)_2$ have been investigated by Mandon et al. [230]. The compound undergoes a chemically and electrochemically reversible one-electron oxidation and an irreversible one-electron reduction. Ferricenium oxidation results in the formation of a dark purple Mo_2^{5+} complex which exhibits an ESR spectrum consistent with an $S = 1/2$ ground state ($g = 1.959$, $A = 32.2 \times 10^{-4}$ cm^{-1}). The X-ray structure of $[Mo_2(tmtaa)_2]PF_6 \cdot CH_2Cl_2$ revealed discrete dinuclear cations composed of four-coordinate Mo(tmtaa) units linked via a direct Mo–Mo bond of length 2.221 Å and with a bond order of 3.5. The molybdenum atoms are displaced 0.57 Å from the N_4 coordination plane toward the other molybdenum atom and the ligands on adjacent molybdenum atoms are staggered by about 90°. The unstable reduced species formed by Na/Hg reduction exhibits an ESR spectrum consistent with electron delocalization over two equivalent molybdenum atoms ($g = 1.964$, $A = 23.3 \times 10^{-4}$ cm^{-1}).

The reaction of $Mo_2(OAc)_4$, N^nBu_4Br and gaseous HBr in refluxing methanol results in the formation of brown $N^nBu_4[Mo_2Br_6]$ [231]. The compound is paramagnetic ($\mu_{eff} = 1.5$ BM) and exhibits a broad ESR signal at $g = 1.98$. It is postulated that the $[Mo_2Br_6]^-$ anion bears a close structural relationship to triply bonded $Mo_2^{III}L_6$ complexes and possesses a $\sigma^2\pi^4\pi^*$ electron configuration. Electrochemical studies [232] suggest that $[Mo_2Br_6]^-$ participates in a disproportionation reaction in solution (eqn. (9)):

$$2[Mo_2Br_6]^- \rightarrow [Mo_2Br_6]^{2-} + Mo_2Br_6 \qquad (9)$$

The $Mo_2X_4(PR_3)_4$ complexes are readily oxidized to yield mixed-valence $Mo^{II}Mo^{III}$ species. Electrochemical oxidation of $Mo_2Cl_4(PR_3)_4$ (R = Et, ^{n}Pr), α-$Mo_2Cl_4(dppe)_2$ and $Mo_2Br_4(dppe)_2$ yields paramagnetic species

which are ESR active although somewhat unstable [233]. Low temperature oxidations using $NOPF_6$ permit the isolation of the cations.

Although structurally characterized, the precise formulation of the compound obtained upon reaction of $MoCl_2(CO)_4$ and $P(OMe)_3$ in dichloromethane remains unknown [234]. A number of formulations, including one containing the $Mo^{II}Mo^{III}$ cation $[Mo_2Cl_3(CO)_4\{P(OMe)_3\}_4]^{2+}$, are possible for the compound, at present formulated as $[Mo_2Cl_3(CO)_4\{P(OMe)_3\}_4]^{n+}$-$[MoOCl_4\{OP(OMe)_2\}]^{n-}$. The cation is a dinuclear seven-coordinate trichloro-bridged complex possessing approximate C_{2v} symmetry and an Mo–Mo distance of 3.575 Å. Structural characterization of other salts of the cation would resolve this dilemma.

Oxidation of $Mo_2(OAc)_4$ in 2 M HCl at high temperatures was first noted by Anderson and coworkers [235,236] who precipitated several salts formulated as $K_6[Mo_3Cl_{12}]$, $(NH_4)_7[Mo_3Cl_{13}] \cdot H_2O$ and $Cs_6[Mo_4Cl_{12}]$. They also described salts of $[Mo_2X_8]^{3-}$ but redox titrations indicating a molybdenum oxidation state of III were inconsistent with this formulation [237]. Subsequently, the reaction of $Mo_2(OAc)_4$ with 12 M HCl at 60 °C was reported to produce the $Mo^{II}Mo^{III}$ anion $[Mo_2Cl_8]^{3-}$, and salts purported to be $A_3[Mo_2Cl_8]$ ($A = Rb^+$ or Cs^+) were isolated [238]. Improved preparations of the chloro complex were subsequently reported [239]. The X-ray structure of the material revealed an anion which appeared to possess a tri-μ-chloro confacial bi-octahedral structure with one-third of the bridging ligands missing. The bromo analogue exhibits a similar structure [240]. The structure determinations were reported before careful magnetic susceptibility measurements showed the compounds to be diamagnetic, indicating the possible presence of a hydride ligand in the "vacant" coordination site. The first evidence for this thesis was chemical [241] but crystallographic evidence appeared later. The disorder problems associated with the structural characterization of the Rb^+ and Cs^+ salts did not arise in the case of the pyH^+ salt and the hydride ligand was revealed [242]. Neutron diffraction studies [243] unambiguously confirmed the presence of the hydride ligand. The isovalent Mo^{III} complexes have confacial bi-octahedral structures; two μ-X and a μ-H ligand form the shared face while the remaining halide ligands are terminally bonded to the molybdenum centres.

The dark brown complex $Mo_2(O^iPr)_4(dmpe)_2$, prepared by reacting $Mo_2(O^iPr)_4(HO^iPr)_4$ and dmpe in toluene, contains an unbridged triple bond uniting Mo^0 and Mo^{IV} centres [244]. As shown in Fig. 26, the bidentate dmpe ligands are bonded to one molybdenum atom only while the four alkoxide ligands are bonded to the other. The complex adopts a staggered conformation and it is proposed that it possesses a $\sigma^2\pi^4$ triple bond. Two electrons on Mo^0 are localized in the d_{xy} orbital (a δ component in other cases) while the d_{xy} orbital of Mo^{IV} is involved in Mo–O π-bonding.

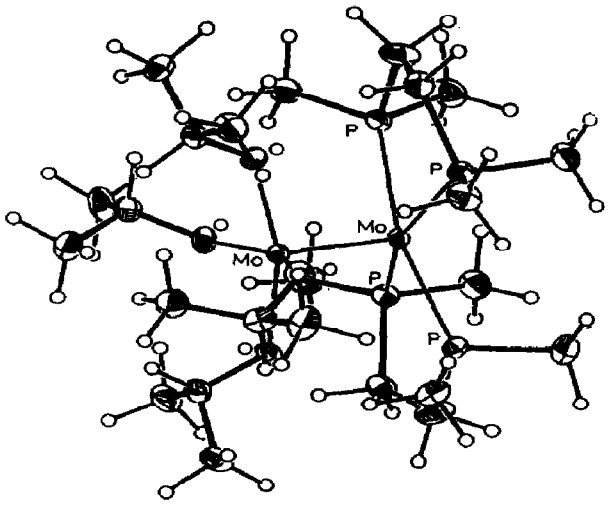

Fig. 26. Structure of $Mo_2(O^iPr)_4(dmpe)_2$. Reproduced with permission from ref. 244.

Dinuclear compounds $(\eta^7\text{-}C_7H_7)MoX_3Mo(\eta^7\text{-}C_7H_7)$ (X = Cl, Br, I) are formed by reaction of $[Mo(CO)_3(\eta^7\text{-}C_7H_7)]^+$ with Me_3SiX [245]. The complexes have been subjected to electronic and photoelectronic spectral studies [246] which are consistent with an unsymmetrical mixed-valence (Mo^0Mo^I) ground state. In the related reaction of $(\eta^7\text{-}C_7H_7)Mo(CO)_2Br$ with sodium alkoxides or phenoxides complexes of the type $(\eta^3\text{-}C_7H_7)(CO)_2Mo(OR)_3\text{-}Mo(\eta^7\text{-}C_7H_7)$ (R = Me (**48**), Et, Ph, C_6H_4Me, C_6H_4Cl) are formed [247]. The paramagnetic complexes were characterized by elemental analysis, IR, ESR and mass spectra, and by an X-ray structure analysis of **48** (Fig. 27). ESR spectra are consistent with the localization of the unpaired electron on

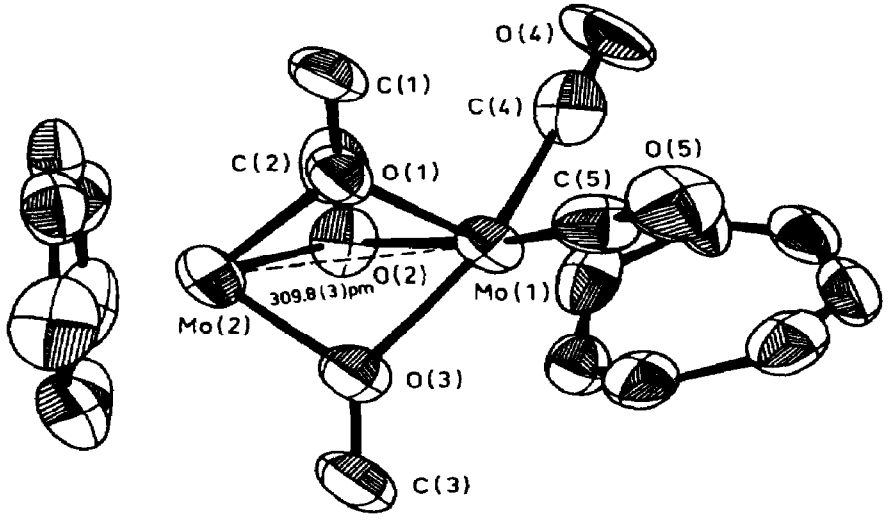

Fig. 27. The molecular structure of **48**. Reproduced with permission from ref. 247.

only one molybdenum centre, and superhyperfine coupling to seven magnetically equivalent protons suggests that Mo(2) is the site of electron localization.

(c) Trinuclear compounds

A number of trinuclear complexes containing $[MoS_4]^{2-}$ fragments have been reported. Black $(NEt_4)_2[S_2Mo(\mu\text{-}S)_2MoS(\mu\text{-}S)_2MoS_2]$ (Fig. 21(b)) is produced when NEt_4Cl and $(NH_4)_2[MoS_4]$ are heated together in dmf [248]. A linear array of molybdenum atoms is observed; the central molybdenum atom features a square-pyramidal structure while the terminal molybdenum atoms possess tetrahedral geometries. The central and terminal molybdenum atoms are assigned oxidation states of IV and VI respectively. Detailed molecular orbital calculations are consistent with the localized mixed-valence formulation [249]. The $[S_2Mo(\mu\text{-}S)_2MoO(\mu\text{-}S)_2MoS_2]^{2-}$ complex has also been reported and structurally characterized [250]. Related species are formed by reductive cleavage of α- and β-$(N^nBu_4)_4[Mo_8O_{26}]$ (7 : 1 ratio) upon reaction with $(Me_3Si)_2S$ [251]. When eight equivalents of $(Me_3Si)_2S$ are used in the reaction, a dark red diamagnetic compound, $(N^nBu_4)_2[Mo_3S_{7.45}O_{2.55}]$, may be isolated. A crystal examined by X-ray diffraction contained approximately equal amounts of two anions, $[(\eta^2\text{-}S_2)MoO(\mu\text{-}S)_2MoO(\mu\text{-}S)_2MoS_2]^{2-}$ (Fig. 21(c)) and $[(\eta^2\text{-}S_2)MoO(\mu\text{-}S)_2MoO(\mu\text{-}S)_2MoOS]^{2-}$, which are postulated to contain central and terminal molybdenum atoms in oxidation states of IV and VI respectively. Recently, the synthesis and characterization of pure $(PPh_4)_2[(\eta^2\text{-}S_2)MoO(\mu\text{-}S)_2MoO(\mu\text{-}S)_2MoS_2]$ was reported [252].

A blue compound, formulated as the $Mo_2^{IV}Mo^{VI}$ compound $K_6[Mo_3O_6(CN)_8]\cdot 2H_2O$ is obtained from an aqueous solution of $K_4[MoO_2(CN)_4]$ by repeated precipitation with methanol [253]. The compound, characterized by elemental analysis and IR spectroscopy only, remains inadequately characterized. Also, the structure of $Mo_3O_4(acac)_3(OEt)_3$ has been determined but details have not been presented [254].

The trinuclear compound $(PPh_4)_2[S_2Mo(\mu\text{-}S)_2Mo(NNMe_2)_2(\mu\text{-}S)_2MoS_2]$ (**49**) is produced upon addition of PPh_4Br to the orange acetonitrile solution formed when $S_2Mo(\mu\text{-}S)_2Mo(NNMe_2)_2(PPh_3)$ is reacted with LiSPh [255]. The diamagnetic anion of **49** is composed of a *trans*-$Mo(NNMe_2)_2$ unit coordinated to two bidentate $[MoS_4]^{2-}$ ligands. The geometry and orientation of the $NNMe_2$ groups suggest that they are best described as coordinated isodiazene ligands. In this case, the central molybdenum atom would possess an oxidation state of II, while the terminal molybdenum atoms retain their original oxidation state of VI. An uncharacterized compound of purported formula $(PPh_4)_2[Mo_3S_8(NNMe_2)(MeCN)]$ results from the direct reaction of $S_2Mo(\mu\text{-}S)_2Mo(NNMe_2)_2(PPh_3)$ with $[MoS_4]^{2-}$.

The reaction of $Mo(CO)_6$ with a refluxing mixture of HOAc and acetic anhydride is complex but suitable work-up of the reaction mixtures, including permanganate oxidation in two cases, results in the isolation of three trinuclear mixed-valence compounds [256,257]. These are $[Mo_3(\mu\text{-}CMe)_2(OAc)_6(H_2O)_3]SbF_6 \cdot 3H_2O$ (**50**) and $[Mo_3(\mu_3\text{-}CMe)_2(OAc)_6(H_2O)_3]X_2$ ($X = CF_3SO_3^-$ (**51**), $C_7H_7SO_3^-$ (**52**)). While the cation in the latter compounds was originally formulated as $[Mo_3(\mu_3\text{-}OEt)_2(OAc)_6(H_2O)_3]^{2+}$ [258], detailed studies subsequently revealed the presence of μ_3-ethylidyne ligands [256,257]. The complexes consist of a triangle of molybdenum atoms bridged above and below the plane of the triangle by μ_3-CMe ligands and along each edge by two acetate ligands; a water molecule is also bonded to each molybdenum atom (see Fig. 13(a)). The compounds are paramagnetic and possess fractional Mo–Mo bond orders of 5/6 for **50** (Mo–Mo = 2.812 Å (average) and 2/3 for **51** and **52** (Mo–Mo = 2.883(1) Å and 2.891(1) Å respectively). Their electronic structure and relationship to other triangular complexes have been discussed [259,260]. The black $Mo^{III}Mo_2^{IV}$ complex $Cp_3Mo_3(\mu_3\text{-}S)(\mu\text{-}S)_3$, predicted to have the triangular structure shown in Fig. 13(b) (each molybdenum atom is bonded to a Cp ligand rather than the three terminal ligands shown), is produced when $CpMoH(CO)_2\{P(OPh)_3\}$ reacts with propylene sulphide [261]. Cyclic voltammograms of $[Mo_3S_4(ida)_3]^{2-}$ show two reversible one-electron waves indicating the existence of $Mo^{III}Mo_2^{IV}$ and $Mo_2^{III}Mo^{IV}$ complexes [262].

The trinuclear $[Mo_3O_4(aq)]^{4+}$ and $[Mo_3O_4(ox)_3(H_2O)_3]^{2-}$ complexes may be reversibly reduced electrochemically in acidic media in two sequential steps which are pH dependent (eqns. (10) and (11)) [263–265]:

$$Mo_3^{IV} + 2e^- \rightarrow Mo_2^{III}Mo^{IV} \quad (10)$$

$$Mo_2^{III}Mo^{IV} + e^- \rightarrow Mo_3^{III} \quad (11)$$

The mixed-valence aqua complex is diamagnetic and protonation of the μ-oxo ligands accompanies reduction [265]. The complex exhibits a broad intervalence CT band at 1050 nm ($\epsilon = 100$ per molybdenum atom). Isotopic exchange experiments show that all the core oxygen atoms of $[Mo_3O_4(aq)]^{4+}$ are retained upon reduction to the $Mo_2^{III}Mo^{IV}$ analogue and reoxidation to the starting material [266]. Recently, the $[Mo_3(S)SO_2(aq)]^{2+}$ ion was shown to undergo a similar stepwise reduction [267].

A number of $Mo_2^{III}Mo^{IV}$ complexes have been isolated in the solid state. Dark blue $[Mo_3(\mu_3\text{-}O)(\mu\text{-}Cl)_3(\mu\text{-}OAc)_3(H_2O)_3](ClO_4)Cl$ is formed upon work-up of the reaction of $MoCl_2(CO)_4$ and acetic acid–acetic anhydride [268]. A related compound, $[Mo_3(\mu_3\text{-}CMe)(\mu\text{-}Br)_3(\mu\text{-}OAc)_3(H_2O)_3]ClO_4$ results from the reaction of $Mo(CO)_6$ and NaBr in acetic acid–acetic anhydride [269]. Both complex cations exhibit the structure shown in Fig. 13(b) with

crystallographically imposed and approximate C_3 symmetry respectively. Similar structures have been established for the complexes $[Mo_3(\mu_3\text{-}O)(\mu\text{-}Br)_3(\mu\text{-}O_2CH)Cl_3]^-$ [270], $[Mo_3(\mu_3\text{-}O)(\mu\text{-}Cl)_3(\mu\text{-}OAc)_2Cl_5]^{2-}$ [271], $[Mo_3(\mu_3\text{-}O)(\mu\text{-}Cl)_3(\mu\text{-}OAc)_3Cl_3]^-$ [271] and $Mo_3(\mu_3\text{-}S)_2(\mu\text{-}Cl)_3\{S_2P(OEt)_2\}_3$ [272]. The electronic structure and structural relationship of the above complexes have been discussed [259,260].

The trinuclear cluster compound $Mo_3HI_7(thf)_3$ (**53**) is formed as a minor product in the reactions of $MoI_2(CO)_3(thf)_2$ or $Mo(CO)_3(thf)_3$ and I_2 in thf at reflux [273]. The major product of the above reactions, likely to be an oligomer such as $[MoI_2(thf)_n]_x$, reacts with nitriles to yield small amounts of analogous $Mo_3HI_7L_3$ (L = MeCN (**54**), PhCN (**55**)) compounds [273]. Compounds **53**, **53** · thf, **54** · MeCN and **55** · PhCN have been structurally characterized by X-ray diffraction techniques; a view of the core of the $Mo_3HI_7L_3$ compounds is shown in Fig. 28 and the interrelationship of this and related fragments of the $[Mo_6X_8]^{4+}$ core is shown in Fig. 29 (see Fig. 29(f) in the case of $Mo_3HI_7L_3$). In the unsolvated compound **53**, the cluster possesses C_{3v} symmetry while the clusters are of lower symmetry in the solvated compounds. In all compounds it is proposed that the hydride ligand (revealed in the ^1H NMR spectrum of **53** at δ −10.31) occupies the triply bridging position opposite to that occupied by the μ_3-I ligand. Fenske–Hall MO calculations support the presence of strong metal–metal interactions in these mixed-valence Mo_3^{8+} compounds which use ten elec-

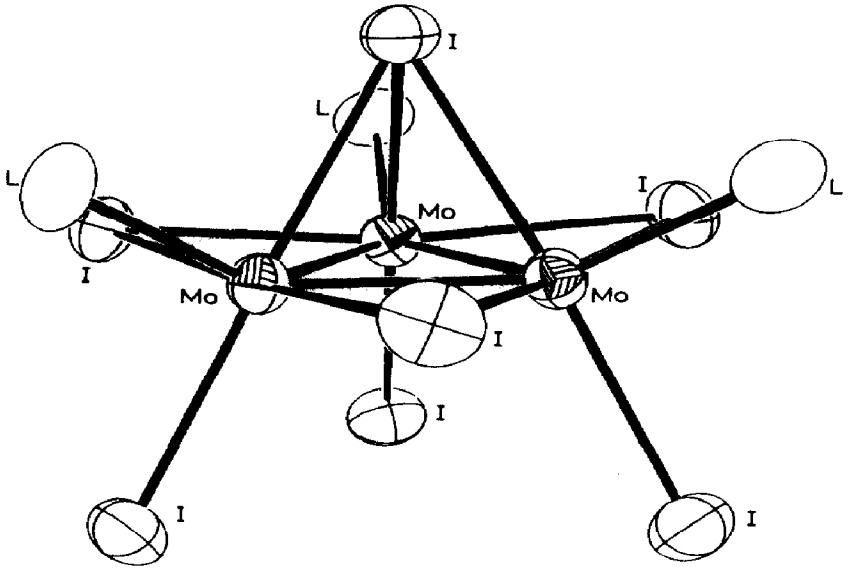

Fig. 28. A view of the core of the $Mo_3HI_7L_3$ compounds **53**–**55**. The hydride ligand has not been located but probably resides opposite the μ_3-I ligand. Reproduced with permission from ref. 273.

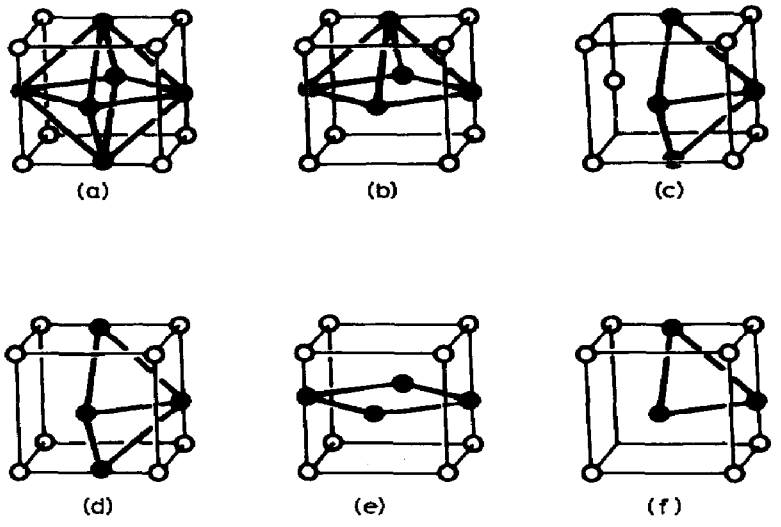

Fig. 29. The relationship of metal clusters derived from the $[M_6(\mu_3\text{-}X)_8]^{n+}$ core. The solid and empty circles represent M and X atoms respectively. In most compounds the M atoms are further coordinated by a terminal ligand (not shown).

trons for cluster bonding and a hydride capping ligand. The $Mo_2^0Mo^{VI}$ compound $(NEt_4)_2[(CO)_4Mo(\mu\text{-}S)_2Mo(\mu\text{-}S)_2Mo(CO)_4]$ has been prepared by reaction of $(NEt_4)_2[WS_4]$ and $Mo(CO)_3(nbd)$ [217].

The reaction of $Cp_2Mo_2(CO)_4$ with ethyl diazoacetate in boiling toluene results in the formation of green diamagnetic $Cp_3Mo_3(\mu_3\text{-}N)(O)(CO)_4$ [274]. The complex, as shown in Fig. 30, exhibits an unusual structure with an almost planar Mo_3N core incorporating a μ_3-nitrido ligand possessing a T-shaped coordination geometry. The Mo(2) and Mo(3) atoms are further coordinated by two carbonyl ligands and a cyclopentadienyl ligand, creating

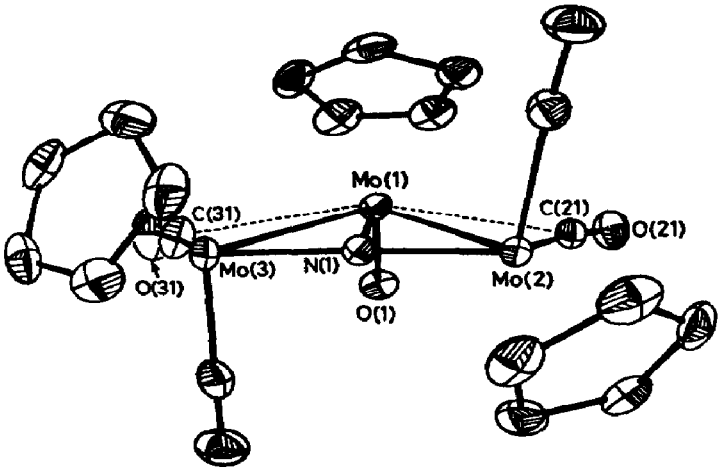

Fig. 30. Structure of $Cp_3Mo_3(\mu_3\text{-}N)(O)(CO)_4$. Reproduced with permission from ref. 274.

an environment typical of low valent molybdenum. In contrast, Mo(1), which is bound to an oxo and a cyclopentadienyl ligand, is in an environment characteristic of high valent molybdenum. However, the valence states of the molybdenum atoms are difficult to determine. A tetranuclear mixed-valence complex possessing T-shaped coordination at two nitrido ligands has been reported (Section D(ii)(d)).

(d) Tetranuclear compounds

A number of tetranuclear $Mo_2^{V}Mo_2^{VI}$ compounds have been reported but it is unlikely that they have been correctly formulated. Attempts to grow crystals of $MeMoCl_2(O^nPr)_2$ produced red crystals (**56**) formulated as $Mo_4O_6Cl_4(O^nPr)_6$ on the basis of an X-ray diffraction study [275]. The $Mo_2^{V}Mo_2^{VI}$ mixed-valence formulation could not be substantiated by magnetic and spectroscopic studies as only a few crystals of the substance were obtained. Subsequently, Koch and Lincoln [276] offered an alternative interpretation of the X-ray diffraction data for **56**. These workers noted that the Mo(2)–O(4) distance of 2.13(1) Å lies outside the range for terminal alkoxide ligands. Further, they suggested that this anomaly could be removed if the ligands involved were in fact propanol ligands. Compound **56**

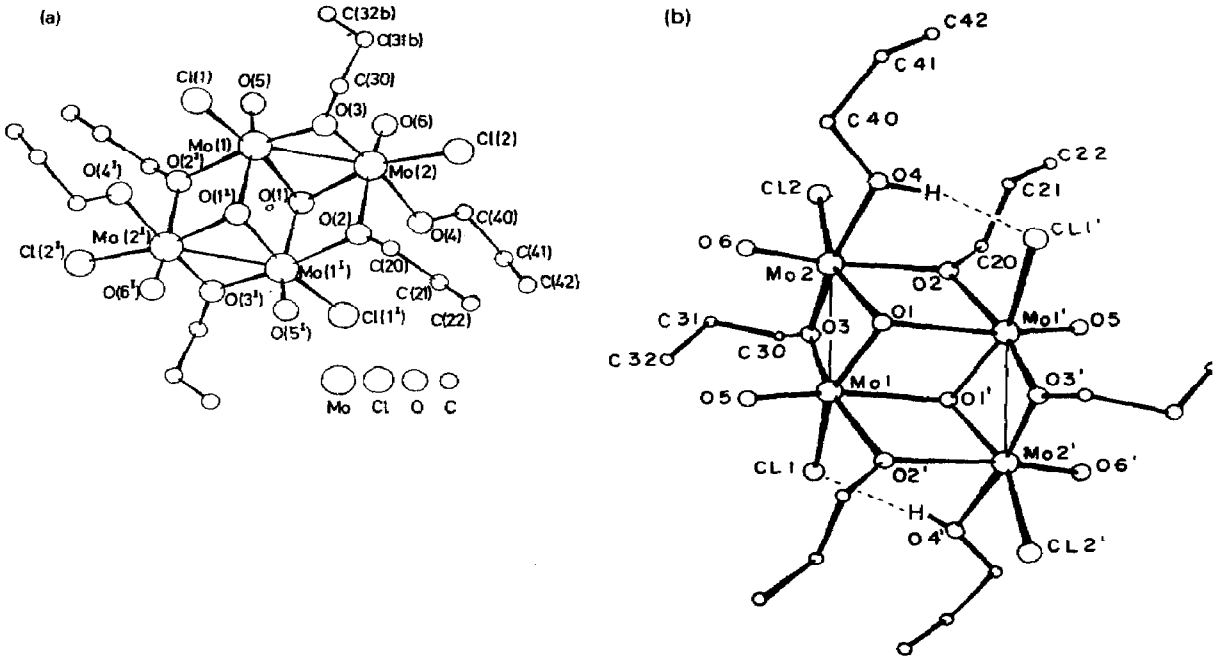

Fig. 31. The structures of **56**. (a) The mixed-valence structure originally proposed by Beaver and Drew. Reproduced with permission from ref. 275. (b) The tetranuclear Mo^{V} structure proposed by Koch and Lincoln. Reproduced with permission from ref. 276.

would then be the isovalent Mo^{V} compound, $Mo_4O_6Cl_4(O^nPr)_4(HO^nPr)_2$. The original structure and that proposed by Koch and Lincoln are shown in Fig. 31. The same argument may apply to another compound which has been structurally characterized as an $Mo_2^{V}Mo_2^{VI}$ tetramer. The orange–brown compound (**57**) obtained upon the reaction of $MoCl_5$ with either 2-(2′-thienyl)benzimidazole or 2-(2′-thienyl)-1-(2′-thienylmethyl)benzimidazole in ethanol–MeCN was originally characterized as $[C_{16}H_{13}N_2S_2]_2[Mo_4O_8Cl_4(OEt)_4]$ (cation = 2-(2′-thienyl)-1-(2′-thienylmethyl)benzimidazolium) [277]. The structure of the tetrameric anion is closely related to that of $Mo_4O_6Cl_4(O^nPr)_4(HO^nPr)_2$ except that μ-oxo ligands replace the two μ-O^nPr ligands which bridge the metal–metal-bonded pairs of molybdenum atoms. The long Mo–O bond distances (2.23(2) Å) established for the terminally bonded "ethoxide" ligands support the actual presence of HOEt ligands in **57** and its reformulation as the Mo^{V} tetramer $[C_{16}H_{13}N_2S_2]_2[Mo_4O_8Cl_4(OEt)_2(HOEt)_2]$ [276].

The black diamagnetic tetranuclear $Mo_2^{IV}Mo_2^{VI}$ diazene compound $(NHEt_3)_2[Mo_4O_{11}(dhphH_2)]$ (**58**) is produced by reacting $MoO_2Cl_2(dmf)_2$, 1,4-dihydrazinophthalazine ($dhphH_6$) and NEt_3 in ethanol [278]. The structure of the anion of **58**, shown in Fig. 32, consists of a planar binuclear $Mo_2^{IV}O_3$ core bridged by a diazene ligand and two essentially tetrahedral $[MoO_4]^{2-}$ ions. It was stated that the mixed-valence formulation had been confirmed by XPS data but no details were given. Protonation of the

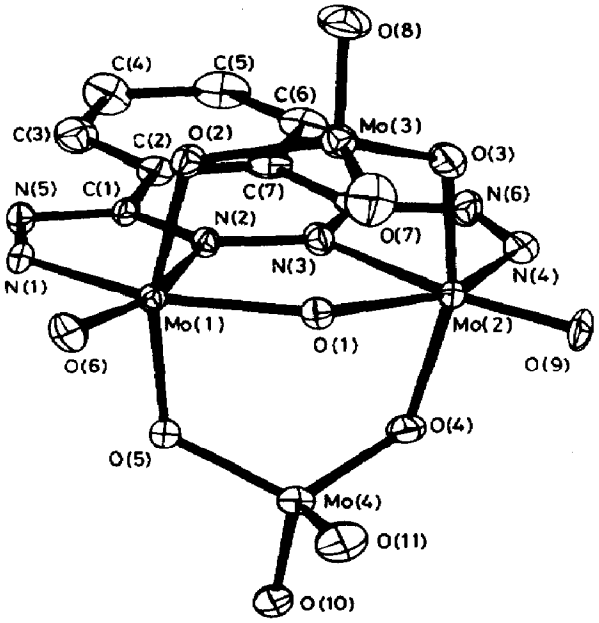

Fig. 32. Structure of the anion in **58**. Reproduced with permission from ref. 278.

complex results in the dissociation of the molybdate ions and the formation of $[Mo_2O_5(dhphH_6)]^{2+}$.

Orange–brown $[(MeCp)_2Mo_2O_4]_2$ is produced upon the reaction of $(MeCp)_2MoCl_2$ and $K_2[MoO_4]$ in water and also via the hydrolysis of $[(MeCp)_2MoH_3]^+$ [180]. The crystal structure of the material isolated by the latter method revealed a tetranuclear complex formed via the coupling of two dinuclear units by two triply bridging oxygen atoms (Fig. 20(b)) [181,182]. The structural parameters are consistent with the assignment of IV and VI oxidation states to the Mo(1) and Mo(2) atoms respectively. Similar structures are proposed for the Cp and ^{n}BuCp derivatives as well as the tungsten analogues (Section D(iii)(d)).

The reaction given in eqn. (12) results in the formation of the green compound shown in Fig. 33 [279]:

$$2(^t\text{BuO})_3\text{MoN} + \text{Mo}_2(\text{O}^i\text{Pr})_6 \xrightarrow{\text{hexane–HO}^i\text{Pr}} \text{Mo}_4(\mu_3\text{-N})_2(\mu\text{-O}^i\text{Pr})_2(\text{O}^i\text{Pr})_{10} \quad (12)$$

The coordination geometry of the nitrogen and molybdenum atoms is T-shaped (cf. $Cp_3Mo_3(N)(O)(CO)_4$, Section D(ii)(c)) and trigonal bipyramidal respectively. The Mo_4^{18+} core contains six electrons for Mo–Mo bonding. The Mo–Mo bond distances, two of 2.92 Å and one of 2.55 Å, along with the trends in the Mo–N distances suggest partial oxidative addition of two d^0 MoN units across an $[Mo_2]^{6+}$ centre. The complex has not been further characterized.

Molybdenum forms a wide variety of mixed-valence compounds having a cubane structure. The ill-defined $Mo_2(S_2CNEt_2)_6$ complex is converted to black diamagnetic $Mo_4(\mu_3\text{-S})_4(\mu\text{-}S_2CNEt_2)_2(S_2CNEt_2)_4$ (**59**) in refluxing toluene [280]. This complex possesses a cubane-like Mo_4S_4 cluster with

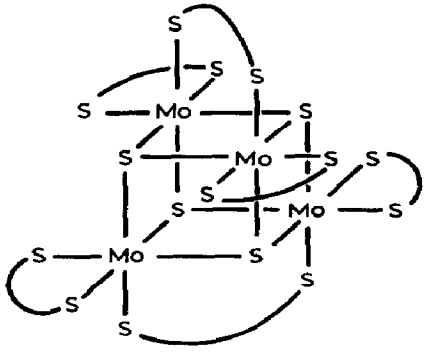

59

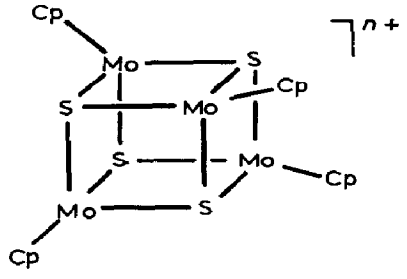

60

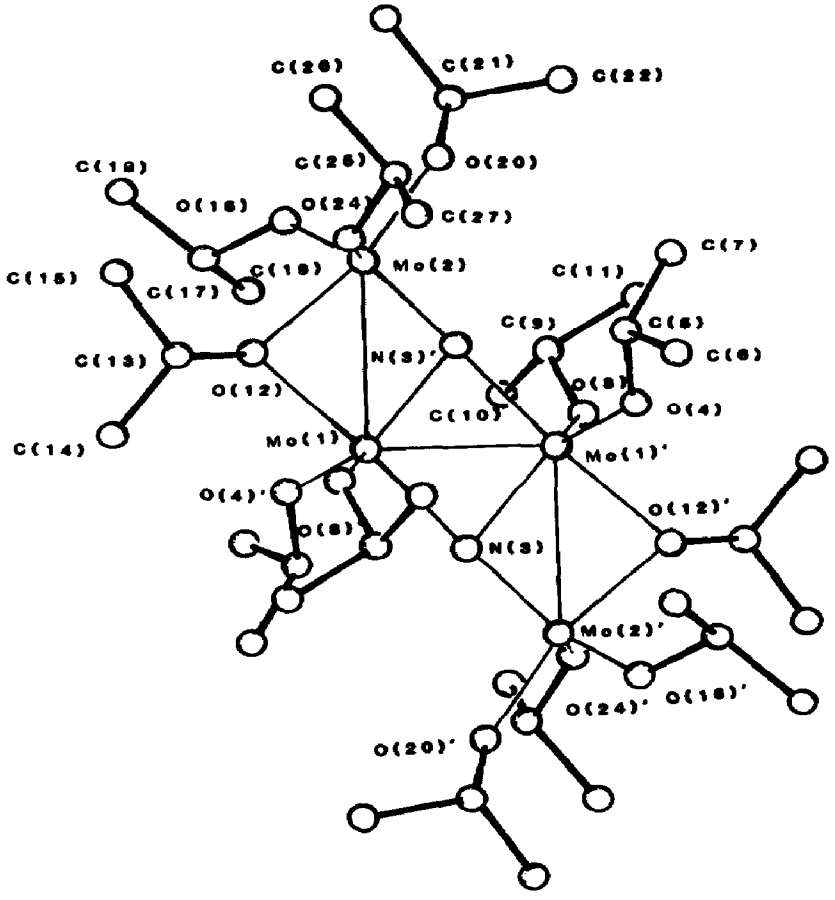

Fig. 33. Structure of the centrosymmetric $Mo_4(\mu_3\text{-}N)_2(\mu\text{-}O^iPr)_2(O^iPr)_{10}$ molecule. Reproduced with permission from ref. 279.

mutually metal–metal-bonded molybdenum atoms. Two Mo–Mo bonds are accompanied by μ-$S_2CNEt_2^-$ ligation while the remaining $S_2CNEt_2^-$ ligands are bidentate on single molybdenum atoms. The complex exhibits intense visible absorptions at 720 ($\epsilon = 1476$), 560 ($\epsilon = 4180$) and 352 nm ($\epsilon = 2313$). The bonding in the complex, which possesses an average oxidation state of 3.5, has been discussed [280]. The members of the series $[(^iPrCp)_4Mo_4(\mu_3\text{-}S)_4]^{n+}$ ($n = 0, 1, 2$) (**60**) are readily interconverted by chemical and electrochemical redox processes [281]. The mixed-valence compounds $[(^iPrCp)_4Mo_4(\mu_3\text{-}S)_4]BF_4$ and $[(^iPrCp)_4Mo_4(\mu_3\text{-}S)_4](I_3)_2$, along with the isovalent parent compound, have been crystallized and structurally characterized. The compounds possess a cubane structure composed of a tetrahedron of molybdenum atoms, each face being capped by a μ_3-S ligand. Very small structural changes accompany oxidation. Photoelectron spectra of the electron-rich isovalent compound have been interpreted in terms of a model developed by Toan et al. [282].

Several high valent tetranuclear complexes containing edta have been reported by Shibahara and coworkers. The reaction of azide with green $K[Mo_2(OH)_2(OAc)(edta)]$ under air-free conditions results in the formation of maroon $K_4[Mo_4O_4(OH)_2(edta)_2] \cdot 12H_2O$ (**61**) via partial displacement of acetate by azide in the conjugate base form of $[Mo_2(OH)_2(OAc)(edta)]^-$, and subsequent oxidation of molybdenum by the azide ligand [201,202]. An analogous sodium salt may be prepared. The X-ray structure of **61** has been determined (Fig. 34(a)); the tetranuclear anion is composed of two $Mo_2(\mu\text{-}O)(\mu\text{-}OH)(edta)$ units bridged face to face by two μ-oxo ligands. The Mo(1)–Mo(2) distance is 2.41 Å, the single oxo bridge possesses Mo–O distances of 1.90 Å and the Mo(1)–O(11)–Mo(2′) angle is 164° [283]. The compound is diamagnetic and the electronic spectrum consists of bands at 473 ($\epsilon = 3800$), 536 ($\epsilon = 3520$) and 730 nm ($\epsilon = 1650$).

A number of mixed-valence cuboidal complexes have been derived from the aqua ions $[Mo_4(\mu_3\text{-}S)(\mu\text{-}S)_3(aq)]^{n+}$ ($n = 5, 6$). The reaction of $Mo(CO)_6$ and Na_2S in acetic anhydride followed by aqueous work-up results in the isolation of $[Mo_3S_4(aq)]^{4+}$ and the $Mo_2^{III}Mo_2^{IV}$ ion $[Mo_4S_4(aq)]^{6+}$ [284]. Reaction of the latter with thiocyanate results in the formation of $(NH_4)_6[Mo_4S_4(NCS)_{12}] \cdot 10H_2O$ (**62**). The anion of **62** possesses a cubane structure with slant and basal edge lengths of 2.791(1) Å and 2.869(1) Å respectively. The molybdenum atoms are bridged via μ_3-S ligands and each is coordinated to three terminal NCS^- ligands. A Jahn–Teller distortion splitting the degenerate t_2 orbitals is proposed to account for the distortion away from t_d symmetry in this ten-electron species. Also, reduction of the

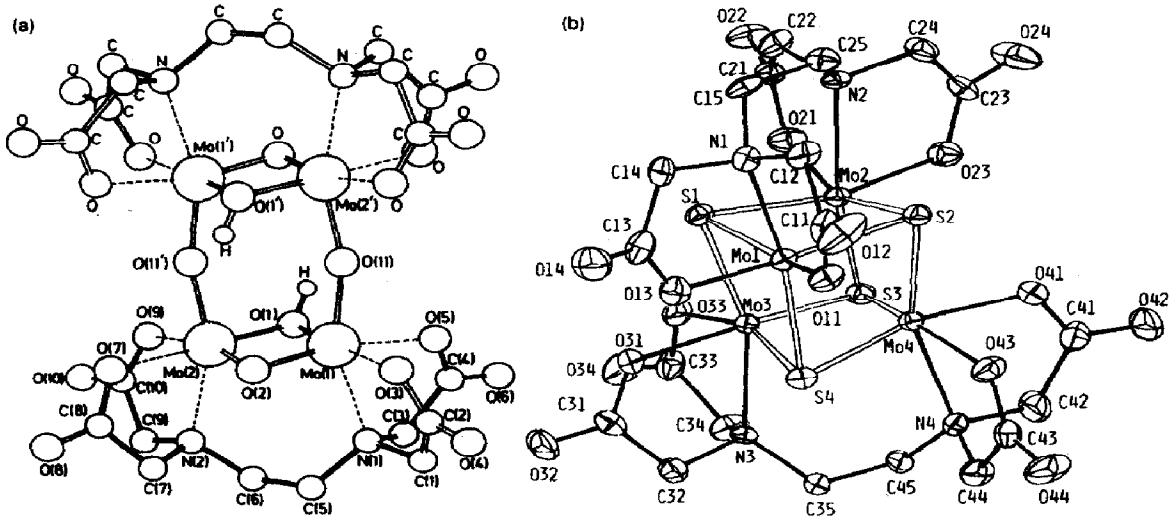

Fig. 34. (a) Structure of the anion in **61**. Reproduced with permission from ref. 283. (b) Structure of the anion in **63**. Reproduced with permission from ref. 285.

Mo^{V} compound $Na_2[Mo_2O_2(\mu\text{-}S)_2(cyst)_2]\cdot 3H_2O$ in 2 M HCl using a mercury pool electrode followed by aerial ion chromatographic work-up yields two green bands containing $[Mo_3S_4(aq)]^{4+}$ and the mixed-valence $Mo_3^{III}Mo^{IV}$ complex $[Mo_4S_4(aq)]^{5+}$ (λ_{max} 645 nm, ϵ 470) [285–287]. Various derivatives of $[Mo_3S_4(aq)]^{5+}$ have been isolated and the X-ray structures of $Ca_3[Mo_4S_4(edta)_2]_2\cdot 26H_2O$ (**63**) [285] $(NMe_4)_7[Mo_4S_4(NCS)_{12}]$ [286] (**64**) and $Mo_4S_4\{HB(pz)_3\}_4(pz)$ (**65**) [288] have been determined. The anion in **63**, shown in Fig. 34(b), has approximate S_4 symmetry and each edta ligand spans two molybdenum atoms at an Mo_2S_2 face. The four molybdenum atoms are structurally indistinguishable and a Class III formulation has been proposed. The complex exhibits near-IR bands at 900 nm ($\epsilon = 86$ sh) and 1150 nm ($\epsilon = 260$) and possesses a large comproportionation constant (7.3×10^{11}). The X-ray structures of salts of $[Mo_4S_4(edta)_2]^{n+}$ ($n = 2, 4$) have also been reported to be similar to the anion of **63** [289]. The core of complex **65** exhibits virtual C_{2v} symmetry. Various studies [286–288] are consistent with retention of the cuboidal structure upon the electrochemical or chemical redox processes represented in eqn. (13):

$$[Mo_4S_4]^{6+} \overset{+e^-}{\rightarrow} [Mo_4S_4]^{5+} \overset{+e^-}{\rightarrow} [Mo_4S_4]^{4+} \qquad (13)$$

The reduction of $Na_2[Mo_2O_4(cyst)_2]\cdot 5H_2O$ results in small yields of $[Mo_4O_4(aq)]^{5+}$, assigned a mixed-valence formulation on the basis of redox titrations [288,290]. Finally, electrolytic methods have been extended to the preparation of seleno and tellurido complexes $[Mo_4E_4(aq)]^{5+}$ [290].

The orange–red $Mo_2^{II}Mo_2^{V}$ complex $Mo_4O_2(\mu_4\text{-}CO_3)(CO)_2(\mu\text{-}O)_2(\mu\text{-}OH)_4(PMe_3)_6$ is formed as a minor product in the reaction of *cis*-$Mo(N_2)_2(PMe_3)_4$ and CO_2 [291]. The complex has been characterized by X-ray diffraction studies only (Fig. 35). The carbonate ligand exhibits a novel coordination mode and bridges all four molybdenum atoms; the two terminal Mo^{II} atoms are seven-coordinate while the two inner Mo^{V} atoms are bonded into a familiar *syn*-$[Mo_2O_4]^{2+}$ core.

Lustrous black crystals of $(NHEt_3)_2[Mo_4O_8(OMe)_2(NNPh)_4]$ result from the reaction of $MoO_2(bdiol)_2\cdot 2bdiolH_2$ with phenylhydrazine and NEt_3 in acidified methanol [292]. The tetranuclear anion (Fig. 36) is composed of two $[Mo(NNPh)_2]^{2+}$ units bridged by two methoxy groups and two tetrahedral $[MoO_4]^{2-}$ groups which function as bidentate ligands. Metal–metal interactions are insignificant. Assuming that the phenyldiazo ligands are three-electron donor $-N_2R^+$ groups, oxidation states of 0 and VI may be assigned to the central and MoO_4 molybdenum atoms respectively. While the authors favour this assignment, the high oxygen content in the coordination sphere of the central atom is at variance with the assigned oxidation state of 0.

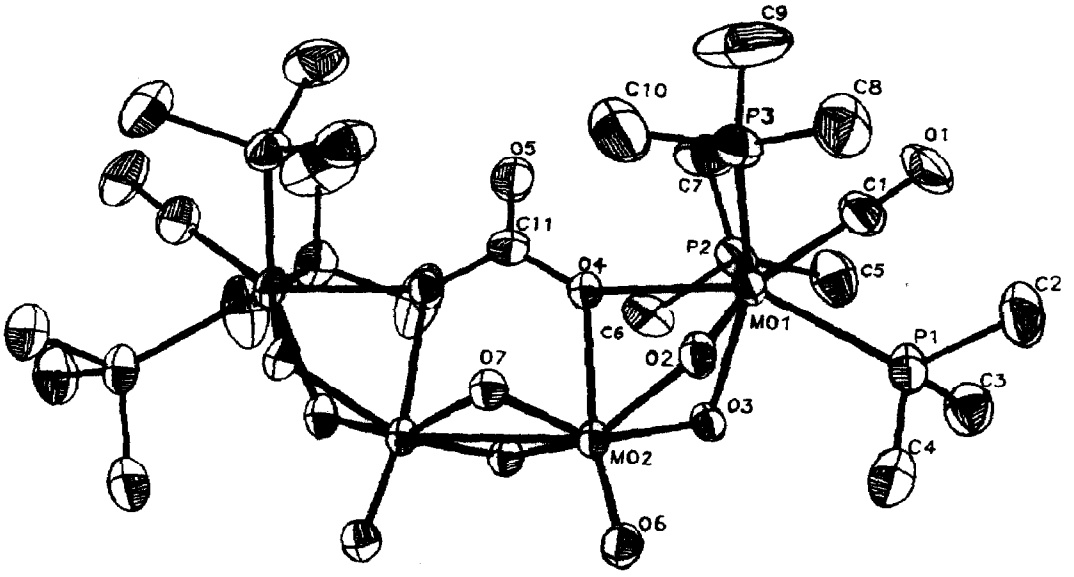

Fig. 35. Structure of $Mo_4O_2(\mu_4\text{-}CO_3)(CO)_2(\mu\text{-}O)_2(\mu\text{-}OH)_4(PMe_3)_6$. Reproduced with permission from ref. 291.

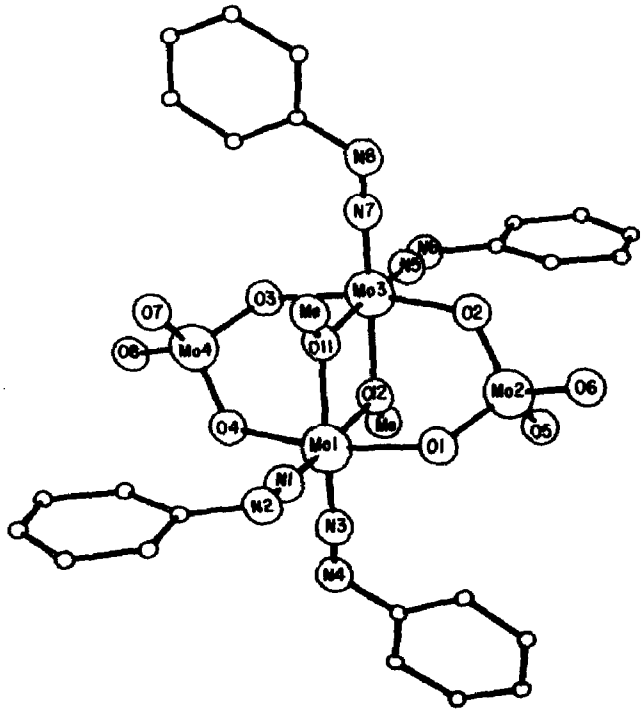

Fig. 36. Structure of the anion in $(NHEt_3)_2[Mo_4O_8(OMe)_2(NNPh)_4]$. Reproduced with permission from ref. 292.

A number of discrete tetranuclear halomolybdenum complexes have recently been reported. The one-electron oxidation of $[Mo_4Cl_{12}]^{4-}$ results in the formation of two isomers of $[Mo_4Cl_{12}]^{3-}$ [293]. Firstly, the reaction of $(NEt_4)_4[Mo_4Cl_{12}]$ with $AsPh_4Cl \cdot HCl$ in CH_2Cl_2 results in the formation of black $(AsPh_4)_2(NEt_4)[Mo_4Cl_{12}] \cdot 2CH_2Cl_2$ according to eqn. (14):

$$(NEt_4)_4[Mo_4Cl_{12}] + 2AsPh_4Cl + HCl \rightarrow (AsPh_4)_2(NEt_4)[Mo_4Cl_{12}] + 1/2H_2 + 3NEt_4Cl \quad (14)$$

Analogous $N^nPr_4^+$ and PPh_4^+ salts may be obtained by the iodine oxidation of the appropriate salt of $[Mo_4Cl_{12}]^{2-}$ in CH_2Cl_2. The anions in the above compounds are isostructural, exhibiting a planar rhombohedral array of molybdenum atoms. Removal of two *trans* MoCl units from $[Mo_6Cl_{14}]^{2-}$ would result in a related cluster (Fig. 29(e)). Secondly, reaction of $(NEt_4)_4[Mo_4Cl_{12}]$ with I_2, Cl_2 or $PhICl_2$ in CH_2Cl_2 produces green $(NEt_4)_3[Mo_4Cl_{12}]$ which possesses a butterfly cluster of four molybdenum atoms. In this case, the cluster may be envisaged to form from the removal of *cis* MoCl units from $[Mo_6Cl_{14}]^{2-}$ (Fig. 29(d)). The structure is related to that of $[Mo_4I_{11}]^{2-}$ (vide infra) produced when I^- is lost from a putative $[Mo_4I_{12}]^{3-}$ cluster. The anion $[Mo_5Cl_{13}]^{2-}$ (see Section D(ii)(f)) can be considered to form by the addition of $MoCl^+$ to $[Mo_4Cl_{12}]^{3-}$. Iodine oxidation of $N^nBu_4[MoI_3(CO)_4]$ results in the formation of black $(N^nBu_4)_2[Mo_4I_{11}]$ in high yield [294]. An alternative synthesis involves the reaction of $Mo_2(OAc)_4$ with HI gas in hot methanol followed by addition of N^nBu_4I [231]. X-ray diffraction studies by Stensvad et al. [294] reveal that the anion possesses a severely distorted tetrahedral cluster of molybdenum atoms bridged on two faces by μ_3-I atoms and on five edges by μ-I atoms; each molybdenum atom is also bonded to a terminal iodine atom (Fig. 29(c)). MO considerations indicate that six bonding and two non-bonding orbitals are available to accommodate the 15 cluster electrons, giving a formal Mo–Mo bond order of 1.0 and three electrons in non-degenerate non-bonding orbitals localized mainly on Mo(1) and Mo(2). The magnetic moment of 1.87 BM is in agreement with this model. The electronic, IR, ESR and photoelectron spectra of the compound have been reported [231] as has the related compound $(N^nBu_4)_2[Mo_4I_{10}Cl]$ [228]. Reaction of $[Mo_4I_{11}]^{2-}$ with dppe produces $Mo_4I_6(dppe)_2$ [231].

(f) Pentanuclear compounds

The reaction of $MoCl_2$ or $K_3[MoCl_6]$ in redox-active molten salts ($AlCl_3$–KCl–$BiCl_3$–Bi) results in the formation of $[Mo_6Cl_{14}]^{2-}$ and $[Mo_5Cl_{13}]^{2-}$ [295]. The latter complex, isolated and characterized as the $N^nBu_4^+$ salt, possesses a structure derived from $[Mo_6Cl_{14}]^{2-}$ by the removal

of an MoCl unit. The molybdenum atoms form a square-pyramidal core surrounded by eight μ_3-Cl atoms in a cubic array. The relationship of the core structure of this molecule to the $[Mo_6X_8]^{4+}$ core is shown in Fig. 29(b). Each molybdenum atom is bonded to a terminal chlorine atom and the Mo–Mo distances of 2.602(3) and 2.563(3) Å are slightly shorter than those of the hexanuclear parent compound $[Mo_6Cl_{14}]^{2-}$ (2.61 Å). The paramagnetic compound possesses 19 cluster electrons and an average molybdenum oxidation state of 2.20.

(g) Hexanuclear compounds

A novel hexanuclear $Mo_4^{V}Mo_2^{VI}$ compound, $Mo_6O_{10}(O^iPr)_{12}$ (**66**), is formed as an intermediate in the synthesis of $[MoO_2(O^iPr)_2]_n$ via the reaction of $Mo_2(O^iPr)_6$ and oxygen [296]. The structure of **66** is shown in Fig. 37. The terminal Mo(3) and Mo(3′) atoms are rich in alkoxide ligands and possess an oxidation state of VI, while the internal Mo(1), Mo(2), Mo(1′) and Mo(2′) atoms exhibit structural features characteristic of dinuclear Mo^{V}. In addition, **66** possesses two unusual "semi-bridging" alkoxide ligands formed

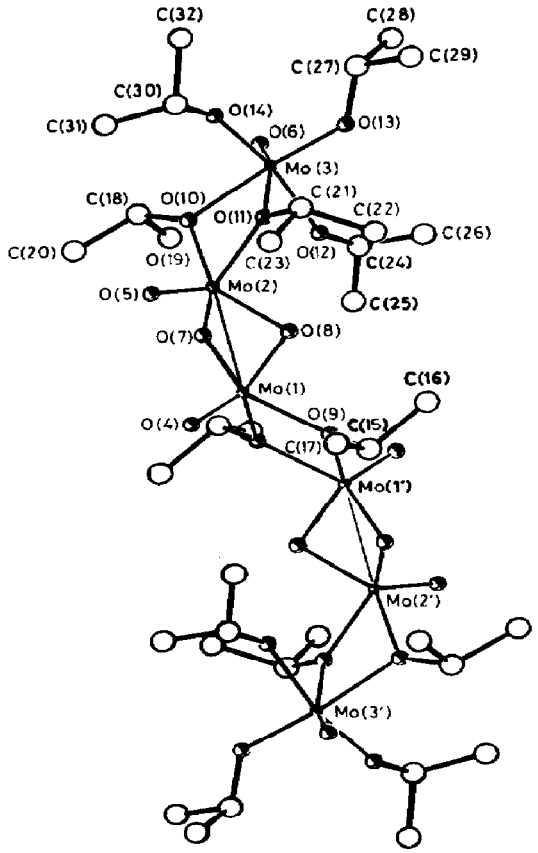

Fig. 37. Structure of **66**. Reproduced with permission from ref. 296.

as a result of the interaction of O(12) and Mo(2) at the site *trans* to the O(5) ligand. Further support for the mixed-valence formulation is provided by the reaction of **66** with py (eqn. (15)) in which tetrameric Mo^{V} and mononuclear Mo^{VI} complexes are formed:

$$Mo_6O_{10}(O^iPr)_{12} + 6py \rightarrow 2MoO(O^iPr)_4(py) + Mo_4O_8(O^iPr)_4(py)_4 \qquad (15)$$

Owing to the scope of this review, the Chevrel phases, which constitute a large and important class of solid state mixed-valence molybdenum complexes, will not be discussed. Readers interested in these materials are advised to consult recent reviews [297]. Interestingly, however, a molecular model of the Chevrel phases has been prepared by the reductive dimerization of the trinuclear thio–Mo cluster $Mo_3S_4Cl_4(PEt_3)_4(MeOH)$ (**67**). The reaction of **67** and magnesium in thf results in the formation of dark purple $Mo_6(\mu_3\text{-}S)_8(PEt_3)_6$, which contains a regular octahedral core of molybdenum atoms with each face capped by a μ_3-S atom (cf. the $[Mo_6X_8]^{4+}$ core in Fig. 14(b)) and each molybdenum atom bound to a PEt_3 ligand [298]. The diamagnetic complex possesses 20 cluster valence electrons and formal molybdenum oxidation states of $Mo_2^{II}Mo_4^{III}$. It participates in one-electron electrochemical reduction and oxidation processes.

In contrast with the situation with niobium and tantalum, mixed-valence molybdenum species based on the core structures shown in Fig. 14 are rare. Electrochemistry on $[Mo_6X_{14}]^{2-}$ ions (X = Cl, Br) allows the formation of $[Mo_6X_{14}]^{-}$ and $[Mo_6X_{14}]^{3-}$ ions in solution. Combination of these ions produces excited $[Mo_6X_{14}]^{2-*}$ which exhibits a red electrochemically generated chemiluminescence upon pulsing the potential applied to a platinum work electrode [299,300].

(g) High nuclearity compounds

Purple $[(H_2O)_9Mo_3(\mu_3\text{-}S)_4Mo(\mu_3\text{-}S)_4Mo_3(H_2O)_9](MeC_6H_4SO_3)_8 \cdot 18H_2O$ (**68**) is obtained by ion chromatography following the reaction of magnesium and $[Mo_3S_4(aq)]^{4+}$ in acidic solution. The structure of the cation in **68** consists of two incomplete cubane-type Mo_3S_4 cores linked by a molybdenum atom. The diamagnetic complex exhibits intense absorptions in the visible and near-IR (950 nm, $\epsilon = 606$ per molybdenum atom) and contains two structurally distinct molybdenum centres with a mean oxidation state of $3\frac{3}{7}$. The assignment of oxidation states is difficult (presuming the cation charge to be correct) [301].

Careful synthetic work has recently yielded an example of thiolate coordination in isopolymolybdate chemistry. Yellow $(NBu_4)_4[Mo_{10}O_{28}(SCH_2CH_2O)_2(MeOH)_2] \cdot 2MeOH$ (**69**) is formed upon reaction of $(NBu_4)_4[Mo_{10}O_{28}]$ with two equivalents of 2-mercaptoethanol in methanol [302]. The X-ray structure of **69** revealed the discrete centrosymmetric decanuclear anions

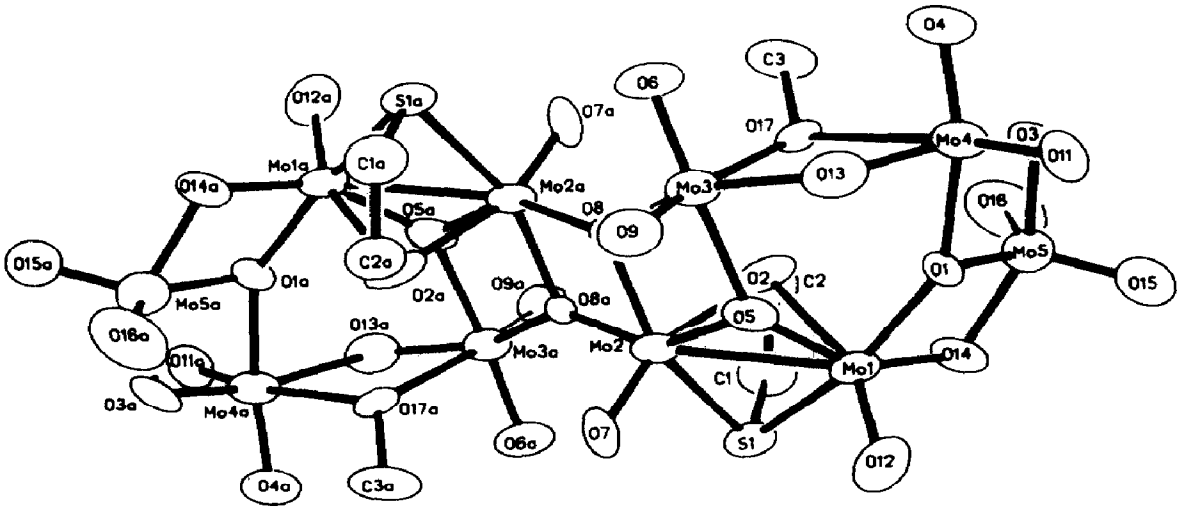

Fig. 38. Structure of the anion in **69**. Reproduced with permission from ref. 302.

shown in Fig. 38. The Mo(1) and Mo(2) atoms bridged by the mercaptoethanolate ligands are Mo^{V} centres. The two dinuclear units involving these atoms display structural features typical of dinuclear Mo^{V} complexes. The remaining molybdenum atoms are ascribed an oxidation state of VI. Construction of the Class I ion depends on the ability of chelating $[Mo_xO_y]^{n-}$ units to aggregate in methanolic solutions so as to bridge the pair of $[Mo_2O_3(SCH_2CH_2O)]^{2+}$ fragments.

A large and intriguing class of mixed-valence molybdenum compounds are the isopoly and heteropoly blues formed upon chemical, electrochemical or photochemical reduction of molybdates. For further information, the reader is directed to excellent reviews of this area [94,95,173,174]. Mention is made here of the recent work of Yamase [303,304], which has revealed through single-crystal ESR and crystallographic studies the sites involved in the photochemical reduction of $[Mo_{10}O_{34}]^{8-}$ and $[Mo_7O_{24}]^{6-}$. Yamase's studies [303,304] have also resulted in systems for the photochemical production of hydrogen from aqueous solutions. The catalytic transformation of organic substrates by the use of reduced molybdate species has also attracted considerable interest [305].

(iii) Tungsten compounds

(a) General survey

Although less developed than that of molybdenum, the mixed-valence chemistry of tungsten resembles that of its second row congener in many ways. In some cases exactly analogous complexes are known for both

molybdenum and tungsten. All oxidation states with the exception of I, −I and −II are represented in the mixed-valence compounds of tungsten. Approximately 15 dinuclear compounds have been characterized and examples having integral and half-integral average oxidation states ranging from +5.5 to +2.0, with the exception of +4.0, have been reported. Like molybdenum, tungsten forms very few $W^{V}W^{VI}$ compounds but one of these, $(AsPh_4)_2[W_2(\mu\text{-}N)Cl_{10}]$, has been structurally characterized. Several $W^{IV}W^{VI}$ complexes of the type $L_2W(\mu\text{-}S)_2WS_2$ (L = Cp, MeCp) are formed upon reaction of $[WS_4]^{2-}$ with L_2WCl_2. In contrast, the reaction of $[WO_4]^{2-}$ with L_2WCl_2 results in the tetranuclear $W_2^{IV}W_2^{VI}$ complexes, $[L_2W_2O_4]_2$. Redox reactions involving isovalent metal–metal-bonded complexes account for the synthesis of a number of mixed-valence tungsten complexes. Electrochemical and chemical redox reactions have been employed to produce dinuclear metal–metal-bonded W_2^{9+}, W_2^{7+} and W_2^{5+} complexes exemplified by $[W_2Cl_4(\mu\text{-}OEt)_2(OEt)_2L_2]^{+}$ (L = py), $W_2Cl_4(\mu\text{-}OEt)_2(hp)_2$ and $[W_2I_4(O_2C^tBu)_2]^{-}$ respectively. Although relatively unimportant in the mixed-valence chemistry of the previously discussed elements, this method comes into its own in the chemistry of rhenium (Section E(iii)). Confacial bi-octahedral structures are a feature of most dinuclear W_2^{7+} complexes and $[W_2X_9]^{2-}$ (X = Cl, Br) anions and μ-SR complexes possess such a structure. Two dinuclear tungsten complexes possess metal atoms with very different oxidation states. Localized W^{0} and W^{VI} sites co-exist in $W_2(O^iPr)_6(CO)_4$ while W^{0} and W^{IV} sites are observed in $Cp_2W(\mu\text{-}SPh)_2W(CO)_4$. The six-unit difference in oxidation state in the former complex is matched by only two other transition metal complexes, the $[(CO)_4Mo(\mu\text{-}S)_2MoS_2]^{2-}$ and $[(CO)_4Mo(\mu\text{-}S)_2Mo(\mu\text{-}S)_2Mo(CO)_4]^{2-}$ anions formed upon reaction of $Mo^{0}(CO)_6$ with $[Mo^{VI}S_4]^{2-}$ (Section D(ii)). Trinuclear compounds are of two general types. The first type contains a "linear" array of high valent thio–tungsten centres and is isolated from acidified solutions of $[WS_4]^{2-}$. Typical examples include $[WS(WS_4)_2]^{2-}$ and $[WO(WS_4)_2]^{2-}$ which possess structures composed of square-pyramidal $[W^{IV}E]^{2+}$ (E = S, O) fragments coordinated by tetrahedral $[W^{VI}S_4]^{2-}$ ligands. Derivatives containing an additional ligand on the W^{IV} atom are also known and recently a unique $W^{II}W_2^{VI}$ complex, $[W(WS_4)_2]^{2-}$, was reported. The second type of trinuclear compound possesses triangular arrays of metal atoms bridged by μ_3-L (L = O, CMe) and μ-carboxylate ligands. Tungsten forms a unique class of tetranuclear $W_2^{V}W_2^{VI}$ compounds which possess roughly square and planar tungsten centres linked by μ-O ligands. The aqua complex $[W_4O_4(\mu\text{-}O)_4Cl_8(H_2O)_4]^{2-}$ has been studied in some detail and several derivatives containing SCN^{-}, ox or dmf ligands have been synthesized. Tetranuclear W_4^{18+} and $W_2^{III}W_2^{V}$ complexes have also been reported. Hexanuclear mixed-valence complexes of tungsten are also known. Finally, a number of very

interesting mixed-valence compounds are produced upon reduction of isopolytungstate and heteropolytungstate ions. These compounds have been extensively reviewed, and the work of others should be consulted for an overview of this area [94,95,173].

Properties of selected mixed-valence compounds of tungsten are summarized in Tables 7 and 8.

(b) Dinuclear compounds

Like molybdenum, tungsten forms very few $W^{V}W^{VI}$ compounds. The only structurally characterized example is brown $(AsPh_4)_2[W_2(\mu\text{-}N)Cl_{10}]$ (**70**), a byproduct in the synthesis of $AsPh_4[WNCl_4]$ [306]. The anion in **70** possesses a corner-shared bi-octahedral structure with an eclipsed ligand conformation and an unsymmetrical (W1–N = 1.657(7) Å, W2–N = 2.072(7) Å) but linear W–N–W bridge. The W1 and W2 atoms are assigned oxidation states of VI and V respectively, the geometry around W2 being indicative of a Jahn–Teller-stabilized W^{V} centre. The W ··· W distance (3.729 Å) is very similar to the 3.728 Å W ··· W separation in $[W_4O_8Cl_8(H_2O)_4]^{2-}$, which contains W^{IV} and W^{V} centres linked via linear W–O–W bridges [307] (Section D(iii)(d)). Another $W^{V}W^{VI}$ complex has been observed in solution. Deep blue $[W_2O_4(\mu\text{-}O)(Me_3tcn)_2]^{+}$ is produced by chemical (Zn/Hg) or electrochemical reduction of $[W_2O_4(\mu\text{-}O)(Me_3tcn)_2]^{2+}$ and is likely to possess a corner-shared bi-octahedral structure analogous to that of the isovalent parent complex [308]. The corresponding molybdenum complex has been discussed in Section D(ii)(b). Blue $W^{V}W^{VI}$ intermediates are also observed upon oxidation of $[W_2O_2(\mu\text{-}O)_2(aq)]^{2+}$ [309,310]. One other $W^{V}W^{VI}$ compound, green W_2OCl_9, has been briefly described but probably has an extended structure [311].

A variety of mixed-valence compounds have been obtained from reactions involving $[WO_4]^{2-}$ and $[WS_4]^{2-}$ (see also Sections D(iii)(c) and D(iii)(d)). The only dinuclear compounds of this type are orange–red $L_2W(\mu\text{-}S)_2WS_2$ (L = Cp, MeCp), formed by the reactions of $(NH_4)_2[WS_4]$ and L_2WCl_2 [180]. The compounds probably possess localized $W^{IV}W^{VI}$ centres and a structure similar to that of a crystallographically characterized molybdenum analogue (Fig. 20(a)) [181,182].

Electrochemical oxidation of the W^{IV} complexes $W_2Cl_4(\mu\text{-}OEt)_2(OEt)_2L_2$ (L = py, 4-Mepy, 4-Phpy) results in the formation of yellow ESR-active (typically $g_1 = 1.88$, $g_2 = 1.70$, $g_3 = 1.66$) monocations, $[W_2Cl_4(\mu\text{-}OEt)_2(OEt)_2L_2]^{+}$ [312]. Isolation of salts has not been achieved although chemical oxidations using $NOPF_6$ are also reported to produce the monocations. The W_2^{9+} complexes possess a W–W bond of order 1.5 and a $\sigma^2\pi$ electronic configuration.

Mention should be made of a W^{IV} compound which was earlier purported

TABLE 7

Properties of selected dinuclear mixed-valence compounds of tungsten

Compound	W oxidation state		Structure	W...W distance (Å)	μ_{eff} (BM)	ESR spectrum	W–W bond order	Electron configuration	Ref.
	Formal	Average							
$(AsPh_4)_2[W_2NCl_{10}]$	V, VI	5.5	–	3.729	–	–	–	–	306
$[W_2O_4(\mu\text{-}O)(Me_3tcn)_2]^{+}$ [a]	V, VI	5.5	–	–	–	–	–	–	308
$Cp_2W(\mu\text{-}S)_2WS_2$	IV, VI	5	Fig. 20(a)	–	Diamagnetic	–	–	–	180–182
$[W_2Cl_4(\mu\text{-}OEt)_2(OEt)_2L_2]^{+}$ [a] (L = py, 4-Mepy, 4-Phpy)	IV, V	4.5	–	–	–	$g_1 = 1.88$ [c] $g_2 = 1.70$ $g_3 = 1.66$	1.5	$\sigma^2\pi$	312
$(Ph_3PNPPh_3)_2[W_2Cl_9]$	III, IV	3.5	Fig. 39	2.540(1)	1.87	–	–	–	216
$(N^iPr_4)_2[W_2Br_9]$	III, IV	3.5	Fig. 39	2.601(2)	1.72	–	–	–	319
$W_2Cl_4(\mu\text{-}SEt)_3(SMe_2)_2$	III, IV	3.5	Fig. 40(a)	2.505(1)	–	$g = 2.00$	2.5	–	321
$(AsPh_4)_2[W_2Cl_6(\mu\text{-}Cl)(\mu\text{-}SPh)_2]$	III, IV	3.5	Fig. 40(b)	2.519(2)	–	$g_1 = 2.238$ [c] $g_2 = 1.907$ $g_3 = 1.754$	2.5	–	322
$[W_2Cl_4(\mu\text{-}OEt)_2(hp)_2]^{-}$ [a]	III, IV	3.5	–	–	–	$g_1 = 1.93$ [c] $g_2 = 1.86$ $g_3 = 1.62$	1.5	$\sigma^2\pi^2\delta^*$	312
$W_2(O^iPr)_6(CO)_4$	O, VI	3	75	3.410(1)	Diamagnetic	–	–	–	218
$[W_2I_4(O_2C^tBu)_2]^{-}$ [b]	II, III	2.5	Fig. 41(a)	2.24	–	–	3.5	$\sigma^2\pi^4\delta$	327
$W_2Br_2(O_2C^tBu)_3 \cdot 2thf$	II, III	2.5	Fig. 41(b)	2.313	–	–	3.5	$\sigma^2\pi^4\delta$	327
$Cp_2W(\mu\text{-}SPh)_2W(CO)_4$	O, IV	2	77	4.011(2)	Diamagnetic	–	–	–	331, 332

[a] Formed and characterized in solution.

[b] As the $[W_2(O_2C^tBu)_5(^tBuCONMe_2)_2]^{+}$ salt.

[c] In frozen CH_2Cl_2 at 77 K.

to be a mixed-valence $W^{III}W^{V}$ compound. The deep violet compound, originally prepared by Olsson and formulated as $K_2[W(OH)Cl_5]$ [313], has been subsequently reformulated as $K_4[W_2(\mu\text{-}O)Cl_{10}]$ [314,315]. König [315] proposed a Class II $W^{III}W^{V}$ formulation for the compound. However, this proposal has been questioned by San Filippo et al. [316] who interpreted magnetic susceptibility data in terms of antiferromagnetically coupled d^2 W^{IV} centres. The crystal structure of $K_4[W_2(\mu\text{-}O)Cl_{10}]$ has also been determined [317] and structural features indicative of a $W^{III}W^{V}$ formulation, such as inequivalent metal sites, were not apparent.

A number of dinuclear mixed-valence tungsten complexes exhibit a confacial bi-octahedral structure. The violet $W^{III}W^{IV}$ complex $[W_2Cl_9]^{2-}$ may be prepared by a variety of methods. Saillant and Wentworth first prepared the complex by oxidizing isovalent $[W_2Cl_9]^{3-}$ with elemental halogens (eqn. (16)) [318]:

$$2[W_2Cl_9]^{3-} + X_2 \rightarrow 2[W_2Cl_9]^{2-} + 2X^- \qquad (X = Cl, Br, I) \qquad (16)$$

Later Delphin and Wentworth reported that the complex is formed during the reaction of $[W(CO)_5Cl]^-$ and WCl_6 [311]. In the same study, a compound formulated as $(N^nBu_4)_2[W_4Cl_{17}]$ was reported to produce $(N^nBu_4)_2[W_2Cl_9]$ upon reaction with chloride. Also, the reduction of WCl_4 with Na/Hg in thf in the presence of $(Ph_3PNPPh_3)Cl$ yields $(Ph_3PNPPh_3)_2[W_2Cl_9]$ (**71**) and this compound has been structurally characterized; the structure of the anion in **71** is shown in Fig. 39 [216]. The W–W bond length of 2.540(1) Å is 0.122 Å longer than the corresponding bond in $[W_2Cl_9]^{3-}$, the increased formal charge of the metal atoms being the basis for the orbital modifications which account for this lengthening. The complex is paramagnetic with $\mu_{eff} = 1.87$ BM [318]. The analogous bromo

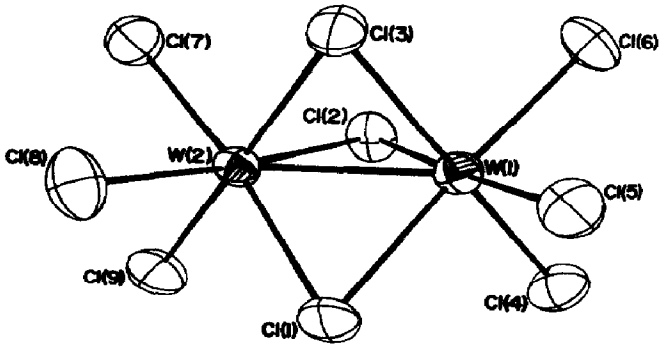

Fig. 39. The structure of the $[W_2Cl_9]^{2-}$ anion in **71**. An analogous structure has been established for $[W_2Br_9]^{2-}$ [319]. Reproduced with permission from ref. 216.

complex has also been reported; oxidative bromination of $N^iPr_4[W(CO)_5Br]$ with 1,2-dibromoethane yields $(N^iPr_4)_2[W_2Br_9]$ (**72**) [319] (eqn. (17)):

$$4[W(CO)_5Br]^- + 7C_2H_4Br_2 \rightarrow 2[W_2Br_9]^{2-} + 7C_2H_4 + 20CO \quad (17)$$

The structure of the anion in **72** is analogous to that of $[W_2Cl_9]^{2-}$ (Fig. 39). As observed in the chloro analogue the W–W bond length (2.601(2) Å) is 0.19 Å longer than that in $[W_2Br_9]^{3-}$, consistent with a bond order of 2.5. A distortion of the anion from D_{3h} symmetry has been attributed to a static Jahn–Teller distortion which results in the separation of e' W–W π-orbitals [319]. However, this conclusion was questioned by Cotton et al. [216]. Compound **72** exhibits simple Curie magnetism over the temperature range 77–300 K, with a magnetic moment of 1.72 BM indicative of a single unpaired electron [319]. The electronic structures of the $[W_2X_9]^{n+}$ (X = Cl, Br; n = 2, 3) complexes have recently been interpreted [320].

A number of thio-bridged $W^{III}W^{IV}$ complexes exhibit the confacial bi-octahedral structure. The first such complex, red–brown $W_2Cl_4(\mu\text{-}SEt)_3(SMe_2)_2$, was produced by the reaction of $WCl_4(SMe_2)_2$ with two equivalents of Me_3SiSEt [321]. The complex has the structure shown in Fig. 40(a), with a W–W distance (2.505(1) Å) indicative of a W–W bond. An unusually short non-bonded contact of 3.054(6) Å between two of the bridging sulphur atoms is observed. A doublet ground state is consistent with the g = 2.00 ESR signal observed for the solid at 77 K. The complex is

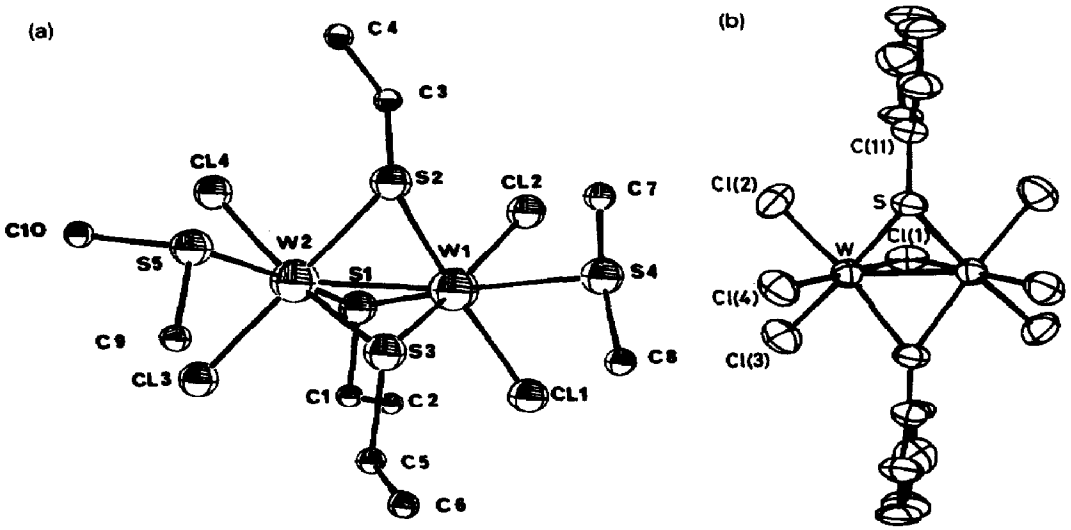

Fig. 40. Structures of thio-bridged confacial bi-octahedral complexes. (a) $W_2Cl_4(\mu\text{-}SEt)_3(SMe_2)_2$. Reproduced with permission from ref. 321. (b) The $[W_2Cl_6(\mu\text{-}Cl)(\mu\text{-}SPh)_2]^{2-}$ anion in **73**. Reproduced with permission from ref. 322.

assigned a Class III mixed-valence classification. The reaction of $WCl_4(SMe_2)_2$ and Me_3SiSPh produced the very air-sensitive complex $W_2Cl_4(SMe_2)_2(\mu\text{-}Cl)(\mu\text{-}SPh)_2$, which was converted to stable burgundy crystals of $(AsPh_4)_2[W_2Cl_6(\mu\text{-}Cl)(\mu\text{-}SPh)_2]\cdot 1.4CH_2Cl_2$ (**73**) by reaction with $AsPh_4Cl$ [322]. The structure of the anion in **73** is shown in Fig. 40(b); the confacial bi-octahedral structure and structural parameters (e.g. a W–W distance of 2.519(2) Å) are consistent with a strong W–W bond of formal bond order 2.5. Low temperature ESR spectra of **73** were interpreted in terms of a rhombic $S = 1/2$ system. A large anisotropy was observed in the g values, with one of the values, associated with the W–W direction, having a value considerably greater than two (CH_2Cl_2, 77 K, $g_1 = 2.238$, $g_2 = 1.907$, $g_3 = 1.754$). The spectra are consistent with the Summerville–Hoffmann treatment of the bonding in such compounds [323].

Electrochemical or chemical (cobaltocene) reduction of $W_2Cl_4(\mu\text{-}OEt)_2(hp)_2$ produces blue (λ_{max} 587 nm, $\epsilon > 2.5 \times 10^3$), ESR active ($g_1 = 1.93$, $g_2 = 1.86$, $g_3 = 1.62$) $[W_2Cl_4(\mu\text{-}OEt)_2(hp)_2]^-$ [312]. The W_2^{7+} complex possesses a W–W bond of order 1.5 and a $\sigma^2\pi^2\delta^*$ electronic configuration. The cobalticenium salt has been isolated.

A number of $W^{II}W^{IV}$ complexes have recently been reported by Ahmed and Chisholm. The best characterized is golden–brown $W_2(NMe_2)_4Cl_2(py)_2$-(CO) (**74**), formed upon the addition of CO to 1,2-$W_2Cl_2(NMe_2)_4$ in toluene–pyridine solution [324]. The chemical and NMR properties of **74** support a $W^{II}W^{IV}$ formulation and an unsymmetrical confacial bi-octahedral structure in which the CO ligand is bound to the "soft" W^{II} centre. Structural characterization of the complex is clearly desirable. Related confacial bi-octahedral complexes, $W_2(NMe_2)_3(O^iPr)Cl_2(py)_2(CO)$ and $W_2(NMe_2)_2(O^iPr)_2Cl_2(py)_2(CO)$, are formed upon reaction of **74** with HO^iPr [324]. Another $W^{II}W^{IV}$ complex, green $W_2H_5(\mu\text{-}PMe_2)(PMe_3)_5$, was reported earlier by Chiu et al. [325]. The complex results from the reaction of $W_2Cl_4(PMe_3)_4$ with hydrogen (3 atm) and Na/Hg in thf at 75 °C and has been characterized by IR, ^1H and ^{31}P NMR spectroscopy and X-ray crystallography. The hydrogen atoms were not located in the crystal structure and thus the compound remains to be unambiguously characterized.

Some mixed-valence complexes of tungsten exhibit extremely different metal oxidation states. The classic example is the W^0W^{VI} complex $W_2(O^iPr)_6(CO)_4$ (**75**), which is formed along with $[W_2(O^iPr)_6(CO)(py)]_2$ upon exposure of $W_2(O^iPr)_6(py)_2$ to two equivalents of CO [218]. The structure of **75** is based on two edge-shared octahedra possessing distinctly different sets of ligands. The coordination sphere of one tungsten atom is composed entirely of O^iPr^- ligands, two of which asymmetrically bridge the tungsten atoms. The other tungsten atom resembles a disubstituted tetracarbonyl–W^0 fragment and the long W–W distance (3.410(1) Å) precludes a

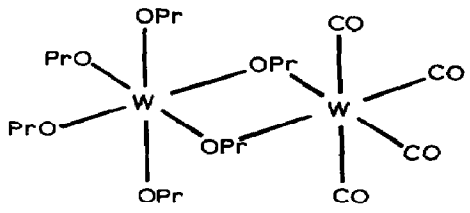

75

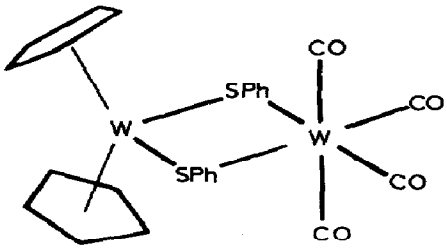

77

W–W bond. The tungsten atoms are assigned oxidation states of VI and 0 respectively; this is the only known tungsten complex possessing metal centres differing by six units of oxidation state. Two molybdenum compounds are also known to possess metal centres differing in oxidation state by six units [217]. These compounds, $(NEt_4)_2[(CO)_4Mo(\mu\text{-}S)_2MoS_2]$ and $(NEt_4)_2[(CO)_4Mo(\mu\text{-}S)_2Mo(\mu\text{-}S)_2Mo(CO)_4]$, are discussed in Section D(ii).

Like molybdenum, technetium and rhenium, tungsten forms a number of dinuclear mixed-valence complexes which are derivatives of well-known $W_2(O_2CR)_4$ complexes. For example, the iodine oxidation of $W_2(O_2C^tBu)_4$ is reported to yield grey paramagnetic $[W_2(O_2C^tBu)_4]I$ which has been characterized by IR and ESR ($g = 1.794$, no ^{183}W coupling) spectroscopy [326]. Later, the reaction of $W_2(O_2C^tBu)_4 \cdot (^tBuCONMe_2)_2$ with iodine was reported to yield $[W_2(O_2C^tBu)_5(^tBuCONMe_2)_2][W_2I_4(O_2C^tBu)_2]$ (**76**) [327]. The structure of the anion in **76** is shown in Fig. 41(a); the W–W bond distance of 2.24 Å is consistent with a formal bond order of 3.5 and a $\sigma^2\pi^4\delta$ bonding configuration. The reaction of $W_2(O_2C^tBu)_4 \cdot 2thf$ with bromine results in the formation of brown $W_2Br_2(O_2C^tBu)_3(thf)_2$ which possesses the structure shown in Fig. 41(b) (W–W = 2.31 Å) [327]. The physical and spectroscopic properties of these materials have not been reported. A related compound, $W_2Cl_2(mhp)_3$, has been isolated in attempts to prepare W_4 clusters from $W_2(mhp)_4$. The molecule possesses a bond order of 3.5 and a *cis* disposition of chloro ligands (as in Fig. 41(b)) [328]. Tungsten also resembles molybdenum and rhenium in the formation of brown or purple monocationic complexes $[W_2Cl_4(PR_3)_4]^+$ ($PR_3 = PMe_3$, PBu_3, PMe_2Ph, $PMePh_2$) upon oxidation of the quadruply bonded $W_2Cl_4(PR_3)_4$ precursors [329]. Oxidation may be effected electrochemically or chemically using $AgPF_6$ (for $PR_3 = PBu_3$) or $[FeCp_2]^+$ (for $PR_3 = PMe_3$).

Another example of a complex with very different oxidation states is the W^0W^{IV} complex $Cp_2W(\mu\text{-}SPh)_2W(CO)_4$ (**77**) [330–332]. Originally, this complex, which is formed by the reaction of $Cp_2W(SPh)_2$ and $W(CO)_6$, was incorrectly formulated as $Cp_2W(\mu\text{-}SPh)_2W(CO)_3$ [330]. A subsequent X-ray crystal structure determination revealed its true identity [331,332]. The long

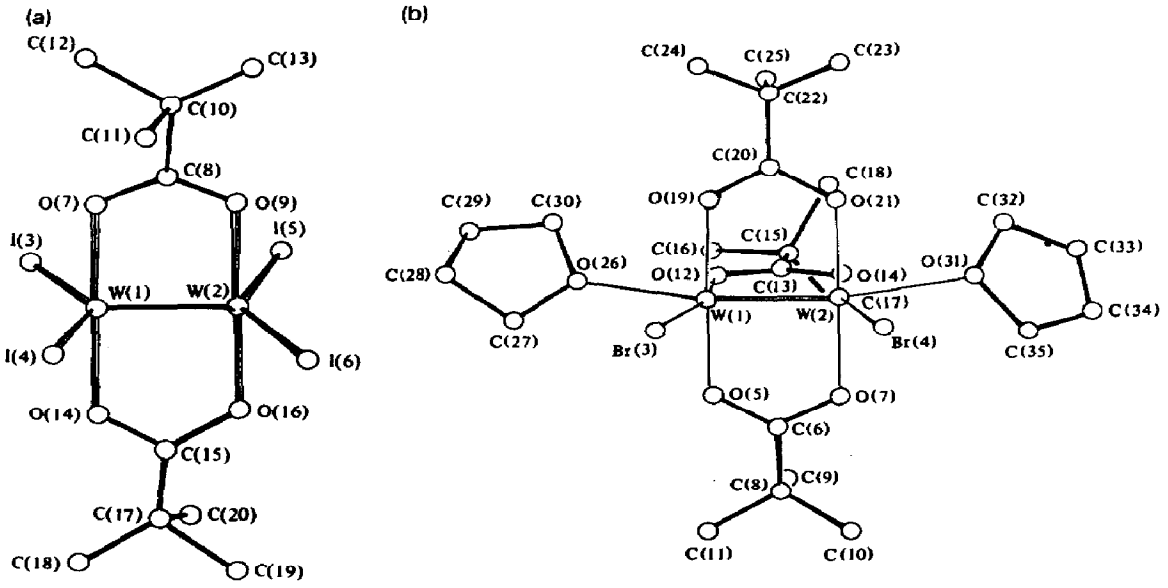

Fig. 41. (a) Structure of the $[W_2I_4(O_2C^tBu)_2]^-$ anion in **76**. (b) Structure of $W_2Br_2(O_2C^tBu)_3(thf)_2$. Reproduced with permission from ref. 327.

W–W distance of 4.011(2) Å precludes the presence of a W–W bond, and carbonyl- and cyclopentadienyl-bearing tungsten atoms are thus assigned oxidation states of 0 and IV respectively.

(c) Trinuclear compounds

In recent years a variety of mixed-valence chalcogenotungsten compounds have been prepared. A mixture of such species is formed upon the acidification of $[WS_4]^{2-}$ and a variety of species may be isolated by varying the reaction conditions. Trinuclear species include $[WS(WS_4)_2]^{2-}$ [333], $[WO(WS_4)_2]^{2-}$ [334], $[WO(WS_4)_2(H_2O)]^{2-}$ [335–337], $[W_3S_8(S_2CH_2)]^{2-}$ [335], $[WO(WS_4)_2(dmf)]^{2-}$ [250] and $[W(WS_4)_2]^{2-}$ (**78**) [338]. With the exception of **78**, these complexes possess central square-pyramidal W^{IV} atoms flanked by terminal tetrahedral $W^{VI}S_4$ ligands (see Fig. 21 for the

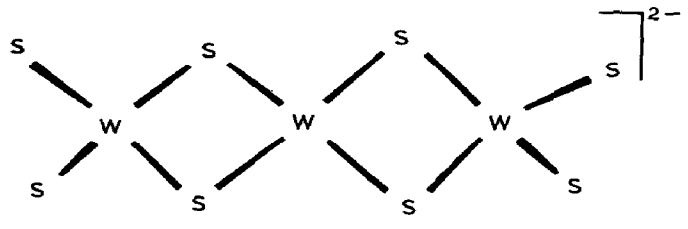

78

structures of related molybdenum complexes). These complexes are all valence-localized $W^{IV}W_2^{VI}$ anions. In contrast, recently described **78** is a valence-localized $W^{II}W_2^{VI}$ species. The central W^{II} atom in $[W(WS_4)_2]^{2-}$ exhibits a novel square-planar geometry while the terminal W^{VI} atoms adopt the usual tetrahedral geometry [338].

Triangular mixed-valence complexes of tungsten are also known. Oxidative work-up of the reaction of $W(CO)_4(pip)_2$ in acetic acid–acetic anhydride yields orange $[W_3(\mu_3\text{-}O)(\mu_3\text{-}CMe)(\mu\text{-}OAc)_6(H_2O)_3]^{2+}$, isolated and structurally characterized as the bromide salt [339]. The formally $W_2^{IV}W^{V}$ cation possesses a bicapped triangular array of tungsten atoms (Fig. 13(a)). The arrangement of the remaining ligands around the $[WO(CMe)]^{8+}$ core resembles that observed in the basic carboxylates of vanadium, chromium and manganese. The cation is an electron-deficient paramagnetic cluster with an average bond order of 5/6. Early reports of the thermal reaction of $W(CO)_6$ and acetic acid–acetic anhydride formulated the yellow–brown products as $W_3O(OAc)_8(OH) \cdot L$ (L = H_2O, MeOH) [340] and $W_3O(OAc)_9$ [341] but the structure of these solids has not been established. The major solution species in this and related reactions are isovalent $[W_3(\mu_3\text{-}O)_2(\mu\text{-}O_2CR)_6(H_2O)_3]^{2+}$ complexes [259,342]. However, mixed-valence compounds possessing a triangular W_3 core have now been prepared and characterized. Cation exchange chromatography of the above (hydrolysed) reaction mixture yielded a blue band which provided crystals of $[W_3(\mu_3\text{-}O)(OAc)_6(H_2O)_3]ZnBr_4 \cdot 8H_2O$ upon addition of $ZnBr_2$ [343]. The structure of the formally $W_2^{III}W^{IV}$ complex is shown in Fig. 10 and is related to that of the major product but with one μ_3-O capping ligand missing. The complex is diamagnetic and the electronic structure has been probed by Fenske–Hall calculations. Very recently, an improved synthesis of $[W_3(\mu_3\text{-}O)(OAc)_6(H_2O)_3]^{2+}$ (involving the reaction of $[WO_4]^{2-}$, zinc and acetic anhydride) and the X-ray structure of $[W_3(\mu_3\text{-}O)(OAc)_6(H_2O)_3]ZnCl_4 \cdot 4H_2O$ were reported [344]. The complex may be converted to $[W_3(\mu_3\text{-}O)(OAc)_5(OMe)(H_2O)_3]^{2+}$ which has also been structurally characterized [344]. A related $W_2^{III}W^{IV}$ fragment was previously observed in the mixed-metal complex $W_3(O_2CH_2{}^tBu)O_3Cr_3(O_2C{}^tBu)_{12}$ [345]. The electronic structure of the above complexes has been discussed [260].

(d) Tetranuclear compounds

In 1974 Launay and coworkers reported the preparation of an anion formulated as $[W_4O_8Cl_8]^{2-}$ via the addition of tungstate to a concentrated solution of W^{V} in 8–12 M HCl [307,346]. The reaction mixture establishes the equilibrium shown in eqn. (18), and although the equilibrium lies to the left, selective precipitation leads to the isolation of the mixed-valence anion:

$$2[WO_2Cl_4]^{2-} + 2[WOCl_5]^{2-} + 2H_2O = [W_4O_8Cl_8]^{2-} + 4H^+ + 10Cl^- \quad (18)$$

The complex was also formed by slow aerial oxidation of a 0.15 M W^V solution in 2 M HCl [307]. The properties of this complex and of its derivatives are summarized in Table 8. An X-ray structure of the $W_2^V W_2^{VI}$ compound $(NHMe_3)_2[W_4O_8Cl_8(H_2O)_4] \cdot 2H_2O$ revealed an anion composed of four $WO_3Cl_2(H_2O)$ octahedra, corner linked via μ-O ligands to form a roughly square and planar array of crystallographically equivalent tungsten atoms, as shown in Fig. 42 [307]. Each tungsten atom is displaced towards the attached terminal oxo ligand (W–O = 1.711(9) Å) and is thus found alternately 0.18 Å above or below the molecular plane. Photoelectron spectroscopy and ESR (powder, $g_1 = 1.809$, $g_2 = 1.777$, $g_3 = 1.748$ for W^V, $S = 1/2$) data at 77 K are consistent with the unpaired electrons being localized on separate W^V centres. At $-50\,°C$ the rate of electron hopping is estimated to be 2.5×10^8 Hz. The compound exhibits two intense absorption bands at 650 and 550 nm which are assigned to intervalence CT transitions. Analogous complexes, $[W_4O_8Cl_6(dmf)_6]$, $[W_4O_8(NCS)_{12}]^{6-}$ and $[W_4O_8(NCS)_4(C_2O_4)_4]^{6-}$, have also been reported [347]. The structure of the anion in $Cs_5(NH_4)[W_4O_8(NCS)_{12}] \cdot 6H_2O$ is related to $[W_4O_8Cl_8(H_2O)_4]^{2-}$, however, the four crystallographically unique tungsten atoms are almost planar (maximum deviation, 0.05 Å) and the terminal oxo ligands reside on the same side of the molecule [347]. The electronic spectra of the above complexes exhibit two intense bands near 550 and 700 nm, which have been assigned to intervalence CT transitions in these Class II complexes [348].

Acidification of $[WS_4]^{2-}$ with acetic acid in anhydrous media results in the formation of the $W_2^V W_2^{VI}$ complex $[W_4S_{12}]^{2-}$ which was isolated and structurally characterized as the PPh_4^+ salt [349]. The complex contains a

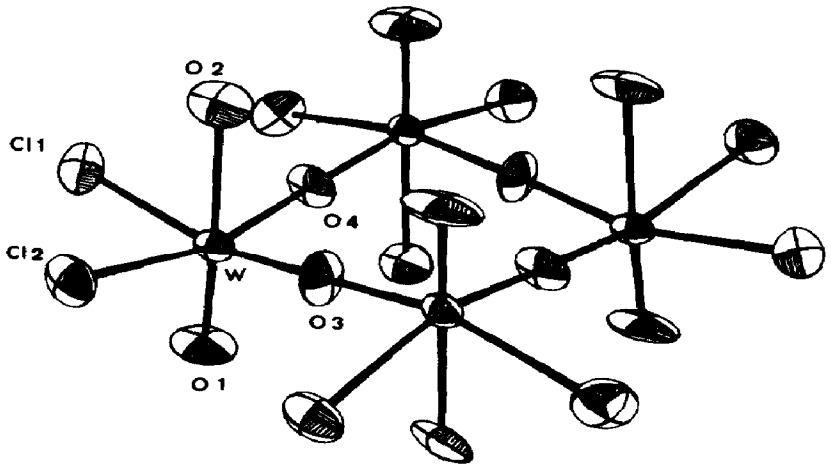

Fig. 42. Structure of the tetranuclear W_2^V W_2^{VI} anion $[W_4O_8Cl_8(H_2O)_4]^{2-}$. Reproduced with permission from ref. 307.

TABLE 8

Properties of tetranuclear *cyclo*-W_2^V W_2^{VI} compounds

Compound	Synthesis	Structure	W ··· W (Å)	ESR spectrum	Electronic spectrum (nm) (ϵ)	XPS (eV)
$(NHMe_3)_2[W_4O_8Cl_8(H_2O)_4]$ [a]	$[WO_2Cl_4]^{2-}$ + $[WOCl_5]^{2-}$ in H_2O	Fig. 42	3.721(2) [c] 3.735(2) [d]	$g_1 = 1.809$ [e] $g_2 = 1.777$ $g_3 = 1.748$ $A = 154$ G	650 (16000) 550 (18000)	W^V, $4f(7/2)$ 35.5 W^V, $4f(5/2)$ 37.7 W^{VI}, $4f(7/2)$ 37.0 W^{VI}, $4f(5/2)$ 39.2
$Cs_5(NH_4)[W_4O_8(NCS)_{12}]$ [b]	Exchange reaction of $[W_4O_8Cl_8(H_2O)_4]^{2-}$	–	$1.72 \pm 1(4)$	–	570 (26000) 710 (42000)	
$W_4O_8Cl_6(dmf)_6$ [b]	Exchange reaction of $[W_4O_8Cl_8(H_2O)_4]^{2-}$	–	–	–	570 (16000) 660 (14000)	
$(quinH)(NMe_4)$-$[W_4O_8(NCS)_4(ox)_4]$ [b]	Exchange reaction of $[W_4O_8Cl_8(H_2O)_4]^{2-}$	–	–	–	550 (12000) 680 (20000)	

[a] Data from ref. 307.

[b] Data from ref. 347.

[c] Along *b*.

[d] Along *c*.

[e] Powdered sample at 77 K.

syn-$[W_2S_4]^{2+}$ core composed of square-pyramidal W^V atoms, which is coordinated by two terminal tetrahedral $[WS_4]^{2-}$ ligands. The central W^V atoms are strongly spin coupled via a direct W–W interaction (W–W = 2.95 Å).

The tetranuclear $W_2^{IV}W_2^{VI}$ complexes $[(RCp)_2W_2O_4]_2$ (R = H, Me, ^{n}Bu) result from the reactions of $(RCp)_2WCl_2$ and $Na_2[WO_4]$. Their structure is likely to be analogous to that of a molybdenum analogue, $[(MeCp)_2Mo_2O_4]_2$ (Fig. 20(b)) [181,182].

The tetranuclear carbido cluster $W_4C(NMe)(O^iPr)_{12}$ is formed during the reaction of $W_2(NMe_2)_6$ and HO^iPr in hexane [279]. The complex exhibits a butterfly structure supported by a system of bridging NMe^{2-}, O^iPr and carbido (C(55)) ligands; the W_4CNO_{12} skeleton of the complex is shown in

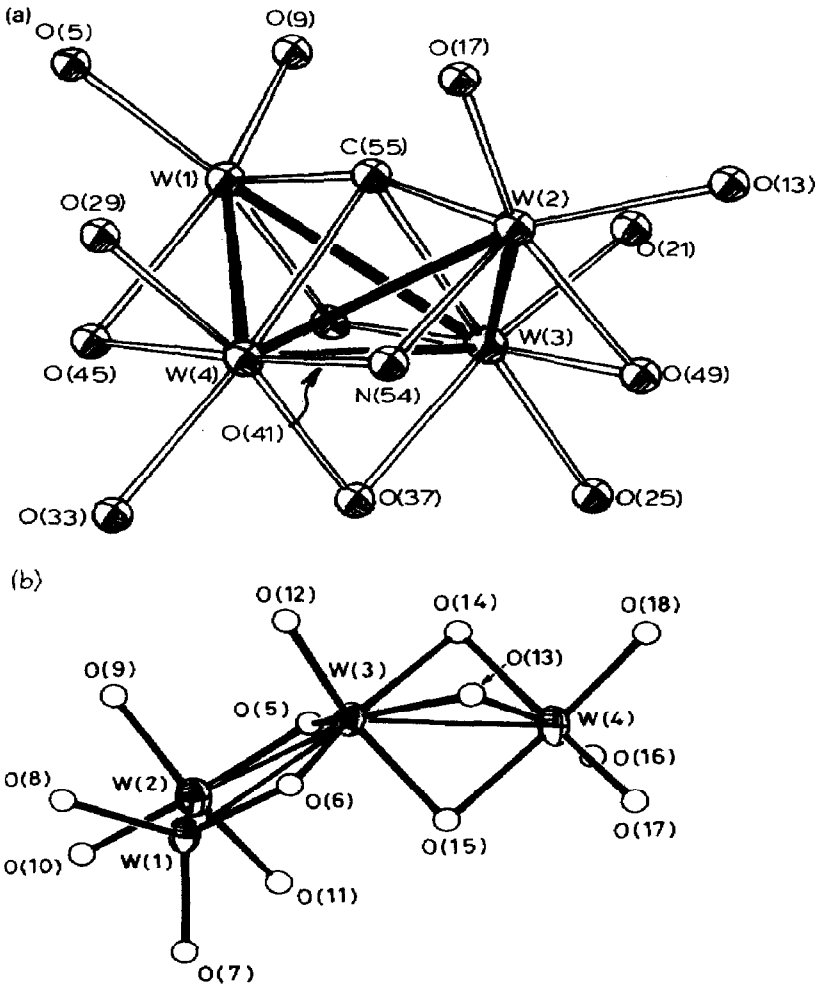

Fig. 43. (a) The central W_4CNO_{12} skeleton of $W_4(C)(NMe)(O^iPr)_{12}$. Reproduced with permission from ref. 279. (b) The central W_4O_{14} skeleton of $W_4O_2(O^iPr)_{12}$. O(5) and O(6) are oxo ligands. Reproduced with permission from ref. 350.

Fig. 43(a). The tetranuclear centre is formally W_4^{18+} and has only six electrons for W–W cluster bonding.

A number of novel mixed-valence alkoxy–tungsten clusters have been reported in recent years. Tetranuclear $W_4O_2(O^iPr)_{12}$, which has the structure shown in Fig. 43(b), is produced in the reaction of $W_2(O^iPr)_6(py)_2$ and acetone [350]. The complex contains one W–W triple bond (W(1)–W(2) 2.404(2) Å) and one W–W single bond (W(3)–W(4) 2.684(2) Å). The asymmetrical bonding of the oxo ligands O(5) and O(6) to the tungsten atoms, viz. W(3)–O(5) 1.86(2) Å and W(3)–O(6) 2.01(1) Å, is representative of formal W=O and W–O bonds respectively, and the W–W bond distances are consistent with localized oxidation states of III for W(1) and W(2) and V for W(3) and W(4). Interestingly, the dinuclear fragment containing the W^V centres exhibits an unusual confacial bi-octahedral structure. Spectroscopic properties have not been reported.

(e) Hexanuclear compounds

Deep red $(Ph_3PNPPh_3)[W_6Br_{14}]$ (**79**) is prepared by the reaction of $(Ph_3PNPPh_3)_2[W_6Br_{14}]$ with $NOPF_6$ [351]. Analogous $[W_6Cl_{14}]^-$, $[W_6Cl_8Br_6]^-$ and $[W_6Br_8Cl_6]^-$ complexes have been isolated as $N^tBu_4^+$ salts. The anion of **79** possesses a nearly octahedral geometry with average W–W distances of 2.649(8) Å.

(f) High nuclearity compounds

The striking blue or brown colours of reduced heteropolytungstates result from the formation of intensely coloured mixed-valence species. The current state of knowledge concerning these species has developed recently through electrochemical and spectroscopic studies. This area has been subject to considerable review [94,95,173] and only some recent or illustrative studies will be cited here. The reduction of heteropolytungstates is not accompanied by substantial structural changes in the anion framework when the electrons enter essentially non-bonding orbitals. Only anions in which the tungsten atoms coordinate to a single terminal oxygen atom, e.g. Keggin, Dawson and W_6O_{19} anions, possess such orbitals and reduction of these species may be electrochemically reversible. Irreversible reduction to heteropoly blues occurs in the case of polyanions containing two terminal oxygen atoms. A classic result was derived from the electrochemical study [352] of the metatungstate anion, α-$[H_2W_{12}O_{40}]^{6-}$, which has a Keggin structure. Six reversible reduction processes result in the progressive formation of blue $W_x^VW_{12-x}^{VI}$ species. Further reduction leads to the formation of brown $W^{IV}W^{VI}$ species and the formation of metal–metal bonds between WO_6 octahedra. The addition of 24 electrons results in the formation of $[H_2W_{12}^{IV}O_{40}H_{24}]^{6-}$ which may be quantitatively re-oxidized to metatungstate

or reduced further with eight electrons. The X-ray structure of the rubidium salt of the brown six-electron-reduced anion, $Rb_4H_8[H_2W_{12}O_{40}] \cdot \sim 18H_2O$ has been determined [353]. While exhibiting the usual Keggin structure with nine tungsten atoms occupying their usual positions, three other tungsten atoms are displaced 0.48 Å in the direction of the centre of a W_3O_{13} group. This result is consistent with the formation of a $W_3^{IV}O_{13}$ cluster within the Keggin anion. The broad absorption bands in the electronic spectrum of heteropoly blue species are attributable to intervalence CT ($W^V \rightarrow W^{VI}$) and *d–d* transitions. The added electrons are delocalized over certain atoms and/or regions of the anion skeleton, although the extent of delocalization depends on the time scale of the observation technique. The electrochemical and photochemical reduction of various salts of the decatungstate ion, $[W_{10}O_{32}]^{4-}$, has been reinvestigated by Chemseddine et al. [354]. The one-electron-reduced species was characterized by electronic and ESR spectroscopy. A 1500 nm band is assigned to an intervalence CT transition within a Class II mixed-valence species. The orthorhombic ESR spectrum shows that the reduction occurs on an equatorial rather than an apical tungsten site of the anion (for the structure see ref. 355). The electronic delocalization in reduced tungstates having W_6O_{19}, $XW_{12}O_{40}$, $As_2W_{18}O_{62}$ and $AsH_2W_{18}O_{60}$ structural types has been reported [356]. Thermally activated electron hopping strongly depends on the junction between adjacent WO_6 octahedra, with more ready delocalization between corner-sharing octahedra. The ^{183}W NMR chemical shifts and relaxation times in polysite mixed-valence heteropolytungstates provide a direct determination of the location of added electrons in ESR-silent heteropoly blues [357]. ESR studies of photochemically reduced $(NH_2{}^iPr_2)_4[W_{10}O_{32}] \cdot 8H_2O$ indicate delocalization of the unpaired electron in the one-electron-reduced form [303].

E. MIXED-VALENCE COMPOUNDS OF THE GROUP 7 ELEMENTS

(i) Manganese compounds

(a) General survey

The presence of manganese in the photosynthetic oxygen-evolving complex (OEC) of green plants and cyanobacteria has provided a major impetus for the development of the mixed-valence chemistry of manganese. Whatever the actual nuclearity and structure of the OEC, it is certain that mixed-valence states are created during oxygen evolution. Thus the investigation of synthetic mixed-valence complexes may provide insight into the structure and function of the biological system. A diversity of compounds, some with complex structures and intriguing properties, has resulted from attempts to model the many and varied active sites proposed for the OEC. To date,

mixed-valence complexes containing manganese in oxidation states 0 through IV and VII have been characterized, with Mn^{II} to Mn^{IV} complexes being most common. No examples containing Mn^{V} and Mn^{VI} have been reported. Dinuclear complexes constitute the largest group of mixed-valence manganese compounds and the most prevalent contain oxo-bridged $Mn^{III}Mn^{IV}$ centres coordinated by N-donor ligands. These complexes, represented by the well-known $[Mn_2(\mu\text{-}O)_2L_4]^{3+}$ (L = bpy, phen) cations, were among the first reported mixed-valence complexes of manganese and they remain a subject of considerable interest. There has been a spate of recent reports of related complexes $[Mn_2(\mu\text{-}O)_2L_2]^{3+}$ where L = bispicen, tpa, cyclam, cyclen and tren. Incorporation of acetate as well as oxo bridges into $Mn^{III}Mn^{IV}$ complexes is exemplified by $[(Me_3tcn)_2Mn_2(\mu\text{-}O)(\mu\text{-}OAc)_2]^{3+}$, $[(tcn)_2Mn_2(\mu\text{-}O)_2(\mu\text{-}OAc)]^{2+}$ and $Mn_2(\mu\text{-}O)_2(\mu\text{-}OAc)Cl_2(bpy)_2$. Complexes of $Mn^{II}Mn^{III}$ and $Mn^{I}Mn^{II}$ are less numerous and show a lower tendency to incorporate oxo ligands. Recent structural studies have characterized a number of $Mn^{II}Mn^{III}$ complexes including $[Mn_2(bpmp)(\mu\text{-}OAc)_2]^{2+}$ and $Mn_2(biphen)_2(biphenH)(bpy)_2$. In all, about 24 dinuclear compounds have been reported. Seven trinuclear mixed-valence compounds are known for manganese, and examples with triangular and extended "linear" structures have been characterized. With the exception of the $Mn^{I}_2Mn^{II}$ complex, $Mn_3(MeC_5H_6)_4$, these trinuclear compounds possess an $Mn^{II}Mn^{III}_2$ formulation. Manganese exhibits a propensity to form stable complexes of exceptionally high nuclearity and structural intricacy. Thus tetranuclear, hexanuclear, heptanuclear, nonanuclear and even dodecanuclear complexes are known. The average oxidation state in such complexes varies from $6\frac{4}{7}$ in the highly oxidized $[Mn(MnO_4)_6]^{2-}$ anion to $2\frac{1}{3}$ in the tetranuclear complex $Mn_4O_2(OAc)_6(py)_3$. An interesting feature of the high nuclearity complexes is their spontaneous formation from mixtures containing mononuclear starting materials. It is also noteworthy that all known mixed-valence compounds of manganese, with the exception of $Mn_2(SPh)_3(CO)_6$ which is a Class IIIA compound, are Class I or Class II compounds. Mixed-valence compounds of manganese have been characterized by a variety of techniques including X-ray crystallography, magnetochemistry, ESR and electronic spectroscopy and electrochemistry. The first three mentioned techniques are particularly valuable for the study of these paramagnetic compounds.

Properties of selected mixed-valence compounds of manganese are summarized in Tables 9 and 10.

(b) Dinuclear compounds

Properties of selected dinuclear mixed-valence compounds of manganese are summarized in Table 9.

TABLE 9

Properties of selected dinuclear mixed-valence compounds of manganese

Compound	Mn oxidation state		Structure	Mn...Mn distance (Å)	Magnetic properties [a] (J in cm^{-1})	ESR spectrum (A in gauss)	Electronic spectrum (nm) (ϵ)	K_{comp}	α^2	Principal ref.
	Formal	Average								
$[Mn_2(\mu\text{-}O)_2(bpy)_4](ClO_4)_3$	III, IV	3.5	Fig. 44(a)	2.716(2)	$g = 2.003$ $J = 150 \pm 7$	$g = 2.003$ $A_1 = 167 \pm 3$ $A_2 = 79 \pm 3$	830 (430)	$10^{15.6}$	0.01	359, 362, 364
$[Mn_2(\mu\text{-}O)_2(phen)_4](PF_6)_3$	III, IV	3.5	Fig. 44(a)	2.695(9)	$g = 1.999$ $J = 148 \pm 12$	$g = 2.003$ $A_1 = 167 \pm 3$ $A_2 = 79 \pm 3$	800 (sh) 680 (550)	10^{16}	–	361, 362, 364
$[Mn_2(\mu\text{-}O)_2(bispicen)_2](ClO_4)_3$	III, IV	3.5	–	2.659(2)	–	–	–	–	–	368
$[Mn_2(\mu\text{-}O)_2(tpa)_2]_2(S_2O_6)_3$	III, IV	3.5	–	2.643(1)	–	–	–	–	–	369
$[Mn_2(\mu\text{-}O)_2(tren)_2](CF_3SO_3)_3$	III, IV	3.5	Fig. 44(b)	2.679(1)	$g = 1.958$ $J = -146$	$g = 1.958$ $A_1 = 150$ [d] $A_2 = 78$ [d]	680 (570) 548 (440)	–	–	371
$[(Me_2tcn)_2Mn_2(\mu\text{-}O)(\mu\text{-}OAc)_2](ClO_4)_2$	III, IV	3.5	Fig. 45(a)	3.230(3)	$g = 2.2$ $J = -40$	–	1400(100)	7×10^8	–	372, 373
$[(tcn)_2Mn_2(\mu\text{-}O)_2(\mu\text{-}OAc)](BPh_4)_2$	III, IV	3.5	Fig. 45(b)	2.588(2)	$g = 2.0$ $J = -220$	$g = 2.00$ $A_1 = 154$ $A_2 = 77$	628 (345) 546 (394)	–	–	374

$Mn_2(\mu\text{-}O)_2(\mu\text{-}OAc)\text{-}Cl_2(bpy)_2$	III, IV	3.5	–	2.667(2)	$\mu = 3.24$ (301 K) $J = -114$	$g = 2.0$	–	–	–	375
$Mn_2L(\mu\text{-}O)(\mu\text{-}OH)$ [b]	III, IV	3.5	–	–	–	–	450 (5000)	–	0.029	376
$[Mn_2X(TPP)]_2\text{-}\mu\text{-}O$ ($X = N_3^-$, NCO^-)	III, IV	3.5	–	–	–	$g = 2.0$ $A = 69.3 \pm 0.7$	–	–	–	379, 380
$[Mn_2(bpmp)\text{-}(\mu\text{-}OAc)_2](ClO_4)_2$	II, III	2.5	Fig. 46	3.447(1)	$g = 2.00$ $J = -6.1$	Complex	–	1.7×10^9	–	385–387
LMn_2Cl_2Br [c]	II, III	2.5	Fig. 47	3.168(3)	$g \approx 2$ $J = -1.7$	Complex	–	–	–	386, 387
$Mn_2(biphen)_2\text{-}(biphenH)(bpy)_2$	II, III	2.5	Fig. 48	3.182(6)	Ferromagnetic $J = +0.89$	Complex	–	–	–	375
$[Mn_2(L\text{-}Im)\text{-}(\mu\text{-}OAc)_2](ClO_4)_2$	II, III	2.5	–	3.54(1)	$\mu = 7.55$ (297 K) $J = -4.5$	Complex	606 (430) 383 (1050)	–	–	388
$Mn_2(SPh)_3(CO)_6$	I, II	1.5	–	–	–	$g = 2.017$ $A = 33$	880 519	–	–	389

[a] Unless specified, compounds are antiferromagnetically coupled high spin systems and magnetic data were fitted using an isotropic Heisenberg model $H = -2JS_1S_2$.

[b] L = Schiff bases derived from (−)-1,2-diaminopropane and 4-*sec*-butylsalicylaldehyde or 4-*sec*-butyl-2-acetylphenol.

[c] L^{2-} is shown in Fig. 47.

[d] A values $\times 10^4\ cm^{-1}$.

TABLE 10

Properties of selected mixed-valence compounds of manganese

Compound	Mn oxidation state		Structure	Mn ··· Mn distance [a]	S, ground state [b]	Magnetic properties		Ref.
	Formal	Average				g	J (cm^{-1})	
$Mn_3(\mu_3\text{-}O)(\mu\text{-}OAc)_6(py)_3$	II, III_2	$2\frac{2}{3}$	Fig. 10	3.363(1)	$\frac{1}{2}$	2.10	$J = -7.7$, $J' = -5.7$ [c]	395, 396
$Mn_3(\mu_3\text{-}O)(\mu\text{-}OAc)_6(py)_3 \cdot py$	II, III_2	$2\frac{2}{3}$	Fig. 10	3.353(1)	$\frac{1}{2}$	2.13	$J = -5.1$, $J' = -8.3$ [c]	396
$Mn_3(\mu_3\text{-}O)(O_2CPh)_6(py)_2(H_2O)$	II, III_2	$2\frac{2}{3}$	Fig. 10	1–2, 3.216 [d] 1–3, 3.384 [d] 2–3, 3.386 [d]	$\frac{1}{2}$	2.11	$J = -7.3$, $J' = -10.9$ [c]	396
$(PPh_4)_2[Mn_3(pdt)_5]$	II, III_2	$2\frac{2}{3}$	Fig. 49	1–2, 3.123(3) 2–3, 3.101(3)	$\frac{3}{2}$	–	$J_{12} = J_{23} = -18.3$ $J_{13} = 0$	399
$Mn_3(\mu\text{-salhp})_2(\mu\text{-}OAc)_4(MeOH)_2$	II, III_2	$2\frac{2}{3}$	Fig. 50	3.551(1)	$\frac{3}{2}$	2.04–2.0	$J_{12} = -7.09$, $J_{11'} = 0$	400
$Mn_3(MeC_5H_6)_4$	I_2, II	$1\frac{1}{3}$	Fig. 51	1–2, 2.517(2) 2–3, 2.515(2)	$\frac{5}{2}$	–	Curie–Weiss behaviour 2.17–300 K	401
$(ImH_2)_2[Mn_4O_3Cl_6(ImH)(OAc)_3]$	III_3, IV	3.25	Fig. 52	1–2, 1–3, 2.818(5) 1–4, 2.806(5) 2–3, 3.323(5) 2–4, 3.285(5) 3–4, 3.246(5)	–	g ca. 2 and 4	–	403

$Mn_4O_2(OAc)_6(bpy)_2$	II_2, III_2	2.5	Fig. 53	1–1′, 2.779(1) 1–2, 3.288(1) 1–2′, 3.481(1)	$1,1' = 2$ [e] $2,2' = \frac{5}{2}$ [e]	–	$J_{12} = -1.97$ $J_{11'} = -3.12$	404
$Mn_6O_2(O_2C^tBu)_{10}(^tBuCO_2H)_4$	II_4, III_2	$2\frac{1}{3}$	Fig. 54	–	–	Antiferromagnetic $\mu = 4.81$		406
$Mn_9O_4(O_2CPh)_8(sal)_4(salH)_2(py)_4$	II, III_8	$2\frac{8}{9}$	Fig. 55	3–4, 2.817(6) 2–3, 3–5, 3.407(6) 2–5, 5.914(6) 2–4, 4–5_{av} 3.43 1–$(2–5)_{av}$ 3.88	$\frac{3}{2}$	2 and 4	See ref. 411	411
$Mn_{12}O_{12}(OAc)_{16}(H_2O)_4$	III_3, IV_4	$2\frac{1}{12}$	Fig. 56	1–2, 2.767(3) 1–1′, 2.820(3) 1–3, 2–3, 3.33–3.45(1)	–	–	–	398

[a] Where more than one distance is quoted the preceding numbers identify the manganese atoms involved, e.g. when prefixed by 1–2, the distance given is that between Mn(1) and Mn(2).

[b] All trinuclear compounds are antiferromagnetically coupled high spin systems.

[c] $J = J_{12} = J_{31}$ and $J' = J_{23}$ where manganese atoms 1, 2 and 3 are assigned oxidation states of II, III and III respectively. The subscripts refer to the coupled manganese atoms.

[d] Average of two independent molecules with no imposed symmetry.

[e] S for the various manganese atoms (identified by number) are given.

In 1960, Nyholm and Turco [358] reported the first dinuclear mixed-valence compounds of manganese; these were the persulphate and perchlorate salts of the green $[Mn_2(\mu\text{-}O)_2(bpy)_4]^{3+}$ complex formed via persulphate oxidation of Mn^{2+} in the presence of bpy. Later, in an attempt to grow crystals of $[Mn(bpy)_3](ClO_4)_3$, Plaksin et al. [359] isolated and structurally characterized crystals of $[Mn_2(\mu\text{-}O)_2(bpy)_4](ClO_4)_3 \cdot 3H_2O$. The $[Mn_2(\mu\text{-}O)_2(bpy)_4]^{3+}$ cation (**80**), shown in Fig. 44(a), contains two six-coordinate manganese atoms bridged by two oxo ligands and separated by a distance of 2.716(2) Å. The presence of discrete Mn^{III} and Mn^{IV} atoms is consistent with the inequivalence of the bond lengths of the two coordination spheres; the shorter Mn(2)–N and Mn(2)–O bond lengths (2.075 Å and 1.784 Å respectively) are indicative of an Mn^{IV} centre, while longer Mn(1)–N and Mn(1)–O

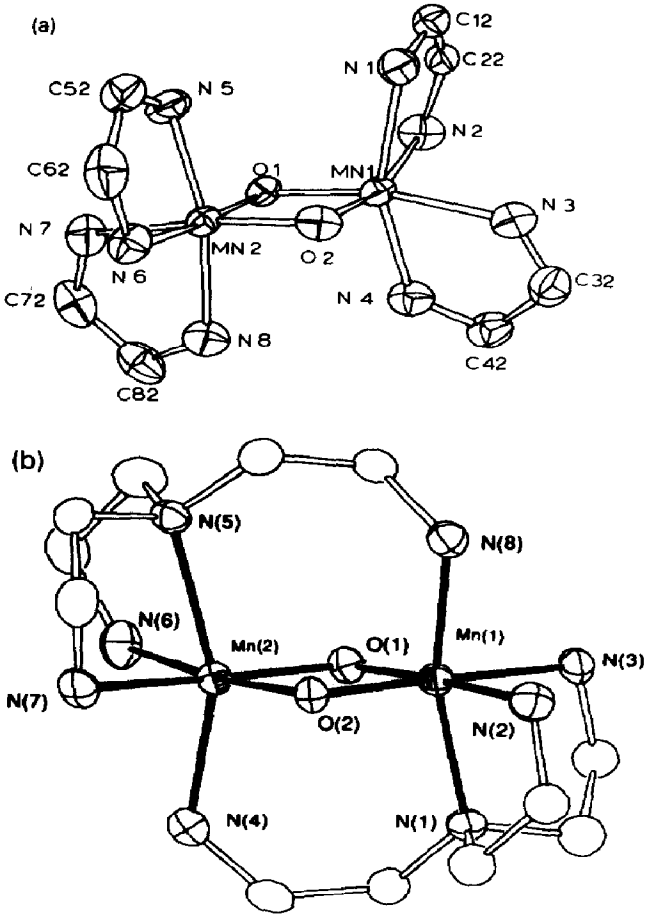

Fig. 44. (a) Structure of the cation in $[Mn_2(\mu\text{-}O)_2(bpy)_4](ClO_4)_3 \cdot 3H_2O$ (**80**). The phenanthroline analogue **81** has a similar structure. Reproduced with permission from ref. 359. (b) Structure of the cation in **84**. Reproduced with permission from ref. 371.

bond lengths (2.132 Å and 1.854 Å respectively) are consistent with a distorted high spin Mn^{III} centre. Analogous complexes of phen, phen-*N*-oxide and bpy-*N*-oxide were reported by Uson et al. [360] and the X-ray structure of $[Mn_2(\mu\text{-}O)_2(phen)_4](PF_6)_3 \cdot Me_3CN$ at 100 and 200 K was ultimately determined by Stebler et al. [361]. The $[Mn_2(\mu\text{-}O)_2(phen)_4]^{3+}$ cation (**81**) exhibits a structure very similar to that of **80** (Fig. 44(a)) but at both temperatures an average structure with two crystallographically equivalent manganese atoms was observed. A detailed analysis of the anisotropic atomic displacement parameters indicated either a dynamic or static disorder between $Mn^{III}Mn^{IV}$ and $Mn^{IV}Mn^{III}$ ions, consistent with a localized Class II structure. Complexes of this general type may also be formed by the reaction of Mn^{2+} and $[MnO_4]^-$ in the presence of ligand [362], the disproportionation of $MnLCl_3(H_2O)$ in ligand buffer [362], and the reaction of $[Mn_3O(OAc)_6](OAc) \cdot HOAc$ and ligand in acidified methanol [363]. In solution the complexes are susceptible to hydrolysis and at low pH they participate in the equilibrium shown in eqn. (19) (L = bpy, phen):

$$H_3O^+ + [Mn_2O_2L_4]^{3+} = [Mn^{III}(OH_2)(OH)L_2]^{2+} + 1/2[Mn^{IV}_2O_2L_4]^{4+} \quad (19)$$

This hydrolysis reaction accounts for the observed pH dependence of spectral and solution magnetic susceptibility data [362]. However, the discovery that the complexes are stable in aqueous bpy or phen buffers at pH 4.5 has permitted extensive solution studies [362,364]. Electrochemically, **80** and **81** are reversibly oxidized to known $[Mn_2O_2L_4]^{4+}$ complexes and irreversibly reduced to unstable $[Mn_2O_2L_4]^{2+}$ complexes [362,365]. From cyclic voltammetric data the comproportionation constants for the formation of **80** and **81** are estimated to be $10^{15.6}$ [362] and 10^{16} [361] respectively. Electrochemical studies [366] have also demonstrated that the one-electron oxidation of $[Mn(bpy)_3]^{2+}$ is followed by a chemical reaction forming **80**, a reaction originally observed by Nyholm and Turco [358]. This observation is clearly relevant to the formation of **80** from $[Mn(bpy)_3](ClO_4)_3$ reported by Plaksin et al. [359]. In the near-IR spectrum of **80**, a broad band at 830 nm (ϵ 430), is assigned to an intervalence CT transition, consistent with a Class II mixed-valence formulation. The following parameters have been derived from the spectrum of **80**: delocalization coefficient $\alpha^2 = 0.01$; activation energy to thermal electron transfer, 36 kJ mol^{-1}; estimated rate of intramolecular electron transfer, 10^6 s^{-1} [362]. For **81**, an intervalence CT transition is observed at 800 nm as a broad shoulder on a 680 nm (ϵ 550) band [361]. Similar bands are observed in the diffuse reflectance spectra of salts of **80** and **81** [360]. Magnetic susceptibility data [359,360,362,364] are consistent with high spin ($S_1 = 2$, $S_2 = 3/2$) antiferromagnetically coupled manganese

centres ($J = -150 \pm 7$ cm^{-1} and $J = -134 \pm 5$ cm^{-1} for **80** and **81** respectively [364]). The ca. 16-line ESR spectra of **80** and **81** exhibit hyperfine coupling to two inequivalent ^{55}Mn nuclei ($I = 5/2$) with $g = 2.003$, $A_1(Mn^{III}) = 167 \pm 3$ G and $A_2(Mn^{IV}) = 79 \pm 3$ G. The large difference between the hyperfine constants indicates that the unpaired electron in the ground state is localized on the Mn^{III} atom or transferred between manganese atoms at a rate much slower than $\| A_1 | - | A_2 \|$ [364]. At 298 K a rate of less than 10^8 s^{-1} is estimated for the thermally activated intramolecular electron transfer (cf. 10^6 estimated from near-IR data [362]). Cooper et al. [364] are critical of related studies reported by Morrison and Sawyer [366]. The complexes have also been investigated by EXAFS spectroscopy [367].

Related complexes in which the two diimine ligands on each metal atom have been replaced by a tetradentate N-donor ligand have recently been reported. Oxidation of aqueous Mn^{2+} in the presence of ligand results in the formation of the green complexes $[Mn_2(\mu\text{-}O)_2(bispicen)_2]^{3+}$ (**82**) [368] and $[Mn_2(\mu\text{-}O)_2(tpa)_2]^{3+}$ (**83**) [369], which were isolated as perchlorate and dithionate salts respectively. X-ray diffraction studies of these salts revealed that both cations bear a strong structural relationship to **80** and **81**. The crystallographically distinct manganese atoms, linked together by two bridging oxo ligands, each bind a tetradentate N-donor ligand in place of the diimine ligands in **80** and **81**. Structural parameters are not consistent with a completely localized $Mn^{III}Mn^{IV}$ complex. The manganese atoms of **82** and **83** are separated by 2.659(2) Å and 2.643(1) Å respectively, distances considerably shorter than the Mn · · · Mn separation in **80** and **81**. Similar preparative methods have been employed in the syntheses of $[Mn_2(\mu\text{-}O)_2L_2](ClO_4)_3$ (L = cyclam, cyclen) [370]. Preliminary X-ray diffraction results indicate a close structural similarity between these complexes and **80** or **81**. A variation on this theme is provided by $[Mn_2(\mu\text{-}O)_2(tren)_2](CF_3SO_3)_3$ (**84**), prepared by the controlled oxidation of $Mn(CF_3SO_3)_2$ in the presence of tren [371]. In the cation in **84** (Fig. 44(b)) the manganese atoms are linked together by the N-donor ligand as well as by the di-μ-oxo bridge. Structural features indicate that the Mn(1) and Mn(2) atoms possess oxidation states of IV and III respectively. The complex exhibits a 16-line ESR spectrum and the manganese atoms are antiferromagnetically coupled ($J = -146$ cm^{-1}).

Manganese, along with vanadium, molybdenum and tungsten, forms dinuclear mixed-valence complexes with triazacyclononane and related ligands. A green $Mn^{III}Mn^{IV}$ compound, $[(Me_3tcn)_2Mn_2(\mu\text{-}O)(\mu\text{-}OAc)_2](ClO_4)_3$ (**85**), is produced by electrochemical or chemical oxidation of $[(Me_3tcn)_2Mn_2(\mu\text{-}O)(\mu\text{-}OAc)_2](ClO_4)_2$ [372,373]. The structure of the cation in **85** is shown in Fig. 45(a); two metrically equivalent manganese atoms, separated by 3.230(3) Å, are linked via one bridging oxo and two bridging acetate ligands. The tridentate Me_3tcn ligands occupy the remaining coordi-

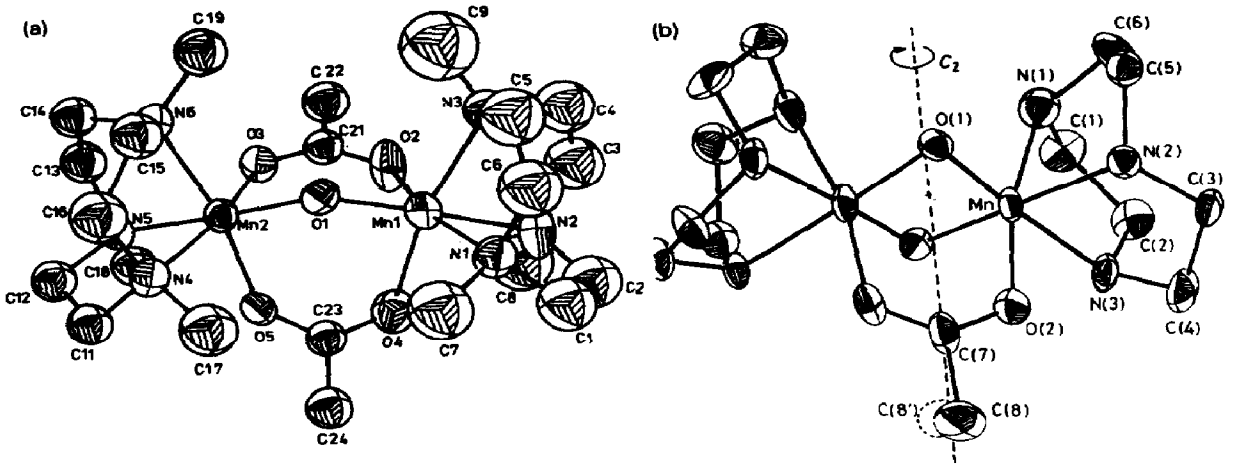

Fig. 45. (a) Structure of the cation in **85**. Reproduced with permission from ref. 373. (b) Structure of the cation in **86** showing the disordered model for the bridging acetate ligand. Reproduced with permission from ref. 374.

nation sites. A disorder involving the ClO_4^- ions prevents an unequivocable statement concerning the equivalence of the manganese atoms. An intervalence CT transition is observed at 1400 nm ($\epsilon = 100$) and magnetic measurements are consistent with antiferromagnetically coupled ($J = -40$ cm^{-1}) high spin manganese centres. A comproportionation constant of 7×10^8 has been derived from cyclic voltammetric data [373]. There is also electrochemical evidence for the formation of a dinuclear $Mn^{II}Mn^{III}$ complex of Me_3tcn but this has not been isolated [372,373]. A related $Mn^{III}Mn^{IV}$ complex, green $[(tcn)_2Mn_2(\mu\text{-}O)_2(\mu\text{-}OAc)](BPh_4)_2 \cdot MeCN$ (**86**), is formed upon hydrolysis of red $[(tcn)_2Mn_2(\mu\text{-}O)(\mu\text{-}OAc)_2]^{2+}$ in the presence of air [374]. Earlier electrochemical studies had revealed the instability of the one-electron-oxidized complex, $[(tcn)_2Mn_2(\mu\text{-}O)(\mu\text{-}OAc)_2]^{3+}$ [372]. The structure of the cation in **86** is shown in Fig. 45(b); two crystallographically equivalent manganese atoms, separated by 2.588(2) Å, are linked via a bridging acetate and two bridging oxo ligands. The tridentate tcn ligands occupy the remaining coordination sites. Although the manganese atoms are crystallographically equivalent, an observed disorder in the position of the methyl group of the bridging acetate ligand may be indicative of a degree of valence localization in the complex. The high spin manganese centres are strongly antiferromagnetically coupled ($J = -220$ cm^{-1}), producing an $S = 1/2$ ground state. The complex is characterized by 16-line ESR spectra ($g = 2.0$, $|A_1| = 154$ G, $|A_2| = 77$ G) quite similar to those of **80** and **81** [364]. Reaction of a slurry of $Mn(OAc)_3 \cdot 2H_2O$ with Me_3SiCl followed by bpy in MeCN resulted in the formation of red–brown $Mn_2(\mu\text{-}O)_2(\mu\text{-}OAc)Cl_2(bpy)_2 \cdot 2MeCN$ which was structurally characterized [375]. This complex exhibits a structure related to **86** except that each tcn ligand is

replaced by a bpy and a terminal chloride ligand. The valence-trapped complex exhibits a 16-line ESR spectrum ($g = 2.0$) and the manganese atoms are antiferromagnetically coupled ($J = -114\ cm^{-1}$).

Other $Mn^{III}Mn^{IV}$ complexes are less well characterized. The oxidation of certain Mn^{III} tetradentate Schiff base complexes under basic conditions yields red–brown $Mn^{III}Mn^{IV}$ complexes, $Mn_2L(\mu\text{-}O)(\mu\text{-}OH)$ (L = Schiff base) [376], which were originally formulated as μ-dioxo–Mn^{IV} complexes [377]. The electronic and circular dichroism spectra of complexes of the optically active tetradentate Schiff bases derived from (−)-1,2-diaminopropane and 4-*sec*-butylsalicylaldehyde or 4-*sec*-butyl-2-acetylphenol have been recorded and tentatively assigned. Electronic absorptions characteristic of Mn^{III} and Mn^{IV} centres are observed along with a prominent band (450 nm, $\epsilon = 5 \times 10^3$) assigned to an intervalence CT transition. The mixed-valence dimers were designated as Class II complexes with integral oxidation states and a substantial delocalization parameter ($\alpha^2 = 0.029$). The structure of these complexes remains obscure.

Partial thermal decomposition of solutions of ESR-silent $[MnX(TPP)]_2$-μ-O (X = OI(Br)Ph$^-$, Br$^-$, N_3^-, NCO$^-$) produced oxo-bridged $Mn^{III}Mn^{IV}$ complexes exhibiting 16-line frozen-glass ESR spectra [378,379]. A strongly antiferromagnetically coupled high spin system involving inequivalent manganese centres is consistent with the ESR spectra of these complexes. A valence-localized structure in which only one manganese atom binds a sixth anionic ligand (X) was postulated. Dismukes et al. [380] have renewed the study of these and related manganese complexes of TPP. Computer simulation of the ESR spectra of the $Mn^{III}Mn^{IV}$ complexes, for which the ^{55}Mn hyperfine field is 1070 G, yields the following parameters: $g = 2.06$, $A_1 = 74$ G, $A_2 = 140$ G. In contrast, an $Mn^{II}Mn^{III}$ species produced by the oxygenation of Mn(TPP) at 10 K exhibits a broader ^{55}Mn hyperfine field (1410 G) as a result of larger hyperfine coupling constants ($g = 2.01$, $A_1 = 99$ G, $A_2 = 181$ G). It is suggested that such spectral differences may find application in distinguishing between $Mn^{II}Mn^{III}$ and $Mn^{III}Mn^{VI}$ centres in chemistry and biology. The $Mn^{II}Mn^{III}$ species has not been identified but mechanisms for the formation of either [(TPP)MnOOMn(TPP)]$^-$ or [(TPP)MnOMn(TPP)]$^-$ have been presented. With regard to mixed-valence manganese porphyrins it would be interesting to investigate the electrospectroscopy of Mn_2(FF) reported by Landrum et al. [381].

Early investigations of dinuclear $Mn^{II}Mn^{III}$ complexes involved rather ill-defined species. The first direct observation of dinuclear $Mn^{II}Mn^{III}$ complexes resulted from the controlled oxidation of the Mn^{II} complexes Mn(saldien) and Mn(5-NO_2-saldien) (magnetic susceptibility data for these Mn^{II} complexes suggest a dinuclear formulation) [382]. The green oxidation products exhibit 16-line ESR spectra, magnetic susceptibilities consistent

with high spin antiferromagnetically coupled manganese centres, and IR spectra indicative of the presence of a bridging peroxide ligand. The complexes are proposed to consist of two valence-trapped $Mn^{II}Mn^{III}$(saldien)$_2$ units linked by a peroxide ligand. Dismukes et al. [380] have suggested that the ESR data are more consistent with an $Mn^{III}Mn^{IV}$ formulation and further study of this system is therefore warranted. It is interesting to note that several years prior to this report, Coleman et al. [383] reported the oxygenation and electrochemistry of a wide range of Mn^{II} Schiff base complexes including Mn(saldien) and Mn(5-NO_2-saldien). The unusual behaviour of these two complexes lead to the suggestion that dinuclear mixed-valence species were formed upon oxidation [383]. In fact, dinuclear mixed-valence Schiff base complexes of manganese had been reported 6 years earlier by Boucher and Coe (vide supra) [376,377].

Dinuclear Mn^{II} complexes of so-called strati-bis Schiff base ligands, Mn_2(dtsb) and Mn_2(bbsc), are air oxidized to yield deep red $Mn^{II}Mn^{III}$ complexes $Mn_2L(OH)(H_2O)$ (L = dtsc or bbsc) [384]. However, only the mixed-valence complex of dtsc could be isolated and it remains uncertain whether the water molecule acts as a ligand. The high spin manganese centres are antiferromagnetically coupled ($g = 1.97$, $J = -6.0$ cm^{-1}) via superexchange through the bridging hydroxo ligand. A near-IR band at 1300 nm, assigned to the intervalence CT transition of a Class II complex, is characteristic of the mixed-valence species.

More recently, $Mn^{II}Mn^{III}$ compounds have been unambiguously characterized by X-ray crystallography. The compound [Mn_2(bpmp)(μ-OAc)$_2$](ClO_4)$_2 \cdot H_2O$ (**87**) has been studied by two groups [385,386]. The compound may be prepared by reacting equimolar amounts of $Mn(ClO_4)_2 \cdot 6H_2O$ and [$Mn(dmso)_6$](ClO_4)$_3$ with bpmpH, HOAc and Et_3N in methanol [385] or by air oxidation of the complex formed from $Mn(OAc)_2$ and bpmp$^-$ [386]. The structure of the cation in **87** is shown in Fig. 46 and features two crystallographically distinct manganese centres bridged by two acetato ligands and the phenoxy oxygen atom of bpmp$^-$ [386]. A valence-trapped structure was inferred from structural data: Mn(1) exhibits a distorted octahedral geometry and bond distances typical of Mn^{II} while Mn(2) exhibits a structure typical of a Jahn–Teller-distorted Mn^{III} centre. In the cyclic voltammogram, two quasi-reversible redox waves are assigned to one-electron reduction and oxidation processes respectively, allowing a comproportionation constant of 1.7×10^9 to be calculated [385]. The complex does not exhibit a near-IR band [385]. Magnetic susceptibility data are indicative of isotropic magnetic exchange between Mn^{II} and Mn^{III} ions with $g = 2.0$ and $J = -6.0$ cm^{-1} [385,386]. ESR spectra exhibit a remarkable temperature dependence and at 7.5 K a $g \approx 2$ signal composed of 29 hyperfine lines is reported [386].

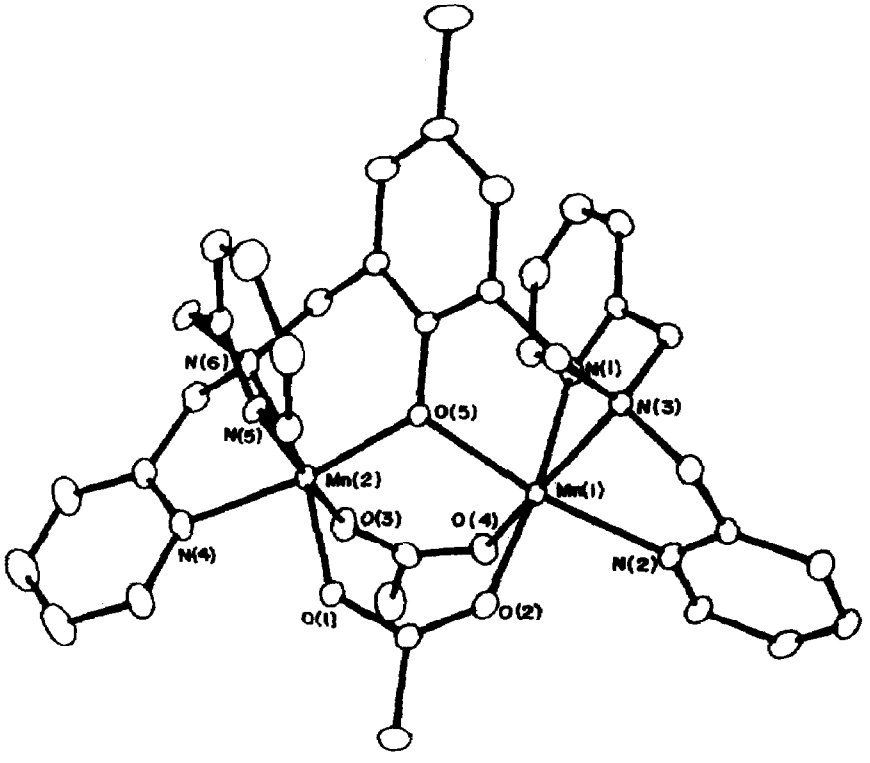

Fig. 46. Structure of the cation in **87**. Reproduced with permission from ref. 386.

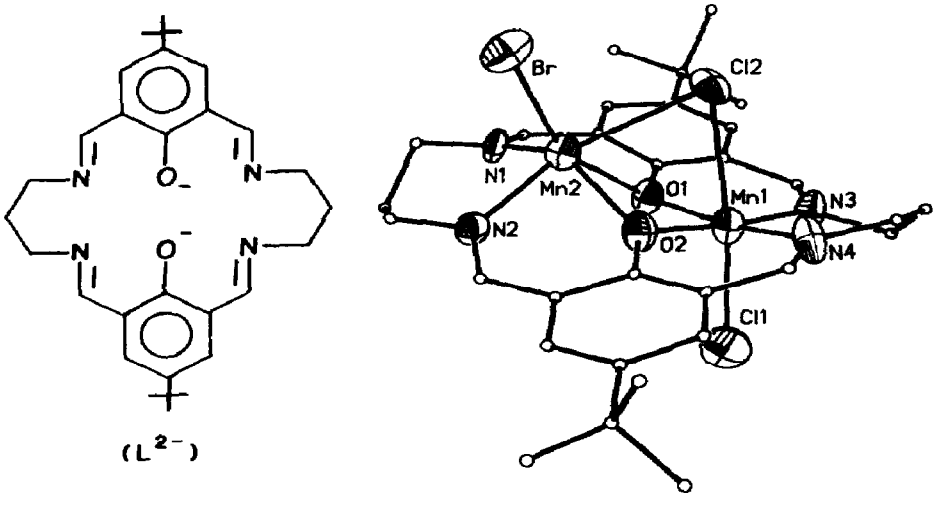

Fig. 47. Structure of LMn_2Cl_2Br where L^{2-} is the ligand shown. Reproduced with permission from ref. 386.

Another $Mn^{II}Mn^{III}$ complex is LMn_2Cl_2Br, formed by oxidation of LMn_2Cl_2 with bromine water (L^{2-} is shown in Fig. 47) [386,387]. The complex (Fig. 47) is composed of manganese centres bridged by a chloro ligand and the two phenoxide oxygen atoms of L; Mn(1) is a Jahn–Teller-distorted Mn^{III} atom while a trigonal prismatic coordination sphere is observed around the Mn^{II} atom (Mn(2)). Magnetic data are consistent with isotropic magnetic exchange between high spin Mn^{II} and Mn^{III} atoms with $J = -1.7$ cm^{-1}. ESR spectra show broad features and little hyperfine resolution even at 7.5 K. Detailed magnetic, electrochemical and ESR data have been reported for this compound and LMn_2Br_3 [387]. The comproportionation constants for the reactions shown in eqn. (20) are 1.7×10^{10} and 2.3×10^{11} for X = Cl and X = Br respectively:

$$[LMn^{III}_2X_2]^{2+} + LMn^{II}_2X_2 = 2[LMn^{II}Mn^{III}X_2]^{+} \quad (20)$$

In the Mn^{II} precursor, LMn_2Cl_2, the bridging halide ligand is absent and a planar diphenoxy bridge links the manganese atoms [387].

Phenoxide bridges feature in two other recently reported $Mn^{II}Mn^{III}$ complexes. Reaction of bpy with $(NHEt_3)[Mn^{III}(biphen)_2(biphenH)]$ in CH_2Cl_2 leads to $Mn_2(biphen)_2(biphenH)(bpy)_2 \cdot 3CH_2Cl_2$ (**88**) which has been structurally characterized [375]. The complex in **88** (Fig. 48) possesses a valence-trapped structure with Mn(1) and Mn(2) assigned oxidation states of II and III (Jahn–Teller distorted) respectively. The ferromagnetic interaction in **88** is characterized by $J = +0.89$ cm^{-1}. Finally, black $[Mn_2(L\text{-}Im)(\mu\text{-}OAc)_2](ClO_4)_2$ is produced when $Mn(OAc)_3 \cdot 3H_2O$, L-ImH and $NaClO_4$ react in MeOH [388]. The complex exhibits a valence-trapped

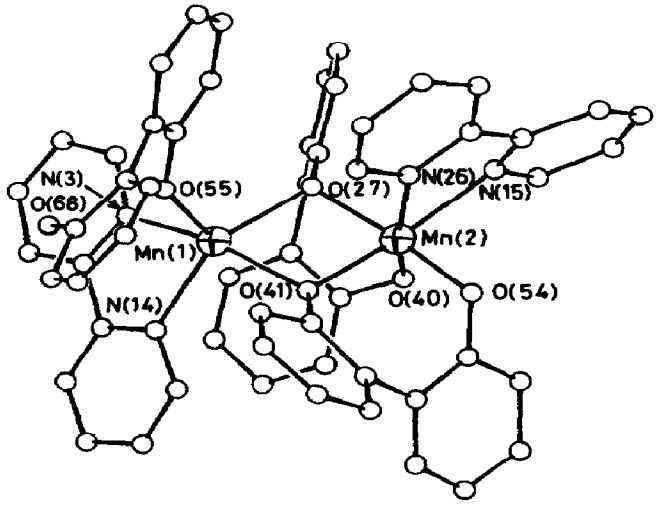

Fig. 48. Structure of $Mn_2(biphen)_2(biphenH)(bpy)_2$. Reproduced with permission from ref. 375.

structure which resembles that of **87**. Magnetic and ESR studies were reported.

Only one $Mn^{I}Mn^{II}$ complex has been reported to date. Electrochemical and chemical (Br_2, $-40\,^{\circ}C$) oxidation of yellow $[Mn_2(\mu\text{-}SPh)_3(CO)_6]^-$ yields the deep red $Mn^{I}Mn^{II}$ complex, $Mn_2(\mu\text{-}SPh)_3(CO)_6$ (**89**) [389]. The complex exhibits new spectral bands at 519 and 880 nm, the latter being assigned to an intervalence CT transition (cf. **80** and **81** [361,362]). ESR spectra of **89** at $-40\,^{\circ}C$ consist of a symmetrical 11-line signal indicative of a single electron interacting with two equivalent ^{55}Mn nuclei. This complex is the only Class IIIA mixed-valence manganese complex isolated to date. Recent studies [390] have also revealed the existence of related complexes. Electrochemical oxidation of the $[Mn_2(\mu\text{-}SR)_3(CO)_6]^-$ and $Mn_2(\mu\text{-}SR)_2L_2(CO)_6$ complexes (R = Me, ^{t}Bu, Ph; L = PMe_3, PPh_3, dppm) occurs in two quasi-reversible steps forming neutral (including **89**) and monocationic complexes. In contrast, electrochemical oxidation of $Mn_2(\mu\text{-}SR)_2(\mu\text{-}CO)L_2(CO)_4$ is accompanied by chemical changes involving the coordination of a solvent molecule (MeCN) and displacement of the μ-CO ligand to a terminal position. These mixed-valence monocations exhibit six-line ESR spectra consistent with coupling to only one manganese atom.

The crystal structure of $Cp(NO_2)Mn(\mu\text{-}NO)_2Mn(NO)Cp$ (**90**) has also

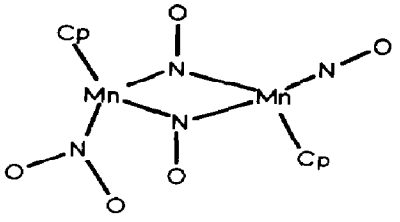

90

been reported [391]. The unsymmetrical complex may be described as an $Mn^{0}Mn^{II}$ species with the nitrito group bound to Mn^{II}.

A dilute low valent $Mn^{0}Mn^{I}$ species is produced upon γ-irradiation of single crystals of $Mn_2(CO)_{10}$ [392,393]. Single-crystal ESR spectra at 85 K are characteristic of anisotropic interactions of a single electron with the magnetic field and with two ^{55}Mn nuclei. The two ^{55}Mn hyperfine tensors have identical components but are inclined at about $120\,^{\circ}C$ to each other, suggesting that the mixed-valence species has lower symmetry than $Mn_2(CO)_{10}$ itself. The mixed-valence species is postulated to be $[Mn_2(CO)_9]^-$ with a single bridging carbonyl ligand and a $^2B_2$ ground state [392]. The complex is not D_{4d} $[Mn_2(CO)_{10}]^-$ as previously proposed by Bratt and Symons [393].

(c) Trinuclear compounds

Manganese forms a number of isovalent and mixed-valence oxo-centred basic carboxylates of general formula $[Mn_3(\mu_3\text{-}O)(O_2CR)_6L_3]^{+/0}$ (Fig. 10). The reaction of $Mn(OAc)_3 \cdot 2H_2O$ with pyridine, once reported to yield $Mn_4O_2(OAc)_8(py)_5$ [394], yields black $Mn_3O(OAc)_6(py)_3$ (**91**) [395]. Unsolvated **91** and the pyridine solvate have been structurally characterized at room temperature and $-50\,^{\circ}C$ respectively [395,396]. In both cases, crystallographically imposed 32 (D_3) symmetry dictates the equivalence of the manganese atoms and a planar array of manganese, central oxygen and N-donor atoms. Variable-temperature susceptibility data show that all the manganese centres are in high spin configurations and are antiferromagnetically coupled ($|J| < 9\ cm^{-1}$) to produce a doublet ground state [396]. The 3-Clpy analogue possesses a similar structure except that one of the manganese atoms is crystallographically unique [397]. Consistent with the observed Mn–O bond lengths, and the balancing of charges, the unique manganese atom is assigned an oxidation state of II while the other two manganese atoms are assigned an oxidation state of III. This complex is also weakly antiferromagnetic.

The reaction of Mn^{2+} and $[MnO_4]^-$ in various media is known to produce a variety of isovalent and mixed-valence carboxylate complexes [362,396,398]. A recent modification of this general reaction, the use of $N^tBu_4[MnO_4]$ and non-aqueous solvents, has been employed in the synthesis of **91** and $Mn_3O(O_2CPh)_6(py)_2(H_2O)$ (**92**) [396]. The latter complex exhibits a valence-trapped structure with the water and py ligands coordinated to the Mn^{II} and Mn^{III} centres respectively (see Fig. 10). The $Mn^{II}Mn^{III}$ interaction in **92** ($J = -10.9\ cm^{-1}$) is close in magnitude to that observed in $[Mn_3O(OAc)_6(py)_3]ClO_4$.

Several trinuclear mixed-valence compounds of manganese possess an extended rather than a triangular array of manganese atoms. The first example of such a compound was reported in 1985 by Seela et al. [399]. Controlled aerial oxidation of an ethanolic reaction mixture containing $MnCl_2$, Na_2pdt and PPh_4Br resulted in the formation of $(PPh_4)_2[Mn_3(pdt)_5]$ (**93**). The structure of the anion in **93** is shown in Fig. 49. The idealized C_2 molecule possesses an approximately linear array of manganese atoms bridged by thiolate S-donor atoms. The central Mn(2) atom, assigned as the Mn^{II} atom, possesses a distorted octahedral geometry while the terminal Mn^{III} atoms (Mn(1) and Mn(3)) possess distorted five-coordinate geometries. In **93**, the high spin manganese centres are antiferromagnetically coupled, producing a quartet ground state with $S_1 = S_3 = 2$, $S_2 = 5/2$, $J_{12} = J_{23} = -18.3\ cm^{-1}$ and $J_{13} \approx 0$. This complex is the only known homoleptic, S-donor ligand, mixed-valence complex of manganese.

The green $Mn^{II}Mn^{III}_2$ complex $Mn_3(salhp)_2(OAc)_4(MeOH)_2$ (**94**) is pro-

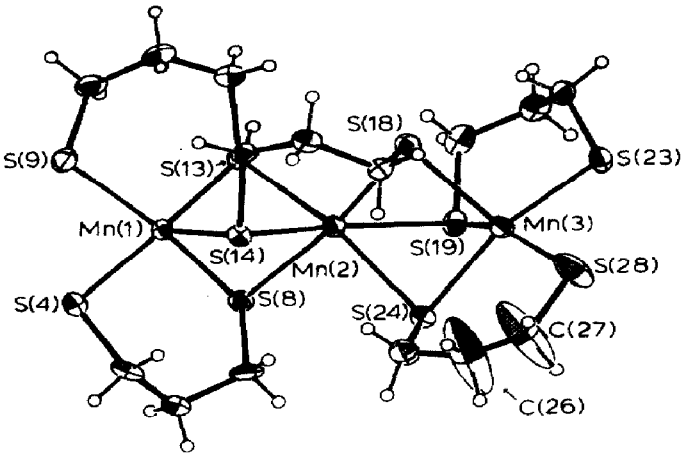

Fig. 49. Structure of the anion in **93**. Reproduced with permission from ref. 399.

duced by the reaction of $Mn(OAc)_2 \cdot 4H_2O$ and salhp in refluxing methanol [400]. The X-ray structure of **94** (Fig. 50) revealed a central Mn^{II} ion (Mn(2)) coordinated by μ-alkoxy and μ-OAc ligands to two terminal Mn^{III} atoms which bear the salhp ligand, two μ-OAc ligands and a terminal methanol ligand. The presence of methanol ligands rather than methoxy ligands was established by preparing the analogous thf adduct which exhibited magnetic and spectroscopic properties identical with those of **94**. In the solid state and in CH_2Cl_2–toluene solution the manganese centres are weakly coupled ($J_{12} = -7.09$, $J_{11'} = 0$ cm^{-1}) and the complex possesses a quartet ground state. In donor solvents, **94** dissociates into Mn^{2+} and Mn^{3+} ions.

The final trinuclear complex to be discussed also possesses an extended structure. Brown $Mn_3(MeC_5H_6)_4$ is formed upon the reaction of $MnCl_2$ and $K(MeC_5H_6)$ [401]. The structure of this unusual complex, shown in Fig. 51, comprises two $Mn(MeC_5H_6)_2$ units linked via two terminal carbon atoms (one from each ligand) to the central Mn(2) atom. The inclusion of

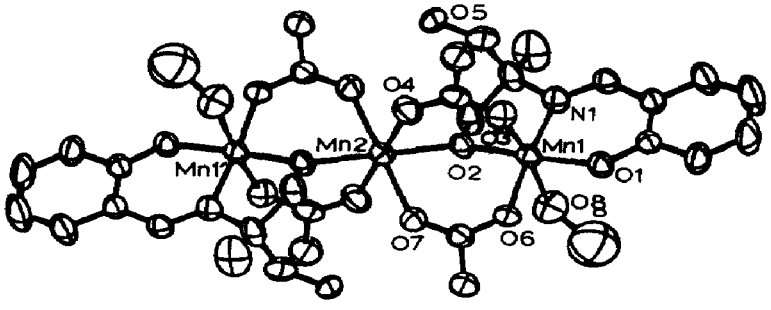

Fig. 50. Structure of **94**. Reproduced with permission from ref. 400.

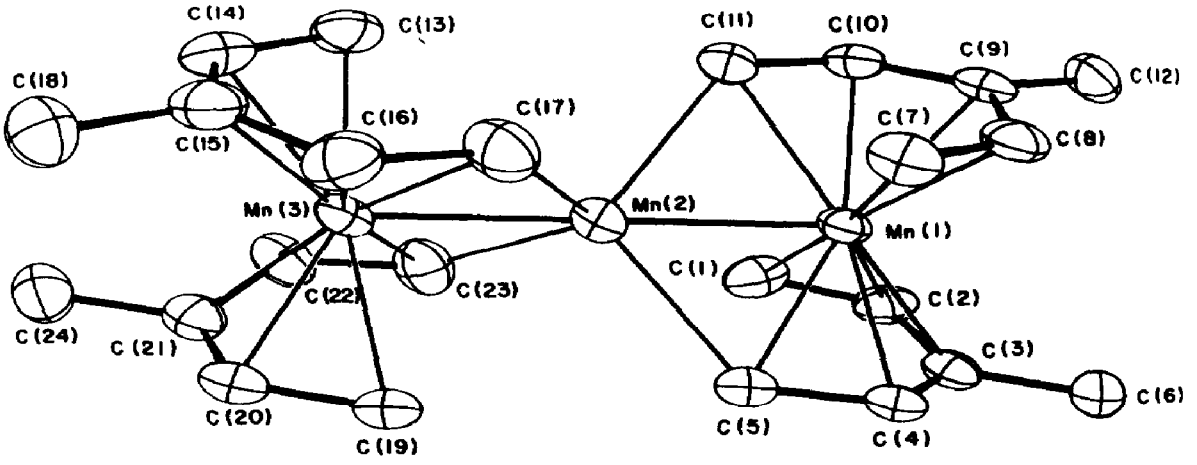

Fig. 51. Structure of $Mn_3(MeC_5H_6)_4$. Reproduced with permission from ref. 401.

the coordinated manganese atoms in the nearly tetrahedral carbon coordination sphere of Mn(2) produces an edge-bicapped tetrahedral geometry around this manganese atom. The terminal manganese atoms, Mn(1) and Mn(3), are postulated to be formally Mn^{I} centres, necessitating the assignment of an oxidation state of II to Mn(2). Magnetic susceptibility data are consistent with the high spin $S = 5/2$ ground state predicted by theoretical studies and the formulation of the complex as an association of high spin Mn^{II} and diamagnetic $[Mn^{I}(MeC_5H_6)_2]^-$ centres.

(d) Tetranuclear compounds

In 1987, Christou and coworkers reported the first tetranuclear mixed-valence compounds of manganese. Such compounds are important models for the proposed manganese tetramer in the oxygen-evolving centre of green plants and cyanobacteria [402]. The $Mn^{III}_3Mn^{IV}$ compound $(ImH_2)_2[Mn_4O_3Cl_6(ImH)(OAc)_3] \cdot 1.5MeCN$ (**95**) is formed via the sequential reaction of **97** (vide infra) with Me_3SiCl, ImH, and then $NaClO_4$ [403]. The novel structure of the anion in **95** is shown in Fig. 52. An Mn_4 pyramid with Mn(1) as apex, a μ_3-Cl ligand (Cl(5)) bridging the basal plane and μ_3-O ligands bridging the remaining three faces is the best description of the $[Mn_4(\mu_3\text{-}O)_3(\mu_3\text{-}Cl)]^{6+}$ core. Three bridging acetate ligands, five terminal chloro ligands and a terminal ImH ligand complete the coordination spheres. Mn(1) is assigned as the Mn^{IV} centre while the remaining manganese atoms are assigned as Mn^{III} centres. Only preliminary magnetic susceptibility and ESR data have been reported. The authors alluded to the synthesis of an analogous uncharged $Mn^{III}_3Mn^{IV}$ complex, $Mn_4O_3Cl_4(OAc)_3(py)_3$, but details were not given [403].

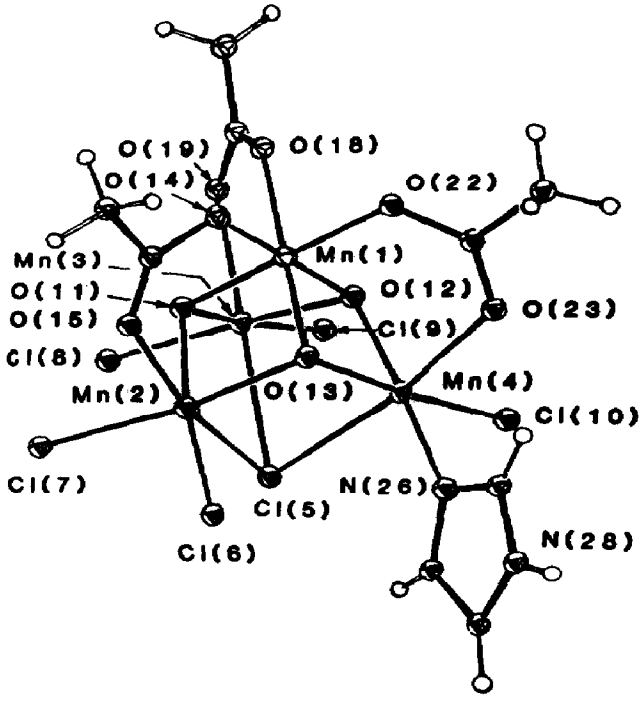

Fig. 52. Structure of the anion in **95**. Reproduced with permission from ref. 403.

The dark brown complex $Mn_4O_2(OAc)_6(bpy)_2$ (**96**) is formed by the reaction of $[Mn_3O(OAc)_6(py)_3] \cdot py$ [396] with bpy [404]. The structure of this $Mn^{II}_2Mn^{III}_2$ complex is shown in Fig. 53. The manganese atoms in the $[Mn_4O_2]^{6+}$ core are strictly planar and are linked via two μ_3-O and six

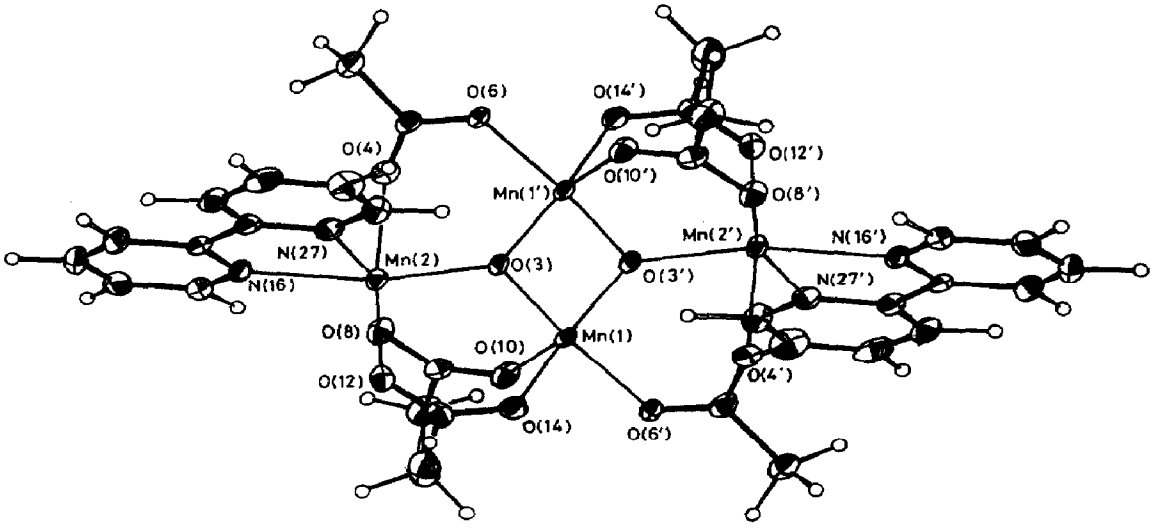

Fig. 53. Structure of **96**. Reproduced with permission from ref. 404.

μ-OAc ligands. The bpy ligands complete the coordination spheres of Mn(2) and Mn(2′). On the basis of structural parameters, Mn(1) and Mn(1′) are assigned an oxidation state of III while Mn(2) and Mn(2′) are assigned an oxidation state of II. Magnetic susceptibility data have been fitted using a model involving isotropic pairwise interactions ($S_1 = S_{1'} = 2$, $S_2 = S_{2'} = 5/2$) with $J_{12} = J_{12'} = J_{1'2} = J_{1'2'} = -1.97$, $J_{11'} = -3.12$ and $J_{22'} = 0$ cm^{-1}. Interestingly, the related isovalent Mn^{III} compound, $[Mn_4O_2(OAc)_7(bpy)_2]ClO_4 \cdot 3H_2O$, has been reported [405] and the $[Mn_4O_2]^{8+}$ core present in this complex exhibits a butterfly rather than a planar structure. Reduction in the dihedral angle between the edge-shared Mn_3O units in the isovalent complex results in the binding of a seventh OAc^- ligand which bridges Mn(1) and Mn(1′).

(e) Hexanuclear compounds

The reaction of $MnCO_3$ with pivalic acid in refluxing toluene deposits the red–brown hexanuclear $Mn^{II}_4Mn^{III}_2$ complex $Mn_6O_2(O_2C^tBu)_{10}(^tBuCO_2H)_4$ [406], the only known hexanuclear mixed-valence complex of manganese. The complex (Fig. 54) is composed of two tetrahedral $Mn_4O(O_2CR)_6$ units which share a common edge. Pivalate ligands bridge pairs of manganese atoms along each edge except that which is shared, and a monodentate pivalic acid molecule is coordinated to each of the four outer manganese atoms. The average manganese oxidation state of $+2\frac{1}{3}$ is accommodated by

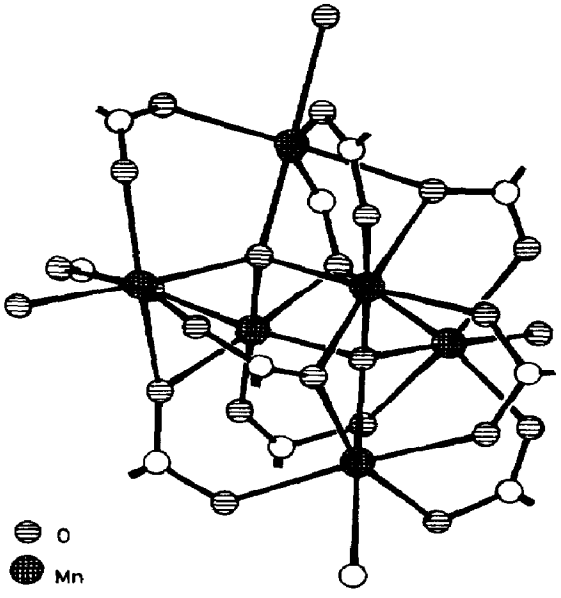

Fig. 54. The central core of the $Mn_6O_2(O_2C^tBu)_{10}(^tBuCO_2H)_4$ cluster. The carboxylate ligands are only partially shown. Reproduced with permission from ref. 406.

assigning oxidation states of III and II to the shared inner and outer manganese atoms respectively. In pyridine, the complex reacts to form $Mn_6O_2(O_2C^tBu)_{10}(py)_4$.

(f) Heptanuclear compounds

Although solids such as Mn_2O_7 do not fall within the scope of this review, it is interesting to note the existence of at least one discrete oxomanganate, the violet compound $(H_3O)_2[Mn(MnO_4)_6] \cdot 11H_2O$ formed upon evaporation of an aqueous solution of permanganic acid [407,408]. The X-ray structure of the compound at $-120\,^\circ C$ reveals a heptanuclear anion composed of six tetrahedral $Mn^{VII}O_4$ units bound to a central six-coordinate Mn^{IV} ion. The Mn^{VII} atoms form a trigonal prismatic arrangement around the central Mn^{IV} atom which has an octahedral coordination sphere formed by the μ-O ligands. This compound has an average manganese oxidation state of $6\frac{4}{7}$ and is by far the most oxidized mixed-valence compound known for any of the group 4–7 elements.

A basic carboxylate fragment is observed in the red–brown mixed-valence polymer $K_2[Mn(H_2O)[Mn_3O(O_2CH)_9]_2]$ formed by the reaction of $KMnO_4$ and 70–95% formic acid [409]. The two distinct types of manganese atom are assigned oxidation states of II and III. The Mn^{II} atoms are bonded to four formate ligands and two water molecules. Each formate ligand binds the Mn^{II} atom to an Mn^{III} atom in a trinuclear unit. Magnetic susceptibility studies demonstrated exchange interactions between the Mn^{II} atoms possibly via superexchange interactions through the bridging oxygen atoms.

(g) High nuclearity compounds

A novel nonanuclear complex has recently been described by Christou and coworkers. The reaction of **92** · 0.5MeCN or $[Mn_3O(O_2CPh)_6(py)_3]ClO_4$ and salicylic acid in MeCN results in black crystals of the $Mn^{II}Mn^{III}_8$ complex $Mn_9O_4(O_2CPh)_8(sal)_4(salH)_2(py)_4$ in 40% yield [410,411]. The structure of the complex is shown in Fig. 55. The central Mn^{II} atom (Mn(1)) exhibits an eight-coordinate distorted dodecahedral geometry. Each of the four μ_3-η^3-salicylate ligands surrounding Mn(1) link it to two other manganese atoms, one in the top and one in the bottom Mn^{III}_4 unit. The eight Mn^{III} atoms are contained in two $Mn_4(\mu\text{-}O)_2$ units which possess a butterfly arrangement similar to that found in $[Mn_4O_2(OAc)_7(bpy)_2]^+$ [405]. A detailed magnetic susceptibility study of the complex has been reported [411].

The characterization of a discrete dodecanuclear mixed-valence complex of manganese highlights the ability of this element to form stable complexes of exceptionally high nuclearity and structural intricacy. Red–black $Mn_{12}O_{12}(OAc)_{16}(H_2O)_4 \cdot 2HOAc \cdot 4H_2O$ (**97**) is isolated from the reaction

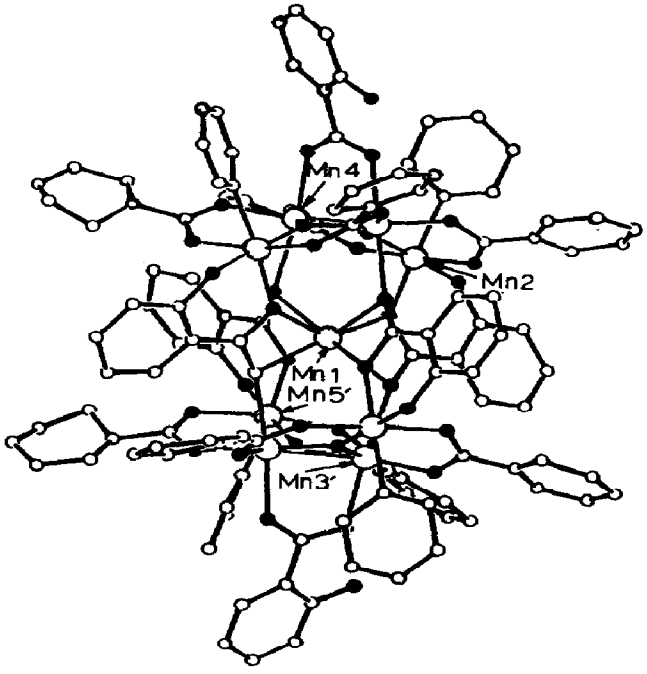

Fig. 55. Structure of $Mn_9O_4(O_2CPh)_8(sal)_4(salH)_2(py)_4$ with only one of each symmetry (C2) related pair of manganese atoms labelled. The oxygen atoms are shown as solid circles. Reproduced with permission from ref. 411.

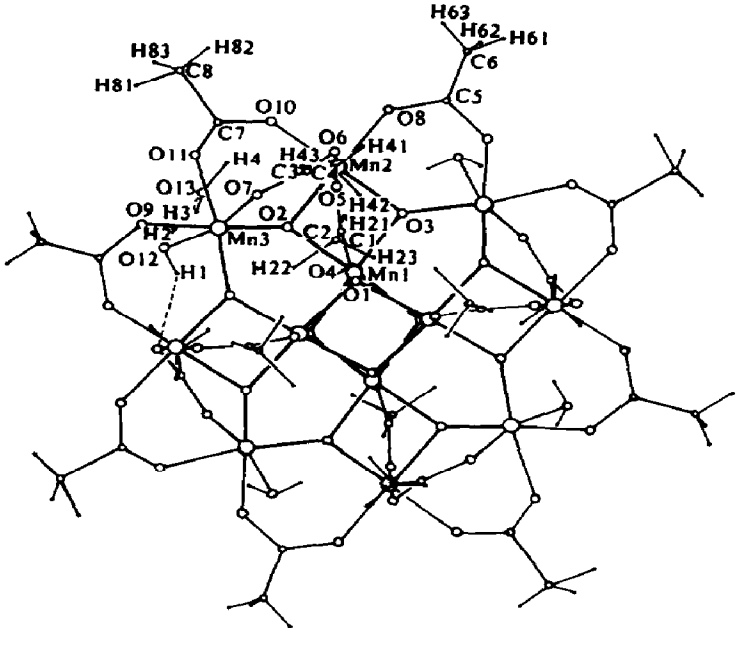

Fig. 56. Structure of $Mn_{12}O_{12}(OAc)_{16}(H_2O)_4$. Reproduced with permission from ref. 398.

of $Mn(OAc)_2 \cdot 4H_2O$ and $KMnO_4$ in acetic acid at 60 °C [398]. The structure of the "snow flake" molecule is shown in Fig. 56. The structural parameters and formula support the assignment of Mn(1) as an Mn^{IV} atom and Mn(2) and Mn(3) as Mn^{III} atoms. The Mn(1) atoms form an almost ideal cubane structure which is linked through a network of μ_3-oxo ligands (O(2) and O(3)) to acetate-bearing Mn(2) and Mn(3) atoms. The μ_3-oxo atoms O(2) and O(3) are displaced from the planes formed by the three coordinated metal atoms. The complex has been exploited in the synthesis of **95**, the only other example of a mixed-valence manganese complex with a "cubane"-like central core [403].

(ii) Technetium compounds

(a) General survey

In contrast with the number and variety of mixed-valence compounds formed by its first and third row congeners, mixed-valence compounds of technetium are relatively rare and are restricted to only three classes of compound: oxo-bridged and metal–metal-bonded dinuclear compounds and metal–metal-bonded polynuclear cluster halides. The limited number and variety of mixed-valence technetium compounds may be a consequence of the recent development of the chemistry of this synthetic element and its propensity, in low oxidation states, to form strong metal–metal bonds. With few exceptions, most notably the μ-oxo-$Tc^{III}Tc^{IV}$ complexes $Tc_2(\mu\text{-}O)X_5L_5$ (X = Cl, Br; L = pyridine derivative), mixed-valence technetium compounds are strongly metal–metal-bonded species with average oxidation states of less than 2.5. In fact the first Tc–Tc-bonded complex to be identified, $[Tc_2Cl_8]^{3-}$, remains the archetypal mixed-valence complex of technetium. In view of the chemistry of its closest analogues, molybdenum and rhenium, it is not surprising that technetium should form such strong metal–metal bonds. It is surprising, however, that metal–metal-bonded technetium compounds appear to be thermodynamically stable as mixed-valence rather than isovalent (cf. molybdenum and rhenium) species. Such compounds have been the subject of extensive investigations by Cotton and Walton [154] and the Russian group lead by Spitsyn [412]. Dinuclear metal–metal-bonded compounds possess an average oxidation state of 2.5, a Tc–Tc bond order of 3.5 and structures related to $[Re_2Cl_8]^{2-}$ or $Mo_2(OAc)_4$. A variety of salts of $[Tc_2Cl_8]^{3-}$ have been intensively investigated by a wide variety of techniques including crystallography, magnetochemistry, and ESR, electronic, vibrational and photoelectron spectroscopy. The paramagnetic ion possesses a delocalized structure and a $\sigma^2\pi^4\delta^2\delta^*$ metal–metal bond. Various derivatives maintaining the $\sigma^2\pi^4\delta^2\delta^*$ core and an average oxidation state of 2.5 have been prepared by reacting $[Tc_2Cl_8]^{3-}$ with various ligands. Compounds of

this type include $Tc_2(hp)_4Cl$ and $Tc_2(OAc)_4X$ (X = Cl, Br). In 1982, Spitsyn and coworkers discovered a new class of polynuclear mixed-valence cluster halides possessing strong metal–metal bonds, and several hexanuclear and octanuclear compounds of this type have now been reported. The hexanuclear clusters $[Tc_6Cl_{12}]^{2-}$ and $[Tc_6Cl_{14}]^{3-}$ possess trigonal prismatic structures with μ-Cl ligands above and along the edges of the triangular faces of the prism. Strong Tc–Tc bonding is maintained between the pairs of metal atoms forming the vertical edges of the prism. A hexanuclear complex $[Tc_6Br_6(\mu_3\text{-}Br)_5]^{n+}$ is proposed to possess a structure similar to octahedral $[M_6X_{14}]^{n+}$ complexes formed by other elements, although some doubts remain about its characterization. Further developments by Spitsyn's group have led to octanuclear clusters which also exhibit strong metal–metal bonding and formal mixed-valence formulations.

Properties of selected mixed-valence compounds of technetium are summarized in Table 11.

(b) Dinuclear compounds

Technetium forms very few mixed-valence compounds in which the average oxidation state exceeds 2.5 and until recently there was little evidence to support the existence of such compounds. For example, a poorly characterized compound of unknown structure was reported by Spitsyn et al. in 1985 [412]. This yellow–green material, formulated as the $Tc^{IV}Tc^{V}$ compound $K_3[Tc_2Cl_8O_2]$, was obtained upon reflux of $K_3[Tc_2Cl_8] \cdot 2H_2O$ in methyl ethyl ketone in air [412]. The compound exhibited a magnetic moment of 4.15 BM and chemical and IR data were interpreted in terms of a dinuclear structure with a weak Tc–Tc bond. More recently, examples of well-characterized $Tc^{III}Tc^{IV}$ compounds have been reported by Clarke and coworkers [413,414]. Two isomeric forms of $Tc_2(\mu\text{-}O)X_5L_5$ (X = Cl, Br; L = py, 4-Mepy, 3,5-Me_2py) are produced upon reaction of common technetium starting materials such as $(NH_4)_2[TcX_6]$, $N^nBu_4[TcOX_4]$, $[TcO_2(py)_4]Cl$ and $TcO(OR)Br_2(py)_2$ with neat pyridine at reflux temperatures. The ultimate products, the dissymmetric isomers $XL_4Tc\text{–}O\text{–}TcX_4L$, appear to be formed via the asymmetric $X_2L_3Tc\text{–}O\text{–}TcX_3L_2$ isomers which may be isolated at intermediate stages of the reactions. The X-ray structures of the asymmetric (**98**) and dissymmetric (**99**) isomers of $Tc_2(\mu\text{-}O)Cl_5(4\text{-}Mepy)_5$ are shown in Fig. 57. In both complexes, the geometry about the technetium is almost octahedral and the metal atoms are linked by a corner-shared μ-oxo ligand. The equatorial ligands on each technetium atom are staggered relative to those on the adjacent technetium atom. The two Tc–O bond distances in **99** are not significantly different. However, in **98** the Tc1–O distance is clearly shorter than the Tc2–O distance. This observation is contrary to conclusions based on the assignment of formal oxidation

TABLE 11

Properties of selected mixed-valence compounds of technetium

Compound	Average Tc oxidation state	Tc–Tc bond order	Tc–Tc distance (Å)	μ_{eff} [a] (BM)	ESR spectrum	XPS Tc $3d_{5/2}$ (eV) [b]	Ref.
$(Mepy)_2Cl_3TcOTcCl_2(Mepy)_3$	3.5	–	Tc1–O 1.800(3) [c] Tc2–O 1.837(3)	1.3	Rhombic	–	414
$(Mepy)_4ClTcOTcCl_4(Mepy)$	3.5	–	Tc1–O 1.84(1) [c] Tc2–O 1.79(1)	1.3	$g_{\parallel} = 1.9275$, $g_{\perp} = 1.997$ $A_{\parallel} = 272.3$, $A_{\perp} = 163.3$ $A'_{\parallel} = 31.0$, $A'_{\perp} = 60.1$ [d]	–	413, 414
$(NH_4)_3[Tc_2Cl_8]\cdot 2H_2O$	2.5	3.5	2.13(1)	1.78	–	255.5	416, 417, 419
$Y[Tc_2Cl_8]\cdot 9H_2O$	2.5	3.5	2.105(1)	1.78	$g_{\parallel} = 1.912$, $g_{\perp} = 2.096$ $\lvert A_{\parallel}\rvert = 166$, $\lvert A_{\perp}\rvert = 67.2$ [e]	–	416, 418, 427

$K_3[Tc_2Cl_8]\cdot 2H_2O$	2.5	3.5	2.117(2)	1.74	–	255.5	419, 424
$Tc_2(hp)_4Cl$	2.5	3.5	2.095(1)	–	$g = 2.046$	–	429
$Tc_2(OAc)_4Cl$	2.5	3.5	2.117(1)	1.73	–	255.8	430–433
$Tc_2(OAc)_4Br$	2.5	3.5	2.112(1)	1.74	–	255.7	430–433
$K[Tc_2(OAc)_4Cl_2]$	2.5	3.5	2.1260(5)	1.73	–	255.8	430–433
$Tc_2py_2Cl_5$	2.5	3.5	–	1.8	–	255.3	412
$(NMe_4)_3[Tc_6Cl_6(\mu\text{-}Cl)_6]Cl_2$	1.83	Edge 4.0 Base 0.5	Edge 2.16(1) Base 2.69(1)	1.7	–	254.6	442–444
$(NMe_4)_2[Tc_6Cl_6(\mu\text{-}Cl)_6]$	1.67	Edge 3.0 Base 1.0	Edge 2.22(1) Base 2.57(1)	1.1	–	–	442–444
$[H(H_2O)_2][Tc_8Br_4(\mu\text{-}Br)_8]Br$ [f]	1.5	Edge 4.0 Diagonal 1.0 Base 0.5	Edge 2.155(3) Diagonal 2.531(2) Base 2.70(2)	1.0	$g < 2$	254.7	445–447
$[H(H_2O)_2]_2[Tc_8Br_4(\mu\text{-}Br)_8]Br_2$ [f]	1.5	Edge 4.0 Diagonal 1.0 Base 0.5	Edge 2.152(9) Diagonal 2.520(9) Base 2.69(1)	1.1	$g \approx 2$	–	445–447

[a] At ca. 298 K.

[b] Data from ref. 450.

[c] No Tc–Tc bond exists in these compounds.

[d] A values in G.

[e] A values $\times 10^4$ cm^{-1}.

[f] In these compounds it is possible that OH^- or H_3O^+ ions are present instead of water molecules.

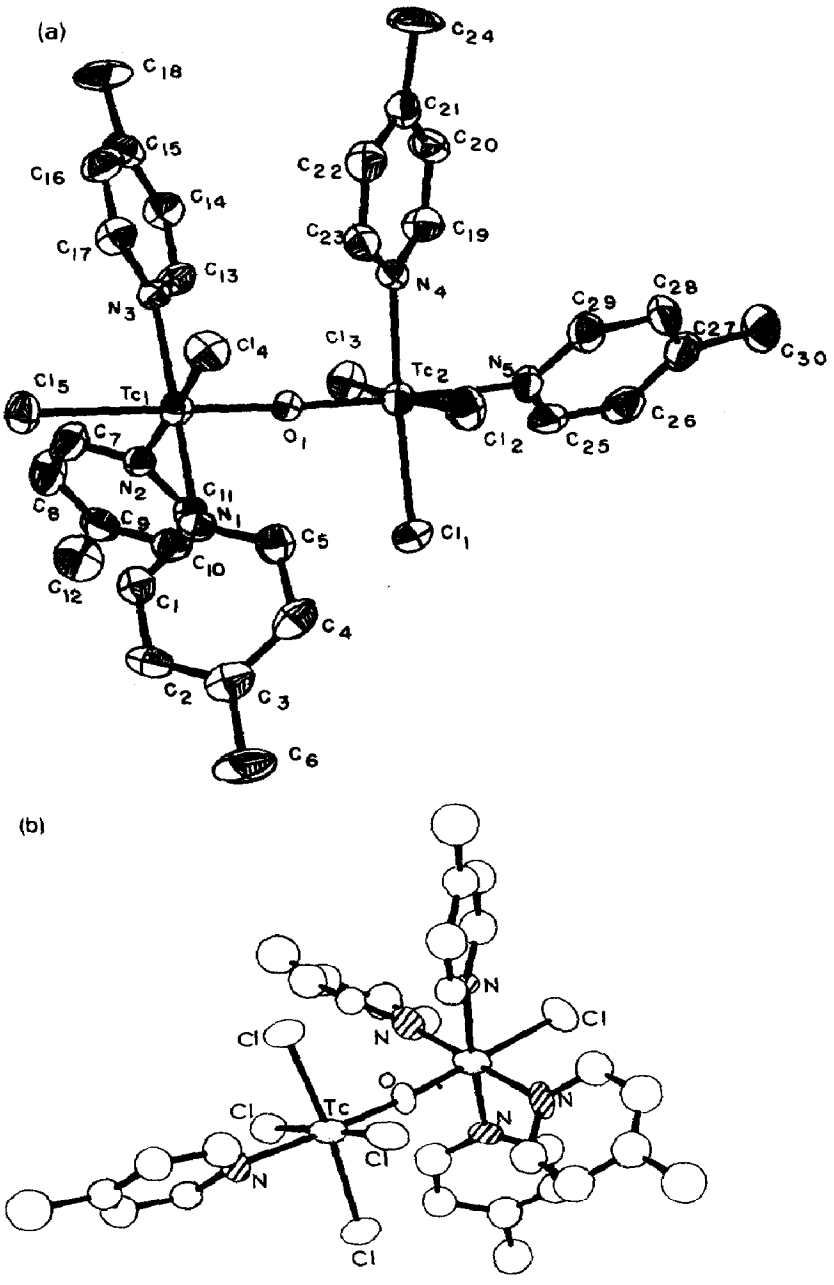

Fig. 57. Structures of (a) **98** and (b) **99**. Reproduced with permission from ref. 414.

states of III and IV to Tc1 and Tc2 respectively and is probably due to a steric effect. The short Tc–O distances in both molecules indicate significant π bonding in the triatomic core. Both types of compound exhibit three near-IR bands assigned to intervalence CT transitions. The bandwidths of these transitions are much narrower than those predicted for Class II

compounds by the theory of Hush [7]. In the solid state, both types of compound exhibit small magnetic moments ($\mu_{eff} \approx 0.9$–1.3 BM) and complex low temperature ESR spectra. For **99**, an axial ESR signal exhibiting unequal coupling to two ^{99}Tc ($I = 5/2$) nuclei is observed at $-173\,^{\circ}C$. The spectrum is simulated using the following parameters: $g_{\|} = 1.9275$, $g_{\perp} = 1.997$, $A_{\|} = 272.3$ G, $A'_{\|} = 31.0$ G, $A_{\perp} = 163.3$ G, $A'_{\perp} = 60.1$ G. A rhombic spectrum with similar parameters is observed for **98**. Magnetic data indicate the presence of a single unpaired electron which is likely to reside in a π orbital based upon d_{xz} and d_{yz} valence orbitals on technetium and p_x and p_y valence orbitals on oxygen. Electrochemical data yield comproportionation constants of 3.4×10^{19} and 1.3×10^{26} for the asymmetric and dissymmetric chloro complexes respectively. XPS studies are consistent with an average technetium oxidation state of 3.5 or the presence of a $Tc^{III}Tc^{IV}$ core. In a compound with the latter formulation, the more oxidized technetium atom would be coordinated to the greater number of halide ligands. Previously, Kuzina et al. [415] had noted the formation of dark crystalline materials when *trans*-$[TcO_2(py)_4]^+$ was reacted with py for extended periods and it is likely that the materials are closely related to the above compounds.

The majority of dinuclear mixed-valence technetium compounds possess strong metal–metal bonds and an average oxidation state of 2.5. Compounds of this type, particularly $[Tc_2Cl_8]^{3-}$, have been extensively studied by Cotton and Spitsyn and their respective coworkers. The ammonium and yttrium salts of the turquoise–blue $[Tc_2Cl_8]^{3-}$ anion were first isolated by Eakins et al. in 1963 [416]. They generated the complex by air oxidation of a hydrochloric acid solution of the brown material obtained upon reduction of $[TcCl_6]^{2-}$ with zinc in concentrated hydrochloric acid at $100\,^{\circ}C$. Modifications of this procedure provide improved syntheses of the NH_4^+ [417,418] and Y^{3+} [418] salts of $[Tc_2Cl_8]^{3-}$. Spitsyn and coworkers [412,419–421] have recently developed another route based on the reduction of $[TcO_4]^-$ with molecular hydrogen under pressure (3–5 MPa) in an autoclave at 120–180 °C. A study of the reduction of $(pyH)_3[TcCl_6]$ using this method revealed the formation of $[Tc_2Cl_8]^{3-}$ via hydrolysed cluster intermediates [420]. The autoclave method has been employed in the synthesis of the NH_4^+ [419], K^+ [419], pyH^+ [420], $quinH^+$ [421] and $N^tBu_4^+$ [412] salts of $[Tc_2Cl_8]^{3-}$. However, structural studies by Koz'min and Novitskaya reveal that compounds produced by this method may vary in composition according to the formula $M'_6M''_{3-x}(H_3O)_x[Tc_2Cl_8]_3 \cdot nH_2O$ ($n = 0$–3) [422,423]. The K^+ [424] and Cs^+ [419] salts have also been prepared by metathesis. The bromo compounds $M_3[Tc_2Br_8] \cdot 2H_2O$ ($M = NH_4^+$, K^+) have been reported [412] but are very unstable with respect to disproportionation to $[Tc_2Br_6]^{2-}$ and $[TcBr_6]^{2-}$ [425] and oxidation to $[TcBr_6]^{2-}$ [412]. Thus the bromo complex remains incompletely characterized.

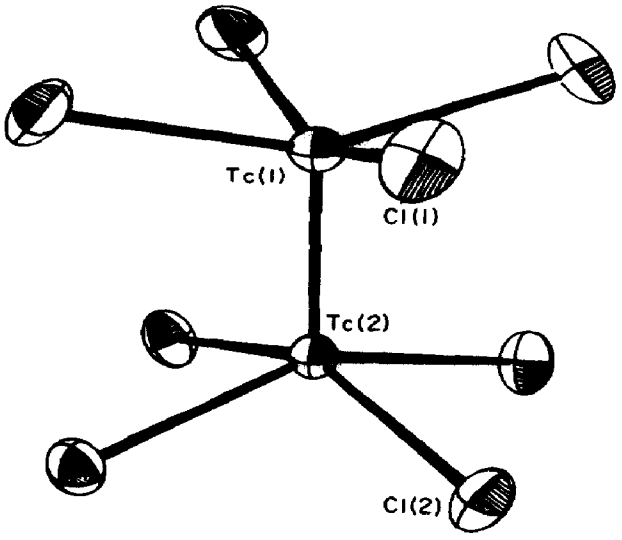

Fig. 58. Structure of the anion in $Y[Tc_2Cl_8]\cdot 9H_2O$. Reproduced with permission from ref. 427.

The NH_4^+ [417,426], K^+ [424] and Y^{3+} [427] salts of $[Tc_2Cl_8]^{3-}$ have been structurally characterized by Cotton and coworkers. The Cs^+ salt is isostructural with the NH_4^+ and K^+ salts [422]. The structure of the $[Tc_2Cl_8]^{3-}$ ion (Fig. 58) is similar to those of the $[Re_2Cl_8]^{2-}$ and $[Mo_2Cl_8]^{4-}$ ions and consists of two equivalent square-pyramidal $TcCl_4$ groups joined by a very short Tc–Tc bond (2.105(1) Å in the Y^{3+} salt) to give an eclipsed rotational conformation. The $[Tc_2Cl_8]^{3-}$ ion is paramagnetic ($\mu_{eff} = 1.78$ BM for K^+ and Y^{3+} salts) and frozen solution ESR spectra reveal the presence of one unpaired electron with hyperfine coupling to two equivalent ^{99}Tc nuclei ($g_{\parallel} = 1.912$, $g_{\perp} = 2.096$, $|A_{\parallel}| = 166 \times 10^{-4}$ cm^{-1}, $|A_{\perp}| = 67.2 \times 10^{-4}$ cm^{-1}) [418]. However, doubts [412] have been raised concerning the accuracy of the preceding ESR study, as $[Tc_2Cl_8]^{3-}$ was subsequently discovered to undergo solvolysis in the solvent employed [428].

In an attempt to produce isovalent $[Tc_2Cl_8]^{2-}$, Cotton et al. [429] isolated $Tc_2(hp)_4Cl$ upon the reaction of $(NH_4)_3[Tc_2Cl_8]$ with molten hpH. The insoluble compound may be sublimed and mass spectrometry shows that individual $Tc_2(hp)_4Cl$ molecules pass into the gas phase. The compound is composed of infinite chains of $[Tc_2(hp)_4]^+$ units symmetrically linked by bridging chloride ions (Fig. 59). The Tc–Tc bond distance is a short 2.095(1) Å. The compound is paramagnetic and exhibits an ESR signal with a g value of 2.046. Polarized single-crystal electronic spectra at 5 K reveal the rich vibrational structure of the $\delta \rightarrow \delta^*$ transition.

The $[Tc_2X_8]^{3-}$ ions also react reversibly with acetic acid in an autoclave to give the green compounds $Tc_2(OAc)_4X$ (X = Cl, Br) which are readily

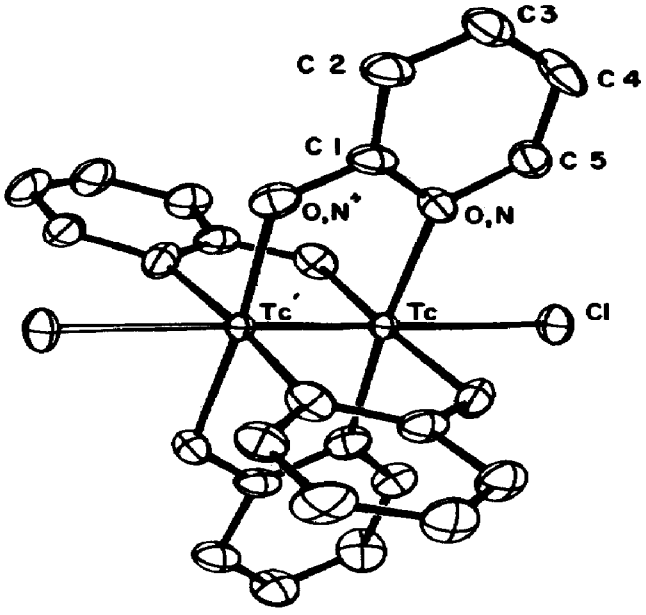

Fig. 59. Structure of $Tc_2(hp)_4Cl$ showing a $Tc_2(hp)_4$ unit and neighbouring chloride ions. The Tc–Cl distance is 2.679(1) Å. Reproduced with permission from ref. 429.

soluble in polar organic solvents [430,431]. Like $Tc_2(hp)_4Cl$, these compounds are volatile but exhibit extended structures in the solid state [432,433]. They possess the familiar tetraacetate structure observed in the group 6 complexes $M_2(OAc)_4 \cdot 2H_2O$ (M = Cr, Mo) with bridging halide ligands in place of the axially bound water molecules. Both compounds have very similar Tc–Tc bond distances but differ in the geometry at the bridging halide. In the chloro compound the Tc–Cl–Tc angle of 120° results in the formation of a zigzag polymeric structure. In the bromo compound the Tc–Br–Tc angle is 180° and a linear polymeric structure results. The compounds exhibit magnetic moments of 1.74 BM [434] and ESR spectra consistent with delocalization of the electron over two equivalent technetium centres [434,435]. The tetraacetate structure is also observed in $K[Tc_2(OAc)_4Cl_2]$ [436]. The thermal decomposition of $(pyH)_3[Tc_2Cl_8]$ in argon at 250–280 °C is reported to yield dark brown $Tc_2Cl_5(py)_2$ which is ascribed a Tc–Tc-bonded structure on the basis of analysis and optical photoelectron spectra [412]. The X-ray structure of the complex has not been reported. Finally, a black powder with the formula $Tc_4O_{10} \cdot 14H_2O$ is obtained by the hydrolysis of $K_3[Tc_2Cl_8]$ under argon [412]. The hydrated oxide dissolves in concentrated hydrochloric acid with the formation of $[Tc_2Cl_8]^{3-}$, suggesting the retention of the metal–metal bond upon hydrolysis. The anhydrous compound Tc_4O_{10} may also be prepared and studies

suggest the presence of one unpaired electron for each pair of technetium atoms. The actual nuclearity of the compounds remains unknown.

The electronic structure of the Tc–Tc-bonded compounds discussed above has attracted much interest. In contrast with very stable quadruply bonded species such as $[Re_2Cl_8]^{2-}$, the technetium compounds possess one electron in excess of the number necessary to produce a quadruple bond. Although the electron was earlier proposed to reside in a non-bonding orbital of σ character [417,437], ESR properties and molecular orbital calculations [438,439] suggest a $\sigma^2\pi^4\delta^2\delta^*$ electron configuration. The ESR spectra of $Tc^{II}Tc^{III}$ compounds are similar and give rise to a well-resolved hyperfine structure due to two equivalent ^{99}Tc nuclei. Seven representative complexes exhibit the following ESR parameters: $g_{\|} = 1.85 \pm 0.03$, $g_{\perp} = 2.13 \pm 0.03$, $A_{\|} = -(188 \pm 5) \times 10^{-4}$ cm^{-1} and $A_{\perp} = -(78 \pm 5) \times 10^{-4}$ cm^{-1} [412,434,435]. The observation that $g_{\|} < 2$, $g_{\perp} > 2$ and $g_{av} > 2$ suggests that the magnetic electron is in the δ^* orbital [412,440]. This bonding description is supported by the satisfactory agreement between observed and calculated electronic spectra [441]. The stability of $[Tc_2Cl_8]^{3-}$ compared with that of $[Tc_2Cl_8]^{2-}$ (cf. $[Re_2Cl_8]^{2-}$) can be rationalized by arguing that the lower oxidation state of technetium in the former is associated with an expansion of the 4*d* orbitals, resulting in an increase in the strengths of the Tc–Tc bond components and increased Tc–Tc bonding [427]. Thus the formal bond order of the Tc–Tc bond in $Tc^{II}Tc^{III}$ compounds is 3.5.

(c) Hexanuclear compounds

In 1982, Spitsyn and coworkers opened a new field of polynuclear cluster chemistry. These workers have prepared a variety of technetium clusters, all with formal mixed-valence formulations, via the autoclave reduction of $[TcO_4]^-$ with molecular hydrogen (3–5 MPa) in concentrated hydrogen halide solution at 140–220 °C [412,442–447]. Depending upon the temperature, a number of different clusters crystallize from these reaction mixtures. The reduction of $NMe_4[TcO_4]$ with hydrogen in concentrated hydrochloric acid yields compounds containing the trigonal prismatic clusters $[Tc_6Cl_{12}]^{2-}$ and $[Tc_6Cl_{14}]^{3-}$ (Fig. 60(a) and (b)) [412,442]. Both clusters are composed of a trigonal prism of metal atoms; a terminal chloro ligand is bonded to each metal atom and six chloro ligands bridge the edges bordering the triangular faces. In $[Tc_6Cl_{14}]^{3-}$, two additional chlorides cap the triangular faces at a distance of 3 Å from the metal atoms. The bonding within these clusters has been discussed in terms of electron-rich triple bonding ($\sigma^2\pi^4\delta^2\delta^{*2}$) within each Tc_2 unit with two additional electrons in a π^* orbital [448,449]. Bonding between Tc_2 units is primarily through the HOMO of the cluster (π bonding between dinuclear units) and localized δ and δ^* orbitals (σ bonding between dinuclear units). The reduction of $HTcO_4$ with hydrogen in

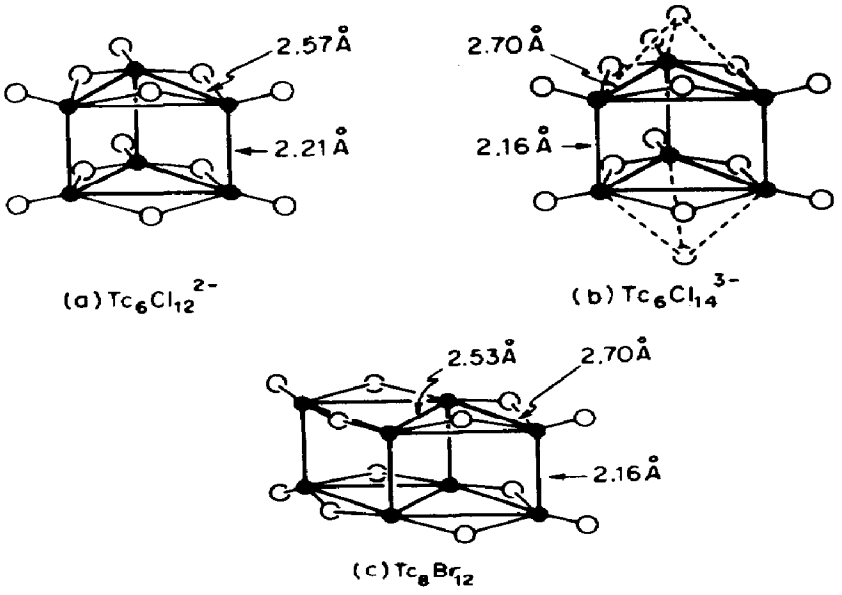

Fig. 60. Structures of (a) $[Tc_6Cl_{12}]^{2-}$, (b) $[Tc_6Cl_{14}]^{3-}$ and (c) $[Tc_8Br_{12}]^{0/+}$. The technetium and halogen atoms are represented by solid and empty circles respectively. Reproduced with permission from ref. 449.

HBr results in the formation of an octahedral cluster [443], along with various octanuclear clusters which will be discussed below. The octahedral cluster compound is formulated as $[H_3O(H_2O)_3]_2[Tc_6Br_6(\mu_3\text{-}Br)_5]$ and is proposed to possess a structure similar to known $[M_6X_{14}]^{2-}$ clusters (Fig. 14(b)) except that the eight equivalent μ_3-bridging sites are not fully occupied in the case of the technetium cluster [445]. However, there is some ambiguity in this assignment as the crystallographic study was originally interpreted in terms of partial and mixed (Br^- and OH^-) bridging ligands [443].

(d) Octanuclear compounds

The reduction of $HTcO_4$ with hydrogen in HBr has led to the isolation of numerous materials [412,443,445–447]. Various X-ray diffraction studies [412,445–447] have failed to provide unambiguous formulations for some of these materials. However, the presence of prismatic Tc_8 clusters is, with one exception [412,445], consistently revealed. The materials appear to be constituted of two clusters, $[Tc_8Br_{12}]^+$ [446] and Tc_8Br_{12} [445–447], co-crystallized with Br^- counter-ions, H_2O and/or $H(H_2O)_nBr$. The general structure of these clusters is exemplified by the structure of Tc_8Br_{12} shown in Fig. 60(c). Very short Tc–Tc distances (ca. 2.16 Å) indicate strong metal–metal bonding in the four Tc_2 units which comprise the vertical edges of the prism.

A terminal bromo ligand is bonded to each metal atom and eight bromo ligands bridge the edges bordering the bases of the prism. In the solid state these clusters are associated with Br^- ions which are located ca. 3 Å away from the prism bases. Again the short Tc–Tc bonds are electron-rich triple bonds which are bonded together by overlap of δ and δ^* orbitals. The electronic structure of the compounds has been discussed [412,445].

(iii) Rhenium compounds

(a) General survey

It is quite evident that the simple oxidation or reduction of isovalent analogues accounts for the preparation of the majority of dinuclear mixed-valence compounds of rhenium (Scheme 1). Section E(iii)(b) highlights this aspect of rhenium chemistry by discussing dinuclear compounds in an order which reflects their synthesis according to this scheme.

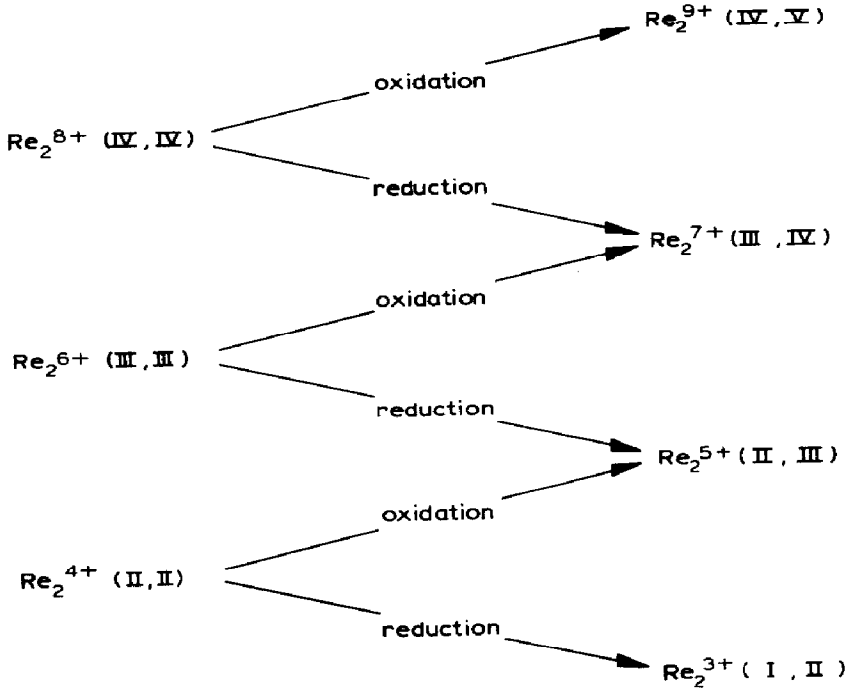

Scheme 1. The formation of dinuclear mixed-valence compounds of rhenium via the oxidation and reduction of isovalent analogues.

Much of the mixed-valence chemistry of rhenium has grown out of a desire to understand the effects of redox processes on the bond order and electron configuration of metal–metal-bonded compounds. In contrast with technetium which forms very stable dinuclear complexes with an average

oxidation state of 2.5, rhenium forms a variety of metal–metal-bonded dinuclear compounds possessing half-integral average oxidation states ranging from 4.5 through 0.5. The only integral average oxidation state exhibited by dinuclear mixed-valence compounds of rhenium is 3.0. As a consequence of metal–metal bonding, dinuclear complexes are generally Class III compounds exhibiting crystallographically equivalent rhenium centres and spectroscopic properties consistent with electron delocalization. Many examples such as $[Re_2(\mu\text{-}H)_4H_4(PR_3)_4]^+$, $[Re_2(\mu\text{-}Cl)_2(\mu\text{-}dppm)_2Cl_4]^+$ and $[Re_2Cl_4(PMe_2Ph)_4]^+$ are discussed in Section E(iii)(b). There are, however, metal–metal-bonded complexes which exhibit Class I structures and these include $Re_2Cl_5(dth)_2$, $Re_2X_4(OR)_2(PPh_3)_2$, $Re_2Cl_5(dppm)_2$ and $Re_2Cl_3(dppm)_2(CO)_2L$ (L = nitrile, isocyanide). Relatively few dinuclear compounds, such as $K_3[Re_2(\mu\text{-}O)Cl_{10}]$ and $(CO)_5Re(\mu\text{-}F)ReF_5$, are devoid of direct metal–metal interactions. X-ray crystallography and ESR and electronic spectroscopy have been important tools in the thorough characterization of these compounds. The last two techniques have also been important in the characterization of unstable electrochemically produced solution species. In contrast with its first row congener and close relative molybdenum, rhenium is not known to form many high nuclearity compounds. The reaction of Cp^*ReO_3 and PPh_3 results in two interesting products. The first, $[Cp^*_3Re_3(\mu\text{-}O)_6][ReO_4]_2$, contains a triangular cation having a structure reminiscent of $[Zr_3(\mu\text{-}Cl)_6(C_6Me_6)_3]^{2+}$ and highly oxidized perrhenate counter-ions. The $[ReO_4]^-$ anions are in fact incorporated into the second product, the tetranuclear $Re^V_2Re^{VII}_2$ complex $Cp^*_2Re_4O_{11}$. Axial coordination of perrhenate to $[Re^{III}_2(O_2C^nPr)_4]^{2+}$ is also a feature of tetranuclear $[Re_2(O_2C^nPr)_4][ReO_4]_2$. The other trinuclear compounds $Re_3O_4(CH_2SiMe_3)_3(PMe_3)_4$ and $Re_3I_6(CO)_6$ possess triangular and linear structures respectively. An $Re^I_2Re^{III}_2$ iodocarbonyl complex, $Re_4I_8(CO)_6$, and a cyclometallophosphine complex, $Re_4Cl_2(CO)_{15}\{MePP(Me)PMe\}$, are also known. The rhenium compound of highest nuclearity is hexanuclear $Re_6(\mu\text{-}Cl)_6H(CH_2SiMe_3)_9$.

Properties of selected mixed-valence compounds of rhenium are summarized in Table 12.

(b) Dinuclear compounds

The oxidation of $[Re_2OCl_{10}]^{4-}$ with hydrogen peroxide in 3 M HCl produces a blood-red complex originally formulated as $[Re_2O_2HCl_{10}]^{3-}$ [451] but later shown to be the $Re^{IV}Re^V$ anion $[Re_2(\mu\text{-}O)Cl_{10}]^{3-}$ upon X-ray structural characterization of the caesium salt [452]. The complex anion exhibits a corner-shared bi-octahedral structure in which the rhenium centres are linked by a linear Re–O–Re bridge (Re–O = 1.832(3) Å). The structure is similar to that of $K_4[W_2(\mu\text{-}O)Cl_{10}]$ [317].

TABLE 12

Properties of selected mixed-valence compounds of rhenium

Compound	Re oxidation state		Structure	Re ··· Re distance [a] (Å)	Electron configuration	μ_{eff} (BM)	ESR spectrum	Ref.
	Formal	Average						
$K_3[Re_2OCl_{10}]$	IV, V	4.5	–	ca. 3.66	–	–	–	452
$[Re_2H_8(PPh_3)_4]PF_6$	IV, V	4.5	–	–	–	–	$g = 2.11–2.13$ $A = 140 \times 10^{-4}$ cm^{-1}	454
$(N^nBu_4)_2[Re_2Cl_9]$	III, IV	3.5	–	–	–	1.5	–	456
$(N^nBu_4)_3[Re_2(NCS)_{10}]$	III, IV	3.5	–	2.613(1)	$\sigma^2\pi^2$	Paramagnetic	–	461
$[Re_2Cl_6(dppm)_2]H_2PO_4 \cdot H_3PO_4$	III, IV	3.5	Fig. 61	2.6823(6)	$\sigma^2\pi^2\delta^{*2}\delta$	–	–	462, 463
$Re_2OCl_3(O_2CEt)_2(PPh_3)_2$	III, IV	3.5	–	2.514(1)	–	2.0	–	464, 465
$Re_2Cl_4(OEt)_2(PPh_3)_2$	II, IV	3.0	Fig. 62(a)	2.231(1)	$\sigma^2\pi^4\delta^2$	Diamagnetic	–	466, 467
$(CO)_5Re(\mu\text{-}F)ReF_5$	I, V	3.0	Fig. 63	–	–	Diamagnetic	–	467 469–471
$Re_2Cl_5(dth)_2$	II, III	2.5	**103**	2.293(2)	$\sigma^2\pi^4$	1.72	–	471 473–475
$[Cp_2Co][Re_2Cl_6(dppm)_2]$	II, III	2.5	–	–	$\sigma^2\pi^2\delta^*\delta^2\pi^*$	Paramagnetic		462

$Re_2Cl_5(dppm)_2$	II, III	2.5	Fig. 64	2.263(1)	–	1.95	$g_{\|} < 2$, $g_{\perp} = 2.2$	486
$[Cp_2Co][Re_2(hp)_2Cl_2]$	II, III	2.5	–	–	$\sigma^2\pi^4\delta^2\delta^*$	Paramagnetic	$g = 2.15$–2.25	489
$Re_2(\mu-OAc)Cl_4(PPh_3)_2$	II, III	2.5	Fig. 62(b)	2.2165(7)	$\sigma^2\pi^4\delta^2\delta^*$	1.63 [b]	–	468
$[Re_2Cl_4(PMe_2Ph)_4]PF_6$	II, III	2.5	–	2.218(1)	$\sigma^2\pi^4\delta^2\delta^*$	1.35	$g_{\|} = 2.19$ ($A = 300$ G) $g_{\perp} = 2.24$ ($A = 120$ G)	479, 490
$Re_2Cl_3(dppm)_2(CO)_2(^iPrNC)$	I, II	1.5	–	2.718(1)	–	–	–	501
$[Cp_3^*Re_3(\mu\text{-}O)_6][ReO_4]_2$	V, VI_2	$\frac{17}{3}$	Fig. 65(a)	2.747(2)		Diamagnetic?	–	504, 505
$Re_3O_4(CH_2SiMe_3)_3(PMe_3)_4$	I, V_2	$\frac{11}{3}$	Fig. 66	2–3, 2.381(1)	–	Diamagnetic	–	507
$Re_3(\mu\text{-}I)_6(CO)_6$	I_2, IV	2.0	Fig. 67(a)	3.379(3)	–	3.59	–	508, 509
$Cp_2^*Re_4O_{11}$	V_2, VII_2	6.0	Fig. 65(b)	1–2, 2.651(1)	$\sigma^2\pi^2$	Diamagnetic	–	506
$[Re_2(O_2C^nPr)_4][ReO_4]_2$	III_2, VII_2	5.0	–	2.251(2)	$\sigma^2\pi^4\delta^2$	Diamagnetic	–	510, 511
$Re_4I_8(CO)_6$	I_2, III_2	2.0	Fig. 67(b)	2–2′, 2.279(1)	–	–	–	508, 509
$Re_6Cl_6H(CH_2SiMe_3)_9$	II_2, III_4	$\frac{16}{6}$	Fig. 69	1–2, 2.993(1)	–	–	–	515

[a] The preceding numbers identify the rhenium atoms involved, e.g. when prefixed by 1–2, the distance given is that between Re(1) and Re(2).

[b] Solution measurement for $Re_2(OAc)Br_4(PPh_2py)_2$.

A variety of hydrido–Re_2^{9+} compounds have recently been reported by Walton and coworkers [453,454]. Electrochemical oxidation of $Re_2(\mu\text{-}H)_4H_4(PR_3)_4$ ($PR_3 = PPh_3$, $PEtPh_2$ or PEt_2Ph) and $Re_2(\mu\text{-}H)_4H_4(AsPh_3)_4$ results in the formation of the corresponding dark blue (PPh_3) or violet (others) paramagnetic ESR-active monocations. Also, the PPh_3 derivative, $[Re_2H_8(PPh_3)_4]PF_6$, may be isolated upon the chemical oxidation of $Re_2H_8(PPh_3)_4$ with Ph_3CPF_6 or $(C_7H_7)PF_6$. The other cations are not stable enough to permit isolation and their study has been restricted to electrochemically generated solution species. The ESR spectra of the cations are characterized by a broad signal at $g = 2.11$–2.13, which exhibits hyperfine features due to two rhenium nuclei ($I = 5/2$, $A = 140 \times 10^{-4}$ cm^{-1}). The related paramagnetic compounds $[Re_2(\mu\text{-}H)_4H_3(PPh_3)_4L](PF_6)_2$ are produced upon the oxidation of $[Re_2(\mu\text{-}H)_4H_3(PPh_3)_4L]PF_6$ with $NOPF_6$ [454]. The above compounds have not been structurally characterized.

The violet Re_2^{7+} complex $[Re_2Cl_9]^{2-}$ was first isolated as the $AsPh_4^+$ salt upon reaction of β-$ReCl_4$ and $AsPh_4Cl$ in methanol–(12 M hydrochloric acid) [455]. Other methods involving the reduction of $ReCl_5$ or β-$ReCl_4$ also yield $[Re_2Cl_9]^{2-}$ [456–458]. The reaction of $ReCl_5$ or β-$ReCl_4$ and PPh_3 in anhydrous acetone yields $(DOTP)_2[Re_2Cl_9] \cdot 2C_3H_6O$ (the cation is formed in the reaction mixture) [456,457]. The reaction of $ReCl_5$ and β-$ReCl_4$ and $OPPh_3$ in acetone solution produces high yields of $[(Ph_3PO)_2H]_2[Re_2Cl_9]$ [458]. In solution, the Re^{IV} complexes $(NBu_4)[Re_2X_9]$ are readily reduced (for example, with iron, copper, mercury and tin) to the mixed-valence analogues, $(NBu_4)_2[Re_2X_9]$ (X = Cl (blue), X = Br (brown)) [459]. The X-ray structures of the $[Re_2X_9]^{2-}$ anions have not been reported but they are likely to be related to the tungsten analogues (Section D(iii)(b)).

Reaction of $(N^nBu_4)_2[Re_2Cl_8]$ and sodium thiocyanate leads to the formation of the green Re_2^{7+} compound $(N^nBu_4)_3[Re_2(NCS)_{10}]$ [460,461]. The complex was originally formulated as $(N^nBu_4)_3[Re_2(NCS)_{10}(CO)_2]$ [460] on the basis of IR data but was reformulated upon the determination of the X-ray structure [461]. The $[Re_2(NCS)_{10}]^{3-}$ ions consist of crystallographically equivalent distorted octahedra sharing an edge formed by the nitrogen atoms of two bridging NCS^- ligands. Eight terminal N-bonded NCS^- ligands occupy the remaining coordination sites. A weak metal–metal bond is indicated by the Re–Re distance of 2.613(1) Å and the unpaired electron in this formally $Re^{III}Re^{IV}$ complex appears to be delocalized equally over both metal centres.

The complex $Re_2(\mu\text{-}Cl)_2(\mu\text{-dppm})_2Cl_4$ (**100**) undergoes a one-electron oxidation upon reaction with $NOPF_6$, the resulting product being $[Re_2(\mu\text{-}Cl)_2(\mu\text{-dppm})_2Cl_4]PF_6$ [462,463]. Deep blue $[Re_2(\mu\text{-}Cl)_2(\mu\text{-dppm})_2Cl_4]^+$ possesses electrochemical properties consistent with the presence of an Re_2^{7+} core. Attempts to grow a crystal of the PF_6^- salt resulted in the hydrolysis of

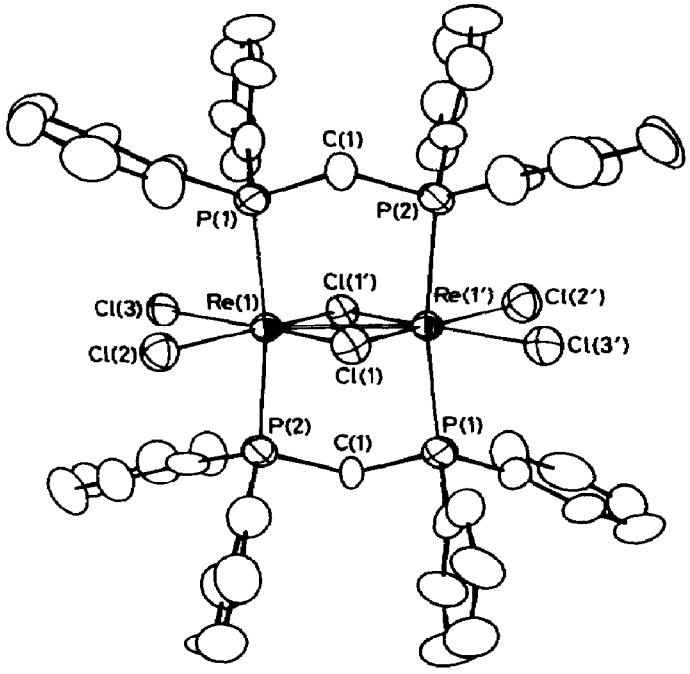

Fig. 61. The structure of the cation in **101**. Reproduced with permission from ref. 462.

the anion and the isolation of $[Re_2(\mu\text{-}Cl)_2(\mu\text{-}dppm)_2Cl_4]H_2PO_4 \cdot H_3PO_4 \cdot 4H_2O$ (**101**). In the cation (Fig. 61) the edge-shared bi-octahedral structure contains two rhenium atoms linked via two μ-dppm and two μ-Cl ligands; two terminal chloro ligands complete the coordination sphere of each rhenium atom. The lengthening of the Re–Re distance (2.6823(6) Å) compared with that in **100** (2.616(1) Å) is consistent with a reduction in the Re–Re bond order from two in **100** to 1.5 in **101** and a $\sigma^2\pi^2\delta^{*2}\delta$ ground state for **101**. The corresponding anion $[Re_2Cl_6(dppm)_2]^-$ is also known [462] (vide infra).

The reactions of *trans*-$ReOX_3(PPh_3)_2$ and *trans*-$ReCl_4(PPh_3)_2$ with carboxylic acids or their anhydrides are complex. In boiling toluene these reactions yield, among other products, purple $Re_2OCl_3(O_2CR)_2(PPh_3)_2$ [464]. These compounds were originally thought to be $Re_2Cl_3(O_2CR)_2(PPh_3)_2$ [464] but were later correctly formulated as $Re_2OCl_3(O_2CR)_2(PPh_3)_2$ after the X-ray structure of the ethyl derivative was obtained [465]. The complex possesses an edge-shared bi-octahedral structure in which two sets of vertices are bridged by propionate groups. The other two bridging ligands (μ-Cl and μ-O) form a plane with the rhenium atoms; this plane is approximately perpendicular to the plane of the bridging propionate ligands. Phosphine and chloro ligands complete the coordination spheres. The Re–Re distance is 2.514(1) Å.

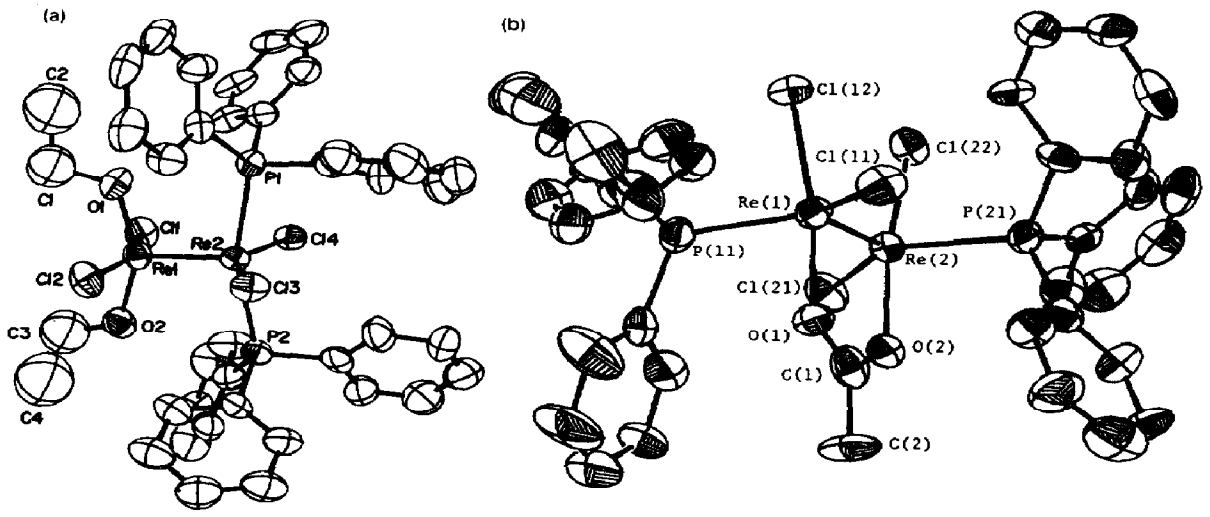

Fig. 62. Products from the reactions of $Re_2(OAc)_2X_4L_2$ with PPh_3 in ethanol. (a) Structure of $Re_2Cl_4(OEt)_2(PPh_3)_2$. Reproduced with permission from ref. 466. (b) Structure of $Re_2(\mu\text{-}OAc)Cl_4(PPh_3)_2$. Reproduced with permission from ref. 468.

A variety of red complexes of general formula $Re_2X_4(OR)_2(PPh_3)_2$ (X = Cl, Br; R = Me, Et, ^{n}Pr, ^{i}Pr) are produced by reaction of $Re_2X_4(O_2CR)_2 \cdot 2H_2O$ with PPh_3 in refluxing alcohols [466,467]. The structure of the $Re_2Cl_4(OEt)_2(PPh_3)_2$ molecule is shown in Fig. 62(a). The presence of an Re–Re quadruple bond is consistent with the essentially eclipsed conformation and the short Re–Re distance of 2.231(1) Å, but in contrast with homopolar quadruple bonds, the ligand distribution in the complex suggests that the Re(1) and Re(2) atoms may be assigned oxidation states of IV and II respectively. The complexes exhibit characteristic electronic absorptions ($\lambda_{max} \approx 1200$ nm, $\epsilon \approx 3000$) assigned to intervalence CT transitions. Analogous reactions using $Re_2(OAc)_2X_4L_2$ (X = Cl, Br; L = py, 4-Mepy) and PPh_3 in refluxing ethanol yield the Re_2^{5+} complexes $Re_2(OAc)X_4(PPh_3)_2$ (vide infra) [468].

Orange $(CO)_5Re(\mu\text{-}F)ReF_5$ (**102**) may be prepared by the reaction of ReF_6 and $Re_2(CO)_{10}$ in anhydrous HF [469] or the fluorination of $Re_2(CO)_{10}$ with XeF_2 in 1,1,2-trichlorotrifluoroethane or anhydrous HF [470,471]. The molecular structure of **102**, as shown in Fig. 63, contains octahedral rhenium centres linked by a bent fluorine bridge. The metrical data favour the covalent formulation $(CO)_5Re(\mu\text{-}F)ReF_5$ in preference to the ionic formula, $[Re(CO)_5][ReF_6]$. Thus **102** may be classified as a Class I mixed-valence species containing Re^I and Re^V centres. In the reaction of ReF_6 and $Re_2(CO)_{10}$ in HF the formation of **102** is accompanied by the formation of green $[Re(CO)_5][Re_2F_{11}]$ which does in fact contain discrete $[Re(CO)_5]^+$ and

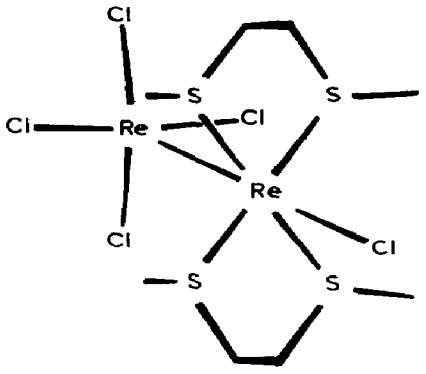

103

$[Re_2F_{11}]^-$ ions [469,470]. Several other ionic solids containing discrete Re^I and Re^V complex ions have been reported [472].

The first mixed-valence metal–metal-bonded rhenium complex discovered was red–black dichroic $Re_2Cl_5(dth)_2$ (**103**) produced upon the reaction of $(NBu_4)_2[Re_2Cl_8]$ and dth in refluxing acidic MeCN [473]. The complex is paramagnetic ($\mu_{eff} = 1.72$ BM) and X-ray diffraction studies revealed an unsymmetrical structure consistent with a Class I $(dth)_2ClRe^{II}Re^{III}Cl_4$ formulation [474,475]. Although the Re–Re bond is retained in the reaction, its length of 2.293(2) Å and the staggered rotational conformation suggest the absence of a δ bond and a bond order of three for this molecule. The molecule is proposed to possess a $\delta^2\pi^4$ Re–Re bond with the extra electron localized on the Re^{II} atom. It is unique among Re–Re triply bonded compounds as all others possess a $\sigma^2\pi^4\delta^2\delta^{*2}$ electronic configuration.

Electrochemical studies of the $[Re_2X_8]^{2-}$ complexes [476,477] indicate irreversible reduction processes, the first of which leads to the formation of $[Re_2X_8]^{3-}$. These rhenium complexes, which are quite unstable, are analo-

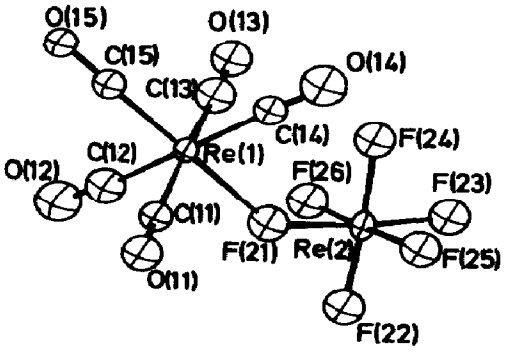

Fig. 63. Structure of one of the independent molecules of $(CO)_5Re(\mu\text{-}F)ReF_5$. Reproduced with permission from ref. 471.

gous to the very stable $[Tc_2Cl_8]^{3-}$. A possible explanation for the instabilities of $[Re_2X_8]^{3-}$ is that the chloro and bromo ligands are less capable than many others of stabilizing the reduced Re_2^{5+} core. In contrast, the phosphine complexes $Re_2X_6(PR_3)_2$ (X = Cl, Br; PR_3 = PEt_3, P^nPr_3, P^nBu_3, $PMePh_2$, PEt_2Ph) exhibit electrochemically reversible reduction processes, and the stability of the electrogenerated monoanions allowed their characterization by ESR spectroscopy [478,479]. Cobaltocene reduction of $Re_2Cl_6(PR_3)_2$ (PR_3 = PEt_3, P^nPr_3, $PMePh_2$, $PEtPh_2$) results in the formation of the $[Cp_2Co][Re_2Cl_6(PR_3)_2]$ salts [480] as shown in Scheme 2. Scheme 2 also shows the course of other electrochemical and chemical transformations involving these and related complexes. Thus the addition of PR_3 to $[Re_2Cl_6(PR_3)_2]^-$ results in the formation of $Re_2Cl_5(PR_3)_3$, a complex which may be prepared from $[Re_2Cl_4(PR_3)_4]^+$ and Cl^- (Scheme 2) or directly from Re_3Cl_9 or $[Re_2Cl_8]^{2-}$ and phosphine as described below. Cobaltocene reduction of **100** results in the formation of light green $[Cp_2Co][Re_2Cl_6(dppm)_2]$, the dinuclear anion of which is proposed to possess a $\sigma^2\pi^2\delta^{*2}\delta^2\pi^*$ ground state and a bond order of 1.5 [462].

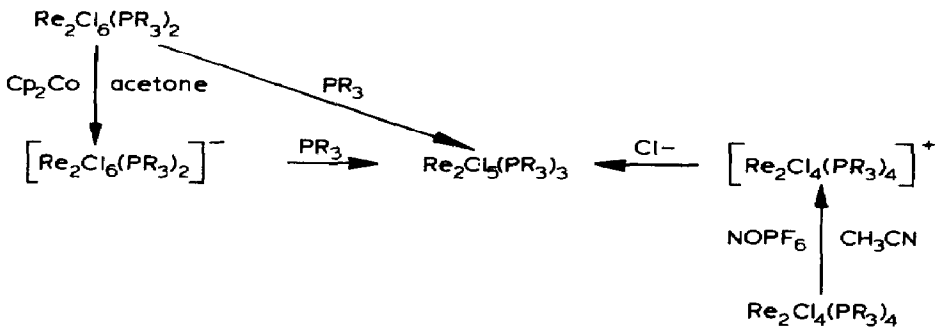

Scheme 2. Redox and chemical transformations of dirhenium chlorophosphine complexes.

The reaction of phosphines with Re_3X_9 or $[Re_2X_8]^{2-}$ depends on the reaction conditions and the basicity of the phosphine [154]. The reaction of $PMePh_2$ or $PEtPh_2$ and Re_3Cl_9 or $(NBu_4)[Re_2Cl_8]$ yields the paramagnetic Re_2^{5+} complexes $Re_2Cl_5(PRPh_2)_3$ which contain an Re–Re bond order of 3.5 and a $\sigma^2\pi^4\delta^2\delta^*$ electronic ground state [481,482]. $Re_2Cl_5(PEtPh_2)_3$ may also be prepared by the reaction of $(NBu_4)[Re_2Cl_9]$ with $PEtPh_2$ [483]. The analogous bromo complex may be prepared by reacting $(NBu_4)_2[Re_2Br_8]$ with phosphine. The $Re_2X_5(PR_3)_3$ complexes exhibit an intense absorption in the near-IR region (1400 nm), which has been assigned to the $\delta \rightarrow \delta^*$ transition [484]. The photoelectron spectra of the halophosphine complexes $Re_2X_6L_2$, $Re_2X_5L_3$ and $Re_2X_4L_4$ show a dependence of the Re $4f_{7/2}$

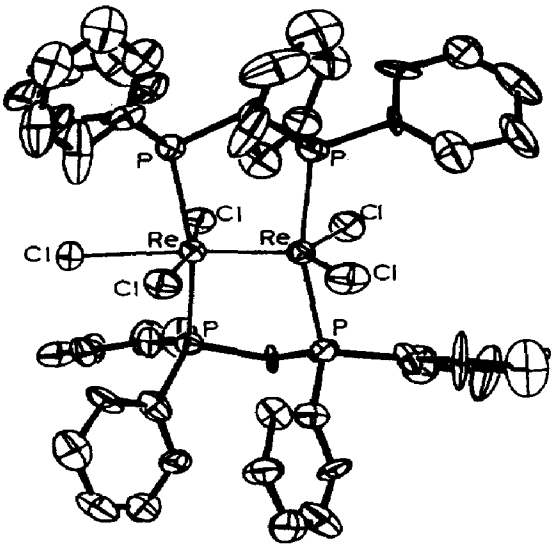

Fig. 64. Structure of **104**. Reproduced with permission from ref. 486.

binding energies on formal oxidation state [485]. More basic phosphines such as PR_3 (R = alkyl) result in a two-electron reduction and the formation of $Re_2X_4(PR_3)_4$ complexes.

The reaction of $(NBu_4)_2[Re_2Cl_8]$ and dppm in refluxing acetone yields brown paramagnetic ($\mu_{eff} = 1.95$ BM) $Re_2Cl_5(dppm)_2$ (**104**) [486], the X-ray structure of which is shown in Fig. 64. The Re–Re distance is 2.263(1) Å and the ligands adopt an eclipsed rotational conformation; the dppm ligands act as bridging ligands. The broad ESR spectrum of **104** has been interpreted in terms of electron delocalization over two rhenium nuclei. The analogous bromo complex is produced by the reaction of $(NBu_4)_2[Re_2Br_8]$ and dppm in acetonitrile [487].

The complexes $Re_2(O_2CR)_4X_2$ (R = alkyl, aryl; X = Cl, Br, I) are electrochemically reduced in dichloromethane solution to the monoanions $[Re_2(O_2CR)_4X_2]^-$, the ESR properties of which are consistent with electron delocalization over two equivalent rhenium atoms and an $\sigma^2\pi^4\delta^2\delta^*$ electronic ground state [440,488]. Recently, the anions $[Re_2(O_2CR)_4Cl_2]^-$ (R = C_3H_7, CMe_3, Ph) have been isolated as green–mustard cobalticenium salts from the cobaltocene reduction of $Re_2(O_2CR)_4Cl_2$ in acetone [480]. The ESR spectra of these compounds are identical with those of the electrochemically generated species. The complexes $Re_2(O_2CR)_2X_4L_2$ (R = Me, Et; X = Cl, Br; L = H_2O, py, 4-Mepy, dmf, dmso) exhibit a one-electron reduction similar to those reported for the $Re_2(O_2CR)_2X_2$ complexes above [466]. Cobaltocene reduction of $Re_2(hp)_4X_2$ (X = Cl, Br, I) in acetone precipitates the related green–black salts $[Cp_2Co][Re_2(hp)_4X_2]$ [489]. The $[Re_2(hp)_4X_2]^-$

anions, which may be electrochemically generated, are paramagnetic and exhibit broad ESR signals displaying hyperfine coupling to two rhenium nuclei. The unpaired electron is proposed to reside in a δ^* orbital. Chemical reduction provides a variation on this theme. Reaction of $Re_2(OAc)_2X_4L_2$ (X = Cl, Br; L = py, 4-Mepy) with PPh_3 in refluxing ethanol yields $Re_2(\mu\text{-}OAc)X_4(PPh_3)_2$ [468]. These complexes and $Re_2(OAc)X_4(PPh_2py)_2$ may also be isolated from analogous reactions in refluxing acetone. The complexes are paramagnetic and electronic spectra are consistent with a $\sigma^2\pi^4\delta^2\delta^*$ electronic configuration. The X-ray structure of $Re_2(OAc)Cl_4(PPh_3)_2$ reveals an eclipsed structure with rhenium atoms linked by an Re–Re bond of 2.2165(7) Å and a bridging acetate ligand (Fig. 62(b)).

As shown in Scheme 2, the oxidation of $Re_2X_4(PR_3)_4$ results in the formation of $[Re_2X_4(PR_3)_4]^+$ which is converted by a chemical process to $Re_2X_5(PR_3)_3$ [478,479]. The green paramagnetic Re_2^{5+} compound $[Re_2Cl_4(PMe_2Ph)_4]PF_6$, produced when $Re_2Cl_4(PMe_2Ph)_4$ is reacted with one equivalent of $NOPF_6$ or $(C_7H_7)PF_6$, has been studied in considerable detail [490]. The paramagnetic compounds exhibit ESR spectra consistent with electron delocalization over both rhenium atoms (e.g. $[Re_2Cl_4(PMe_2Ph)_4]^+$, $\mu_{eff} = 1.35$ BM, $g_{\|} = 2.19$, $g_{\perp} = 2.24$, $A_{\|} = 300$ G, $A_{\perp} = 120$ G). The analogous dications, $[Re_2Cl_4(PR_3)_4]^{2+}$, may be prepared using an excess of $NOPF_6$ but the second oxidation step does not work for all phosphines. The X-ray structure of $[Re_2Cl_4(PMe_2Ph)_4]PF_6$ has been determined. The ligand set around the Re_2 core exhibits an eclipsed conformation in which chlorine and phosphorus donor atoms are staggered with respect to one another. The molecule has virtual D_{2d} symmetry and an Re–Re bond distance of 2.218(1) Å. A $\sigma^2\pi^4\delta^2\delta^*$ electronic configuration and a bond order of 3.5 has been postulated. The cation in $[Re_2Cl_4(PMe_2Ph)_4](PF_6)_2$ possesses an Re–Re quadruple bond with a length of 2.215(2) Å; as argued in the case of the $[Tc_2Cl_8]^{3-/2-}$ complexes, the increased bond order in $[Re_2Cl_4(PMe_2Ph)_4]^{2+}$ is largely offset by a lessening of the σ and/or π bonding as a result of orbital contraction with increasing charge. Molecular orbital and spectroscopic studies of the $[Re_2Cl_4(PR_3)_4]^+$ complexes have been reported [491].

Similarly, the complexes $Re_2X_4L_2$ (X = Cl, Br; L = dppe, arphos) are electrochemically and chemically (using $NOPF_6$) oxidized to the corresponding monocations, $[Re_2X_4L_2]^+$ [492]. However, in contrast with the electrochemical oxidation of $Re_2X_4(PR_3)_4$ complexes, the oxidation of $Re_2X_4L_2$ complexes is not followed by chemical reactions. However, $[Re_2Cl_4(arphos)_2]^+$ will react with added Cl^-, and with respect to the formation of $Re_2Cl_5L_2$ complexes it is interesting to note the synthesis and X-ray structural characterization of $Re_2Cl_5(dppm)_2$ (vide supra). The paramagnetic ($\mu_{eff} = 2.2$ BM) salt, $[Re_2Cl_4(dppe)_2]PF_6$, is believed to retain the staggered

structure of the neutral parent compound and the triple metal–metal bond. Unlike in the $[Re_2X_4(PR_3)_4]^+$ complexes, no near-IR band in the region 1000–2000 nm is observed in the $[Re_2X_4L_2]^+$ complexes. Reaction of $[Re_2X_4L_2]PF_6$ (X = Cl, Br; L = dppe, arphos) with RNC (R = ^{i}Pr, ^{t}Bu) yields $[Re_2X_3L_2(RNC)]PF_6$ [493]. These may be oxidized to the corresponding Re_2^{5+} dications using $NOPF_6$ [493,494]. The $[Re_2X_4L_2]PF_6$ compounds may be converted directly to $[Re_2X_3L_2(RNC)](PF_6)_2$ by reaction with RNC (R = Me, Et) in the presence of $TlPF_6$.

A byproduct of the reaction of $Re_2Cl_4(dppm)_2$ with ^{t}BuNC in the presence of PF_6^- is the blue paramagnetic μ-iminyl compound $[Re_2(\mu\text{-Cl})(\mu\text{-CNH}^t\text{Bu})(\mu\text{-dppm})_2Cl_2(CN^t\text{Bu})_2]PF_6 \cdot H_2O \cdot 0.5CH_2Cl_2$ (**105**) [495]. The cation in **105** possesses an edge-shared bi-octahedral structure, with rhenium atoms linked via two μ-dppm ligands, a single μ-Cl and μ-iminyl ligands. The dirhenium core may be formally Re_2^{3+} or Re_2^{5+} depending on the as yet undetermined donor character of the μ-iminyl ligand. The complex exhibits a well-defined ESR spectrum at −160 °C [495]; the anisotropic signal exhibits rhenium and phosphorus hyperfine coupling.

A mixed-valence structure (**106**) has been assigned to the purple powders of stoichiometry Re_2Cl_4L (L = bpy, phen) formed upon the reaction of bpy

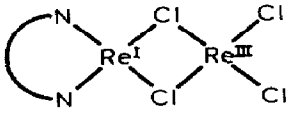

106

or phen with Re_3Cl_9 [496,497]. However, these reactions are quite complex and the products, best formulated as $(LH)_xRe_3Cl_9L$, are very dependent upon the reaction conditions [498,499]. While the formal oxidation state of rhenium appears to be lower than III, a formulation such as **106** has not been supported by subsequent studies [498,499].

The first metal–metal-bonded Re_2^{3+} complexes, blue paramagnetic $Re_2Cl_3(dppm)_2(CO)_2L$ (L = nitrile, isocyanide), were prepared by the cobaltocene reduction of $[Re_2Cl_3(dppm)_2(CO)_2L]PF_6$ [500]. ESR spectra ($g \approx 2.28$) of the complexes exhibit hyperfine coupling to rhenium and phosphorus nuclei and are similar to those obtained for other dirhenium complexes containing chloride and phosphine ligands [440,479,490]. Recently, a detailed report on this chemistry, including the X-ray structure of $Re_2Cl_3(dppm)_2(CO)_2(^i\text{PrNC})$, appeared [501]. The porphyrin complex $[Re_2(\mu\text{-TPP})(CO)_6]SbCl_6$ has been structurally characterized but a reliable synthetic route and the electronic nature of the complex remain to be established [502].

The radical anions $[Re_2(\mu\text{-}H)_2(CO)_8]^-$ and $[Re_2(\mu\text{-}H)_2(\mu\text{-dppm})(CO)_6]^-$ are produced by γ-irradiation of the neutral parent compounds in methyltetrahydrofuran at 77 K [503]. On the basis of elegant ESR experiments, the radical anions are proposed to possess the same symmetry as the parent molecules (D_{2h} and C_{2v} for $Re_2(\mu\text{-}H)_2(CO)_8$ and $Re_2(\mu\text{-}H)_2(\mu\text{-dppm})(CO)_6$ respectively). The unpaired electron is delocalized over both rhenium centres and occupies a π^*_{Re-Re} orbital.

(c) Trinuclear compounds

The treatment of Cp^*ReO_3 with excess PPh_3 in aerated thf leads to the precipitation of green–blue crystals of $[Cp^*_3Re_3(\mu\text{-}O)_6][ReO_4]_2$ [504]. The X-ray crystal structure of $[Cp^*_3Re_3(\mu\text{-}O)_6][ReO_4]_2 \cdot 0.5CH_2Cl_2$ reveals a highly symmetric trinuclear dication consisting of three equivalent Cp^*ReO_2 units linked via oxo bridges (Fig. 65(a)). The triangular Re_3 plane is sandwiched between two triangular arrays of oxygen atoms which together form a trigonal prism. In this dication the rhenium atoms have formal oxidation states of $5\frac{2}{3}$. With 46 valence electrons the complex is electron deficient with an Re–Re bond order of 2/3 (Re–Re = 2.747(2) Å). Molecular orbital calculations predict a triplet ground state for $[Cp^*_3Re_3O_6]^{2+}$, in contrast with the originally reported diamagnetism inferred from NMR studies [505]. Interestingly, the reaction also produces a tetranuclear complex, $Cp^*_2Re_4O_{11}$, when the amount of oxygen available is limited (vide infra) [506].

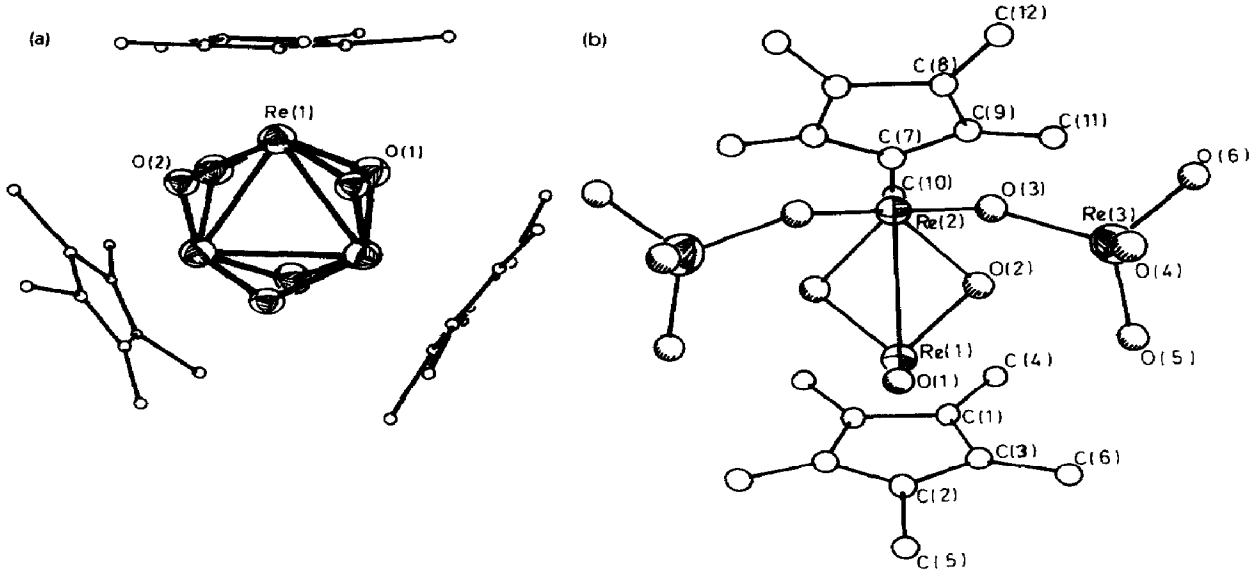

Fig. 65. Products from the reaction of Cp^*ReO_3 and PPh_3–O_2. (a) Structure of the cation in $[Cp^*_3Re_3O_6][ReO_4]_2 \cdot 0.5CH_2Cl_2$. Reproduced with permission from ref. 504. (b) Structure of $Cp^*_2Re_4O_{11}$. Reproduced with permission from ref. 506.

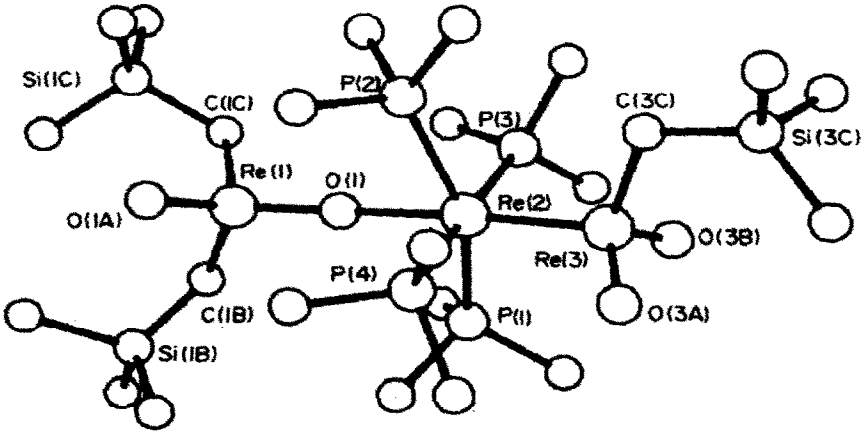

Fig. 66. Structure of $Re_3O_4(CH_2SiMe_3)_3(PMe_3)_4$. Reproduced with permission from ref. 507.

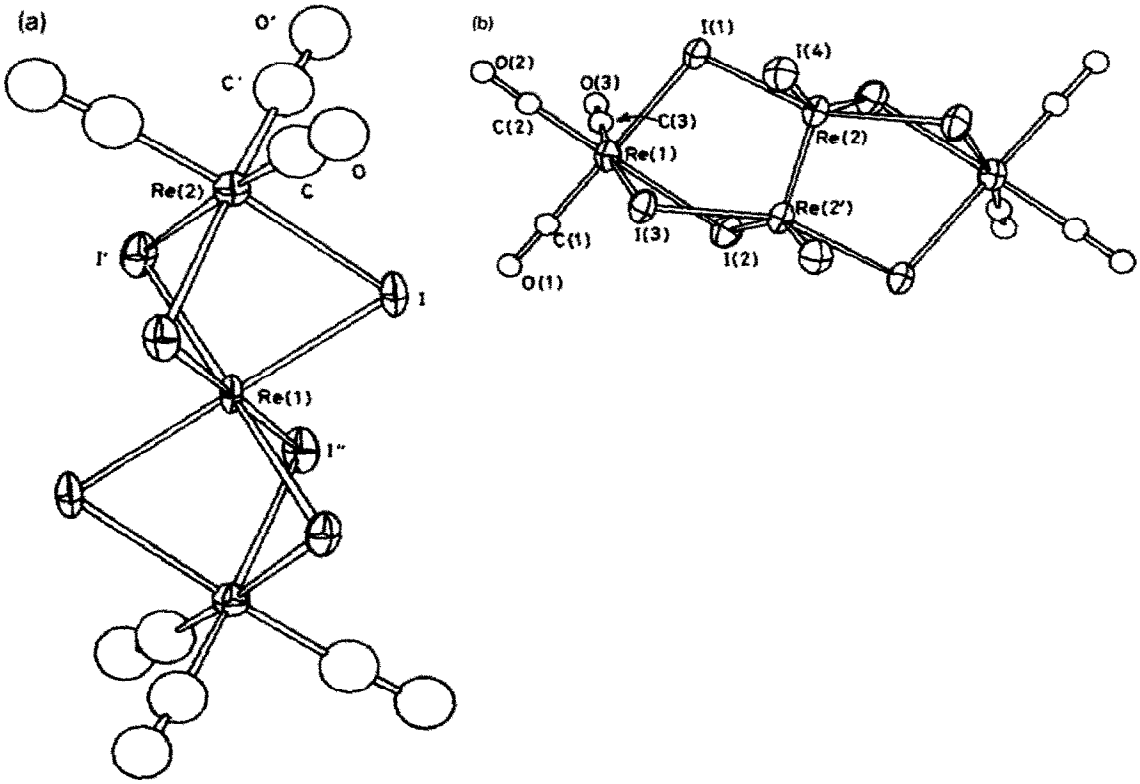

Fig. 67. Products from the reaction of $Re_2I_2(CO)_8$ and I_2. Structures of (a) $Re_3I_6(CO)_6$ and (b) $Re_4I_8(CO)_6$. Reproduced with permission from ref. 509.

A red trinuclear $Re^{I}Re^{V}_{2}$ complex, $Re_3O_4(CH_2SiMe_3)_3(PMe_3)_4$, results from the reaction of $Re(NPh)Cl_3(PMe_3)_2$ with PMe_3 and $(Me_3SiCH_2)_2Si$ [507]. The complex exhibits an unusual molecular structure (Fig. 66) in which two oxo–Re^{V} units (Re(1) and Re(3)) are bonded to a central tetrakis(phosphine)–Re^{I} centre (Re(2)). The Re(2)–Re(3) distance of 2.381(1) Å and electron counting considerations support the presence of a double Re=Re bond between Re(2) and Re(3). The large asymmetry in the Re(1)–O–Re(2) bridge suggests that the Re(1) atom attains an 18-electron configuration by Re–O(1) π-bonding. The oxygen atoms are believed to arise from the thf solvent.

The black trinuclear $Re^{I}_{2}Re^{IV}$ complex $Re_3(\mu\text{-}I)_6(CO)_6$ is produced upon iodine oxidation of $Re_2I_2(CO)_8$ in refluxing heptane [508,509]. The structure of the complex, as shown in Fig. 67(a), consists of an octahedral $[Re^{IV}I_6]^{2-}$ centre bridged via iodine atoms to two terminal $[Re^{I}(CO)_3]^{+}$ units. The Re $\cdots$ Re distance of 3.379(3) Å precludes the presence of a metal–metal bond. The magnetic moment ($\mu_{eff} = 3.59$ BM) is slightly lower than the spin-only value for a magnetically dilute six-coordinate Re^{IV} d^3 centre.

(d) Tetranuclear compounds

The reaction of Cp^*ReO_3 and PPh_3 in the presence of limited amounts of oxygen results in the formation of a brown diamagnetic $Re^{V}_{2}Re^{VII}_{2}$ complex, $Cp^{*}_{2}Re_4O_{11}$, which exhibits the structure shown in Fig. 65(b) [506]. The complex is composed of two perrhenate groups bonded asymmetrically via an oxygen atom to one end of a μ-dioxo–Re^{V}_{2} unit. The Re(1)–Re(2) distance of 2.651(1) Å is indicative of a metal–metal double bond between these d^2 atoms. A mixed-valence product from a related reaction was discussed in Section E(iii)(c).

Orange $[Re_2(O_2C^{n}Pr)_4][ReO_4]_2$, originally formulated as $Re_2O_2(\mu\text{-}O)_2(O_2C^{n}Pr)_2$ by Taha and Wilkinson [510], is formed upon reaction of $ReCl_3$ and hot butyric acid in the presence of oxygen [511]. In the crystal state, the compound is composed of central $[Re^{III}_{2}(O_2CR)_4]^{2+}$ units bonded along their Re–Re axis to two $[Re^{VII}O_4]^{-}$ units. The Re–$OReO_3$ bond distances are 2.18(3) Å while the Re–Re bond in the central fragment is 2.251(2) Å in length. The reaction of $ReCl_3$ and hot $^{i}PrCO_2H$ results in the formation of $[Re_2Cl_2(O_2C^{i}Pr)_3][ReO_4]$ which exhibits a related but extended solid state structure [512].

The preparation of $Re_3I_6(CO)_6$ by the reaction of $Re_2I_2(CO)_8$ and iodine has already been mentioned. Another mixed-valence complex, the tetranuclear $Re^{I}_{2}Re^{III}_{2}$ complex $Re_4I_8(CO)_6$ (**107**), is produced by the reaction of $Re_2I_2(CO)_6(thf)_2$ and iodine, followed by prolonged crystallization of the crude product [508,509]. The structure of **107** is shown in Fig. 67(b); a central multiply metal–metal-bonded $[Re_2I_8]^{2-}$ core is bound through iodine

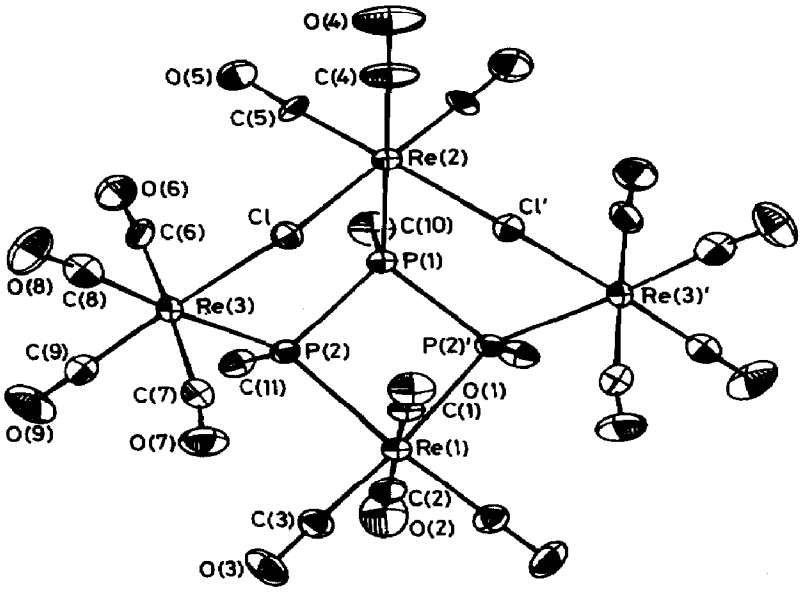

Fig. 68. Structure of **108**. Reproduced with permission from ref. 513.

bridges to two terminal $[Re(CO)_3]^+$ units. The two multiply bonded Re^{III} centres possess non-eclipsed square-pyramidal geometries while the *fac*-tricarbonyl–Re^{I} units possess distorted octahedral geometries. As only a few crystals of **107** were obtained, magnetic and spectroscopic studies were precluded.

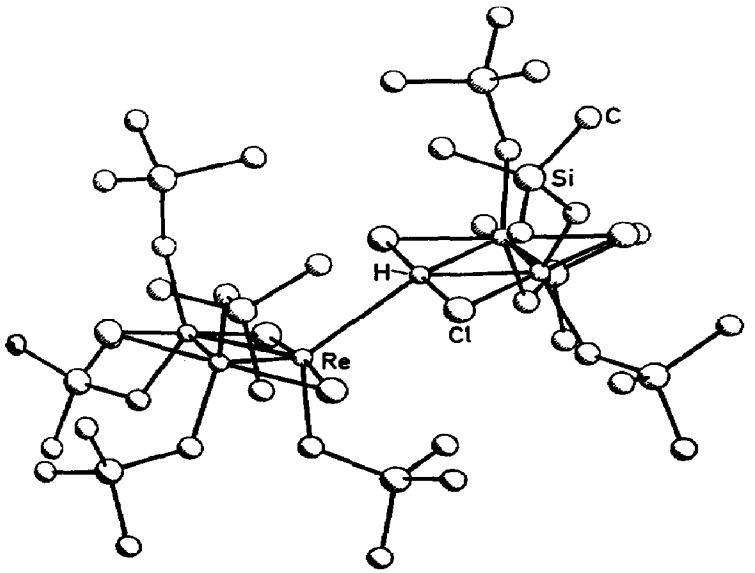

Fig. 69. Structure of $Re_6(\mu\text{-}Cl)_6H(CH_2SiMe_3)_9$. Reproduced with permission from ref. 515.

The white tetranuclear cyclometallophosphine complex $Re_4Cl_2(CO)_{15}$-{MePP(Me)PMe} (**108**), the structure of which is shown in Fig. 68, is formed upon the reaction of $Ni(PMeCl_2)_4$ and $Re_2(CO)_{10}$ [513]. Pyrolysis of **108** at 230–250°C leads to the formation of the red clusters $Re_6(CO)_{18}(\mu_4\text{-PMe})_3$ and $Re_5(CO)_{14}(\mu_4\text{-PMe})(\mu\text{-PMe}_2)\{\mu_3\text{-P[Re(CO)}_5]\}$ [514].

(e) Hexanuclear compounds

Hydrogenolysis of a thf solution of $Re_3(\mu\text{-Cl})_3(CH_2SiMe_3)_6$ results in the formation of green $Re_6(\mu\text{-Cl})_6H(CH_2SiMe_3)_9$ according to eqn. (21) [515]:

$$2Re_3Cl_3(CH_2SiMe_3)_6 + 2H_2 \rightarrow Re_6Cl_6H(CH_2SiMe_3)_9 + 3SiMe_4 \qquad (21)$$

The X-ray structure of the compound is shown in Fig. 69 and consists of two triangular Re_3 clusters (Re–Re = 2.390–2.420(1) Å) linked by a long (2.993(1) Å) Re–Re bond (cf. Re–Re distances of 2.39–2.42 Å in the triangles). The mixed-valence aspect of the complex has not been addressed but formally each triangular unit must possess an $Re^{II}Re_2^{III}$ formulation.

F. CONCLUDING REMARKS

This review has exposed the breadth, diversity and novelty of early transition metal mixed-valence chemistry. As the detail of this chemistry has been outlined in the individual general survey it only remains to make a few general observations. The distribution of compounds according to transition metal is represented in the pie graph given in Fig. 70. The greatest number of mixed-valence compounds are formed by the group 6 elements, followed closely by the group 7 elements. Relatively few compounds are known for the group 4 and 5 elements, particularly the former where zirconium and

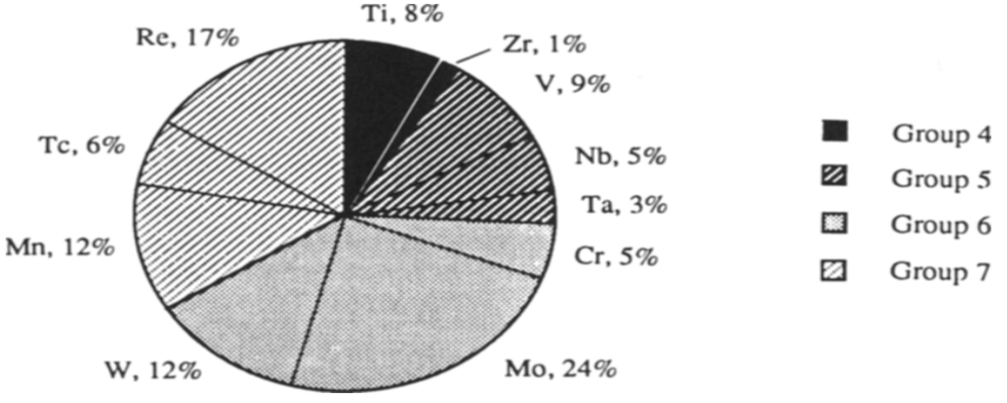

Fig. 70. Distribution of mixed-valence compounds according to element and group.

TABLE 13

Approximate number of compounds according to nuclearity and element

Nuclearity	Element											
	Ti	Zr	Hf	V	Nb	Ta	Cr	Mo	W	Mn	Tc	Re
Di-	10	–	–	12	2	2	10	45	18	30	16	48
Tri-	5	2	–	5	12	3	5	18	10	6	–	3
Tetra-	5	–	–	1	1	–	–	16	12	2	–	4
Penta-	2	–	–	2	–	–	1	1	–	–	–	–
Higher	5	–	–	>10	Many	Many	2	Many	Many	5	4	3

hafnium together are known to form only two compounds. The number of publications in this area follows a roughly similar distribution. The distribution of compounds according to nuclearity and metal is shown in Table 13. The majority of compounds are dinuclear although a large number of high nuclearity species are known for niobium, tantalum, molybdenum and tungsten. This distribution reflects the problems associated with the rational synthesis of high nuclearity compounds compared with the relatively simple low nuclearity species. Spontaneous formation of high nuclearity compounds in general is a characteristic feature of the elements which form mixed-valence compounds of this type. Many of the compounds described have been prepared inadvertently and their mixed valency has often been an aspect of secondary interest. Accordingly, a thorough and systematic description of the electronic structure of these compounds is often prevented by a lack of crucial experimental information relating to their mixed valency. Fortunately, this situation is rapidly changing and the rational synthesis and systematic study of mixed-valence compounds is attracting growing interest. The collection of compounds described herein may be likened to a zoo of exotic animals. Many of the species are unique and exhibit remarkable behaviour. Studies aimed at the discovery of new species will broaden knowledge and assist the formulation of interrelationships and commonalities of origin and behaviour. As the zoo arouses the interest and curiosity of the visitor and serves as a focal point for the continued study of the species therein, so too we hope this review will function in the area of mixed-valence chemistry.

NOTE ADDED IN PROOF

This section extends coverage of the literature available to us up to April 1989. The organization of compounds follows that of the main text.

Group 4. No further reports.

Group 5. The $V^{IV}V_7^V$ compound $(NH_4)_8[V_{19}O_{41}(OH)_9]\cdot 11H_2O$ has been prepared and characterized by physical, spectroscopic and crystallographic methods [516]. The complex $Nb_3O_2Cl_7(thf)$ contains an Nb_2^{III} unit bridged by an $Nb^VO_2Cl_3(thf)$ bridging ligand [517]. A variety of mixed-valence chalcogenide complexes of niobium and tantalum have been reported by Fenske et al. [518]. Tetranuclear $Nb_4(\mu_3\text{-}Cl)_2(\mu\text{-}Cl)_4Cl_4(PMe_3)_6$ contains a core of fused Nb_3 units forming a rhombus linked by chloride ligands [519].

Group 6. Dinuclear molybdenum mixed-valence complexes have also been reviewed by Casewit and Rakowski DuBois [520]. A report concerning

$[(Me_3tcn)_2Mo_2(\mu\text{-}O)(\mu\text{-}OAc)_2]^{3+}$ and related species, including the analogous $Mo^{II}Mo^{III}$ monocation, has appeared [521]. The synthesis and structures of salts of $[Mo_4(\mu\text{-}E)(\mu\text{-}S)_3(H_2O)_{12}]^{5+}$ (E = O, S) have been reported [522]. Another example (cf. **69**) of a mixed-valence polyoxomolybdate, the $Mo^{V}_4Mo^{VI}_4$ compound $(NBu_4)_4[Mo_8O_{24}(OMe)_2]$, has been reported [523]. Ring currents in reduced molybdenum and tungsten heteropoly blues have been investigated by susceptibility measurements [524]. Mixed-valence molybdenum chalcogenide complexes have been described [518]. The synthesis, X-ray structure and physicochemical properties of $(PPh_4)[W_2Cl_8(thf)]$ have been reported [525] and the electronic structure of $[W(WS_4)_2]^{2-}$ has been probed by MO methods [526].

Group 7. Mixed-valence manganese centres in biology have been reviewed [527] and ESR evidence for a dinuclear mixed-valence active site in *Lactobacillus plantarum* manganese catalase has been reported [528]. The chemistry of $Mn^{III}Mn^{IV}$ and related isovalent complexes of tcn and Me_3tcn (e.g. **85** and **86**) has been described in detail [529]. An $[Mn_2(\mu\text{-}O)_2]^{3+}$ complex of *N,N*-bis(2-pyridylmethyl)glycinate has been prepared and characterized by crystallographic, spectroscopic and magnetic studies [530]. The synthesis, structure and magnetic properties of a second form of **94**, containing a bent rather than linear (see Fig. 50) $Mn^{II}Mn^{III}_2$ unit, have been reported [531]. Christou and Vincent have reviewed mixed-valence manganese clusters [532]. The synthesis and characterization of $Mn_4O_3Cl_4(OAc)_3(py)_3$, which is closely related to **95**, has been reported [533]. While the controlled aerial oxidation of $Mn(CF_3SO_3)_2$ in the presence of tren yields **84** [371], exposure to excess oxygen leads to the $Mn^{III}_4Mn^{IV}_6$ compound $[Mn_{10}O_{14}(tren)_6](CF_3SO_3)_8 \cdot 6MeCN$ which exhibits a structure resembling that of layered manganese oxides [534]. The $Mn^{III}_8Mn^{IV}_4$ complex $Mn_{12}O_{12}(O_2CPh)_{16}(H_2O)_4$ possesses a structure related to that reported for **97** [535]. The mechanism of formation of oxo-bridged $Tc^{III}Tc^{IV}$ complexes **98** and **99** and their intramolecular isomerization have been studied by Lu and Clarke [536]. Details of the interesting polynuclear clusters of technetium have appeared: the synthesis [537], X-ray structures [537] and physicochemical properties [538] of hexanuclear and octanuclear complexes have been described.

ACKNOWLEDGEMENTS

My thanks to Dr. A.G. Wedd and Mr. P.R. Traill for critically reviewing the manuscript, to Ms. J. White for the photographic reproduction of the figures and to those who gave permission for reproduction of figures. I would especially like to thank my wife Brooke for her patience during the preparation of this review and her valuable assistance in the later stages.

REFERENCES

1 M.B. Robin and P. Day, Adv. Inorg. Chem. Radiochem., 10 (1967) 247–422.
2 P. Day, Int. Rev. Phys. Chem., 1 (1981) 149–193.
3 J. Woodward, Philos. Trans. R. Soc. London, 33 (1724) 15. Translated in H.M. Powell, Proc. Chem. Soc., London, (1959) 73.
4 A.G. Sharpe, The Chemistry of Cyano-Complexes of the Transition Metals, Academic Press, New York, 1976, p. 99.
5 D.B. Brown (Ed.), Mixed-Valence Compounds, Theory and Application in Chemistry, Physics, Geology and Biology, Reidel, Dordrecht, 1980.
6 G.C. Allen and N.S. Hush, Prog. Inorg. Chem., 8 (1967) 357–389.
7 N.S. Hush, Prog. Inorg. Chem., 8 (1967) 391–444.
8 C. Creutz, Prog. Inorg. Chem., 30 (1983) 1–73.
9 A.E. Underhill and D.M. Watkins, Chem. Soc. Rev., 9 (1980) 429–448.
A.H. Reis, Jr., and S.W. Peterson, Ann. N.Y. Acad. Sci., 313 (1978) 560–579.
10 M. Dunaj-Jurco, G. Ondrejovic, M. Melnik and J. Garaj, Coord. Chem. Rev., 83 (1988) 1–28.
11 T.J. Meyer, Ann. N.Y. Acad. Sci., 313 (1978) 496–508.
12 D.B. Brown and J.T. Wrobleski, in D.B. Brown (Ed.), Mixed-Valence Compounds, Theory and Application in Chemistry, Physics, Geology and Biology, Reidel, Dordrecht, 1980, p. 49–71.
13 K.Y. Wong and P.N. Schatz, Prog. Inorg. Chem., 28 (1981) 369–449.
14 D.E. Richardson and H. Taube, Coord. Chem. Rev., 60 (1984) 107–129.
15 A. Flamini, D.J. Cole-Hamilton and G. Wilkinson, J. Chem. Soc., Dalton Trans., (1978) 454–459.
16 S. Sabo, R. Choukroun and D. Gervais, J. Chem. Soc., Dalton Trans., (1981) 2328–2330.
17 F.J. Kristine and R.E. Shepherd, Inorg. Chem., 20 (1981) 215–222.
18 J.N. Armor, Inorg. Chem., 17 (1978) 203–213.
19 J.N. Armor, Inorg. Chem., 17 (1978) 213–221.
20 G.P. Pez and J.N. Armor, Adv. Organomet. Chem., 19 (1981) 1–50.
21 G.P. Pez, J. Am. Chem. Soc., 98 (1976) 8072–8078.
22 G.P. Pez and S.C. Kwan, J. Am. Chem. Soc., 98 (1976) 8079–8083.
23 G.P. Pez, P. Apgar and R.K. Crissey, J. Am. Chem. Soc., 104 (1982) 482–490.
24 A.R. Middleton and G. Wilkinson, J. Chem. Soc., Dalton Trans., (1980) 1888–1890.
25 J.F. Plummer and E.P. Schram, Inorg. Chem., 14 (1975) 1505–1512.
26 S. Wongnawa and E.P. Schram, Inorg. Chem., 16 (1977) 1001–1006.
27 G. Fachinetti, C. Biran, C. Floriani, A.C. Villa and C. Guastini, J. Chem. Soc., Dalton Trans., (1979) 792–800.
28 E.O. Fischer and F. Röhrscheid, J. Organomet. Chem., 6 (1966) 53–66.
29 S. Dzierzgowski, R. Giezynski, M. Jarosz and S. Pasynkiewicz, J. Organomet. Chem., 152 (1978) 281–285.
30 E.E. van Tamelen, B. Åkermark and K.B. Sharpless, J. Am. Chem. Soc., 91 (1969) 1552–1554.
31 S. Sabo and D. Gervais, C. R. Acad. Sci., Ser. C, 291 (1980) 207.
32 L. Maya, Inorg. Chem., 25 (1986) 4213–4217.
33 F. Bottomley, G.O. Egharevba and P.S. White, J. Am. Chem. Soc., 107 (1985) 4353–4354.
34 J.C. Huffman, J.G. Stone, W.C. Krusell and K.G. Caulton, J. Am. Chem. Soc., 99 (1977) 5829–5831.
35 F. Bottomley, I.J.B. Lin and M. Mukaida, J. Am. Chem. Soc., 102 (1980) 5238–5242.

36 F. Bottomley and F. Grein, Inorg. Chem., 21 (1982) 4170–4178.
37 A. Roth, C. Floriani, A. Chiesi-Villa and C. Gaustini, J. Am. Chem. Soc., 108 (1986) 6823–6825.
38 M. Kilner, G. Parkin and A.G. Talbot, J. Chem. Soc., Chem. Commun., (1985) 34–35.
39 R.L. Daake and J.D. Corbett, Inorg. Chem., 17 (1978) 1192–1195.
40 J.D. Corbett, Acc. Chem. Res., 14 (1981) 239–246.
41 H. Imoto, J.D. Corbett and A. Cisar, Inorg. Chem., 20 (1981) 145–150.
42 J.D. Smith and J.D. Corbett, J. Am. Chem. Soc., 108 (1986) 1927–1934.
43 A. Simon, Angew. Chem., Int. Ed. Engl., 20 (1981) 1–22.
44 F. Stollmaier and U. Thewalt, J. Organomet. Chem., 208 (1981) 327–334.
45 J. Kleppinger, J. Wrazel, J.C. Calabrese and E.M. Larsen, Inorg. Chem., 19 (1980) 3172–3175.
46 F.A. Cotton, P.A. Kibala and W.J. Roth, J. Am. Chem. Soc., 110 (1988) 298–300.
47 L.V. Boas and J.C. Pessoa, in G. Wilkinson (Ed.), Comprehensive Coordination Chemistry, Pergamon, Oxford, 1987, Vol. 3, 453–583.
48 T.L. Riechel and D.T. Sawyer, Inorg. Chem., 14 (1975) 1869–1875.
49 T.K. Myser and R.E. Shepherd, Inorg. Chem., 26 (1987) 1544–1555.
50 M.A. Hepler and T.L. Riechel, Inorg. Chim. Acta, 54 (1981) L255–L257.
51 Y. Jeannin, J.P. Launay and M.A. Seid Sedjadi, J. Coord. Chem., 11 (1981) 27–34.
52 Y. Jeannin, J.P. Launay, C. Sanchez, J. Livage and M. Fournier, Nouv. J. Chim., 4 (1980) 587–592.
53 S. Yamada, C. Katayama, J. Tanaka and M. Tanaka, Inorg. Chem., 23 (1984) 253–255.
54 H. Taguchi, K. Isobe, Y. Nakamura and S. Kawaguchi, Bull. Chem. Soc. Jpn., 51 (1978) 2030–2035.
55 A. Kojima, K. Okazaki, S. Ooi and K. Saito, Inorg. Chem., 22 (1983) 1168–1174.
56 M. Nishizawa, K. Hirotsu, S. Ooi and K. Saito, J. Chem. Soc., Chem. Commun., (1979) 707–708.
57 M. Nishizawa and K. Saito, Inorg. Chem., 19 (1980) 2284–2288.
58 F. Babonneau, C. Sanchez, J. Livage, J.P. Launay, M. Daoudi and Y. Jeannin, Nouv. J. Chim., 6 (1982) 353–357.
59 J.P. Launay, Y. Jeannin and M. Daoudi, Inorg. Chem., 24 (1985) 1052–1059.
60 P. Blanc, C. Madic and J.P. Launay, Inorg. Chem., 21 (1982) 2923–2928.
61 T.W. Newton and F.B. Baker, Inorg. Chem., 3 (1964) 569–573.
62 F.J. Kristine, D.R. Gard and R.E. Shepherd, J. Chem. Soc., Chem. Commun., (1976) 994–995.
63 F.J. Kristine and R.E. Shepherd, J. Am. Chem. Soc., 100 (1978) 4398–4404.
64 J.C. Smart and B.L. Pinsky, J. Am. Chem. Soc., 102 (1980) 1009–1014.
65 B.G. Bennett and D. Nicholls, J. Chem. Soc. A, (1971) 1204–1206.
66 K.S. Murray and R.M. Sheahan, J. Chem. Soc., Dalton Trans., (1973) 1182–1187.
67 F. Calderazzo and S. Bacciarelli, Inorg. Chem., 2 (1963) 721–723.
68 J.H. Osborne, A.L. Rheingold and W.C. Trogler, J. Am. Chem. Soc., 107 (1985) 6292–6297.
69 H. Funk, C. Müller and A. Paul, Z. Chem., 6 (1966) 277.
70 B.G. Bennett and D. Nicholls, J. Inorg. Nucl. Chem., 34 (1972) 673–677.
71 B.J. Allin and P. Thornton, Inorg. Nucl. Chem. Lett., 9 (1973) 449–452.
72 F.A. Cotton, G.E. Lewis and G.N. Mott, Inorg. Chem., 21 (1982) 3316–3321.
73 T.G. Richmond, Q.-Z. Shi, W.C. Trogler and F. Basolo, J. Am. Chem. Soc., 106 (1984) 76–80.
74 W. Hieber, J. Peterhans and E. Winter, Chem. Ber., 94 (1961) 2572–2578.

75 W. Hieber, E. Winter and E. Schubert, Chem. Ber., 95 (1962) 3070–3076.
76 M. Schneider and E. Weiss, J. Organomet. Chem., 121 (1976) 365–371.
77 F. Bottomley, J. Darkwa and P.S. White, J. Chem. Soc., Chem. Commun., (1982) 1039–1040.
78 F. Bottomley and P.S. White, J. Chem. Soc., Chem. Commun., (1981) 28–29.
79 F. Bottomley, D.E. Paez and P.S. White, J. Am. Chem. Soc., 104 (1982) 5651–5657.
80 F. Bottomley, D.E. Paez and P.S. White, J. Am. Chem. Soc., 107 (1985) 7226–7227.
81 F. Bottomley, D.F. Drummond, D.E. Paez and P.S. White, J. Chem. Soc., Chem. Commun., (1986) 1752–1753.
82 C.M. Bolinger, J. Darkwa, G. Gammie, S.D. Gammon, J.W. Lyding, T.B. Rauchfuss and S.R. Wilson, Organometallics, 5 (1986) 2386–2388.
83 N. Gharbi, C. Sanchez, J. Livage, J. Lemerle, L. Nejem and J. Lefebvre, Inorg. Chem., 21 (1982) 2758–2765, and references therein.
84 S. Ostrowetsky, Bull. Soc. Chim. Fr., (1964) 1012–1018 and 1018–1035.
85 C. Heitner-Wirguin and J. Selbin, J. Inorg. Nucl. Chem., 30 (1968) 3181–3188.
86 A. Bino, S. Cohen and C. Heitner-Wirguin, Inorg. Chem., 21 (1982) 429–431.
87 C. Heitner-Wirguin and J. Selbin, Isr. J. Chem., 7 (1969) 27–30.
88 A. Müller, E. Krickemeyer, M. Penk, H.-J. Walberg and H. Bögge, Angew. Chem., Int. Ed. Engl., 26 (1987) 1045–1046.
89 E. Hayek and E. Pallasser, Monatsh. Chem., 99 (1968) 2494.
90 G.K. Johnson, Ph.D. Thesis, University of Missouri-Columbia, 1977. Diss. Abstr., B, 38 (1978) 4801.
91 G.K. Johnson and E.O. Schlemper, J. Am. Chem. Soc., 100 (1978) 3645–3646.
92 S.P. Harmalker and M.T. Pope, J. Am. Chem. Soc., 103 (1981) 7381–7383.
93 M.M. Mossoba, C.J. O'Connor, M.T. Pope, E. Sinn, G. Herv and A. Teze, J. Am. Chem. Soc., 102 (1980) 6864–6866.
94 M.T. Pope, in G. Wilkinson (Ed.), Comprehensive Coordination Chemistry, Pergamon, Oxford, 1987, Vol. 3, 1023–1058.
95 M.T. Pope, Heteropoly and Isopoly Oxometallates, Inorganic Chemistry Concepts 8, Springer-Verlag, Berlin, 1983.
96 D.L. Kepert and K. Vrieze, in V. Gutmann (Ed.), Halogen Chemistry, Academic Press, New York, 1967, Vol. 3, p. 1.
97 D. Brown, in J.C. Bailar, Jr., H.J. Emeleus, R. Nyholm and A.F. Trotman-Dickenson (Eds.), Comprehensive Inorganic Chemistry, Pergamon, Oxford, 1973, Vol. 3, pp. 553–622.
98 H. Schäfer and H.G. Schnering, Angew. Chem., 76 (1964) 833–849.
99 R.A. Walton, Prog. Inorg. Chem., 16 (1972) 1–226.
100 R.E. McCarley, in D.B. Brown (Ed.), Mixed-Valence Compounds, Theory and Application in Chemistry, Physics, Geology and Biology, Reidel, Dordrecht, 1980, pp. 337–364.
101 L.G. Hubert-Pfalzgraf, M. Postel and J.G. Riess, in G. Wilkinson (Ed.), Comprehensive Coordination Chemistry, Pergamon, Oxford, 1987, Vol. 3, 585–697.
102 C.E. Holloway and M. Melnik, Rev. Inorg. Chem., 7 (1985) 161–250.
103 A. Antinolo, M. Fajardo, A. Otero and P. Royo, J. Organomet. Chem., 234 (1982) 309–314.
104 A. Fakhr, Y. Mugnier, R. Broussier, B. Gautheon and E. Laviron, J. Organomet. Chem., 317 (1986) 201–213.
105 Y. Matsuda, S. Sakamoto, T. Takaki and Y. Murakami, Chem. Lett., (1985) 107–110.
106 J.E. Anderson, Y.H. Liu, R. Gillard, J.-M. Barbe and K.M. Kadish, Inorg. Chem., 25 (1986) 2250–2255.

107 A.V. Saha, R.K. Maiti, R.N. Gupta and B.K. Sen, Indian J. Chem., 15A (1977) 43–44.
108 F. Ott, Electrochem. Z., 18 (1912) 349.
109 S.J. Kiehl and D. Hardt, J. Am. Chem. Soc., 50 (1928) 1608–1620.
110 S.J. Kiehl and D. Hardt, J. Am. Chem. Soc., 50 (1928) 2337–2345.
111 S.J. Kiehl, R.L. Fox and H.B. Hardt, J. Am. Chem. Soc., 59 (1937) 2395–2399.
112 E.W. Golibersuch and R.C. Young, J. Am. Chem. Soc., 71 (1949) 2402–2405.
113 E.I. Krylov and N.N. Kalugina, Russ. J. Inorg. Chem., 4 (1959) 1138.
114 Y.G. Goroshchenko and M.I. Andreeva, Russ. J. Inorg. Chem., 11 (1966) 1197–1199.
115 A. Bino, J. Am. Chem. Soc., 102 (1980) 7990–7991.
116 A. Bino, Inorg. Chem., 21 (1982) 1917–1920.
117 F.A. Cotton, M.P. Diebold, R. Llusar and W.J. Roth, J. Chem. Soc., Chem. Commun., (1986) 1276–1278.
118 F.A. Cotton, M.P. Diebold and W.J. Roth, Inorg. Chem., 27 (1988) 2347–2352.
119 F.A. Cotton, S.A. Duraj and W.J. Roth, J. Am. Chem. Soc., 106 (1984) 3527–3531.
120 A.P. Ginsberg and A.L. Wayda, Inorg. Chem., 24 (1985) 4749–4751.
121 L.G. Hubert-Pfalzgraf, M. Tsunoda and J.G. Riess, Inorg. Chim. Acta, 41 (1980) 283–286.
122 V.T. Kalinnikov, A.A. Pasynskii, G.M. Larin, V.M. Novotortsev, Y.T. Struchkov, A.I. Gusev and N.I. Kirillova, J. Organomet. Chem., 74 (1974) 91–96.
123 F.A. Cotton and W.J. Roth, J. Am. Chem. Soc., 105 (1983) 3734–3735.
124 F.A. Cotton, S.A. Duraj and W.J. Roth, J. Am. Chem. Soc., 106 (1984) 6987–6993.
125 F.A. Cotton and W.J. Roth, Inorg. Chim. Acta, 126 (1987) 161–166.
126 R.B. King, D.M. Braitsch and P.N. Kapoor, J. Chem. Soc., Chem. Commun., (1972) 1072.
127 R.B. King, D.M. Braitsch and P.N. Kapoor, J. Am. Chem. Soc., 97 (1975) 60–64.
128 M.R. Churchill and S.W.-Y. Chang, J. Chem. Soc., Chem. Commun., (1974) 248–249.
129 F. Stollmaier and U. Thewalt, J. Organomet. Chem., 222 (1981) 227–233.
130 S.Z. Golberg, B. Spivack, G. Stanley, R. Eisenberg, D.M. Braitsch, J.S. Miller and M. Abkowitz, J. Am. Chem. Soc., 99 (1977) 110–117.
131 D.C. Boyd, M. Gebhard and K.R. Mann, Inorg. Chem., 25 (1986) 119–120.
132 A. Simon and H.-G. von Schnering, J. Less-Common Met., 11 (1966) 31.
133 F.A. Cotton, M.P. Diebold and W.J. Roth, J. Am. Chem. Soc., 109 (1987) 2833–2834.
134 A.J. Benton, M.G.B. Drew and D.A. Rice, J. Chem. Soc., Chem. Commun., (1981) 1241–1242.
135 J. Rijnsdorp and F. Jellinek, J. Solid State Chem., 28 (1979) 149–156.
136 D.D. Klendworth and R.A. Walton, Inorg. Chem., 20 (1981) 1151–1155.
137 R.A. Mackay and R.F. Schneider, Inorg. Chem., 6 (1967) 549–552.
138 F. Ueno and A. Simon, Acta Crystallogr. Sect. C, 41 (1985) 308–310.
139 A. Simon, H.-G. von Schnering and H. Schäfer, Z. Anorg. Allg. Chem., 361 (1968) 235–248.
140 A. Simon, Z. Anorg. Allg. Chem., 355 (1967) 311–322.
141 H. Imoto and A. Simon, Inorg. Chem., 21 (1982) 308–319.
142 H. Imoto and J.D. Corbett, Inorg. Chem., 19 (1980) 1241–1245.
143 F. Stollmaier and A. Simon, Inorg. Chem., 24 (1985) 168–171.
144 R.G. Woolley, Inorg. Chem., 24 (1985) 3519–3525, and references therein.
145 D.C. Bradley, M.B. Hursthouse and P.F. Rodesiler, J. Chem. Soc., Chem. Commun., (1968) 1112–1113.
146 C.E. Holloway and M. Melnik, Rev. Inorg. Chem., 7 (1985) 1–74.
147 J. Reed, Inorg. Chim. Acta, 21 (1977) L36.

148 A. Antinolo, M. Fajardo, A. Otero and P. Royo, J. Organomet. Chem., 246 (1983) 269–278.
149 N. Bricevic, Z. Ruzic-Toros and B. Kojic-Prodic, J. Chem. Soc., Dalton Trans., (1985) 455–458.
150 C.B. Thaxton and R.A. Jacobson, Inorg. Chem., 10 (1971) 1460–1463.
151 A. Vogler and H. Kunkely, Inorg. Chem., 23 (1984) 1360–1363.
152 S.P. Christiano, J. Wang and T.J. Pinnavaia, Inorg. Chem., 24 (1985) 1222–1227.
153 L.F. Larkworthy, K.B. Nolan and P. O'Brien, in G. Wilkinson (Ed.), Comprehensive Coordination Chemistry, Pergamon, Oxford, Vol. 3, 1987, 699–969.
154 F.A. Cotton and R.A. Walton, Multiple Bonds Between Metal Atoms, Wiley, New York, 1982.
155 H. Behrens and H. Zizlsperger, Z. Naturforsch., Teil B, 16 (1961) 349.
156 H. Behrens and R. Schwab, Z. Naturforsch., Teil B, 19 (1964) 768–769.
157 E. Lindner and H. Behrens, Spectrochim. Acta, Part A, 23 (1967) 3025–3033.
158 L.B. Handy, J.K. Ruff and L.F. Dahl, J. Am. Chem. Soc., 92 (1970) 7327–7337.
159 H. Behrens and D. Herrmann, Z. Anorg. Allg. Chem., 351 (1967) 225–236.
160 C. Elschenbroich and J. Heck, J. Am. Chem. Soc., 101 (1979) 6773–6776.
161 N. Van Order, Jr., W.E. Geiger, T.E. Bitterwolf and A.L. Rheingold, J. Am. Chem. Soc., 109 (1987) 5680–5690.
162 A.M. Arif, J.G. Hefner, R.A. Jones, T.A. Albright and S.-K. Kang, J. Am. Chem. Soc., 108 (1986) 1701–1703.
163 F.A. Cotton and W. Wang, Inorg. Chem., 21 (1982) 2675–2678.
164 F.A. Cotton and G.W. Rice, Inorg. Chim. Acta, 27 (1978) 75–78.
165 H. Behrens and W. Haag, Chem. Ber., 94 (1961) 320–322.
166 F. Bottomley, D.E. Paez and P.S. White, J. Am. Chem. Soc., 103 (1981) 5581–5582.
167 A.A. Pasynskii, I.L. Eremenko, Y.V. Rakitin, V.M. Novotortsev, O.G. Ellert, V.T. Kalinnikov, V.E. Shklover, Y.T. Struchkov, S.V. Lindeman, T.K. Korbanov and G.S. Gasanov, J. Organomet. Chem., 248 (1983) 309–320.
168 A.A. Pasynskii, I.L. Eremenko, O. Orazsakhatov, G.S. Gasanov, V.E. Shklover and Y.T. Struchkov, J. Organomet. Chem., 269 (1984) 147–153.
169 L.C.A. Barreswil, Ann. Chim. Phys., 20 (1847) 364.
170 J.A. Connor and E.A.V. Ebsworth, Adv. Inorg. Chem. Radiochem., 6 (1964) 279–381.
171 B. Upadyay, A.N. Upadhyay, A. Upadhyay and S.C. Tripathi, Transition Met. Chem., 3 (1978) 60–61.
172 B. Upadhyay, A. Upadhyay, H.N. Singh, D. Chaturvedi and A.N. Upadhyay, Transition Met. Chem., 3 (1978) 313–315.
173 M.T. Pope, in D.B. Brown (Ed.), Mixed-Valence Compounds, Theory and Application in Chemistry, Physics, Geology and Biology, Reidel, Dordrecht, 1980, pp. 365–386.
174 R.I. Buckley and R.J.H. Clark, Coord. Chem. Rev., 65 (1985) 167–218.
175 K. Wieghardt, G. Backes-Dahmann, W. Herrmann and J. Weiss, Angew. Chem., Int. Ed. Engl., 23 (1984) 899–900.
176 W. Herrmann and K. Wieghardt, Polyhedron, 5 (1986) 513–520.
177 M. Chaudhury, J. Chem. Soc., Dalton Trans., (1983) 857–860.
178 R.K. Wharton, J.F. Ojo and A.G. Sykes, J. Chem. Soc., Dalton Trans., (1975) 1526–1530.
179 G.A. Chappelle, A. MacStay, S.T. Pittenger, K. Ohashi and K.W. Hicks, Inorg. Chem., 23 (1984) 2768–2771.
180 G.J.S. Adam and M.L.H. Green, J. Organomet. Chem., 208 (1981) 299–308.
181 J.-C. Daran, K. Prout, G.J.S. Adam, M.L.H. Green and J. Sala-Pala, J. Organomet. Chem., 131 (1977) C40–C42.

182 K. Prout and J.-C. Daran, Acta Crystallogr., Sect. B, 34 (1978) 3586–3591.
183 M. Draganjac, E. Simhon, L.T. Chan, M. Kanatzidis, N.C. Baenziger and D. Coucouvanis, Inorg. Chem., 21 (1982) 3321–3332.
184 D. Coucouvanis and A. Hadjikyriacou, Inorg. Chem., 25 (1986) 4317–4319.
185 M.W. Bishop, J. Chatt, J.R. Dilworth, J.R. Hyde, S. Kim, K. Venkatasubramanian and J. Zubieta, Inorg. Chem., 17 (1978) 2917–2928.
186 J.A. Broomhead, M. Sterns and C.G. Young, J. Chem. Soc., Chem. Commun., (1981) 1262–1263.
187 J.A. Broomhead, M. Sterns and C.G. Young, Inorg. Chem., 23 (1984) 729–737.
188 C.D. Garner, N.C. Howlader, F.E. Mabbs, A.T. McPhail and K.D. Onan, J. Chem. Soc., Dalton Trans., (1979) 962–969.
189 C.D. Garner, personal communication, 1986.
190 A.M. Bond, J.A. Broomhead and A.F. Hollenkamp, Inorg. Chem., 27 (1988) 978–985.
191 A.F. Isbell, Jr., and D.T. Sawyer, Inorg. Chem., 10 (1971) 2449–2457.
192 L.J. de Hayes, H.C. Faulkner, W.H. Doub, Jr., and D.T. Sawyer, Inorg. Chem., 14 (1975) 2110–2116.
193 A.W. Edelblut, K. Folting, J.C. Huffman and R.A.D. Wentworth, J. Am. Chem. Soc., 103 (1981) 1927–1931.
194 F.A. Schultz, V.R. Ott, D.S. Rolison, D.C. Bravard, J.W. McDonald and W.E. Newton, Inorg. Chem., 17 (1978) 1758–1765.
195 V.R. Ott, D.S. Swieter and F.A. Schultz, Inorg. Chem., 16 (1977) 2538–2545.
196 B. Kathirgamanathan, M. Martinez and A.G. Sykes, J. Chem. Soc., Chem. Commun., (1985) 1437–1439.
M. Martinez, B.-L. Ooi and A.G. Sykes, J. Am. Chem. Soc., 109 (1987) 4615–4619.
197 K.F. Miller, A.E. Bruce, J.L. Corbin, S. Wherland and E.I. Stiefel, J. Am. Chem. Soc., 102 (1980) 5102–5104.
198 J.D. Rush and B.H.J. Bielski, Inorg. Chem., 24 (1985) 3895–3898.
199 J.R. Bradbury, A.F. Masters, A.C. McDonell, A.A. Brunette, A.M. Bond and A.G. Wedd, J. Am. Chem. Soc., 103 (1981) 1959–1964.
200 G.D. Hinch, D.E. Wycoff and R.K. Murmann, Polyhedron, 5 (1986) 487–495.
201 T. Shibahara, B. Sheldrick and A.G. Sykes, J. Chem. Soc., Chem. Commun., (1976) 523–524.
202 T. Shibahara and A.G. Sykes, J. Chem. Soc., Dalton Trans., (1978) 100–104.
203 E. Herdtweck, C. Schumacher and K. Dehnicke, Z. Anorg. Allg. Chem., 526 (1985) 93–102.
204 P.M. Boorman, T. Chivers, K.N. Mahadev and B.D. O'Dell, Inorg. Chim. Acta, 19 (1976) L35–L37.
205 M. Rakowski DuBois, R.C. Haltiwanger, D.J. Miller and G. Glatzmaier, J. Am. Chem. Soc., 101 (1979) 5245–5252.
206 C.J. Casewit, R.C. Haltiwanger, J. Noordik and M. Rakowski DuBois, Organometallics, 4 (1985) 119–129.
207 C.J. Casewit and M. Rakowski DuBois, Inorg. Chem., 25 (1986) 74–80.
208 C.J. Casewit and M. Rakowski DuBois, J. Am. Chem. Soc., 108 (1986) 5482–5489.
209 R.T. Weberg, R.C. Haltiwanger, J.C.V. Laurie and M. Rakowski DuBois, J. Am. Chem. Soc., 108 (1986) 6242–6250.
210 N.G. Connelly and L.F. Dahl, J. Am. Chem. Soc., 92 (1970) 7470–7472.
211 A. Müller, W. Eltzner, R. Jostes, H. Bögge, D. Diemann, J. Schimanski and H. Lueken, Angew. Chem., Int. Ed. Engl., 23 (1984) 389–390.
212 F.A. Cotton and R. Poli, Polyhedron, 6 (1987) 2181–2186.

213 W.H. Delphin and R.A.D. Wentworth, J. Am. Chem. Soc., 95 (1973) 7920–7921.
214 W.H. Delphin, R.A.D. Wentworth and M.S. Matson, Inorg. Chem., 13 (1974) 2552–2555.
215 M.Y. Subbotin and L.A. Aslanov, Russ. J. Inorg. Chem., 31 (1986) 222–225, and references therein.
216 F.A. Cotton, L.R. Falvello, G.N. Mott, R.R. Schrock and L.G. Sturgeoff, Inorg. Chem., 22 (1983) 2621–2623, and references therein.
217 L.D. Rosenhein and J.W. McDonald, Inorg. Chem., 26 (1987) 3414–3416.
218 F.A. Cotton and W. Schwotzer, J. Am. Chem. Soc., 105 (1983) 5639–5641.
219 F.A. Cotton, B.A. Frenz and T.R. Webb, J. Am. Chem. Soc., 95 (1973) 4431–4432.
220 F.A. Cotton, B.A. Frenz, E. Pedersen and T.R. Webb, Inorg. Chem., 14 (1975) 391–398.
221 W.C. Trogler, D.K. Erwin, G.L. Geoffroy and H.B. Gray, J. Am. Chem. Soc., 100 (1978) 1160–1163.
222 A. Bino and F.A. Cotton, Inorg. Chem., 18 (1979) 1159.
223 A. Bino, F.A. Cotton, D.O. Marler, S. Farquharson, B. Hutchinson, B. Spencer and J. Kincaid, Inorg. Chim. Acta, 133 (1987) 295–300.
224 A. Loewenschuss, J. Shamir and M. Ardon, Inorg. Chem., 15 (1976) 238–241.
225 A. Pernick and M. Ardon, J. Am. Chem. Soc., 97 (1975) 1255–1256.
226 A. Bino, Inorg. Chem., 20 (1981) 623–626.
227 F.A. Cotton and E. Pedersen, Inorg. Chem., 14 (1975) 399–400.
228 R.E. McCarley, J.L. Templeton, T.J. Colburn, V. Katovic and R.J. Hoxmeier, Adv. Chem. Ser., 150 (1976) 318–334.
229 J.H. Baxendale, C.D. Garner, R.G. Senior and P. Sharpe, J. Am. Chem. Soc., 98 (1976) 637–638.
230 D. Mandon, J.M. Giraudon, L. Toupet, J. Sala-Pala and J.E. Guerchais, J. Am. Chem. Soc., 109 (1987) 3490–3491.
231 H.D. Glicksman and R.A. Walton, Inorg. Chem., 17 (1978) 3197–3202.
232 J. Latorre, J. Soto, P. Salagre and J.E. Sueiras, Transition Met. Chem., 9 (1984) 447–449.
233 T. Zietlow, D.D. Klendworth, T. Nimry, D.J. Salmon and R.A. Walton, Inorg. Chem., 20 (1981) 947–949.
234 M.G.B. Drew and J.D. Wilkins, J. Chem. Soc., Dalton Trans., (1975) 1984–1989.
235 I.R. Anderson and J.C. Sheldon, Aust. J. Chem., 18 (1965) 271–276.
236 G.B. Allison, I.R. Anderson and J.C. Sheldon, Aust. J. Chem., 20 (1967) 869–876.
237 G.B. Allison, I.R. Anderson, W. van Bronswyk and J.C. Sheldon, Aust. J. Chem., 22 (1969) 1097–1102.
238 M.J. Bennett, J.V. Brencic and F.A. Cotton, Inorg. Chem., 8 (1969) 1060–1065.
239 J. San Filippo, Jr., H.J. Sniadoch and R.L. Grayson, Inorg. Chem., 13 (1974) 2121–2130.
240 F.A. Cotton, B.A. Frenz and Z.C. Mester, Acta Crystallogr. Sect. B, 29 (1973) 1515–1519.
241 F.A. Cotton and B.J. Kalbacher, Inorg. Chem., 15 (1976) 522–524.
242 A. Bino and F.A. Cotton, Angew. Chem., Int. Ed. Engl., 18 (1979) 332–333.
243 F.A. Cotton, P.C.W. Leung, W.J. Roth, A.J. Schultz and J.M. Williams, J. Am. Chem. Soc., 106 (1984) 117–120.
244 M.H. Chisholm, J.C. Huffman and W.G. Van Der Sluys, J. Am. Chem. Soc., 109 (1987) 2514–2515.
245 M. Bochmann, M. Cooke, M. Green, H.P. Kirsch, F.G.A. Stone and A.J. Welch, J. Chem. Soc., Chem. Commun., (1976) 381–383.
246 G.C. Allen, M. Green, B.J. Lee, H.P. Kirsch and F.G.A. Stone, J. Chem. Soc., Chem. Commun., (1976) 794–795.
247 B. Kanellakopulos, D. Nöthe, K. Weidenhammer, H. Wienand and M.L. Ziegler, Angew. Chem., Int. Ed. Engl., 16 (1977) 261–262.

248 W.-H. Pan, M.E. Leonowicz and E.I. Stiefel, Inorg. Chem., 22 (1983) 672–678.
249 J. Bernholc and E.I. Stiefel, Inorg. Chem., 24 (1985) 1323–1330.
250 A. Müller, W. Hellmann, C. Römer, M. Römer, H. Bögge, R. Jostes and U. Schimanski, Inorg. Chim. Acta, 83 (1984) L75–L77.
251 Y. Do, E.D. Simhon and R.H. Holm, Inorg. Chem., 24 (1985) 2827–2832.
252 D. Coucouvanis, A. Toupadakis and A. Hadjikyriacou, Inorg. Chem., 27 (1988) 3272–3273.
253 J. van de Poel and H.M. Neumann, Inorg. Chem., 7 (1968) 2086–2091.
254 S. Scavnicar and M. Herceg, Acta Crystallogr., 21 (1966) A151.
255 J.R. Dilworth, J. Zubieta and J.R. Hyde, J. Am. Chem. Soc., 104 (1982) 365–367.
256 A. Bino, F.A. Cotton and Z. Dori, J. Am. Chem. Soc., 103 (1981) 243–244.
257 M. Ardon, A. Bino, F.A. Cotton, Z. Dori, M. Kaftory, B.W.S. Kolthammer, M. Kapon and G. Reisner, Inorg. Chem., 20 (1981) 4083–4090.
258 A. Bino, M. Ardon, I. Maor, M. Kaftory and Z. Dori, J. Am. Chem. Soc., 98 (1976) 7093–7095.
259 F.A. Cotton, Polyhedron, 5 (1986) 3–14.
260 Y. Jiang, A. Tang, R. Hoffmann, J. Huang and J. Lu, Organometallics, 4 (1985) 27–34.
261 W. Beck, W. Danzer and G. Thiel, Angew. Chem., Int. Ed. Engl., 12 (1973) 582.
262 T. Shibahara and H. Kuroya, Polyhedron, 5 (1986) 357–361.
263 D.T. Richens and A.G. Sykes, Inorg. Chim. Acta, 54 (1981) L3–L4.
264 D.T. Richens and A.G. Sykes, Inorg. Chem., 21 (1982) 418–422.
265 M.T. Paffett and F.C. Anson, Inorg. Chem., 22 (1983) 1347–1355.
266 K.R. Rodgers, R.K. Murmann, E.O. Schlemper and M.E. Shelton, Inorg. Chem., 24 (1985) 1313–1322.
267 T. Shibahara, T. Yamada, H. Kuroya, E.F. Hills, P. Kathirgamanathan and A.G. Sykes, Inorg. Chim. Acta, 113 (1986) L19–L21.
268 A. Bino, F.A. Cotton and Z. Dori, Inorg. Chim. Acta, 33 (1979) L133–L134.
269 A. Birnbaum, F.A. Cotton, Z. Dori, M. Kapon, D. Marler, G.M. Reisner and W. Schwotzer, J. Am. Chem. Soc., 107 (1985) 2405–2410.
270 W. Dingming, H. Jinling and H. Jianquan, Acta Crystallogr. Sect. C, 41 (1985) 888–890.
271 J. Huang, M. Shang, J. Huang, H. Zhang, S. Lu and J. Lu, J. Struct. Chem. (USSR) (Engl. Transl.), 1 (1982) 1.
S. Maoyu, H. Jingling and L. Jiaxi, Acta Crystallogr. Sect. C, 40 (1984) 761.
272 L. Shaofang, L. Yuhui, H. Jinling, L. Jiaxi and H. Jianquan, Jiegou Huaxue, 3 (1984) 147 (Chem. Abstr. (1986) 103, 62905e).
273 F.A. Cotton and R. Poli, J. Am. Chem. Soc., 110 (1988) 830–841.
274 N.D. Feasey, S.A.R. Knox and A.G. Orpen, J. Chem. Soc., Chem. Commun., (1982) 75–76.
275 J.A. Beaver and M.G.B. Drew, J. Chem. Soc., Dalton Trans., (1973) 1376–1380.
276 S.A. Koch and S. Lincoln, Inorg. Chem., 21 (1982) 2904–2905.
S. Lincoln and S.A. Koch, Inorg. Chem., 25 (1986) 1594–1602.
277 M.F. Belicchi, G.G. Fava and C. Pelizzi, J. Chem. Soc., Dalton Trans., (1983) 65–69.
278 D. Attanasio, V. Fares and P. Imperatori, J. Chem. Soc., Chem. Commun., (1986) 1476–1477.
279 M.H. Chisholm, K. Folting, J.C. Huffman, J. Leonelli, N.S. Marchant, C.A. Smith and L.C.E. Taylor, J. Am. Chem. Soc., 107 (1985) 3722–3724.
280 T.C.W. Mak, K.S. Jasim and C. Chieh, Inorg. Chem., 24 (1985) 1587–1591.
281 J.A. Bandy, C.E. Davies, J.C. Green, M.L.H. Green, K. Prout and D.P.S. Rodgers, J. Chem. Soc., Chem. Commun., (1983) 1395–1397.

282 T. Toan, B.K. Teo, J.A. Ferguson, T.J. Meyer and L.F. Dahl, J. Am. Chem. Soc., 99 (1977) 408–416.
283 B. Sheldrick, Acta Crystallogr. Sect. B, 32 (1976) 2884–2886.
284 F.A. Cotton, M.P. Diebold, Z. Dori, R. Llusar and W. Schwotzer, J. Am. Chem. Soc., 107 (1985) 6735–6736.
285 T. Shibahara, H. Kuroya, K. Matsumoto and S. Ooi, J. Am. Chem. Soc., 106 (1984) 789–791.
286 P. Kathirgamanathan, M. Martinez and A.G. Sykes, J. Chem. Soc., Chem. Commun., (1985) 953–954.
287 B.-L. Ooi, C. Sharp and A.G. Sykes, J. Am. Chem. Soc., 111 (1989) 125–130.
288 F.A. Cotton, Z. Dori, R. Llusar and W. Schwotzer, Inorg. Chem., 25 (1986) 3529–3532.
289 T. Shibahara, H. Kuroya, K. Matsumoto and S. Ooi, Inorg. Chim. Acta, 116 (1986) L25–L27.
290 P. Kathirgamanathan, M. Martinez and A.G. Sykes, Polyhedron, 5 (1986) 505–506.
291 E. Carmona, F. Gonzalez, M.L. Poveda, J.L. Atwood and R.D. Rogers, J. Am. Chem. Soc., 105 (1983) 3365–3366.
292 T.-C. Hsieh and J. Zubieta, Inorg. Chem., 24 (1985) 1287–1288.
293 B.A. Aufdembrink and R.E. McCarley, J. Am. Chem. Soc., 108 (1986) 2474–2476.
294 S. Stensvad, B.J. Helland, M.W. Babich, R.A. Jacobson and R.E. McCarley, J. Am. Chem. Soc., 100 (1978) 6257–6258.
295 K. Jödden, H.G. von Schnering and H. Schäfer, Angew. Chem., Int. Ed. Engl., 14 (1975) 570–571.
296 M.H. Chisholm, K. Folting, J.C. Huffman and C.C. Kirkpatrick, J. Chem. Soc., Chem. Commun., (1982) 189–190.
297 R. Chevrel, M. Hirrien and M. Sergent, Polyhedron, 5 (1986) 87–94, and references therein.
298 T. Saito, N. Yamamoto, T. Yamagata and H. Imoto, J. Am. Chem. Soc., 110 (1988) 1646–1647.
299 D.G. Nocera and H.B. Gray, J. Am. Chem. Soc., 106 (1984) 824–825.
300 R.D. Mussell and D.G. Nocera, Polyhedron, 5 (1986) 47–50.
301 T. Shibahara, T. Yamamoto, H. Kanadani and H. Kuroya, J. Am. Chem. Soc., 109 (1987) 3495–3496.
302 S. Liu, X. Sun and J. Zubieta, J. Am. Chem. Soc., 110 (1988) 3324–3326.
303 T. Yamase, Polyhedron, 5 (1986) 79–86, and references therein.
304 T. Yamase, J. Chem. Soc., Dalton Trans., (1985) 2585–2590.
T. Yamase and T. Kurozumi, J. Chem. Soc., Dalton Trans., (1983) 2205–2209, and references therein.
305 C.L. Hill and D.A. Bouchard, J. Am. Chem. Soc., 107 (1985) 5148–5157, and references therein.
306 F. Weller, W. Liebelt and K. Dehnicke, Angew. Chem., Int. Ed. Engl., 19 (1980) 220.
307 Y. Jeannin, J.-P. Launay, J. Livage and A. Nel, Inorg. Chem., 17 (1978) 374–377.
308 G. Backes-Dahmann and K. Wieghardt, Inorg. Chem., 24 (1985) 4049–4054.
309 C. Sharp, E.F. Hills and A.G. Sykes, J. Chem. Soc., Dalton Trans., (1987) 2293–2297.
310 C. Sharp and A.G. Sykes, Inorg. Chem., 27 (1988) 501–503.
311 W.H. Delphin and R.A.D. Wentworth, Inorg. Chem., 12 (1973) 1914–1917.
312 W.S. Harwood, D. DeMarco and R.A. Walton, Inorg. Chem., 23 (1984) 3077–3080.
313 O. Olsson, Chem. Ber., 46 (1913) 566–582.
314 R. Colton and G.G. Rose, Aust. J. Chem., 21 (1968) 883–889.
315 E. König, Inorg. Chem., 8 (1969) 1278–1281.

316 J. San Filippo, Jr., P.J. Fagan and F.J. Di Salvo, Inorg. Chem., 16 (1977) 1016–1021.
317 T. Glowiak, M. Sabat and B. Jezowska-Trzebiatowska, Acta Crystallogr. Sect. B, 31 (1975) 1783–1784.
318 R. Saillant and R.A.D. Wentworth, J. Am. Chem. Soc., 91 (1969) 2174–2175.
319 J.L. Templeton, R.A. Jacobson and R.E. McCarley, Inorg. Chem., 16 (1977) 3320–3328.
320 W.C. Trogler, Inorg. Chem., 19 (1980) 697–700.
321 P.M. Boorman, V.D. Patel, K.A. Kerr, P.W. Codding and P. Van Roey, Inorg. Chem., 19 (1980) 3508–3511.
322 J.M. Ball, P.M. Boorman, K.J. Moynihan, V.D. Patel, J.F. Richardson, D. Collison and F.E. Mabbs, J. Chem. Soc., Dalton Trans., (1983) 2479–2485.
323 R.H. Summerville and R. Hoffmann, J. Am. Chem. Soc., 101 (1979) 3821–3831.
324 K.J. Ahmed and M.H. Chisholm, Organometallics, 5 (1986) 185–189.
325 K.W. Chiu, R.A. Jones, G. Wilkinson, A.M.R. Galas and M.B. Hursthouse, J. Chem. Soc., Dalton Trans., (1981) 1892–1897.
326 D.J. Santure, J.C. Huffman and A.P. Sattelberger, Inorg. Chem., 24 (1985) 371–378.
327 M.H. Chisholm, H.T. Chiu and J.C. Huffman, Polyhedron, 5 (1986) 1377–1380.
328 T.R. Ryan, Energy Res. Abstr. 7 (1982) Abstr. No. 30313. Chem. Abstr. 97:228998v.
329 R.R. Schrock, L.G. Sturgeoff and P.R. Sharp, Inorg. Chem., 22 (1983) 2801–2806.
330 A.R. Dias and M.L.H. Green, J. Chem. Soc., Chem. Commun., (1969) 962.
331 T.S. Cameron, C.K. Prout, G.V. Rees, M.H.L. Green, K.K. Joshi, G.R. Davies, B.T. Kilbourne, P.S. Braterman and V.A. Wilson, J. Chem. Soc., Chem. Commun., (1971) 14–15.
332 K. Prout and G.V. Rees, Acta Crystallogr. Sect. B, 30 (1974) 2717–2720.
333 E. Königer-Ahlborn and A. Müller, Angew. Chem., Int. Ed. Engl., 14 (1975) 573–574.
334 F. Secheresse, G. Lavigne, Y. Jeannin and J. Lefebvre, J. Coord. Chem., 11 (1981) 11–16.
335 A. Müller, R.G. Bhattacharyya, E. Königer-Ahlborn, R.C. Sharma, W. Rittner, A. Neumann, G. Henkel and B. Krebs, Inorg. Chim. Acta, 37 (1979) L493.
336 A. Müller, W. Rittner, A. Neumann, E. Königer-Ahlborn and R.G. Bhattacharyya, Z. Anorg. Allg. Chem., 461 (1980) 91–95.
337 A. Müller, H. Bögge, E. Krickemeyer, G. Henkel and B. Krebs, Z. Naturforsch., Teil B, 37 (1982) 1014–1019.
338 S. Bhaduri and J.A. Ibers, Inorg. Chem., 25 (1986) 3–4.
339 F.A. Cotton, Z. Dori, M. Kapon, D.O. Marler, G.M. Reisner, W. Schwotzer and M. Shaia, Inorg. Chem., 24 (1985) 4381–4384.
340 T.A. Stephenson and D. Whittaker, Inorg. Nucl. Chem. Lett., 5 (1969) 569–573.
341 F.A. Cotton and M. Jeremic, Synth. Inorg. Met.–Org. Chem., (1971) 265–278.
342 A. Bino, F.A. Cotton, Z. Dori, S. Koch, H. Küppers, M. Miller and J.C. Sekutowski, Inorg. Chem., 17 (1978) 3245–3253.
343 M. Ardon, F.A. Cotton, Z. Dori, A. Fang, M. Kapon, G.M. Reisner and M. Shaia, J. Am. Chem. Soc., 104 (1982) 5394–5398.
344 A. Bino, F.A. Cotton, Z. Dori, M. Shaia-Gottlieb and M. Kapon, Inorg. Chem., 27 (1988) 3592–3596.
345 V. Katovic, J.L. Templeton and R.E. McCarley, J. Am. Chem. Soc., 98 (1976) 5705–5706.
346 J.P. Launay, J. Electroanal. Chem. Interfacial Electrochem., 54 (1974) 197.
347 J.P. Launay, Y. Jeannin and A. Nel, Inorg. Chem., 22 (1983) 277–281.
348 Y. Jeannin, J.P. Launay, C. Sanchez, J. Livage and M. Fournier, Nouv. J. Chim., 4 (1980) 587–592.
349 F. Secheresse, J. Lefebvre, J.C. Daran and Y. Jeannin, Inorg. Chim. Acta, 45 (1980) L45–L46; Inorg. Chem., 21 (1982) 1311–1314.

350 T.P. Blatchford, M.H. Chisholm, K. Folting and J.C. Huffman, J. Chem. Soc., Chem. Commun., (1984) 1295–1296.
351 T.C. Zietlow, W.P. Schaefer, B. Sadeghi, N. Hua and H.B. Gray, Inorg. Chem., 25 (1986) 2195–2198.
T.C. Zietlow, W.P. Schaefer, B. Sadeghi, D.G. Nocera and H.B. Gray, Inorg. Chem., 25 (1986) 2198–2201.
352 J.P. Launay, J. Inorg. Nucl. Chem., 38 (1976) 807–816.
353 Y. Jeannin, J.P. Launay and M.A. Seid Sedjadi, Inorg. Chem., 19 (1980) 2933–2935.
354 A. Chemseddine, C. Sanchez, J. Livage, J.P. Launay and M. Fournier, Inorg. Chem., 23 (1984) 2609–2613.
355 J. Fuchs, H. Hartl, W. Schiller and U. Gerlach, Acta Crystallogr. Sect. B, 32 (1976) 740–749.
356 C. Sanchez, J. Livage, J.P. Launay and M. Fournier, J. Am. Chem. Soc., 105 (1983) 6817–6823.
357 M. Kozik, C.F. Hammer and L.C.W. Baker, J. Am. Chem. Soc., 108 (1986) 2748–2749.
358 R.S. Nyholm and A. Turco, Chem. Ind. (London), (1960) 74–75.
359 P.M. Plaksin, R.C. Stoufer, M. Mathew and G.J. Palenik, J. Am. Chem. Soc., 94 (1972) 2121–2122.
360 R. Uson, V. Riera and M. Laguna, Transition Met. Chem., 1 (1975/6) 21–25.
361 M. Stebler, A. Ludi and H.-B. Bürgi, Inorg. Chem., 25 (1986) 4743–4750.
362 S.R. Cooper and M. Calvin, J. Am. Chem. Soc., 99 (1977) 6623–6630.
363 R. Uson, V. Riera and M.A. Ciriano, Transition Met. Chem., 1 (1976) 98–99.
364 S.R. Cooper, G.C. Dismukes, M.P. Klein and M. Calvin, J. Am. Chem. Soc., 100 (1978) 7248–7252.
365 M.M. Morrison and D.T. Sawyer, J. Am. Chem. Soc., 99 (1977) 257–258.
366 M.M. Morrison and D.T. Sawyer, Inorg. Chem., 17 (1978) 333–337.
367 J.A. Kirby, A.S. Robertson, J.P. Smith, A.C. Thompson, S.R. Cooper and M.P. Klein, J. Am. Chem. Soc., 103 (1981) 5529–5537.
368 M.A. Collins, D.J. Hodgson, K. Michelsen and D.K. Towle, J. Chem. Soc., Chem. Commun., (1987) 1659–1660.
369 D.K. Towle, C.A. Botsford and D.J. Hodgson, Inorg. Chim. Acta, 141 (1988) 167–168.
370 K.J. Brewer, A. Liegeois, J.W. Otvos, M. Calvin and L.O. Spreer, J. Chem. Soc., Chem. Commun., (1988) 1219–1220.
371 K.S. Hagen, W.H. Armstrong and H. Hope, Inorg. Chem., 27 (1988) 967–969.
372 K. Wieghardt, U. Bossek, D. Ventur and J. Weiss, J. Chem. Soc., Chem. Commun., (1985) 347–349.
373 K. Wieghardt, U. Bossek, J. Bonvoisin, P. Beauvillain, J.-J. Girerd, B. Nuber, J. Weiss and J. Heinze, Angew. Chem., Int. Ed. Engl., 25 (1986) 1030–1031.
374 K. Wieghardt, U. Bossek, L. Zsolnai, G. Huttner, G. Blondin, J.-J. Girerd and F. Bobonneau, J. Chem. Soc., Chem. Commun., (1987) 651–653.
375 J.S. Bashkin, A.R. Schake, J.B. Vincent, H.-R. Chang, Q. Li, J.C. Huffman, G. Christou and D.N. Hendrickson, J. Chem. Soc., Chem. Commun., (1988) 700–702.
376 L.J. Boucher and C.G. Coe, Inorg. Chem., 15 (1976) 1334–1340.
377 L.J. Boucher and C.G. Coe, Inorg. Chem., 14 (1975) 1289–1295.
378 J.A. Smegal, B.C. Schardt and C.L. Hill, J. Am. Chem. Soc., 105 (1983) 3510–3515.
379 M. Camenzind, B.C. Schardt and C.L. Hill, Inorg. Chem., 23 (1984) 1984–1986.
380 G.C. Dismukes, J.E. Sheats and J.A. Smegal, J. Am. Chem. Soc., 109 (1987) 7202–7203.
381 J.T. Landrum, D. Grimmett, K.J. Haller, W.R. Scheidt and C.A. Reed, J. Am. Chem. Soc., 103 (1981) 2640–2650.
382 B. Mabad, J.-P. Tuchagues, Y.T. Hwang and D.N. Hendrickson, J. Am. Chem. Soc., 107 (1985) 2801–2802.

383 W.M. Coleman, R.K. Boggess, J.W. Hughes and L.T. Taylor, Inorg. Chem., 20 (1981) 700–706.
384 H. Okawa, A. Honda, M. Nakamura and S. Kida, J. Chem. Soc., Dalton Trans., (1985) 59–64.
385 M. Suzuki, S. Murata, A. Uehara and S. Kida, Chem. Lett., (1987) 281–284.
386 H. Diril, H.-R. Chang, X. Zhang, S.K. Larsen, J.A. Potenza, C.G. Pierpont, H.S. Schugar, S.S. Isied and D.N. Hendrickson, J. Am. Chem. Soc., 109 (1987) 6207–6208.
387 H.-R. Chang, S.K. Larsen, P.D.W. Boyd, C.G. Pierpont and D.N. Hendrickson, J. Am. Chem. Soc., 110 (1988) 4565–4576.
388 R.M. Buchanan, K.J. Oberhausen and J.F. Richardson, Inorg. Chem., 27 (1988) 973–974.
389 J.W. McDonald, Inorg. Chem., 24 (1985) 1734–1736.
390 L.J. Lyons, M.H. Tegen, K.J. Haller, D.H. Evans and P.M. Treichel, Organometallics, 7 (1988) 357–365.
391 J.L. Calderon, F.A. Cotton, B.G. DeBoer and N. Martinez, J. Chem. Soc., Chem. Commun., (1971) 1476–1477.
392 T. Lionel, J.R. Morton and K.F. Preston, Inorg. Chem., 22 (1983) 145–147.
393 S.W. Bratt and M.C.R. Symons, J. Chem. Soc., Dalton Trans., (1977) 1314–1316.
394 R.F. Weinland and G. Fischer, Z. Anorg. Chem., 120 (1921) 161.
395 A.R.E. Baikie, M.B. Hursthouse, D.B. New and P. Thornton, J. Chem. Soc., Chem. Commun., (1978) 62–63.
396 J.B. Vincent, H.-R. Chang, K. Folting, J.C. Huffman, G. Christou and D.N. Hendrickson, J. Am. Chem. Soc., 109 (1987) 5703–5711.
397 A.R.E. Baikie, M.B. Hursthouse, L. New, P. Thornton and R.G. White, J. Chem. Soc., Chem. Commun., (1980) 684–685.
398 T. Lis, Acta Crystallogr. Sect. B, 36 (1980) 2042–2046.
399 J.L. Seela, K. Folting, R.-J. Wang, J.C. Huffman, G. Christou, H.-R. Chang and D.N. Hendrickson, Inorg. Chem., 24 (1985) 4454–4456.
400 X. Li, D.P. Kessissoglou, M.L. Kirk, C.J. Bender and V.L. Pecoraro, Inorg. Chem., 27 (1988) 1–3.
401 M.C. Böhm, R.D. Ernst, R. Gleiter and D.R. Wilson, Inorg. Chem., 22 (1983) 3815–3821.
402 J.C. de Paula, W.F. Beck and G.W. Brudvig, J. Am. Chem. Soc., 108 (1986) 4002–4009, and references therein.
403 J.S. Bashkin, H.-R. Chang, W.E. Streib, J.C. Huffman, D.N. Hendrickson and G. Christou, J. Am. Chem. Soc., 109 (1987) 6502–6504.
404 C. Christmas, J.B. Vincent, J.C. Huffman, G. Christou, H.-R. Chang and D.N. Hendrickson, J. Chem. Soc., Chem. Commun., (1987) 1303–1305.
405 J.B. Vincent, C. Christmas, J.C. Huffman, G. Christou, H.-R. Chang and D.N. Hendrickson, J. Chem. Soc., Chem. Commun., (1987) 236–238.
406 A.R.E. Baikie, A.J. Howes, M.B. Hursthouse, A.B. Quick and P. Thornton, J. Chem. Soc., Chem. Commun., (1986) 1587.
407 B. Krebs and K.-D. Hasse, Z. Naturforsch., Teil B, 28 (1972) 218–219.
408 B. Krebs and K.-D. Hasse, Angew. Chem., Int. Ed. Engl., 13 (1974) 603.
409 T. Lis and B. Jezowska-Trzebiatowska, Acta Crystallogr. Sect. B, 33 (1977) 2112–2116.
410 C. Christmas, J.B. Vincent, J.C. Huffman, G. Christou, H.-R. Chang and D.N. Hendrickson, Angew. Chem., Int. Ed. Engl., 26 (1987) 915–916.
411 C. Christmas, J.B. Vincent, H.-R. Chang, J.C. Huffman, G. Christou and D.N. Hendrickson, J. Am. Chem. Soc., 110 (1988) 823–830.
412 V.I. Spitsyn, A.F. Kuzina, A.A. Oblova and S.V. Kryuchkov, Russ. Chem. Rev., 54 (1985) 637–670.

413 M.E. Kastner, P.H. Fackler, L. Podbielski, J. Charkoudian and M.J. Clarke, Inorg. Chim. Acta, 114 (1986) L11–L15.
414 M.J. Clarke, M.E. Kastner, L.A. Podbielski, P.H. Fackler, J. Schriefels, G. Meinken and S.C. Srivastava, J. Am. Chem. Soc., 110 (1988) 1818–1827.
415 A.F. Kuzina, A.A. Oblova and V.I. Spitsyn, Russ. J. Inorg. Chem., 17 (1972) 1377–1379.
416 J.D. Eakins, D.G. Humphreys and C.E. Mellish, J. Chem. Soc., (1963) 6012–6016.
417 W.K. Bratton and F.A. Cotton, Inorg. Chem., 9 (1970) 789–793.
418 F.A. Cotton and E. Pedersen, Inorg. Chem., 14 (1975) 383–387.
419 M.I. Glinkina, A.F. Kuzina and V.I. Spitsyn, Russ. J. Inorg. Chem., 18 (1973) 210–213.
420 V.I. Spitsyn, A.F. Kuzina, A.A. Oblova and L.I. Belyaeva, Dokl. Akad. Nauk SSSR, 237 (1977) 1126–1129 (Engl. 1173–1176).
421 V.I. Spitsyn, A.F. Kuzina, A.A. Oblova, S.V. Kryuchkov and L.I. Belyaeva, Dokl. Akad. Nauk SSSR, 237 (1977) 1412–1413 (Engl. 1211–1212).
422 P.A. Koz'min and G.N. Novitskaya, Russ. J. Inorg. Chem., 17 (1972) 1652–1653.
423 P.A. Koz'min and G.N. Novitskaya, Koord. Khim., 1 (1975) 248.
424 F.A. Cotton and L.W. Shive, Inorg. Chem., 14 (1975) 2032–2035.
425 S.V. Kryuchkov, A.F. Kuzina and V.I. Spitsyn, Russ. J. Inorg. Chem., 28 (1983) 1124–1129.
426 F.A. Cotton and W.K. Bratton, J. Am. Chem. Soc., 87 (1965) 921.
427 F.A. Cotton, A. Davison, V.W. Day, M.F. Fredrich, C. Orvig and R. Swanson, Inorg. Chem., 21 (1982) 1211–1214.
428 V.I. Spitsyn, A.K. Kuzina and S.V. Kryuchkov, Russ. J. Inorg. Chem., 25 (1980) 406–409.
429 F.A. Cotton, P.E. Fanwick and L.D. Gage, J. Am. Chem. Soc., 102 (1980) 1570–1577.
430 V.I. Spitsyn, B. Baierl, S.V. Kryuchkov, A.F. Kuzina and M. Varen, Dokl. Akad. Nauk SSSR, 256 (1981) 608–612.
431 S.V. Kryuchkov, A.F. Kuzina and V.I. Spitsyn, Dokl. Akad. Nauk SSSR, 266 (1982) 127–130.
432 P.A. Koz'min, T.B. Larina and M.D. Surazhskaya, Koord. Khim., 7 (1981) 1719.
433 P.A. Koz'min, T.B. Larina and M.D. Surazhskaya, Koord. Khim., 9 (1983) 1114.
434 Y.V. Rakitin, S.V. Kryuchkov, A.I. Aleksandrov, A.F. Kuzina, N.V. Nemtsev, B.G. Ershov and V.I. Spitsyn, Dokl. Akad. Nauk SSSR, 269 (1983) 1123–1126 (Engl. 253–256).
435 Y.V. Ratikin and V.I. Nefedov, Russ. J. Inorg. Chem., 29 (1984) 294–298.
436 P.A. Koz'min, T.B. Larina and M.D. Surazhskaya, Koord. Khim., 8 (1982) 851.
437 F.A. Cotton, Rev. Pure Appl. Chem., 17 (1967) 25–40.
438 M. Biagini Cingi and E. Tondello, Inorg. Chim. Acta, 11 (1974) L3–L4.
439 F.A. Cotton and B.J. Kalbacher, Inorg. Chem., 16 (1977) 2386–2396.
440 F.A. Cotton and E. Pedersen, J. Am. Chem. Soc., 97 (1975) 303–308.
441 F.A. Cotton, P.E. Fanwick, L.D. Gage, B. Kalbacher and D.S. Martin, J. Am. Chem. Soc., 99 (1977) 5642–5645.
442 K.E. German, S.V. Kryuchkov, A.F. Kuzina and V.I. Spitsyn, Dokl. Akad. Nauk SSSR, 288 (1986) 381–384 (Engl. 139–142).
443 P.A. Koz'min, T.B. Larina and M.D. Surazhskaya, Dokl. Akad. Nauk SSSR, 271 (1983) 1157–1159 (Engl., 577–579).
444 P.A. Koz'min, M.D. Surazhskaya and T.B. Larina, Koord. Khim., 11 (1985) 1559.
445 S.V. Kryuchkov, A.F. Kuzina and V.I. Spitsyn, Dokl. Akad. Nauk SSSR, 287 (1986) 1400–1403 (Engl. 112–115).
446 S.V. Kryuchkov, M.S. Grigor'ev, A.F. Kuzina, B.F. Gulev and V.I. Spitsyn, Dokl. Akad. Nauk SSSR, 288 (1980) 893–897 (Engl. 172–176).

447 P.A. Koz'min, M.D. Surazhskaya and T.B. Larina, Dokl. Akad. Nauk SSSR, 265 (1982) 1420–1423 (Engl. 656–658).
448 R.A. Wheeler and R. Hoffmann, Angew. Chem., Int. Ed. Engl., 25 (1986) 822–823.
449 R.A. Wheeler and R. Hoffmann, J. Am. Chem. Soc., 108 (1986) 6605–6610.
450 V.N. Gerasimov, S.V. Kryuchkov, A.F. Kuzina, V.M. Kulakov, S.V. Pirozhkov, V.I. Spitsyn, Dokl. Akad. Nauk SSSR, 266 (1982) 148–152 (Engl. 688–691).
451 B. Jezowska-Trzebiatowska, J. Mrozinski and W. Wojciechowski, Bull. Acad. Polon. Sci. Ser. Sci. Chim., 11–12 (1969) 629–635.
452 T. Lis and B. Jezowska-Trzebiatowska, Acta Crystallogr. Sect. B, 32 (1976) 867–869.
453 J.D. Allison, C.J. Cameron, R.E. Wild and R.A. Walton, J. Organomet. Chem., 218 (1981) C62–C66.
454 J.D. Allison and R.A. Walton, J. Am. Chem. Soc., 106 (1984) 163–168.
455 F.A. Cotton, W.R. Robinson and R.A. Walton, Inorg. Chem., 6 (1967) 223–228.
456 H. Gehrke, Jr., G. Eastland and M. Leitheiser, J. Inorg. Nucl. Chem., 32 (1970) 867–872.
457 H. Gehrke, Jr., and G. Eastland, Inorg. Chem., 9 (1970) 2722–2725.
458 H. Gehrke, Jr., G. Eastland, L. Haas and G. Carlson, Inorg. Chem., 10 (1971) 2328–2329.
459 F. Bonati and F.A. Cotton, Inorg. Chem., 6 (1967) 1353–1356.
460 F.A. Cotton, W.R. Robinson, R.A. Walton and R. Whyman, Inorg. Chem., 6 (1967) 929–935.
461 F.A. Cotton, A. Davison, W.H. Ilsley and H.S. Trop, Inorg. Chem., 18 (1979) 2719–2723.
462 K.R. Dunbar, D. Powell and R.A. Walton, J. Chem. Soc., Chem. Commun., (1985) 114–116.
463 K.R. Dunbar, D. Powell and R.A. Walton, Inorg. Chem., 24 (1985) 2842–2846.
464 G. Rouschias and G. Wilkinson, J. Chem. Soc. A, (1966) 465–472.
465 F.A. Cotton, R. Eiss and B.M. Foxman, Inorg. Chem., 8 (1969) 950–957.
466 A.R. Chakravarty, F.A. Cotton, A.R. Cutler and R.A. Walton, Inorg. Chem., 25 (1986) 3619–3624.
467 A.R. Chakravarty, F.A. Cotton, A.R. Cutler, S.M. Tetrick and R.A. Walton, J. Am. Chem. Soc., 107 (1985) 4795–4796.
468 A.R. Cutler, P.E. Fanwick and R.A. Walton, Inorg. Chem., 26 (1987) 3811–3814.
469 D.M. Bruce, J.H. Holloway and D.R. Russell, J. Chem. Soc., Chem. Commun., (1973) 321–322.
470 D.M. Bruce, A.J. Hewitt, J.H. Holloway, R.D. Peacock and I.L. Wilson, J. Chem. Soc., Dalton Trans., (1976) 2230–2235.
471 D.M. Bruce, J.H. Holloway and D.R. Russell, J. Chem. Soc., Dalton Trans., (1978) 64–67.
472 D.M. Bruce and J.H. Holloway, Transition Met. Chem., 3 (1978) 217–220.
473 F.A. Cotton, C. Oldham and R.A. Walton, Inorg. Chem., 6 (1967) 214–223.
474 M.J. Bennett, F.A. Cotton and R.A. Walton, J. Am. Chem. Soc., 88 (1966) 3866–3867.
475 M.J. Bennett, F.A. Cotton and R.A. Walton, Proc. R. Soc. London, Ser. A, 303 (1968) 175.
476 F.A. Cotton, W.R. Robinson and R.A. Walton, Inorg. Chem., 6 (1967) 1257–1258.
477 R.R. Hendriksma and H.P. van Leeuwen, Electrochim. Acta, 18 (1973) 39.
478 D.J. Salmon and R.A. Walton, J. Am. Chem. Soc., 100 (1978) 991–993.
479 P. Brandt, D.J. Salmon and R.A. Walton, J. Am. Chem. Soc., 100 (1978) 4424–4430.
480 K.R. Dunbar and R.A. Walton, Inorg. Chem., 24 (1985) 5–10.
481 F.A. Cotton, B.A. Frenz, J.R. Ebner and R.A. Walton, J. Chem. Soc., Chem. Commun., (1974) 4–5.
482 J.R. Ebner and R.A. Walton, Inorg. Chem., 14 (1975) 1987–1992.

483 C.A. Hertzer and R.A. Walton, Inorg. Chim. Acta, 22 (1977) L10.
484 J.R. Ebner and R.A. Walton, Inorg. Chim. Acta, 14 (1975) L45–L46.
485 J.R. Ebner and R.A. Walton, Inorg. Chem., 14 (1975) 2289–2291.
486 F.A. Cotton, L.W. Shive and B.R. Stults, Inorg. Chem., 15 (1976) 2239–2244.
487 J.R. Ebner, D.R. Tyler and R.A. Walton, Inorg. Chem., 15 (1976) 833–840.
488 V. Srinivasan and R.A. Walton, Inorg. Chem., 19 (1980) 1635–1640.
489 A.R. Cutler and R.A. Walton, Inorg. Chim. Acta, 105 (1985) 219–222.
490 F.A. Cotton, K.R. Dunbar, L.R. Falvello, M. Tomas and R.A. Walton, J. Am. Chem. Soc., 105 (1983) 4950–4954.
491 B.E. Bursten, F.A. Cotton, P.E. Fanwick, G.G. Stanley and R.A. Walton, J. Am. Chem. Soc., 105 (1983) 2606–2611.
492 P. Brand, H.D. Glicksman, D.J. Salmon and R.A. Walton, Inorg. Chem., 17 (1978) 3203–3206.
493 L.B. Anderson, S.M. Tetrick and R.A. Walton, J. Chem. Soc., Dalton Trans., (1986) 55–60.
494 L.B. Anderson, T.J. Barder, D. Esjornson, R.A. Walton and B.E. Bursten, J. Chem. Soc., Dalton Trans., (1986) 2607–2612.
495 T.J. Barder, D. Powell and R.A. Walton, J. Chem. Soc., Chem. Commun., (1985) 550–551.
496 R. Colton, R. Levitus and G. Wilkinson, J. Chem. Soc., (1960) 4121–4126.
497 R. Colton, R. Levitus and G. Wilkinson, J. Chem. Soc., (1960) 5275–5276.
498 F.A. Cotton and R.A. Walton, Inorg. Chem., 5 (1966) 1802–1808.
499 D.G. Tisley and R.A. Walton, Inorg. Chem., 11 (1972) 179–181.
500 F.A. Cotton, K.R. Dunbar, L.R. Falvello and R.A. Walton, Inorg. Chem., 24 (1985) 4180–4187.
501 L.B. Anderson, F.A. Cotton, K.R. Dunbar, L.R. Falvello, A.C. Price, A.H. Reid and R.A. Walton, Inorg. Chem., 26 (1987) 2717–2725.
502 S. Kato, M. Tsutsui, D.L. Cullen and E.F. Meyer, Jr., J. Am. Chem. Soc., 99 (1977) 620–622.
503 T. Sowa, T. Kawamura, T. Yamabe and T. Yonezawa, J. Am. Chem. Soc., 107 (1985) 6471–6475.
504 W.A. Herrmann, R. Serrano, M.L. Ziegler, H. Pfisterer and B. Nuber, Angew. Chem., Int. Ed. Engl., 24 (1985) 50–52.
505 P. Hofmann and N. Rösch, J. Chem. Soc., Chem. Commun., (1986) 843–844.
506 W.A. Herrmann, R. Serrano, U. Küsthardt, M.L. Ziegler, E. Guggolz and T. Zahn, Angew Chem., Int. Ed. Engl., 23 (1984) 515–517.
507 K.W. Chiu, W.-K. Wong, G. Wilkinson, A.M.R. Galas and M.B. Hursthouse, Polyhedron, 1 (1982) 31–36.
508 F. Calderazzo, F. Marchetti, R. Poli, D. Vitali and P.F. Zanazzi, J. Chem. Soc., Chem. Commun., (1981) 893–894.
509 F. Calderazzo, F. Marchetti, R. Poli, D. Vitali and P.F. Zanazzi, J. Chem. Soc., Dalton Trans., (1982) 1665–1670.
510 F. Taha and G. Wilkinson, J. Chem. Soc., (1963) 5406–5412.
511 C. Calvo, N.C. Jayadevan, C.J.L. Lock and R. Restivo, Can. J. Chem., 48 (1970) 219–224.
512 C. Calvo, N.C. Jayadevan and C.J.L. Lock, Can. J. Chem., 47 (1969) 4213–4220.
513 N.J. Taylor, J. Chem. Soc., Chem. Commun., (1985) 476–477.
514 N.J. Taylor, J. Chem. Soc., Chem. Commun., (1985) 478–479.
515 K. Mertis, P.G. Edwards, G. Wilkinson, K.M.A. Malik and M.B. Hursthouse, J. Chem. Soc., Chem. Commun., (1980) 654–656.

516 A. Müller, M. Penk, E. Krickemeyer, H. Bögge and H.-J. Walberg, Angew. Chem., Int. Ed. Engl., 27 (1988) 1719–1720.
517 D.H. Dotson and T.M. Brown, in Proceedings of the XXVII International Conference on Coordination Chemistry Porto, Portugal, Abstract D11.
518 D. Fenske, J. Ohmer, J. Hachgenei and K. Merzweiler, Angew. Chem., Int. Ed. Engl., 27 (1988) 1277.
519 F.A. Cotton and M. Shang, J. Am. Chem. Soc., 110 (1988) 7719–7722.
520 C.J. Casewit and M. Rakowski DuBois, Rev. Inorg. Chem., 9 (1988) 199–218.
521 K. Wieghardt, U. Bossek, A. Neves, B. Nuber and J. Weiss, Inorg. Chem., 28 (1989) 432–440.
522 H. Akaski, T. Shibahara, T. Narahara, H. Tsuru and H. Koroya, Chem. Lett., (1989) 129–132.
523 S. Liu and J. Zubieta, Polyhedron, 8 (1989) 537–539.
524 M. Kozik, N. Casan-Pastor, C.F. Hammer and L.C.W. Baker, J. Am. Chem. Soc., 110 (1988) 7697–7701.
525 D.J. Bergs, M.H. Chisholm, K. Folting, J.C. Huffman and K.A. Stahl, Inorg. Chem., 27 (1988) 2950–2954.
526 M.A. Makhyoun, Polyhedron, 7 (1988) 2675–2678.
527 G.W. Brudvig, in L. Que, Jr. (Ed.), Metal Clusters in Proteins, ACS Symposium 372, American Chemical Society, Washington, 1988, pp. 221–237.
528 R.M. Fronko, J.E. Penner-Hahn and C.J. Bender, J. Am. Chem. Soc., 110 (1988) 7554–7555.
529 K. Wieghardt, U. Bossek, B. Nuber, J. Weiss, J. Bonvoisin, M. Corbella, S.E. Vitols and J.J. Girerd, J. Am. Chem. Soc., 110 (1988) 7398–7411.
530 M. Suzuki, H. Senda, Y. Kobayashi, H. Oshio and A. Uehara, Chem. Lett., (1988) 1763–1766.
531 D.P. Kessissoglou, M.L. Kirk, C.A. Bender, M.S. Lah and V.L. Pecoraro, J. Chem. Soc., Chem. Commun., (1989) 84–86.
532 G. Christou and J.B. Vincent, in L. Que, Jr. (Ed)., Metal Clusters in Proteins, ACS Symposium 372, American Chemical Society, Washington, 1988, pp. 239–255.
533 Q. Li, J.B. Vincent, E. Libby, H.-R. Chang, J.C. Huffman, P.D.W. Boyd, G. Christou and D.N. Hendrickson, Angew. Chem., Int. Ed. Engl., 27 (1988) 1731–1733.
534 K.S. Hagen, W.H. Armstrong and M.M. Olmstead, J. Am. Chem. Soc., 111 (1989) 774–775.
535 P.D.W. Boyd, Q. Li, J.B. Vincent, K. Folting, H.-R. Chang, W.E. Streib, J.C. Huffman, G. Christou and D.N. Hendrickson, J. Am. Chem. Soc., 110 (1988) 8537–8539.
536 J. Lu and M.J. Clarke, Inorg. Chem., 27 (1988) 4761–4766.
537 V.I. Spitzin, V.S. Kryutchkov, M.S. Grigoriev and A.F. Kuzina, Z. Anorg. Allg. Chem., 563 (1988) 136–152.
538 S.V. Kryutchkov, A.F. Kuzina and V.I. Spitzin, Z. Anorg. Allg. Chem., 563 (1988) 153–166.